

**NATIONAL TECHNICAL UNIVERSITY OF ATHENS  
SCHOOL OF CIVIL ENGINEERING  
DEPARTMENT OF WATER  
RESOURCES AND ENVIRONMENTAL ENGINEERING**

**DEVELOPMENT OF A  
METHODOLOGY FOR THE  
ESTIMATION OF THE DYNAMIC  
EVOLUTION OF THE  
FLOOD-RELATED HYDROLOGICAL  
BEHAVIOR  
OF PERIURBAN CATCHMENTS  
UNDER POST - FIRE CONDITIONS**

**DOCTORAL THESIS**

**CHRYSOULA PAPATHANASIOU**  
Civil Engineer

**ATHENS, 2018**



**NATIONAL TECHNICAL UNIVERSITY OF ATHENS  
SCHOOL OF CIVIL ENGINEERING  
DEPARTMENT OF WATER RESOURCES AND ENVIRONMENTAL  
ENGINEERING**

**DEVELOPMENT OF A METHODOLOGY  
FOR THE ESTIMATION OF THE DYNAMIC EVOLUTION  
OF THE FLOOD-RELATED HYDROLOGICAL BEHAVIOR  
OF PERIURBAN CATCHMENTS  
UNDER POST - FIRE CONDITIONS**

**Advisory Committee**

**Prof. M.A.Mimikou (Supervisor)**

**Assoc.Prof. N. Mamassis**

**Assoc.Prof. C. Makropoulos**

Copyright © Chrysoula Papathanasiou, 2018

Με επιφύλαξη παντός δικαιώματος. All rights reserved.

Απαγορεύεται η αντιγραφή, αποθήκευση και διανομή της παρούσας διατριβής, εξ ολοκλήρου ή τμήματος αυτής, για εμπορικό σκοπό. Επιτρέπεται η ανατύπωση, αποθήκευση και διανομή για σκοπό μη κερδοσκοπικό, εκπαιδευτικής ή ερευνητικής φύσης, υπό την προϋπόθεση να αναφέρεται η πηγή προέλευσης. Ερωτήματα που αφορούν τη χρήση της διατριβής για κερδοσκοπικό σκοπό πρέπει να απευθύνονται προς τη συγγραφέα.

Η έγκριση της Διδακτορικής Διατριβής από τη Σχολή Πολιτικών Μηχανικών του Εθνικού Μετσόβιου Πολυτεχνείου δεν υποδηλώνει αποδοχή των απόψεων της συγγραφέως (Ν. 5343/1932, Άρθρο 202, Παρ. 2).

# TABLE OF CONTENTS

TABLE OF CONTENTS .....	i
TABLE OF FIGURES .....	iv
TABLE OF TABLES .....	vii
A C K N O W L E D G E M E N T S .....	ix
EXECUTIVE SUMMARY .....	x
ΕΚΤΕΝΗΣ ΠΕΡΙΛΗΨΗ .....	xix
CHAPTER 1: INTRODUCTION .....	1
1.1 Context.....	1
1.2 Aim and objectives .....	2
1.3 Methodology .....	3
1.4 Innovative aspects of the research.....	4
1.5 Structure .....	6
CHAPTER 2: BACKGROUND – NATURAL HAZARDS, FOCUSING ON FLOODS AND FOREST FIRES .....	10
2.1 Natural hazards.....	10
2.1.1 <i>Facts and statistics about natural hazards</i> .....	10
2.1.2 <i>Disaster management</i> .....	14
2.2 Floods .....	16
2.2.1 <i>Facts and statistics about floods</i> .....	16
2.2.1.1 <i>Principal cause and generation mechanisms</i> .....	16
2.2.1.2 <i>Flood characteristics</i> .....	17
2.2.1.3 <i>Flood types</i> .....	19
2.2.1.4 <i>Flood impacts and statistics</i> .....	20
2.2.1.5 <i>Flood Early Warnings Systems</i> .....	24
2.3 Forest fires .....	26
2.3.1 <i>Facts and statistics about forest fires</i> .....	26
2.3.1.1 <i>Forest fire ignition sources</i> .....	26
2.3.1.2 <i>Fire characteristics</i> .....	28
2.3.1.3 <i>Fire severity</i> .....	28
2.3.1.4 <i>Forest fires impacts and statistics</i> .....	29
2.3.1.5 <i>Prescribed fires</i> .....	33
CHAPTER 3: FLOODS–FIRES INTERACTION .....	35
3.1 Impacts of forest fires on ecosystems from a hydrological perspective... 35	35
3.1.1 <i>Direct impacts</i> .....	35
3.1.2 <i>Indirect impacts</i> .....	37
3.2 Assessment of forest fires impacts on typical catchment characteristics 43	43
3.3 Recovery.....	45
3.3.1 <i>Environmental recovery</i> .....	46
3.3.2 <i>Hydrological recovery</i> .....	49
3.3.2.1 <i>Factors that affect hydrological recovery</i> .....	50
3.3.2.2 <i>Temporal dimension of hydrological recovery</i> .....	51
3.4 Effect of floods on imminent forest fires .....	52
3.5 Identification of existing gap in literature .....	53
CHAPTER 4: FLOOD MODELLING .....	56
4.1 Hydrological modelling .....	56
4.2 Hydrological models.....	57
4.2.1 <i>Review on lumped (and semi-distributed) hydrological models</i> .....	59

4.2.1.1	HEC-HMS.....	59
4.2.1.2	TOPMODEL.....	60
4.2.1.3	ARNO.....	61
4.2.1.4	SWAT.....	62
4.2.1.5	Hydrological modules provided by hydraulic models.....	63
4.2.1.5.1	NAM and UHM.....	63
4.2.1.5.2	Hydrological module of SWMM.....	64
4.2.2	Review on distributed (GIS-based) hydrological models.....	65
4.2.2.1	CASC2D & GSSHA™.....	65
4.2.2.2	Vflo™.....	67
4.2.2.3	MIKE SHE.....	68
4.2.2.4	LISFLOOD.....	69
4.2.2.5	CHYM.....	70
4.2.2.6	TOPKAPI.....	71
4.2.2.7	WATFLOOD/SPL.....	72
4.2.3	Evaluation of identified hydrological models.....	73
4.3	Hydraulic modelling.....	74
4.4	Hydraulic models.....	75
4.4.1	Review on 1D hydraulic models.....	76
4.4.1.1	HEC-RAS.....	76
4.4.1.2	MIKE11.....	77
4.4.1.3	SWMM.....	78
4.4.2	Review on 1D2D hydraulic models.....	79
4.4.2.1	LISFLOOD-FP.....	80
4.4.2.2	FLO2D.....	80
4.4.3	Evaluation of identified hydraulic models.....	81
4.5	Coupled hydrological – hydraulic modelling.....	82
4.5.1	“Fixed” platforms for integrated modelling.....	82
4.5.2	“Customized” platforms for integrated modelling.....	84
4.6	Flood models applied in this research.....	85
CHAPTER 5: METHODOLOGY.....		87
5.1	Estimating fire impact.....	87
5.1.1	Examining fire impact from a spatial perspective.....	88
5.1.2	Examining fire impact from a temporal perspective.....	89
5.2	Estimating initial soil moisture.....	91
5.3	Hydrological modelling – selected simulation methods and hydrological parameters.....	92
5.3.1	Hydrological loss method.....	93
5.3.1.1	Estimating CN for pre-fire and normal SM conditions.....	94
5.3.1.2	Estimating IA for pre-fire and normal SM conditions.....	94
5.3.2	Transform Method.....	95
5.3.3.1	Estimating TP for pre-fire and normal SM conditions.....	96
5.3.3.2	Estimating CP for pre-fire and normal SM conditions.....	97
5.3.3	Routing Method.....	97
5.3.3.1	Estimating K for pre-fire and normal SM conditions.....	99
5.4	Estimating the temporal evolution of the selected hydrological parameters for variable initial conditions.....	99
5.5	The 1 <sup>st</sup> post-fire flood: a particular situation.....	102
5.5.1	Particularly erosive rainfall.....	102
5.5.2	Particular geomorphological features.....	103

5.5.3	<i>Extended livestock activities</i>	106
5.5.4	<i>Successively burnt forest land</i>	106
CHAPTER 6: STUDY AREA		108
6.1	Geomorphological and hydrogeological properties	109
6.2	Hydrometeorological regime and monitoring	111
6.2.1	<i>Hydrometeorological characteristics</i>	111
6.2.2	<i>Hydrometeorological monitoring</i>	112
6.3	Land cover and land uses	113
6.3.1	<i>Forested land</i>	114
6.3.2	<i>Urban areas and demographic data</i>	115
		117
6.3.3	<i>Industrial units</i>	117
6.4	Vulnerability to floods and forest fires	118
6.5	First post-fire floods in the study area	122
CHAPTER 7: ADJUSTING THE METHODOLOGY TO THE STUDY AREA		125
7.1	Estimating fire impact	125
7.2	Estimating initial soil moisture conditions for selected rainfall events ...	128
7.3	Setting up the hydrological model for the study area	129
7.3.1	<i>Setting up HEC-GeoHMS</i>	129
7.3.2	<i>Setting up HEC-HMS</i>	131
7.4	Estimating parameter values for variable initial conditions	133
7.4.1	<i>Estimating CN for variable initial conditions</i>	134
7.4.2	<i>Estimating IA for variable initial conditions</i>	136
7.4.3	<i>Estimating TP for variable initial conditions</i>	137
7.4.4	<i>Estimating CP for variable initial conditions</i>	138
7.4.5	<i>Estimating K for variable initial conditions</i>	140
7.5	Running the hydrological model for the study area	143
CHAPTER 8: RESULTS AND DISCUSSION		145
8.1	Application of the methodology	145
8.2	Sensitivity analyses	150
8.2.1	<i>Quantification of the impact of each parameter on runoff volume</i> .....	151
8.2.2	<i>Efficiency testing of the proposed methodology</i>	152
8.3	Flood Mapping	157
8.3.1	<i>Hydraulic modelling</i>	157
8.3.2	<i>Flood hazard mapping</i>	158
8.3.3	<i>Flood risk mapping</i>	160
CHAPTER 9: CONCLUSIONS		164
9.1	Conclusions	164
9.2	Overview of main findings	166
9.1.1	<i>Main findings of the methodology</i>	166
9.1.2	<i>Main findings for the case study</i>	168
9.3	Further research	169
9.4	Epilogue	172
CHAPTER 10: REFERENCES		173

## TABLE OF FIGURES

<i>Figure 2.1. Statistics for the impact of natural disasters on humans (total killed top, total affected bottom) for the period 2002-2012 on a global scale (Source: PreventionWeb of the UNISDR).....</i>	<i>11</i>
<i>Figure 2.2. Statistics for the impact of natural disasters on the economy for the period 1980-2012 on a global scale (Source: PreventionWeb of the UNISDR). .....</i>	<i>12</i>
<i>Figure 2.3. Statistics for the frequency of occurrence of significant natural disasters for the period 2002-2012 on a global scale (Source: PreventionWeb of the UNISDR).....</i>	<i>14</i>
<i>Figure 2.4. Disaster Management Cycle (Source: Schoupe, 2008). .....</i>	<i>15</i>
<i>Figure 2.5. Clogging of sewer systems from tree leaves and litter (personal archive). .....</i>	<i>17</i>
<i>Figure 2.6. Flood events reported during the period 1980-2008 on a global scale (Source: PreventionWeb of the UNISDR). .....</i>	<i>21</i>
<i>Figure 2.7. Flood disasters by country reported during the period 1974-2003 on a global scale (Source: EM-DAT: The Emergency Events Database – Université catholique de Louvain (UCL) – CRED, D. Guha-Sapir – www.emdat.be, Brussels, Belgium). .....</i>	<i>22</i>
<i>Figure 2.8. Flood hazard distribution during the period 1985-2003 on a global scale (Dilley et al., 2005).....</i>	<i>22</i>
<i>Figure 2.9. The number of people affected by floods during the period 1980-2008 on a global scale (Source: PreventionWeb of the UNISDR). .....</i>	<i>23</i>
<i>Figure 2.10. The number of people killed by floods during the period 1980-2008 on a global scale (Source: PreventionWeb of the UNISDR). .....</i>	<i>23</i>
<i>Figure 2.11. The reported economic damages (in 10<sup>3</sup> Million US dollars) from floods that occurred during the period 1980-2008 on a global scale (Source: PreventionWeb of the UNISDR).....</i>	<i>24</i>
<i>Figure 2.12. The annual average cost of flood damages as a percentage of the Gross Domestic Product (GDP) during the period 1998-2002 for the most affected EU countries (Source: EM-DAT – The International Disaster Database). .....</i>	<i>24</i>
<i>Figure 2.13. Close up of tree ring with fire scars (Source: Laboratory of Tree-Ring Research, University of Arizona, Photo by Tom Swetnam, available at: <a href="http://www.ltrr.arizona.edu/~sheppard/swland/scartree.html">http://www.ltrr.arizona.edu/~sheppard/swland/scartree.html</a>). .....</i>	<i>26</i>
<i>Figure 2.14. Wildfires reported during the period 1980-2008 on a global scale (Source: PreventionWeb of the UNISDR). .....</i>	<i>31</i>
<i>Figure 2.15. The number of people killed by wildfires during the period 1980-2008 on a global scale (Source: PreventionWeb of the UNISDR). .....</i>	<i>32</i>
<i>Figure 2.16. The reported economic damages (in 10<sup>3</sup> Million US dollars) from wildfires that occurred during the period 1980-2008 on a global scale (Source: PreventionWeb of the UNISDR).....</i>	<i>32</i>
<i>Figure 2.17. The burnt area (in ha) and the number of fires in 1.000 during the period 1980-2002 in the five Southern EU Member States (Source: EEA, 2004). .....</i>	<i>33</i>
<i>Figure 2.18. The average fire size (in ha) during the period 1980-2012 in the five Southern EU Member States (Source: JRC, 2014).....</i>	<i>33</i>
<i>Figure 3.1. Modification in soil water repellency prior to (a), during (b) and after (c) a fire (adapted from DeBano (1981)). .....</i>	<i>36</i>

Figure 3.2. The four types of erosion that affect exposed slopes (Source: IUM, 2013).....	38
Figures 3.3a-c. Desertification due to successive fire events in different parts of the Torres del Paine National Park, Chile (personal archive). ....	42
Figure 3.4. Vegetation recovery of Tidbinbilla Nature Reserve (Australia), one month after extended fires in 2003 (Source: Technical Report 17, Wildfires in the ACT 2003, by Carey et al., 2003).....	47
Figure 3.5. Vegetation recovery of Ginini Wetlands (Australia), two months after extended fires in 2003 (Source: Technical Report 17, Wildfires in the ACT 2003, by Carey et al., 2003).....	48
Figure 3.6. Resprouting of a Coast Live Oak seven months after the Grand Prix Fire, in Claremont Hills, California, 2003 (Photo by Cliff McLean, available at: <a href="http://www.natureathand.com/Main/NAHEssays_StationFireRecovery.htm">http://www.natureathand.com/Main/NAHEssays_StationFireRecovery.htm</a> , originally published in Southern Sierran, Vol. 65 No. 12, December, 2009, Angeles Chapter of the Sierra Club). ....	48
Figure 5.1. The impact of K and X on routed hydrographs. ....	98
Figure 5.2 Debris flow generated from a catchment near Glenwood Springs, Colorado burnt in 2002 (Source: Cannon et al., 2003).....	104
Figure 5.3 European Landslide Susceptibility Map (Source: Günther et al., 2014).....	105
Figure 5.4. Actual soil erosion risk map for Europe, based on the USLE approach (Source: Grimm et al., 2002).....	105
Figure 6.1. Zooming in the study area: in the red square in Figures 6.1a (upper left) and 6.1b (upper right) and highlighted in blue font in Figure 6.1c (lower middle).....	108
Figure 6.2. The geological structures of the south eastern part of the study area: (1) Holocene deposits, (2) Neogene formations, carbonates, marls, conglomerates, sands, etc., (3) schists and phyllites, (4) carbonates of Upper Cretaceous, (5) Rafina marbles, Mesozoic; A–A0, hydrogeological section (Source: Stamatis et al., 2006). ....	109
Figure 6.3. Hydrogeological section between Spata and Vravrona (see cross section A-A' in Figure 6.2) (1: Neogene deposits, 2: Carbonates, 3: Schists and phyllites, 4: Level of ground water) (Source: Stamatis et al., 2006). ....	110
Figure 6.4. The 5m X 5m DSM of the study area.....	111
Figure 6.5. The locations of meteorological and flow measurement stations used in this research.....	113
Figure 6.6. A hybrid land use-land cover map of the study area. ....	114
Figure 6.7. Fuel mapping for the study area (Source: Eftychidis and Varela, 2013).....	115
Figure 6.8. The Municipalities included in the study area. ....	116
Figure 6.9. The three large-scale public works in the study area: The AIA (Source: <a href="http://www.ana-mpa.gr">www.ana-mpa.gr</a> ) in Figure 6.9a, at the upper left, Rafina port (Source: <a href="http://www.irafina.gr">www.irafina.gr</a> ) in Figure 6.9b, at the upper right and the airport junction of Attiki Odos motorway (Source: <a href="http://en.aodos.gr/">http://en.aodos.gr/</a> ) in Figure 6.9c, at the lower middle. ....	117
Figure 6.10. Locations of industrial units in the study area. ....	118
Figure 6.11. Pictures depicting the floodplain and the damages caused in private properties in the area of Rafina during the flood event of 22/02/2013 (personal archive). ....	119



Figure 6.12. Forest fires in the greater area of Rafina catchment for the period 2000-2012 (Source: Eftychidis and Varela, 2013).....	121
Figure 6.13. Rainfall erosivity map of Europe (adapted from: Panagos et al., 2015).....	123
Figure 6.14. The event cloud of HOA, where the size of the font is proportional to the magnitude of the event (Source: www.hoa.ntua.gr).....	124
Figure 7.1. The procedure to estimate fire impact according to the suggested methodology. ....	125
Figure 7.2. Landsat TM images of $NBR_{PRE-FIRE}$ (Figure 7.2a on the left) and $NBR_{POST-FIRE}$ (Figure 7.2b on the left) (Source: Mitsopoulos, 2013).....	126
Figure 7.3. The DNBR map and the fire severity classes of the greater area affected by the fire event of August 2009.....	126
Figure 7.4. The different fire severity classes from the fire event of 2009 at the total affected area (Figure 7.4a on the left) and in the study area (Figure 7.4b on the right).....	127
Figure 7.5. The subbasins of the study area and its hydrographic network, as drawn on its DSM.....	130
Figure 7.6. The HEC-HMS simplified schematic of the study area. ....	132
Figure 7.7. The procedure to estimate the values of the examined parameters for variable conditions. ....	134
Figure 7.8. The proposed post-fire changes in the values of the five examined parameters for normal SM conditions. ....	142
Figure 8.1. Simulated flows when applying and when ignoring the methodology and estimated peak flow for the flood event of 10-11/12/2009 ( <b>Rafina station</b> ). .....	145
Figure 8.2. Observed and simulated flows when applying and when ignoring the methodology for the flood event of 03/02/2011 ( <b>Drafi station</b> ).....	146
Figure 8.3. Observed and simulated flows when applying and when ignoring the methodology for the flood event of 22/02/2013 for <b>Drafi</b> (top left), <b>Rafina</b> (top right) and <b>Rafina2</b> (bottom) stations. ....	146
Figure 8.4. The relative change [%] in all parameter values after a fire event, when applying the proposed methodology.....	152
Figure 8.5. A Google Earth map with the flood hazard maps for T=5 years (blue line), T=200 years (green line) and T=1000 years (purple line) for normal SM, recently burnt conditions. ....	159
Figure 8.6. A Google Earth map with the flood hazard maps for T=5 years (blue line), T=200 years (green line) and T=1000 years (purple line) for wet SM, unburnt conditions.....	160
Figure 8.7. The static flood vulnerability map of Rafina catchment.....	161
Figure 8.8. The different layers used in the production of the flood risk maps. ....	162
Figure 8.9. Flood risk maps for T=5, 200 and 1000 years for wet and no longer affected by recent fire conditions (upper row) and for normal and recently burnt conditions (lower row). ....	162

## TABLE OF TABLES

Table 2.1 Statistics for the geographical extent of natural disasters in 2012 (Source: PreventionWeb of the UNISDR).....	13
Table 4.1. Evaluation of the identified hydrological models. ....	74
Table 4.2. Evaluation of the identified hydraulic models. ....	82
Table 5.1. Different classes of Antecedent Moisture Conditions.....	92
Table 6.1. PROMETHEUS fuel categories in the study area.....	115
Table 6.2. Water stress of vegetation species dominant in the forested areas of Rafina catchment (Source: Xanthopoulos and Caballero, 2007). ....	122
Table 7.1 The total area [km <sup>2</sup> ], total burnt area [km <sup>2</sup> ] and % of burnt area of each subbasin of the study area.....	128
Table 7.2 The area [km <sup>2</sup> ] of each subbasin of the study area affected by different severity. ....	128
Table 7.3 The area [%] of each subbasin of the study area affected by different severity. ....	128
Table 7.4. AMC for each one of the examined flood events. ....	129
Table 7.5. Name, ID and area covered by each subbasin of the catchment ..	131
Table 7.6. The Thiessen weights for every raingauge and each subbasin. ....	132
Table 7.7. The values of c and d for different SM conditions for CN, IA, TP, CP and K. ....	141
Table 7.8. The values of $h_{CN,FS,t_{upper}}$ and $h_{CN,FS,t_{lower}}$ , $h_{IA,FS,t_{upper}}$ and $h_{IA,FS,t_{lower}}$ , $h_{TP,FS,t_{upper}}$ and $h_{TP,FS,t_{lower}}$ , $h_{CP,FS,t_{upper}}$ and $h_{CP,FS,t_{lower}}$ and $h_{K,FS,t_{upper}}$ and $h_{K,FS,t_{lower}}$ for different FS classes.....	141
Table 7.9 The values of $a_{CN,FS}$ and $b_{CN,FS}$ , $a_{IA,FS}$ and $b_{IA,FS}$ , $a_{TP,FS}$ and $b_{TP,FS}$ , $a_{CP,FS}$ and $b_{CP,FS}$ and $a_{K,FS}$ and $b_{K,FS}$ for different FS classes.....	142
Table 7.10. The final values of CN, IA, TP, CP and K for each event and each subbasin and reach of Rafina catchment.....	144
Table 8.1. Comparative analysis of simulated and observed runoff volumes and peak and other discharges for three flood events. ....	149
Table 8.2. The quantification of the impact of each parameter on runoff volume. ....	151
Table 8.3. Suggested parameter values from the methodology and average parameter values of the best 100 runs of HEC-HMS, for dry SM conditions in Drafi and Rafina-big subbasins.....	154
Table 8.4. Suggested parameter values from the methodology and average parameter values of the best 100 runs of HEC-HMS, for wet SM conditions in Drafi, Rafina big and Rafina small subbasins. ....	154
Table 8.5. Suggested parameter values from the methodology and average parameter values of the best 100 runs of HEC-HMS, for dry SM conditions in Rafina-big subbasins, for moderate limits.....	155
Table 8.6. Suggested parameter values from the methodology and average parameter values of the best 100 runs of HEC-HMS, for wet SM conditions in Rafina big and Rafina small subbasins, for moderate limits.....	155
Table 8.7. Suggested parameter values from the methodology and average parameter values of the best 100 runs of HEC-HMS, for dry SM conditions in Drafi and Rafina-big subbasins, for wide limits. ....	156
Table 8.8. Suggested parameter values from the methodology and average parameter values of the best 100 runs of HEC-HMS, for wet SM conditions in Rafina big subbasin, for wide limits.....	156

*Table 8.9 Manning’s roughness coefficients for the riverbed and the river banks of all subbasins of Rafina catchment. .... 158*

*Table 8.10 The weights attributed to each layer of the static flood vulnerability map..... 161*

## A C K N O W L E D G E M E N T S

Usually (hopefully not always) in this part of a Doctoral thesis, one sees a couple of pages in mushy and overly sentimental wording, written by a thrilled author, who, due to the excitement originating from the completion of his work, tends to acknowledge every single mate in academic, professional and personal life. In an attempt to abstain from this and since I believe that acknowledgments in a Doctoral thesis should have nothing in common with ordinary thank you speeches in Oscar awards, I am writing the following brief, yet honest acknowledgments.

First of all, I owe special and truly cordial thanks to Associate Professor Nikos Mamassis. Besides offering me his valuable scientific advice, always to the point, whenever asked and always customized to my needs, he also served another irreplaceable role in my committee: he believed in me, he kept encouraging me to keep trying to complete this research, even during periods when disappointment prevailed and he inspired me to move forward. He would systematically assign a philosophical perspective in all our discussions for my thesis, leaving a permanent and distinct touch on my way of thinking. Had it not been for him, I would have certainly given up my efforts long ago.

I would also like to thank Associate Professor Christos Makropoulos for his contribution to the implementation of this dissertation. He co-supervised my thesis since its very early stages, he would discuss my scientific concerns several times during its implementation and enlighten me at critical stages on how to proceed. His guidance to identify and exploit appropriate state-of-the-art tools and techniques to reinforce the efficiency of my research has been decisive for its completion.

I would also like to thank my supervisor, Professor Maria Mimikou for offering me the opportunity to work for the Laboratory of Hydrology and Water Resources Management of NTUA, participate in several EU research projects and have a key role in the FLIRE Project (LIFE11 ENV GR 975) while being a Doctoral candidate and have a close-up collaboration with the other two members of my Committee, Prof. Nikos Mamassis and Prof. Christos Makropoulos.

Finally, besides my advisory committee, I would like to thank the other four members of my examination committee, *i.e.* Professor Demetris Koutsoyiannis, Professor Evangelos Baltas, Professor Vassilios Tsihrintzis and Professor George Karatzas for their valuable comments on my thesis. Their comments offered me the opportunity to examine my Doctoral thesis through different, interdisciplinary perspectives before finalizing it.

## EXECUTIVE SUMMARY

Floods are a natural hazard directly associated with loss of life and severe socioeconomic and environmental impacts. At the same time, they constitute one of the most frequently occurring hazards that affect both urban and rural areas with similar severity, yet with variable consequences, depending on the human activities undertaken and the ecosystem services provided in the affected areas. Due to the inestimable damages which are frequently caused by floods, reliable flood risk assessment and efficient flood risk management emerge as issues of priority not only on a local but also on a national scale. To this end numerous methodologies and practices have been developed in order to deal with this hazard. Yet, the extent of flood impacts and the continuous threats posed on human lives and properties reveal the inadequacy of applied concepts and practices for effective flood risk assessment and management.

Forest fires are another devastating natural hazard that is also especially high in national priority agendas due to their tremendous socioeconomic and environmental impacts. Besides posing a direct threat on human lives and being related with damage on public and private properties, forest fires also affect, sometimes irrevocably, ecosystem services. In the last decades forest fire activity has been particularly increased, especially in the Mediterranean areas (Esteves *et al.*, 2012; Pausas *et al.*, 2008).

Periurban areas are particularly prone to both floods and forest fires. These areas are hybrid landscapes characterized by a mosaic of different and, to a certain extent, conflicting land uses. In these areas, forested land is often succeeded by cultivated regions and pasture land, with industrial and urban zones prevailing usually at the downstream regions. In the complex environment formed by this interface between different land uses, complicated problems may arise in case of occurrence of a flood event. In addition, zones close to the Wildland-Urban Interface (WUI), *i.e.* the transition zones between areas with intense urban development and unoccupied land, are exposed to greater risks from forest fires, and consequently impacts on humans, society, the economy and the environment are magnified due to nearby human activity.

The threats of floods and forest fires on humans and the environment have long been identified in the European Union, and several environmental policies and legislative measures had been proposed. However, an integrated approach to manage the combined effects of these hazards is still missing. Further to the dire consequences of floods and forest fires, when examined as individual natural hazards, particular attention needs to be paid on the combined impact of these hazards as a result of their interaction, which is usually intensified.

The impact of floods on forest fires is ambiguous and often underestimated; yet it is not negligible. In general, the occurrence of flood events during the wet periods is associated with reduced fire activity during the dry seasons, since the soil is saturated, the vegetation has absorbed significant amounts of water and thus forest fuels are less flammable. In apparent self-contradiction, severe floods can be followed by fires either on a short-term basis (due to increased lightning activity preceding a flood event or damages in the electric installations or even in gas

pipes during floods) or in the long run (due to increased production of biomass fuel in forests).

This research focuses on the inverse way of the floods-fires interaction, *i.e.* the impact of forest fires on the hydrological behaviour of a river basin and thus on upcoming floods, and verifies that efficient flood risk assessment and management necessitate the consideration of this impact. More specifically, fires provoke both direct and indirect impacts on the hydrological response of affected catchments. In general, the alteration, and in many cases destruction, of forested land due to a forest fire is associated strongly with decreased infiltration, increased discharges and peak flows and decreased time to peak flows, rendering the downstream parts of the affected area particularly prone to flooding.

The combined impact of floods and forest fires is magnified in the complex environment of periurban areas, thus rendering flood modelling in these areas even more challenging. In addition, the periurban environment is a “dynamic”, constantly changing environment, the hydrological behaviour of which reflects the constant impacts of man-made interventions and natural changes. Aiming to interpret the behaviour of this complicated environment, decipher its underlying mechanisms and eventually realistically simulate its response, a holistic and flexible approach to flood risk assessment needs to be adopted.

The primary aim of this dissertation is the development of a methodological framework to theoretically estimate the dynamic evolution of hydrological parameters that affect flood risk as a function of time, following the occurrence of forest fires. The research focuses on flood risk assessment under post-fire conditions for Mediterranean periurban catchments. To this end, a methodological framework to theoretically estimate the dynamic evolution of hydrological parameters that affect flood risk as a function of time, following the occurrence of forest fires has been developed.

Following a detailed literature review on natural hazards and disaster management, the research focuses on floods and forest fires in periurban environments. Initially, their generation mechanisms, particular characteristics, impacts and risk management issues are analyzed. Then, research goes beyond the significance of floods and forest fires as natural hazards that act independently and examines their interaction and its importance in representative flood analyses. In particular, the impact of forest fires on the hydrological behavior of a catchment and its assessment has been analyzed in detail.

At this stage of the research the term “*hydrological recovery*” (Papathanasiou *et al.*, 2015a) was introduced to describe the (post-fire) stage when the hydrological response of a burnt catchment has recovered, for all practical (hydrological response) purposes, to its pre-fire state. It is suggested that hydrological recovery may occur earlier than (a more complete) “*environmental recovery*”, which is achieved when the catchment’s natural reforestation and ecosystem rebalance occur – a process that often takes several years (if at all) after a major fire event.

An innovative, coherent and robust methodology has been developed for the quantification of the impact of forest fires under variable initial soil moisture

conditions on the hydrological response of a typical Mediterranean periurban catchment and its incorporation in hydrological modelling. The methodology has been developed for deterministic, physically-based, lumped or (semi-) distributed, event-based or continuous hydrological models.

First, the impact of forest fires on a catchment has been examined from a spatiotemporal perspective. This impact depends strongly on fire extent and Fire Severity (FS), which serve as measures to quantify the effects of fire on soil and overstory (Keeley, 2009; De Santis and Chuvieco, 2007).

Regarding the spatial impact of fires, FS mapping techniques which make use of satellite remote sensing supported by *in-situ* fieldwork and complemented with statistical and simulation modelling are considered as the most popular and effective (Gitas *et al.*, 2012; Lhermitte *et al.*, 2011; Veraverbeke *et al.*, 2010; Viedma *et al.*, 1997). A technique for FS mapping, which involves properly processed satellite images and an analysis in GIS, was standardized and applied in this research. As such, a burnt area can be discretized into patches of land affected by different FS. Five FS classes were used, namely very high FS (i), high FS (ii), moderate FS (iii), low FS (iv) and no severity (referring to unburnt land).

Regarding the impact of fires on a catchment from a temporal perspective, time periods of variable duration and different hydrological impact, directly associated with the status of vegetation regrowth, were identified within each severity class. Following an extended literature review on the conditions of typical Mediterranean vegetation, in terms of annual changes in foliage, post-fire regrowth *etc.*, the duration of each time period has been defined, while the characteristic, transitional periods that can be identified in post-fire vegetation regrowth and are related with hydrological recovery were also taken into consideration.

Regarding the post-fire recovery rate of a typical Mediterranean catchment, increased recovery is often observed during the first post-fire years, and is usually followed by a decreased recovery rate (*e.g.* Thanos and Marcou, 1991; Trabaud *et al.*, 1985; Eccher *et al.*, 1987; Marzano *et al.*, 2012). The first post-fire spring is also critical when examining vegetation recovery (Keeley, 2009). Hence, a sharply descending hydrological impact with time was assumed for each FS class. In the proposed methodology, which is developed for areas covered by successively burnt Mediterranean forests, it is considered that hydrological recovery takes place 4 years after the fire, with the first 2 years being more critical (Brown, 1972; Moody and Martin, 2001a; Springer and Hawkins, 2005; Inbar *et al.*, 1998; Rulli and Rosso, 2007; Robichaud, 2000).

In an attempt to associate FS with the temporal evolution of hydrological recovery, it is assumed that in order to reach hydrological recovery, areas affected by low or moderate severity need approx. 2 years, areas affected by high FS need approx. 3 years and areas affected by very high FS need approx. 4 years. Thus, the time windows of 7 months (1<sup>st</sup> post-fire spring), 12 months (1<sup>st</sup> year), 19 months (2<sup>nd</sup> post-fire spring), 24 months (2<sup>nd</sup> year), 36 months (3<sup>rd</sup> year) and 48 months (4<sup>th</sup> year) after a fire event have been used in this research, as transitional periods in hydrological recovery. These considerations are often case-specific and may need to be readjusted for different areas.

Then, initial conditions are examined in terms of soil moisture (SM). In this research, initial SM conditions depend on the total rainfall depth of the five (5) days preceding a flood event and are estimated according to the SCS Curve Number method (USDA-SCS, 1985; USDA-NRCS, 2004b).

In order to quantify the impact of initial conditions, in terms of forest fire and SM, on the hydrological response of a catchment and examine its evolution in time, appropriate simulation methods need to be applied and representative hydrological parameters need to be examined. Five typical hydrological parameters that depend strongly on catchment characteristics, *i.e.* Curve Number (CN), Initial Abstraction (IA), Standard Lag (TP), Peaking Coefficient (CP) and Muskingum K coefficient, were selected in this research and the change in their values for different initial conditions has been quantified. The time interval between the occurrence of a fire event and the analyzed flood events was also taken into consideration.

Initially, the values of each one of these parameters for pre-fire and normal conditions are estimated. Based on these values, the corresponding values for pre-fire and variable SM conditions (either wet or dry) are estimated through a pre-fire calibration process. This procedure results in the extraction of a set of rules that directly associate pre-fire values for normal conditions with pre-fire values for wet and dry conditions.

The values of the examined hydrological parameters are expected to be significantly affected for post-fire conditions, especially for areas that have been affected severely by fire. A sharply descending impact of fire with time has been considered in the suggested changes in the values of the examined hydrological parameters. Given that post-fire vegetation regrowth determines the post-fire values of the examined hydrological parameters, this logical assumption is verified. Therefore, the logarithmic profile of the characteristic time-windows in post-fire vegetation development can be directly associated with a dynamic post-fire evolution of hydrological parameters in time with regards to their pre-fire values, with changes following a logarithmic profile (Papathanasiou *et al.*, 2015a).

A set of equations was developed to express the post-fire evolution in time of each examined hydrological parameter for normal SM conditions. In these equations post-fire values depend on the corresponding pre-fire values, the time (in months) after the fire event and the parameters  $a$  and  $b$ , which in turn depend on FS and boundary conditions for the post-fire values of each parameter for each FS class. These boundary conditions are classified into upper boundary conditions, which refer to the first post-fire period and lower boundary conditions, which refer to the period just prior to hydrological recovery. Given that the research performed so far on the estimation of the post-fire change of hydrological parameters for different FS is limited, a co-evaluation of threshold values identified in literature, calibration results and, when relevant, particular conditions and restrictions, needs to take place for each case study.

After the estimation of the post-fire values of the examined parameters for normal SM conditions, the corresponding values for wet and dry SM conditions can be



estimated applying the rules mentioned above, which associate normal pre-fire SM conditions with wet and dry pre-fire SM conditions.

Based on the percentage of the affected area within each FS class (as estimated from the GIS analysis performed for FS mapping) and the suggested parameter values for each severity class (as estimated from the developed equations), a composite, weighted parameter value for each subbasin of the examined catchment is estimated and this value is imported in the hydrological model for the necessary simulations.

In this research, the particularities of typical Mediterranean periurban areas were considered, while particular attention was paid on the transferability of the methodology to other areas with similar, yet not identical, hydrometeorological and geomorphological characteristics. Special conditions under which deviations from the proposed methodology can be observed, such as the first post-fire floods, were also thoroughly investigated.

The methodology was incorporated in a semi-automated way in a properly selected deterministic, physically-based, semi-distributed, event-based hydrological model. Following extended literature review and testing of different models, the incorporation of the methodology in the HEC-HMS (Hydrologic Engineering Center – Hydrologic Modeling System) hydrological model of USACE has been concluded. HEC-HMS was effectively calibrated and run for historic flood events recorded at a selected study area.

A typical Mediterranean periurban area in Greece, Rafina catchment, has been used as a study area for the testing of the methodology. This area extends over approx. 123 km<sup>2</sup> and is located in Eastern Attica region. Due to its particular geomorphological and hydrogeological properties, as well as its increased urbanization rate, especially during the last 30 years, Rafina catchment is particularly prone to flooding. At the same time, its flammable vegetation renders the area also vulnerable to forest fires. For all these factors, post-fire hydrological modelling becomes an issue of high priority for the selected study area.

Regarding the results retrieved from the application of the methodology, for all examined flood events the simulated peak flows, runoff volumes and times to peak match well to the corresponding values derived from observed datasets, when available. As expected, simulation results when the methodology is not applied and especially for adverse conditions (wet SM conditions and flood events after a recent forest fire) are poor when compared against the corresponding results when the methodology is applied.

A detailed sensitivity analysis which involved two independent analyses was performed. Initially, a sensitivity analysis was performed in order to quantify the impact of each one of the five examined hydrological parameters on simulated runoff volumes. Then, the efficiency of the proposed methodology was tested through an innovative sensitivity analysis.

More specifically, the model ran for three sets of 1.000 random values for the five examined hydrological parameter and all six subbasins of the study area and its

performance was assessed using the Nash-Sutcliffe indicator. The sampling approach selected, which ensures the representativeness of the ensemble of random values in terms of real variability is Latin Hypercube Sampling (LHS) (McKay *et al.*, 1979; Iman and Conover, 1980; McKay M.D., 1992; van Griensven *et al.*, 2006). For this purpose an original programming code was developed in Matlab7.11.0 (version R2010b) and an additional analysis of the produced matrixes with sampling values was performed. The set with the random values that yielded the best results was compared against the exact values suggested by the methodology and the proximity of the optimum values with the suggested ones was checked.

The hydrological model was also set up and run for floods with return periods that correspond to high, medium and low probability of occurrence and more specifically for T=5, 200 and 1000 years, respectively. The outputs of this hydrological analysis were imported in the HEC-RAS (Hydrologic Engineering Center – River Analysis System) hydraulic model of USACE and eventually representative flood hazard and flood risk maps were produced for the examined return periods for the study area.

Given that the incorporation of the proposed methodology in a hydrological model yields accurate and representative simulations, its incorporation in a flood model chain results in the production of accurate flood hazard and flood risk maps. Hence, it can be safely concluded that the developed methodology can be used effectively in flood risk assessment and support near-real time flood forecasting platforms and operational civil protection systems, as well as flood risk management on a planning basis at a later stage.

The analysis highlights the importance of considering initial SM conditions, even in the application of an event-based hydrological model and verifies that the consideration of constantly normal SM conditions for reasons of simplification or constantly wet SM conditions during the rainy season for adverse conditions undermines the robustness and the accuracy of hydrological simulations.

This research concludes that the calibration of CN, IA, TP, CP and K, which are typical parameters, included in the vast majority of modelling structures, yields optimum simulation results, contrary to current calibration practice which usually involves the calibration of only CN and IA. TP, CP and K are definitely less sensitive calibration parameters than CN and IA since they have a less intense impact on runoff volume; however, they still need to be properly calibrated for more representative hydrological simulations (Papathanasiou *et al.*, 2015a).

The comprehensive methodology developed for this dissertation, allows for the dynamic estimation of this footprint in time, without restricting its application to particular case studies and considering also the fact that some time after fire occurrence, hydrological recovery occurs. It is concluded that the post-fire impact is very intense during the first post-fire period, while it is sharply decreasing with time, until hydrological recovery occurs and the post-fire hydrological footprint vanishes (Papathanasiou *et al.*, 2015a). This impact is not the same on all examined hydrological parameters. CN and IA are more sensitive parameters to fire impact than TP and CP and to a lesser extent K and are thus associated with

more severe post-fire changes and longer lasting post-fire impact. Also, during the first post-fire years the post-fire impact is more intense on the examined parameters than the impact of initial SM.

The generalized methodological framework developed for this research for the estimation of the dynamical changes in time of five representative hydrological parameters under variable initial conditions, in terms of forest fire occurrence and SM conditions, serves the overall purpose of this research, *i.e.* the accurate flood risk assessment in typical Mediterranean periurban areas under post-fire conditions. The robustness of the developed methodology and its suitability for further applications is enhanced by the use of state-of-art tools, modern technologies and comprehensive analyses, the exploitation of well documented relevant knowledge and experience, as well as its easy adjustability and thus applicability to other areas (Papathanasiou *et al.*, 2015a).

The innovative aspects of the methodology are as follows:

First, as mentioned above, a clear distinction has been made between environmental and hydrological recovery. The term “*post-fire forest recovery*”, or else called “*relaxation time*” (Moody and Martin, 2001) is frequent in literature. Both terms refer to the so-called in this research “*environmental recovery*”, which concerns the canopy cover replacement and the recovery of the ecosystem services and may take a lot of years to occur, if at all. Nevertheless, a key factor in hydrological studies, which is of particular interest and needs to be considered, on the contrary to the current practice, is the recovery of the hydrological behaviour of a burnt catchment to its pre-fire status. This is the so-called in this research “*hydrological recovery*”, which is other than full vegetation recovery and may occur several years after a forest fire. This distinction is necessary for research on the post-fire hydrological response of a catchment, in order to avoid misinterpretations and misunderstandings.

In addition, this research quantifies the impact of forest fires on the hydrological behavior of typical periurban catchments and eventually supports the incorporation of fire severity in hydrological modelling. Despite relevant, individual attempts to estimate the impact of forest fires on the values of some of the examined in this research parameters made in the past (Higginson and Jarnecke, 2007; Foltz *et al.*, 2009), no other integrated and widely accepted approach was identified in literature.

The temporal evolution of fire impact in typical Mediterranean areas is also examined and quantified. The common practice is the examination of the fire impact only for recently burnt areas, focusing on the limited period between fire occurrence and the next growing season (*e.g.* Cerrelli, 2005; Higginson and Jarnecke, 2007) or the first couple of post-fire years (Cannon *et al.*, 2008; Rulli and Rosso, 2007; Inbar *et al.*, 1998; Scott and Van Wyk, 1990). The proposed approach is innovative since it considers in an original way the fact that fire impact changes dynamically in time and estimates not only an initial fire impact on hydrology, but also its temporal evolution and of course the period when this impact can safely be considered negligible, *i.e.* the time when hydrological recovery occurs.

Further to that, another scientific gap identified in literature and effectively addressed with this research is the consideration of SM conditions in fire impact studies. Usually, the impacts of SM and a forest fire are examined individually. However, the concurrent conditions of a recent forest fire and wet SM conditions have an adverse impact on a catchment's response, as they are associated with increased runoff volumes and peak flows and decreased times to peak. To this end, both initial conditions and their interaction need to be co-evaluated in order to avoid underestimated catchment's responses and achieve more accurate results in flood simulations.

Besides, the methodology has been developed for typical Mediterranean periurban areas and is expressed in a generic way, so as to be easily adapted to areas with similar hydrometeorological and geomorphological characteristics. The particular characteristics of those areas were examined in detail and the developed methodology is expressed via generalized equations adjusted to different case studies following specific guidelines. For applications to areas other than the study area, the temporal dimension of fire impact needs to be reexamined, taking into consideration local features such as indigenous vegetation, canopy and local climatic characteristics, vegetation development, fire-tolerance, regrowth *etc.* Particular cases when deviations from the proposed methodology may be observed and readjustment of the generic approach would be necessary are also discussed.

Additionally, state-of-the-art tools and methods were applied for the testing of the efficiency of the methodology. Innovative aspects include an original code written in Matlab programming language for the generation of matrixes with random values for the selected hydrological parameters, the consideration in this code of Latin Hypercube Sampling (LHS), an efficient sampling method appropriate for this research, as well as an original procedure typified for the statistical analysis of the results of this research.

The proposed methodology can also be easily automated and integrated in Early Warning Systems for floods and other operational systems for civil protection. Besides the fact that such systems are very sensitive in the accuracy of their inputs, no integrated approach for the incorporation of the combined fire and SM impact on the hydrological response of a catchment supported by a Flood Early Warning System is identified in literature. The import of more accurate information, in terms of the examined initial conditions, in these systems is another innovation that can be supported by this research.

For further research, the methodology could be tested to other case studies, with similar characteristics, in terms of land use/land cover properties, urbanization rate, hydrometeorological, geomorphological features *etc.* Further research could also focus on the expansion of the applicability of this methodology to other Mediterranean areas, which are of course typical periurban ones, yet they do not share the specific particularities during the first post-fire period. In either case different parts of the proposed methodology may need major readjustment, as suggested in Chapter 5.

The incorporation of the proposed methodology in deterministic, physically-based models, set up in lumped and event-based or continuous mode or semi-distributed and continuous mode, *i.e.* in hydrological models other than HEC-HMS or even in HEC-HMS set up in a mode other than semi-distributed and event-based, would also be interesting.

Another recommendation for further research concerns the use of remotely sensed SM datasets instead of estimated SM using the total rainfall during the 5 previous days, which is used in this research. Research could also be made on the examination of different inter-event time periods and the estimation of the impact of those periods on SM for the period preceding a flood event and more specifically the 5 days preceding a flood event, as specified in Chapter 9.

Further research could also be made on the standardization of the rules for the implementation of the procedure for the estimation of fire impact in terms of its spatial extend and severity, as applied in this research, so as to be easily automated and potentially constitute a stand-alone software.

In the absence of detailed information for certain pre- and/or post-fire forest conditions, further research could focus on safe assumptions that could be made, as well as combined use of different sources of this information (*in-situ* estimations, satellite imagery, existing studies *etc.*), so as to extract as accurate as possible conclusions on fire effect and proceed to the application of the methodology avoiding significant errors.

The recognition of post-fire vegetation, so as to estimate as accurately as possible the potential of the affected vegetation for hydrological recovery and of course environmental recovery, constitutes another field for further research. The accurate estimation of post-fire vegetation and potential adaptation mechanisms of affected species can also support more accurate estimation of the period when hydrological recovery is expected.

Finally, a recommendation for further research concerns the automation of the incorporation of the proposed methodology in a rainfall-runoff model for hydrological simulations or even in a hydrological – hydraulic model chain for the production of flood hazard maps, as is for example the FLIRE platform (Kochilakis *et al.*, 2016a; Kochilakis *et al.*, 2016b; Kotroni *et al.*, 2015; Papathanasiou *et al.*, 2015b; Poursanidis *et al.*, 2015a).

## ΕΚΤΕΝΗΣ ΠΕΡΙΛΗΨΗ

Οι πλημμύρες προκαλούν φυσικές καταστροφές που ενδέχεται να οδηγήσουν σε απώλειες ανθρώπινων ζωών, ενώ έχουν και σημαντικές κοινωνικοοικονομικές και περιβαλλοντικές επιπτώσεις. Ταυτόχρονα, επηρεάζουν τόσο τις αστικές όσο και τις αγροτικές περιοχές με παρόμοια σφοδρότητα, αλλά με διαφορετικές συνέπειες, που εξαρτώνται από τις ανθρωπογενείς δραστηριότητες και τις λειτουργίες των οικοσυστημάτων στις πληγείσες περιοχές. Εξαιτίας των ανυπολόγιστων ζημιών που προκαλούνται συχνά από τις πλημμύρες, η αξιόπιστη εκτίμηση και η αποτελεσματική διαχείριση του πλημμυρικού κινδύνου αποτελούν θέματα προτεραιότητας όχι μόνο σε τοπική, αλλά και σε εθνική κλίμακα. Για το λόγο αυτό, έχουν αναπτυχθεί πολυάριθμες μεθοδολογίες και πρακτικές προκειμένου να αντιμετωπιστούν οι κίνδυνοι. Παρόλα αυτά, η έκταση των πλημμυρικών επιπτώσεων και οι συνεχείς απειλές στις ανθρώπινες ζωές και περιουσίες αποκαλύπτουν την ανεπάρκεια των εφαρμοζόμενων πρακτικών για αποτελεσματική εκτίμηση και διαχείριση του πλημμυρικού κινδύνου.

Μία ακόμα ολέθρια φυσική καταστροφή που βρίσκεται ψηλά στην ατζέντα των εθνικών προτεραιοτήτων εξαιτίας των ιδιαίτερα δυσμενών κοινωνικοοικονομικών και περιβαλλοντικών επιπτώσεων με τις οποίες συνδέεται, είναι οι δασικές πυρκαγιές. Πέραν του ότι αποτελούν άμεση απειλή για ανθρώπινες ζωές και σχετίζονται με ζημιές σε δημόσιες εκτάσεις και ιδιωτικές περιουσίες, οι δασικές πυρκαγιές επηρεάζουν επιπλέον, ενίοτε μη αναστρέψιμα, τις λειτουργίες των οικοσυστημάτων στις περιοχές που εκδηλώνονται. Τις τελευταίες δεκαετίες η δραστηριότητα των δασικών πυρκαγιών είναι ιδιαίτερα αυξημένη, κυρίως στις Μεσογειακές περιοχές (Esteves *et al.*, 2012; Pausas *et al.*, 2008).

Οι περιαστικές περιοχές είναι ιδιαίτερα επιρρεπείς τόσο στις πλημμύρες όσο και στις δασικές πυρκαγιές. Οι περιοχές αυτές αποτελούν υβριδικά τοπία που χαρακτηρίζονται από ένα μωσαϊκό διαφορετικών και, σε κάποιο βαθμό, αντικρουόμενων χρήσεων γης. Στις περιοχές αυτές, τις δασικές εκτάσεις συχνά διαδέχονται καλλιεργήσιμες και αγροτικές εκτάσεις, με βιομηχανικές και αστικές ζώνες να επικρατούν συνήθως στις κατάντη περιοχές. Στο πολύπλοκο περιβάλλον που διαμορφώνεται στη διεπιφάνεια μεταξύ διαφορετικών χρήσεων γης, μπορεί να προκύψουν σύνθετα προβλήματα σε περίπτωση εκδήλωσης ενός πλημμυρικού γεγονότος. Επιπλέον, οι περιοχές που βρίσκονται κοντά στις μεταβατικές ζώνες μεταξύ ακατοίκητων και έντονα ανεπτυγμένων αστικών εκτάσεων εκτίθενται σε μεγαλύτερους κινδύνους από δασικές πυρκαγιές και κατά συνέπεια οι επιπτώσεις στους ανθρώπους, την κοινωνία, την οικονομία και το περιβάλλον μεγεθύνονται εξαιτίας της ανθρώπινης δραστηριότητας σε κοντινή απόσταση.

Οι απειλές των πλημμυρών και των δασικών πυρκαγιών στους ανθρώπους και το περιβάλλον έχουν αναγνωριστεί εκτός από εθνικό και σε ευρωπαϊκό επίπεδο και έχουν προταθεί διάφορες περιβαλλοντικές πολιτικές και νομοθετικά μέτρα. Ωστόσο, ακόμα δεν έχει υιοθετηθεί μία ολοκληρωμένη προσέγγιση για τη διαχείριση των συνδυασμένων επιπτώσεων αυτών των καταστροφών. Πέραν των δεινών επιπτώσεων των πλημμυρών και των δασικών πυρκαγιών όταν εξετάζονται μεμονωμένα, ιδιαίτερη προσοχή χρειάζεται να δοθεί στη συνδυαστική

επίδραση των καταστροφών αυτών ως αποτέλεσμα της αλληλεπίδρασής τους, η οποία είναι συνήθως πιο έντονη.

Οι επιπτώσεις των πλημμυρών στις δασικές πυρκαγιές είναι αμφίσημες και συχνά υποεκτιμώνται, ωστόσο δεν είναι αμελητέες. Εν γένει, η εκδήλωση πλημμυρικών επεισοδίων κατά τις υγρές περιόδους σχετίζεται με μειωμένη δραστηριότητα πυρκαγιών κατά τις ξηρές περιόδους, καθώς το έδαφος είναι κορεσμένο, η βλάστηση έχει απορροφήσει σημαντικές ποσότητες νερού και έτσι η δασική καύσιμη ύλη είναι λιγότερο εύφλεκτη. Σε προφανή αντίθεση με τα προηγούμενα, σημαντικές πλημμύρες μπορεί να συνοδεύονται από πυρκαγιές είτε βραχυπρόθεσμα (εξαιτίας της αυξημένης κεραυνικής δραστηριότητας που προηγείται του πλημμυρικού επεισοδίου ή βλαβών σε ηλεκτρικές εγκαταστάσεις ή ακόμα σε αγωγούς αερίου στη διάρκεια των πλημμυρών) είτε μακροπρόθεσμα (εξαιτίας αυξημένης παραγωγής βιομάζας στα δάση).

Η παρούσα έρευνα εστιάζει στο άλλο σκέλος της αλληλεπίδρασης πλημμυρών – δασικών πυρκαγιών, δηλαδή στην επίδραση των δασικών πυρκαγιών στην υδρολογική συμπεριφορά λεκανών απορροής και κατ' επέκταση σε επερχόμενες πλημμύρες και επαληθεύει ότι για την αποτελεσματική εκτίμηση και κατ' επέκταση διαχείριση του πλημμυρικού κινδύνου καθίσταται αναγκαία η εξέταση αυτής της επίδρασης. Ειδικότερα, οι πυρκαγιές έχουν τόσο άμεσες όσο και έμμεσες επιπτώσεις στην υδρολογική απόκριση των λεκανών που έχουν πληγεί. Γενικά, η αλλαγή, και σε πολλές περιπτώσεις καταστροφή, των δασικών εκτάσεων λόγω πυρκαγιών σχετίζεται άρρηκτα με μειωμένη διήθηση, αυξημένες απορροές και παροχές αιχμής και μειωμένο χρόνο ανόδου, καθιστώντας τις κατάντη περιοχές των εκτάσεων που έχουν πληγεί, ιδιαίτερα επιρρεπείς στις πλημμύρες.

Η συνδυαστική επίδραση πλημμυρών και δασικών πυρκαγιών μεγεθύνεται στο πολύπλοκο περιβάλλον των περιαστικών περιοχών, καθιστώντας κατ' αυτό τον τρόπο τις πλημμυρικές προσομοιώσεις στις περιοχές αυτές ακόμα πιο ενδιαφέρουσες από επιστημονική άποψη. Επιπλέον, το περιαστικό περιβάλλον είναι ένα «δυναμικό», συνεχώς μεταβαλλόμενο περιβάλλον, η υδρολογική συμπεριφορά του οποίου αντικατοπτρίζει τις συνεχείς επιδράσεις ανθρωπογενών παρεμβάσεων και φυσικών αλλαγών. Έχοντας ως στόχο την ερμηνεία της συμπεριφοράς αυτού του πολύπλοκου περιβάλλοντος, την αποκρυπτογράφηση των μηχανισμών του και εν τέλει τη ρεαλιστική προσομοίωση της απόκρισής του, καθίσταται αναγκαίο να υιοθετηθεί μία ολιστική και ευέλικτη προσέγγιση για την εκτίμηση και κατ' επέκταση τη διαχείριση του πλημμυρικού κινδύνου.

Πρωταρχικός στόχος της παρούσας έρευνας είναι η ανάπτυξη ενός ολοκληρωμένου πλαισίου για αποτελεσματική εκτίμηση του πλημμυρικού κινδύνου στο πολύπλοκο, ευμετάβλητο και ευαίσθητο περιαστικό περιβάλλον. Η έρευνα εστιάζει στην εκτίμηση του πλημμυρικού κινδύνου υπό μεταπυρικές συνθήκες για Μεσογειακές περιαστικές λεκάνες απορροής. Έτσι, αναπτύχθηκε ένα μεθοδολογικό πλαίσιο για τη θεωρητική εκτίμηση της δυναμικής εξέλιξης των υδρολογικών παραμέτρων που επηρεάζουν τον πλημμυρικό κίνδυνο ως συνάρτηση του χρόνου, μετά την εκδήλωση δασικών πυρκαγιών.

Μετά από ενδελεχή βιβλιογραφική επισκόπηση των φυσικών καταστροφών και της διαχείρισης κινδύνων, η έρευνα εστιάζει στις πλημμύρες και τις δασικές

πυρκαγιές σε περιαστικό περιβάλλον. Αρχικά, αναλύονται τα γενεσιουργά αίτια, τα ιδιαίτερα χαρακτηριστικά και οι επιπτώσεις των δύο φαινομένων, ενώ αναδεικνύονται επίσης τα ζητήματα διαχείρισης κινδύνου. Στη συνέχεια, η έρευνα επεκτείνεται πέραν της σημασίας των πλημμυρών και των δασικών πυρκαγιών ως φυσικών καταστροφών που δρουν μεμονωμένα και εξετάζει την αλληλεπίδρασή τους και τη σημασία της για αποτελεσματικές πλημμυρικές αναλύσεις. Ειδικότερα, αναλύεται λεπτομερώς η επίδραση των δασικών πυρκαγιών στην υδρολογική συμπεριφορά λεκάνης απορροής και η εκτίμησή της.

Σε αυτή τη φάση της έρευνας εισήχθη ο όρος «*υδρολογική επαναφορά*» (Parathanasiou *et al.*, 2015a) για να περιγράψει το (μεταπυρικό) στάδιο όταν η υδρολογική απόκριση λεκάνης απορροής που έχει καεί, έχει επανέλθει, από κάθε πρακτική (υδρολογικής απόκρισης) απόψη, στην κατάσταση που βρισκόταν πριν την πυρκαγιά. Προτείνεται ότι η υδρολογική επαναφορά μπορεί να επέλθει νωρίτερα από την (πιο πλήρη) «*περιβαλλοντική επαναφορά*», η οποία επιτυγχάνεται με φυσική αναδάσωση και επανάκτηση της ισορροπίας των οικοσυστημάτων – μία διαδικασία που συχνά χρειάζεται αρκετά χρόνια μετά από μία σημαντική δασική πυρκαγιά για να επέλθει, αν τελικά επέλθει.

Για την ποσοτικοποίηση της επίδρασης των δασικών πυρκαγιών υπό μεταβαλλόμενες αρχικές συνθήκες εδαφικής υγρασίας στην υδρολογική απόκριση τυπικής Μεσογειακής περιαστικής λεκάνης απορροής και την ενσωμάτωσή της σε υδρολογικό μοντέλο αναπτύχθηκε μία συνεκτική και καινοτόμα μεθοδολογία. Η μεθοδολογία αναπτύχθηκε για προσδιοριστικά, φυσικής βάσης, αδιαμέριστα ή (ημί-) κατανεμημένα, μεμονωμένων γεγονότων ή συνεχή υδρολογικά μοντέλα.

Αρχικά εξετάζεται η χωροχρονική επίδραση των δασικών πυρκαγιών σε μία λεκάνη. Η επίδραση αυτή εξαρτάται σε μεγάλο βαθμό από την έκταση και τη σφοδρότητα της πυρκαγιάς, που χρησιμοποιούνται ως μέτρα για την ποσοτικοποίηση των επιδράσεων της πυρκαγιάς στο έδαφος και τον ανώροφο (Keeley, 2009; De Santis and Chuvieco, 2007).

Σε ό,τι αφορά τη χωρική επίδραση των πυρκαγιών, τεχνικές απεικόνισης της σφοδρότητας της πυρκαγιάς που κάνουν χρήση δορυφορικής τηλεπισκόπησης, υποστηρίζονται από επί τόπου εργασίες πεδίου και συμπληρώνονται με στατιστικές μεθόδους και προσομοιώσεις θεωρούνται ως οι πιο δημοφιλείς και αποτελεσματικές (Gitas *et al.*, 2012; Lhermitte *et al.*, 2011; Veraverbeke *et al.*, 2010; Viedma *et al.*, 1997). Στην παρούσα έρευνα τυποποιήθηκε και εφαρμόστηκε μία τεχνική για απεικόνιση της σφοδρότητας της πυρκαγιάς, η οποία περιλαμβάνει κατάλληλα επεξεργασμένες δορυφορικές εικόνες και ανάλυση σε περιβάλλον Συστημάτων Γεωγραφικής Πληροφορίας (ΣΓΠ). Έτσι, μία καμένη έκταση μπορεί να διακριτοποιηθεί σε επιμέρους τμήματα που έχουν επηρεαστεί από διαφορετική σφοδρότητα πυρκαγιάς. Στην έρευνα χρησιμοποιήθηκαν πέντε κλάσεις σφοδρότητας πυρκαγιάς: πολύ μεγάλη σφοδρότητα (i), μεγάλη σφοδρότητα (ii), μέτρια σφοδρότητα (iii), χαμηλή σφοδρότητα (iv) και μηδενική σφοδρότητα (αφορά σε εκτάσεις που δεν επλήγησαν από την πυρκαγιά).

Εξετάζοντας από οπτική άποψη τις επιπτώσεις των πυρκαγιών σε μία λεκάνη απορροής, σε κάθε κλάση σφοδρότητας εντοπίστηκαν χρονικές περιόδους



μεταβλητής διάρκειας και διαφορετικής υδρολογικής επίδρασης, σε άμεση συσχέτιση με την κατάσταση αναγέννησης της βλάστησης. Ακολουθώντας εκτενή βιβλιογραφική επισκόπηση επί των συνθηκών της τυπικής Μεσογειακής βλάστησης αναφορικά με τις ετήσιες αλλαγές στο φύλλωμα, τη μεταπυρική αναγέννηση κτλ., ορίστηκε η διάρκεια κάθε χρονικής περιόδου, ενώ ελήφθησαν υπόψη και οι χαρακτηριστικές μεταβατικές περίοδοι που μπορούν να εντοπιστούν στη μεταπυρική αναγέννηση της βλάστησης και σχετίζονται με την υδρολογική επαναφορά.

Αναφορικά με το ρυθμό επαναφοράς μίας τυπικής Μεσογειακής λεκάνης μετά από πυρκαγιά, συχνά παρατηρείται αυξανόμενη επαναφορά κατά τη διάρκεια των πρώτων ετών μετά την πυρκαγιά, την οποία συνήθως διαδέχεται μειούμενος ρυθμός επαναφοράς (Thanos and Marcou, 1991; Trabaud *et al.*, 1985; Eccher *et al.*, 1987; Marzano *et al.*, 2012). Η πρώτη άνοιξη μετά την πυρκαγιά είναι επίσης κρίσιμη όταν εξετάζεται η επαναφορά της βλάστησης (Keeley, 2009). Έτσι, στηρίζεται η υπόθεση μίας απότομα μειούμενης με το χρόνο υδρολογικής επίδρασης για κάθε κλάση σφοδρότητας πυρκαγιάς. Στην προτεινόμενη μεθοδολογία, η οποία αναπτύχθηκε για περιοχές που καλύπτονται από Μεσογειακά δάση που έχουν καεί επανειλημμένα, γίνεται η θεώρηση ότι η υδρολογική επαναφορά λαμβάνει χώρα 4 έτη μετά την πυρκαγιά, με τα πρώτα 2 έτη να είναι τα πλέον κρίσιμα (Brown, 1972; Moody and Martin, 2001a; Springer and Hawkins, 2005; Inbar *et al.*, 1998; Rulli and Rosso, 2007; Robichaud, 2000).

Σε μία προσπάθεια να συσχετιστεί η σφοδρότητα πυρκαγιάς με την εξέλιξη στο χρόνο της υδρολογικής επαναφοράς, γίνεται η υπόθεση ότι προκειμένου να επέλθει η υδρολογική επαναφορά, οι περιοχές που έχουν επηρεαστεί από χαμηλή ή μέτρια σφοδρότητα χρειάζονται κατά προσέγγιση 2 έτη, οι περιοχές που έχουν επηρεαστεί από υψηλή σφοδρότητα χρειάζονται κατά προσέγγιση 3 έτη και οι περιοχές που έχουν επηρεαστεί από πολύ υψηλή σφοδρότητα χρειάζονται κατά προσέγγιση 4 έτη. Έτσι, στην έρευνα αυτή χρησιμοποιήθηκαν τα χρονικά παράθυρα των 7 μηνών (1<sup>η</sup> άνοιξη μετά την πυρκαγιά), 12 μηνών (1<sup>ο</sup> έτος), 19 μηνών (2<sup>η</sup> άνοιξη μετά την πυρκαγιά), 24 μηνών (2<sup>ο</sup> έτος), 36 μηνών (3<sup>ο</sup> έτος) και 48 μηνών (4<sup>ο</sup> έτος) μετά την πυρκαγιά ως μεταβατικές περίοδοι στην υδρολογική επαναφορά.

Στη συνέχεια, εξετάζονται οι αρχικές συνθήκες ως προς την εδαφική υγρασία. Στην παρούσα έρευνα οι αρχικές συνθήκες εδαφικής υγρασίας εξαρτώνται από το ολικό ύψος βροχόπτωσης των πέντε (5) ημερών που προηγούνται πλημμυρικού επεισοδίου και εκτιμώνται σύμφωνα με τη μέθοδο Αριθμού Καμπύλης (SCS Curve Number, USDA-SCS, 1985; USDA-NRCS, 2004b).

Προκειμένου να ποσοτικοποιηθεί η επίδραση των αρχικών συνθηκών ως προς την πυρκαγιά και την εδαφική υγρασία στην υδρολογική απόκριση της λεκάνης απορροής και να εξεταστεί η εξέλιξή της στο χρόνο, χρειάζεται να εφαρμοστούν κατάλληλες μέθοδοι προσομοίωσης και να εξεταστούν αντιπροσωπευτικές υδρολογικές παράμετροι. Για την έρευνα αυτή επιλέχθηκαν πέντε τυπικές υδρολογικές παράμετροι που εξαρτώνται σε μεγάλο βαθμό από τα χαρακτηριστικά της λεκάνης απορροής: ο Αριθμός Καμπύλης (CN), οι Αρχικές Απώλειες (IA), Τυπική Υστέρηση (TP), ο Συντελεστής Αιχμής (CP) και ο Συντελεστής Muskingum K και ποσοτικοποιήθηκε η αλλαγή των τιμών τους για

διαφορετικές αρχικές συνθήκες. Το χρονικό διάστημα μεταξύ της εκδήλωσης της πυρκαγιάς και του υπό εξέταση πλημμυρικού επεισοδίου επίσης ελήφθη υπόψη.

Αρχικά εκτιμήθηκαν οι τιμές κάθε μίας εκ των παραμέτρων αυτών για κανονικές συνθήκες πριν την πυρκαγιά. Βάσει αυτών των τιμών εκτιμήθηκαν οι αντίστοιχες τιμές για διαφορετικές συνθήκες εδαφικής υγρασίας (είτε υγρές είτε ξηρές) πριν την πυρκαγιά, μέσω μίας διαδικασίας βαθμονόμησης για συνθήκες πριν την πυρκαγιά. Έτσι προέκυψε ένα σύνολο κανόνων που συσχετίζουν άμεσα τις τιμές για κανονικές συνθήκες πριν την πυρκαγιά με τις τιμές για υγρές και ξηρές συνθήκες πριν την πυρκαγιά.

Οι τιμές των υπό εξέταση υδρολογικών παραμέτρων αναμένεται να επηρεάζονται σημαντικά για μεταπυρκαγιά, ιδιαίτερα για περιοχές που έχουν πληγεί σε μεγάλο βαθμό από πυρκαγιά. Για το λόγο αυτό, θεωρήθηκε απότομα μειούμενη με το χρόνο η επίδραση της πυρκαγιάς στις προτεινόμενες αλλαγές στις τιμές των υπό εξέταση υδρολογικών παραμέτρων. Η λογική αυτή υπόθεση επαληθεύεται από το ότι η αναγέννηση της βλάστησης μετά την πυρκαγιά καθορίζει τις τιμές των υπό εξέταση υδρολογικών παραμέτρων μετά την πυρκαγιά. Έτσι, το λογαριθμικό προφίλ των χαρακτηριστικών χρονικών παραθύρων στην ανάπτυξη της βλάστησης μετά την πυρκαγιά μπορεί να συσχετιστεί άμεσα με μία δυναμική μεταπυρκαγιά εξέλιξη των υδρολογικών παραμέτρων στο χρόνο αναφορικά με τις τιμές τους πριν την πυρκαγιά, με τις αλλαγές των τιμών να ακολουθούν ένα λογαριθμικό προφίλ (Parathanasiou *et al.*, 2015a).

Στο πλαίσιο αυτό, αναπτύχθηκαν οι εξισώσεις που παρουσιάζονται στη συνέχεια για τον υπολογισμό της μεταπυρκαγιάς εξέλιξης στο χρόνο των εξεταζόμενων υδρολογικών παραμέτρων για κανονικές συνθήκες εδαφικής υγρασίας.

$$CN_{pf,FS}(t) = CN_{af} + h_{CN,FS}(t) \quad (\text{Εξ. a1})$$

$$IA_{pf,FS}(t) = IA_{af} + h_{IA,FS}(t) \quad (\text{Εξ. a2})$$

$$TP_{pf,FS}(t) = h_{TP,FS}(t) * TP_{af} \quad (\text{Εξ. a3})$$

$$CP_{pf,FS}(t) = MAX[(CP_{af} + h_{CP,FS}(t)), p] \quad (\text{Εξ. a4})$$

$$K_{pf,FS}(t) = h_{K,FS}(t) * K_{af} \quad (\text{Εξ. a5})$$

όπου:

$$h_{CN,FS}(t) = a_{CN,FS} * \ln(t) + b_{CN,FS} \quad (\text{Εξ. b1})$$

$$h_{IA,FS}(t) = a_{IA,FS} * \ln(t) + b_{IA,FS} \quad (\text{Εξ. b2})$$

$$h_{TP,FS}(t) = a_{TP,FS} * \ln(t) + b_{TP,FS} \quad (\text{Εξ. b3})$$

$$h_{CP,FS}(t) = a_{CP,FS} * \ln(t) + b_{CP,FS} \quad (\text{Εξ. b4})$$

$$h_{K,FS}(t) = a_{K,FS} * \ln(t) + b_{K,FS} \quad (\text{Εξ. b5})$$

και όπου:

ο δείκτης pf: αντιστοιχεί σε μεταπυρκαγιάς συνθήκες (post-fire),

ο δείκτης af: αντιστοιχεί σε συνθήκες πριν την πυρκαγιά (ante-fire),

ο δείκτης FS: υποδεικνύει τη σφοδρότητα της πυρκαγιάς (fire severity) που εξαρτάται από το % των εκτάσεων που έχουν πληγεί εντός κάθε κλάσης σφοδρότητας πυρκαγιάς,

t: ο χρόνος μετά την εκδήλωση της πυρκαγιάς [μήνες] και

a, b: παράμετροι που εξαρτώνται από τη σφοδρότητα της πυρκαγιάς και οριακές συνθήκες για την εκτίμηση των μεταπυρκαγιάς τιμών κάθε παραμέτρου.

Για τον υπολογισμό των παραμέτρων  $a$  και  $b$  στις Εξισώσεις b1-b5 παραπάνω, χρειάζεται να είναι γνωστές οι οριακές συνθήκες για κάθε κλάση σφοδρότητας πυρκαγιάς. Οι οριακές αυτές συνθήκες ταξινομούνται σε ανώτερες οριακές συνθήκες, που αναφέρονται στην πρώτη μεταπυρική περίοδο και εκφράζονται από τις τιμές του  $h$  για διαφορετικές συνθήκες σφοδρότητας για  $t_{upper}$  και κατώτερες οριακές συνθήκες, που αναφέρονται στην περίοδο μόλις πριν την υδρολογική επαναφορά και εκφράζονται από τις τιμές του  $h$  για διαφορετικές συνθήκες σφοδρότητας για  $t_{lower}$ . Δεδομένου ότι μέχρι τώρα έχουν γίνει περιορισμένες έρευνες για τον υπολογισμό της μεταπυρικής αλλαγής των υδρολογικών παραμέτρων για διαφορετικές συνθήκες σφοδρότητας πυρκαγιάς, η συνεκτίμηση των οριακών τιμών που υπάρχουν στη βιβλιογραφία, των αποτελεσμάτων βαθμονόμησης και, όταν είναι σχετικό, των ιδιαίτερων συνθηκών και περιορισμών, πρέπει να λαμβάνει χώρα για κάθε περιοχή μελέτης.

Έτσι, προκειμένου να εκτιμηθούν οι τιμές των πέντε εξεταζόμενων υδρολογικών παραμέτρων μετά την πυρκαγιά για κανονικές συνθήκες εδαφικής υγρασίας, πρέπει πρώτα να καθοριστούν τα  $t_{upper}$  και  $t_{lower}$ , όπως επίσης και οι αντίστοιχες τιμές του  $h$  για όλες τις παραμέτρους και τις διαφορετικές κλάσεις σφοδρότητας πυρκαγιάς. Βάσει αυτών των οριακών συνθηκών, μπορούν να εφαρμοστούν οι οι Εξισώσεις b1-b5 για τον υπολογισμό των παραμέτρων  $a$  και  $b$  και στη συνέχεια οι Εξισώσεις a1-a5 για τον τελικό υπολογισμό των τιμών των πέντε υδρολογικών παραμέτρων για μετά την πυρκαγιά.

Σε ό,τι αφορά τις τιμές των υδρολογικών παραμέτρων μετά την πυρκαγιά για υγρές και ξηρές συνθήκες εδαφικής υγρασίας, οι κανόνες που αναφέρονται παραπάνω, οι οποίοι συσχετίζουν τις κανονικές συνθήκες εδαφικής υγρασίας πριν την πυρκαγιά με τις υγρές και ξηρές συνθήκες εδαφικής υγρασίας πριν την πυρκαγιά, μπορούν να εφαρμοστούν για την εκτίμηση των τιμών για υγρές και ξηρές συνθήκες εδαφικής υγρασίας μετά την πυρκαγιά σε σχέση με τις τιμές για κανονικές συνθήκες εδαφικής υγρασίας μετά την πυρκαγιά, όπως προκύπτουν από τις Εξισώσεις a1-a5 και b1-b5. Μία γενικευμένη εξίσωση που εκφράζει τη σχέση μεταξύ των τιμών των παραμέτρων για κανονικές, υγρές και ξηρές συνθήκες εδαφικής υγρασίας είναι η Εξ. c.

$$X_{af,dry/wet} = c * X_{af,normal} + d, \text{ (Εξ. c)},$$

όπου:

$X$ : μία υδρολογική παράμετρος και

$c, d$ : συντελεστές που εξαρτώνται από κατά περίπτωση συνθήκες.

Βάσει του ποσοστού των εκτάσεων που έχουν πληγεί για κάθε κλάση σφοδρότητας πυρκαγιάς (όπως αυτό εκτιμάται από ανάλυση σε περιβάλλον ΣΓΠ που γίνεται για αποτύπωση της σφοδρότητας πυρκαγιάς) και των προτεινόμενων τιμών των παραμέτρων για κάθε κλάση σφοδρότητας (όπως αυτές υπολογίζονται από τις Εξισώσεις a1-a5), εκτιμάται μία συνθετική, σταθμισμένη τιμή παραμέτρων για κάθε υπολεκάνη της υπό εξέταση λεκάνης απορροής και η τιμή αυτή εισάγεται στο υδρολογικό μοντέλο για τις απαραίτητες προσομοιώσεις.

Στην παρούσα έρευνα, εξετάστηκαν οι ιδιαιτερότητες τυπικών Μεσογειακών περιαστικών περιοχών, ενώ ιδιαίτερη προσοχή δόθηκε στη δυνατότητα της μεθοδολογίας να εφαρμοστεί σε άλλες περιοχές με παρόμοια, αλλά όχι

ταυτόσημα, υδρομετεωρολογικά και γεωμορφολογικά χαρακτηριστικά. Παράλληλα, μελετήθηκαν εκτενώς ιδιαίτερες συνθήκες υπό τις οποίες μπορούν να παρατηρηθούν αποκλίσεις από την προτεινόμενη μεθοδολογία, όπως για παράδειγμα οι πρώτες πλημμύρες μετά την πυρκαγιά.

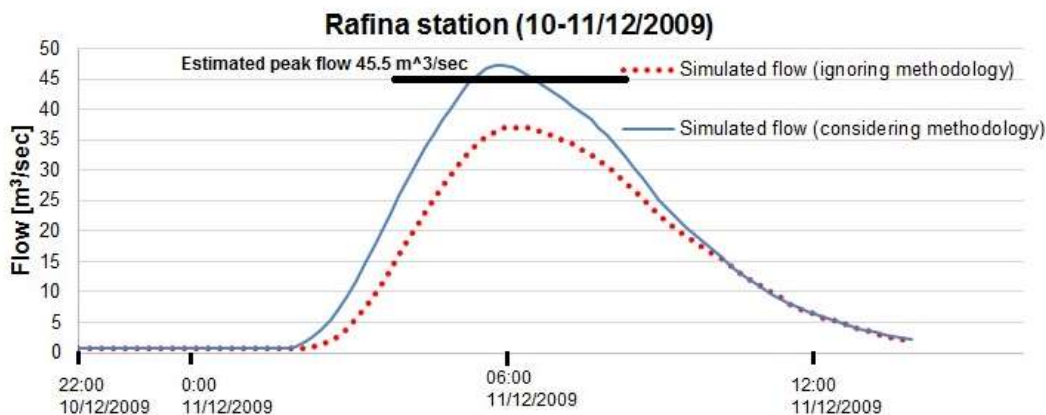
Η μεθοδολογία ενσωματώθηκε με ημιαυτόματο τρόπο σε ένα κατάλληλα επιλεγμένο προσδιοριστικό, φυσικής βάσης, ημι-καταναμημένο, μεμονωμένων γεγονότων υδρολογικό μοντέλο. Μετά από εκτενή βιβλιογραφική έρευνα και δοκιμές διαφορετικών μοντέλων, επιλέχθηκε η ενσωμάτωση της μεθοδολογίας στο HEC-HMS (Hydrologic Engineering Center – Hydrologic Modeling System) υδρολογικό μοντέλο του USACE. Το HEC-HMS βαθμονομήθηκε κατάλληλα και εφαρμόστηκε για ιστορικά πλημμυρικά επεισόδια που καταγράφηκαν στην επιλεγμένη περιοχή μελέτης.

Μία τυπική Μεσογειακή περιαστική περιοχή στην Ελλάδα, η λεκάνη απορροής του ρέματος Ραφήνας, επιλέχθηκε ως περιοχή μελέτης για τη δοκιμή της μεθοδολογίας. Η περιοχή αυτή εκτείνεται σε κατά προσέγγιση 123 km<sup>2</sup> και βρίσκεται στην Ανατολική Αττική. Εξαιτίας των ιδιαίτερων γεωμορφολογικών και υδρογεωλογικών χαρακτηριστικών της, όπως επίσης και λόγω του αυξανόμενου ρυθμού αστικοποίησης, ιδιαίτερα κατά τη διάρκεια των τελευταίων 30 ετών, η λεκάνη απορροής του ρέματος Ραφήνας είναι ιδιαίτερα επιρρεπής στις πλημμύρες. Ταυτόχρονα, η περιοχή είναι ευάλωτη και σε δασικές πυρκαγιές εξαιτίας της επικρατούσας εύφλεκτης βλάστησης σε αυτή. Για αυτούς τους λόγους, οι μεταπυρικές υδρολογικές προσομοιώσεις αποτελούν ζήτημα υψηλής προτεραιότητας για την επιλεγμένη περιοχή μελέτης.

Οι υδρολογικές προσομοιώσεις γίνονται για την περίοδο μετά τον Αύγουστο του 2009, όπου η περιοχή μελέτης επλήγη από σημαντική δασική πυρκαγιά. Αρχικά υπολογίζονται οι τιμές των επιλεγμένων υδρολογικών παραμέτρων για κανονικές, υγρές και ξηρές συνθήκες εδαφικής υγρασίας πριν την πυρκαγιά και οι κανόνες που τις συσχετίζουν. Στη συνέχεια παρέχονται οδηγίες για την προσαρμογή των Εξισώσεων a1-a5 στην περιοχή μελέτης για κανονικές συνθήκες εδαφικής υγρασίας και στις προσαρμοσμένες εξισώσεις εφαρμόζονται οι κανόνες που αναφέρονται παραπάνω. Έτσι, προκύπτουν οι εξισώσεις για τις τιμές των πέντε υδρολογικών παραμέτρων για τις κλάσεις σφοδρότητας πυρκαγιάς που έχουν προαναφερθεί και για υγρές και ξηρές συνθήκες εδαφικής υγρασίας.

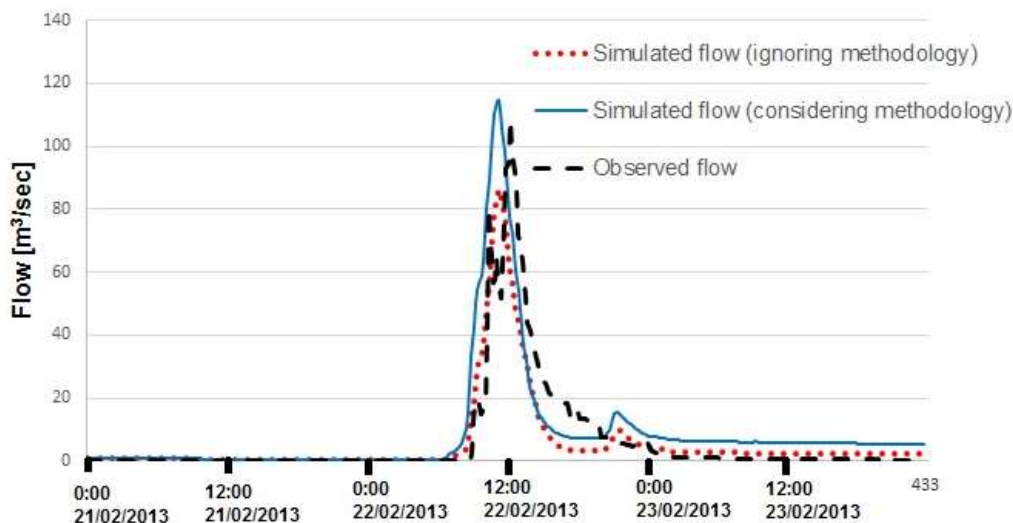
Η εφαρμογή των εξισώσεων έδωσε τις τελικές τιμές των υδρολογικών παραμέτρων για κάθε υπολεκάνη, οι οποίες εισήχθησαν στο υδρολογικό μοντέλο και έγιναν προσομοιώσεις ιστορικών πλημμυρών. Αναφορικά με τα αποτελέσματα της εφαρμογής της μεθοδολογίας, για όλα τα εξεταζόμενα πλημμυρικά επεισόδια οι προσομοιωμένες παροχές αιχμής, όγκοι απορροής και χρόνοι ανόδου είναι σε καλή συμφωνία με τις αντίστοιχες τιμές που προκύπτουν από παρατηρήσεις, όταν διατίθενται. Η σύγκλιση των παρατηρημένων υδρογραφήματων με τα προσομοιωμένα υδρογραφήματα όταν λαμβάνεται υπόψη η μεθοδολογία είναι πολύ μεγαλύτερη της σύγκλισης όταν η μεθοδολογία αγνοείται και ιδιαίτερα για δυσμενείς αρχικές συνθήκες (υγρές αρχικές συνθήκες εδαφικής υγρασίας και πλημμυρικά επεισόδια μετά από πρόσφατη πυρκαγιά).

Αντίστοιχα είναι τα συμπεράσματα και για τις παροχές αιχμής. Ενδεικτικά παρατίθενται τα Γραφήματα 1 και 2, που απεικονίζουν τα προαναφερόμενα.



Γράφημα 1. Προσομοιωμένες απορροές όταν εφαρμόζεται και όταν αγνοείται η μεθοδολογία και εκτιμώμενη παροχή αιχμής για το πλημμυρικό επεισόδιο στις 10-11/12/2009 (Σταθμός Ραφήνας –πλημμυρικό επεισόδια σύντομα μετά την πυρκαγιά).

Rafina station (22/02/2013)



Γράφημα 2. Παρατηρημένες και προσομοιωμένες απορροές όταν εφαρμόζεται και όταν αγνοείται η μεθοδολογία για το πλημμυρικό επεισόδιο στις 22/02/2013 (Σταθμός Ραφήνας – πλημμυρικό επεισόδιο με υγρές αρχικές συνθήκες).

Στη συνέχεια έγινε λεπτομερής ανάλυση ευαισθησίας, η οποία περιλάμβανε δύο ανεξάρτητες αναλύσεις. Αρχικά, έγινε ανάλυση ευαισθησίας προκειμένου να ποσοτικοποιηθεί η επίδραση κάθε μίας από τις πέντε εξεταζόμενες υδρολογικές παραμέτρους στους προσομοιωμένους όγκους απορροής. Η ανάλυση κατέληξε στο συμπέρασμα ότι οι παράμετροι CN και IA έχουν σημαντικότερο υδρολογικό αποτύπωμα από τις άλλες τρεις εξεταζόμενες υδρολογικές παραμέτρους. Ταυτόχρονα, οι παράμετροι CN, IA και TP, οι οποίες σχετίζονται στην προτεινόμενη μεθοδολογία με πιο σημαντικές αλλαγές στην τιμή τους μετά την πυρκαγιά και μεγαλύτερης διάρκειας μεταπυρική επίδραση, είναι πιο ευαίσθητες

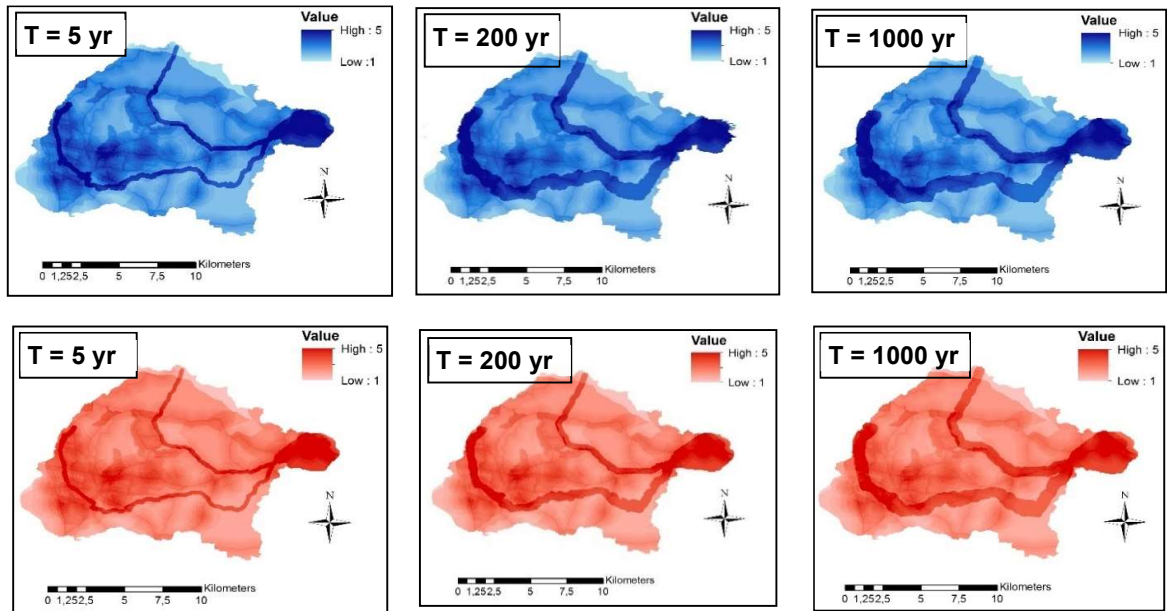
στην επίδραση της πυρκαγιάς και οι μεταπτυρικές τιμές τους συνιστάται να εκτιμώνται με προσοχή. Ωστόσο, παρόλο που οι μεταπτυρικές αλλαγές στις παραμέτρους CP και K υπό διαφορετικές συνθήκες εδαφικής υγρασίας είναι μικρότερες, παραμένουν αρκετά σημαντικές ώστε να μην υποεκτιμώνται.

Εν συνεχεία, ελέγχθηκε η αποτελεσματικότητα τη προτεινόμενης μεθοδολογίας μέσω μίας πρωτότυπης ανάλυσης ευαισθησίας. Πιο συγκεκριμένα, το υδρολογικό μοντέλο εφαρμόστηκε για τρία σύνολα των 1.000 τυχαίων τιμών για τις πέντε εξεταζόμενες υδρολογικές παραμέτρους και όλες τις 6 υπολεκάνες της περιοχής μελέτης και η επίδοσή του αξιολογήθηκε χρησιμοποιώντας το δείκτη Nash-Sutcliffe. Η επιλεγείσα προσέγγιση τυχαίας δειγματοληψίας, η οποία διασφαλίζει την αντιπροσωπευτικότητα του συνόλου των τυχαίων τιμών ως προς την πραγματική μεταβλητότητα είναι η δειγματοληψία Latin Hypercube Sampling (LHS) (McKay *et al.*, 1979; Iman and Conover, 1980; McKay M.D., 1992; van Griensven *et al.*, 2006). Για το σκοπό αυτό αναπτύχθηκε ένας πρωτότυπος προγραμματιστικός κώδικας σε περιβάλλον Matlab7.11.0 (version R2010b) και εφαρμόστηκε και έγιναν επιπλέον αναλύσεις των παραχθέντων πινάκων με τυχαίες τιμές. Το σύνολο των τυχαίων τιμών που έδωσε τα καλύτερα αποτελέσματα συγκρίθηκε με τις ακριβείς τιμές που προτάθηκαν από τη μεθοδολογία και ελέγχθηκε η εγγύτητα των βέλτιστων τιμών με τις προτεινόμενες. Ενδεικτικά παρατίθεται ο Πίνακας 1, όπου παρατίθενται οι προτεινόμενες από τη μεθοδολογία τιμές των πέντε παραμέτρων για τρεις υπολεκάνες της περιοχής μελέτης, οι αντίστοιχες τιμές που έχουν προκύψει ως μέσοι όροι των 100 καλύτερων προσομοιώσεων και η σχετική διαφορά τους και αποδεικνύεται η αποτελεσματικότητα της προτεινόμενης μεθοδολογίας.

*Πίνακας 1. Προτεινόμενες από τη μεθοδολογία τιμές των παραμέτρων και μέσες τιμές παραμέτρων που έχουν προκύψει από τις 100 καλύτερες προσομοιώσεις στο HEC-HMS, για υγρές συνθήκες εδαφικής υγρασίας στις υπολεκάνες Ντράφι, Ραφήνα και Ραφήνα2.*

Υπολεκάνη	Παράμετρος	Προτεινόμενη από μεθοδολογία	Μ.ο. των 100 βέλτιστων προσομοιώσεων	Σχετική διαφορά [%]
<b>Ντράφι (W15460)</b>	CN	48	47	2.1
	IA	11	12	-9.1
	TP	0.49	0.49	0
	CP	0.4	0.4	0
	K	0.50	0.49	2
<b>Ραφήνα (W15020)</b>	CN	57	57	0
	IA	11	12	-9.1
	TP	0.80	0.79	1.3
	CP	0.4	0.4	0
	K	0.91	0.92	-1.1
<b>Ραφήνα2 (W16340)</b>	CN	57	57	0
	IA	10	10	0
	TP	0.70	0.69	1.4
	CP	0.4	0.4	0
	K	0.65	0.65	0

Επίσης, το υδρολογικό μοντέλο προσομοίωσε πλημμύρες με περιόδους επαναφοράς που αντιστοιχούν σε μεγάλη, μεσαία και μικρή πιθανότητα εκδήλωσης και συγκεκριμένα για T=5, 200 and 1000 έτη, αντίστοιχα. Τα αποτελέσματα της υδρολογικής ανάλυσης εισήχθησαν στο υδραυλικό μοντέλο HEC-RAS (Hydrologic Engineering Center – River Analysis System) του USACE και τελικά καταρτίστηκαν αντιπροσωπευτικοί χάρτες επικινδυνότητας πλημμύρας και χάρτες κινδύνου πλημμύρας για τις εξεταζόμενες περιόδους επαναφοράς για την περιοχή μελέτης. Ενδεικτικά παρατίθεται το Γράφημα 3, όπου παρουσιάζονται οι χάρτες κινδύνου πλημμύρας και για τις τρεις επιλεγθείσες περιόδους επαναφοράς για διαφορετικές αρχικές συνθήκες.



*Γράφημα 3. Χάρτες κινδύνου πλημμύρας για T=5, 200 and 1000 έτη για υγρές συνθήκες εδαφικής υγρασίας και όταν δεν έχει πλήξει την περιοχή πρόσφατη πυρκαγιά (επάνω γραμμή) και για κανονικές συνθήκες εδαφικής υγρασίας και μετά από πρόσφατη πυρκαγιά (κάτω σειρά).*

Δεδομένου ότι η ενσωμάτωση της προτεινόμενης μεθοδολογίας σε υδρολογικό μοντέλο καταλήγει σε ακριβείς και αντιπροσωπευτικές προσομοιώσεις, η ενσωμάτωσή της σε υδρολογικό μοντέλο που συνδέεται με υδραυλικό, όπως αναφέρεται παραπάνω, καταλήγει στην κατάρτιση αντιπροσωπευτικών χαρτών επικινδυνότητας πλημμύρας και χαρτών πλημμυρικού κινδύνου. Συμπεραίνεται έτσι ότι η μεθοδολογία που αναπτύχθηκε μπορεί να χρησιμοποιηθεί αποτελεσματικά στην εκτίμηση του πλημμυρικού κινδύνου και να υποστηρίξει πλατφόρμες πρόγνωσης πλημμυρών σε σχεδόν πραγματικό χρόνο και επιχειρησιακά συστήματα πολιτικής προστασίας, όπως επίσης και διαχείριση του πλημμυρικού κινδύνου σε επίπεδο σχεδιασμού σε επόμενο στάδιο.

Τα αποτελέσματα της ανάλυσης υπογραμμίζουν τη σημασία της θεώρησης των αρχικών συνθηκών εδαφικής υγρασίας κατά την εφαρμογή υδρολογικών μοντέλων μεμονωμένου γεγονότος και επαληθεύουν ότι η θεώρηση μόνιμα κανονικών συνθηκών εδαφικής υγρασίας για λόγους απλούστευσης ή μόνιμα υγρών συνθηκών εδαφικής υγρασίας κατά τη διάρκεια των βροχερών περιόδων

επί το δυσμενέστερο, υπονομεύει την ευρωστία και την ακρίβεια των υδρολογικών προσομοιώσεων.

Η έρευνα καταλήγει ότι η βαθμονόμηση των CN, IA, TP, CP και K, που είναι τυπικές παράμετροι που περιλαμβάνονται στην πλειοψηφία των μοντέλων, δίνει βέλτιστα αποτελέσματα προσομοίωσης, σε αντίθεση με την τρέχουσα πρακτική βαθμονόμησης, η οποία συνήθως περιλαμβάνει τη βαθμονόμηση μόνο των CN και IA. Οι παράμετροι TP, CP και K είναι σαφώς λιγότερο ευαίσθητες παράμετροι βαθμονόμησης από τις παραμέτρους CN και IA καθώς έχουν μικρότερη επίδραση στην πλημμυρική απορροή, ωστόσο για πιο αντιπροσωπευτικές υδρολογικές προσομοιώσεις χρειάζεται να βαθμονομούνται κατάλληλα (Parathanasiou *et al.*, 2015a).

Συμπεραίνεται ότι η επίδραση της πυρκαγιάς είναι πολύ έντονη κατά την πρώτη μεταπυρική περίοδο, ενώ μειώνεται απότομα με το χρόνο μέχρι να επέλθει υδρολογική επαναφορά και να εξαφανιστεί το μεταπυρικό υδρολογικό αποτύπωμα (Parathanasiou *et al.*, 2015a). Αυτή η επίδραση δεν είναι η ίδια σε όλες τις εξεταζόμενες υδρολογικές παραμέτρους. Οι παράμετροι CN και IA είναι πιο ευαίσθητες παράμετροι στην επίδραση της πυρκαγιάς από τις παραμέτρους TP και CP και σε μικρότερο βαθμό από την παράμετρο K και έτσι σχετίζονται με σημαντικότερες μεταπυρικές αλλαγές και μεγαλύτερης διάρκειας μεταπυρική επίδραση. Επίσης, κατά τη διάρκεια των πρώτων ετών μετά την πυρκαγιά η μεταπυρική επίδραση είναι πιο έντονη στις εξεταζόμενες περιόδους από την επίδραση των αρχικών συνθηκών εδαφικής υγρασίας.

Το γενικευμένο μεθοδολογικό πλαίσιο που αναπτύχθηκε για αυτή την έρευνα για την εκτίμηση των δυναμικών αλλαγών στο χρόνο πέντε αντιπροσωπευτικών υδρολογικών παραμέτρων υπό διαφορετικές αρχικές συνθήκες, ως προς την εκδήλωση πυρκαγιάς και τις συνθήκες εδαφικής υγρασίας, εξυπηρετεί το γενικότερο στόχο της έρευνας, που είναι η ακριβής εκτίμηση του πλημμυρικού κινδύνου σε τυπικές Μεσογειακές περιαστικές περιοχές υπό μεταπυρικές συνθήκες. Η ευρωστία της μεθοδολογίας που αναπτύχθηκε και η καταλληλότητά της για περαιτέρω εφαρμογές ενισχύεται από τη χρήση εργαλείων προηγμένης τεχνολογίας, μοντέρνων τεχνολογιών και εμπειριστατωμένων αναλύσεων, την αξιοποίηση επαρκώς τεκμηριωμένης σχετικής γνώσης και εμπειρίας, όπως επίσης και την ευκολία προσαρμογής και κατ' επέκταση εφαρμογής σε άλλες περιοχές (Parathanasiou *et al.*, 2015a).

Τα καινοτόμα στοιχεία της μεθοδολογίας παρατίθενται στη συνέχεια:

Καταρχήν, όπως έχει προαναφερθεί, γίνεται σαφής διάκριση μεταξύ της περιβαλλοντικής και της υδρολογικής επαναφοράς. Ο όρος «*επαναφορά των δασών μετά από πυρκαγιά*», ή όπως αλλιώς αναφέρεται «*χρόνος χαλάρωσης (relaxation time)*» (Moody and Martin, 2001) είναι συχνός στη βιβλιογραφία. Και οι δύο όροι αναφέρονται σε αυτό που ορίζεται σε αυτή την έρευνα ως «*περιβαλλοντική επαναφορά*», η οποία αφορά στην αντικατάσταση της κομοστέγης και την επαναφορά των λειτουργιών των οικοσυστημάτων και μπορεί να επέλθει πολλά χρόνια μετά από μία πυρκαγιά, αν τελικά επέλθει. Παρόλα αυτά, μία βασική παράμετρος στις υδρολογικές μελέτες, η οποία είναι ιδιαίτερης σημασίας και χρειάζεται να λαμβάνεται υπόψη, εν αντιθέσει με την τρέχουσα



πρακτική, είναι η επαναφορά της υδρολογικής συμπεριφοράς μίας καμένης λεκάνης στην κατάσταση της πριν την πυρκαγιά. Αυτή η κατάσταση ορίζεται στην παρούσα έρευνα ως «υδρολογική επαναφορά», η οποία είναι διαφορετική από την πλήρη επαναφορά της βλάστησης και μπορεί να επέλθει μερικά χρόνια μετά από μία πυρκαγιά. Η διάκριση αυτή είναι απαραίτητη για την έρευνα της υδρολογικής απόκρισης λεκάνης απορροής μετά από πυρκαγιά, προκειμένου να αποφευχθούν εσφαλμένες ερμηνείες και παρανοήσεις.

Επιπροσθέτως, στην έρευνα αυτή ποσοτικοποιείται η επίδραση των δασικών πυρκαγιών στην υδρολογική συμπεριφορά τυπικών περιστατικών λεκανών απορροής και εν τέλει υποστηρίζεται η ενσωμάτωση της σφοδρότητας πυρκαγιάς σε υδρολογικές προσομοιώσεις. Παρά σχετικές, μεμονωμένες προσπάθειες να εκτιμηθεί η επίδραση των δασικών πυρκαγιών στις τιμές μερικών εκ των εξεταζόμενων στην παρούσα έρευνα παραμέτρων που έχουν γίνει στο παρελθόν (Higginson and Jarnecke, 2007; Foltz *et al.*, 2009), δεν υπάρχει στη βιβλιογραφία κάποια ολοκληρωμένη και ευρέως αποδεκτή προσέγγιση.

Επίσης, εξετάζεται και ποσοτικοποιείται η εξέλιξη στο χρόνο της επίδρασης της πυρκαγιάς σε τυπικές Μεσογειακές περιοχές. Η κοινή πρακτική είναι η εξέταση της επίδρασης της πυρκαγιάς μόνο για πρόσφατα καμένες εκτάσεις, εστιάζοντας στην περιορισμένη χρονική περίοδο μεταξύ της εκδήλωσης της πυρκαγιάς και της επόμενης εποχής βλάστησης (e.g. Cerrelli, 2005; Higginson and Jarnecke, 2007) ή στα πρώτα ένα με δύο έτη μετά την πυρκαγιά (Cannon *et al.*, 2008; Rulli and Rosso, 2007; Inbar *et al.*, 1998; Scott and Van Wyk, 1990). Η προτεινόμενη προσέγγιση είναι καινοτόμα, καθώς λαμβάνει υπόψη με πρωτότυπο τρόπο το γεγονός ότι η επίδραση της πυρκαγιάς αλλάζει δυναμικά στο χρόνο και εκτιμά όχι μόνο μία αρχική επίδραση της πυρκαγιάς στην υδρολογία, αλλά επίσης και την εξέλιξή της στο χρόνο και επιπλέον την περίοδο όταν αυτή η επίδραση μπορεί με ασφάλεια να θεωρηθεί αμελητέα, δηλαδή το χρόνο που επέρχεται υδρολογική επαναφορά.

Ένα ακόμη επιστημονικό κενό που εντοπίστηκε στη βιβλιογραφία και καλύπτεται αποτελεσματικά με την παρούσα έρευνα είναι η θεώρηση των συνθηκών εδαφικής υγρασίας στις μελέτες επίδρασης δασικών πυρκαγιών. Συνήθως, η επίδραση των συνθηκών εδαφικής υγρασίας εξετάζεται χωριστά από την επίδραση των πυρκαγιών. Ωστόσο, οι ταυτόχρονες συνθήκες μίας πρόσφατης δασικής πυρκαγιάς και υγρών συνθηκών εδαφικής υγρασίας έχουν δυσμενείς επιπτώσεις στην απόκριση μίας λεκάνης απορροής, καθώς σχετίζονται με αυξημένους όγκους απορροής και παροχές αιχμής και μειωμένους χρόνους ανόδου. Για αυτό το λόγο, και οι δύο αυτοί παράγοντες που καθορίζουν τις αρχικές συνθήκες, όπως επίσης και η αλληλεπίδρασή τους χρειάζεται να συνεκτιμώνται προκειμένου να αποφευχθούν υποεκτιμημένες αποκρίσεις λεκανών και να επιτευχθούν ακριβέστερα αποτελέσματα σε πλημμυρικές προσομοιώσεις.

Επιπλέον, η μεθοδολογία αναπτύχθηκε για τυπικές Μεσογειακές περιστατικές περιοχές και εκφράζεται με γενικό τρόπο, προκειμένου να μπορεί εύκολα να προσαρμοστεί σε περιοχές με παρόμοια υδρομετεωρολογικά και γεωμορφολογικά χαρακτηριστικά. Τα ιδιαίτερα χαρακτηριστικά των περιοχών αυτών εξετάστηκαν λεπτομερώς και η μεθοδολογία που αναπτύχθηκε εκφράζεται

μέσω γενικευμένων εξισώσεων που προσαρμόζονται σε διαφορετικές περιοχές μελέτης ακολουθώντας συγκεκριμένες οδηγίες. Για εφαρμογές σε άλλες περιοχές, χρειάζεται να επανεξεταστεί η χρονική διάσταση της επίδρασης των πυρκαγιών, λαμβάνοντας υπόψη τοπικά χαρακτηριστικά όπως τα ιθαγενή είδη της βλάστησης, την κομοστέγη, και τοπικά κλιματικά χαρακτηριστικά, η ανάπτυξη της βλάστησης, η αντοχή στην πυρκαγιά, η αναγέννηση της βλάστησης κτλ. Επίσης, εξετάζονται και ιδιαίτερες περιπτώσεις όπου μπορεί να παρατηρηθούν αποκλίσεις από την προτεινόμενη μεθοδολογία και θα μπορούσε να χρειάζεται επαναπροσαρμογή της γενικευμένης προσέγγισης.

Ακόμη, εργαλεία και μέθοδοι προηγμένης τεχνολογίας εφαρμόστηκαν για τον έλεγχο της αποδοτικότητας της μεθοδολογίας. Καινοτόμα στοιχεία περιλαμβάνουν ένα πρωτότυπο κώδικα γραμμένο σε Matlab για την παραγωγή πινάκων τυχαίων τιμών για τις επιλεγμένες υδρολογικές παραμέτρους, τη θεώρηση στον κώδικα αυτό της μεθόδου δειγματοληψίας Latin Hypercube Sampling (LHS), μίας αποτελεσματικής μεθόδου δειγματοληψίας κατάλληλης για αυτή την έρευνα, όπως επίσης και την πρωτότυπη τυποποίηση της στατιστικής ανάλυσης των αποτελεσμάτων της έρευνας.

Η προτεινόμενη μεθοδολογία μπορεί επίσης να αυτοματοποιηθεί και να ενσωματωθεί σε Συστήματα Έγκαιρης Ειδοποίησης για πλημμύρες και άλλα επιχειρησιακά συστήματα πολιτικής προστασίας. Εκτός του ότι τα συστήματα αυτά είναι πολύ ευαίσθητα στην ακρίβεια των δεδομένων εισόδου τους, δεν έχει βρεθεί στη βιβλιογραφία κάποια ολοκληρωμένη προσέγγιση για την ενσωμάτωση της συνδυαστικής επίδρασης δασικών πυρκαγιών και εδαφικής υγρασίας στην υδρολογική απόκριση λεκάνης που υποστηρίζεται από Σύστημα Έγκαιρης Ειδοποίησης Πλημμύρας. Η εισαγωγή περισσότερο έγκυρης, ως προς τις εξεταζόμενες αρχικές συνθήκες, πληροφορίας σε αυτά τα συστήματα είναι μία ακόμη καινοτομία που μπορεί να υποστηριχθεί από την παρούσα έρευνα.

Αναφορικά με προτάσεις για περαιτέρω έρευνα, η μεθοδολογία θα μπορούσε να δοκιμαστεί σε άλλες περιοχές μελέτης, με παρόμοια χαρακτηριστικά ως προς τη χρήση / κάλυψη γης, το ρυθμό αστικοποίησης, υδρομετεωρολογικά και γεωμορφολογικά στοιχεία κτλ. Περαιτέρω έρευνα θα μπορούσε να εστιάσει στην επέκταση της δυνατότητας της μεθοδολογίας να εφαρμοστεί σε άλλες Μεσογειακές περιοχές, οι οποίες είναι μεν τυπικές περιαστικές, αλλά δεν έχουν τις ίδιες ιδιαιτερότητες κατά την πρώτη περίοδο μετά την πυρκαγιά. Σε κάθε περίπτωση, οι επιμέρους συνιστώσες της προτεινόμενης μεθοδολογίας ενδέχεται να χρειάζονται σημαντική επαναπροσαρμογή, όπως προτείνεται στο Κεφάλαιο 5.

Η ενσωμάτωση της προτεινόμενης μεθοδολογίας σε προσδιοριστικά, φυσικής βάσης μοντέλα, αδιαμέριστα και μεμονωμένων γεγονότων ή συνεχή ή ημί-κατανεμημένα και συνεχή, δηλαδή σε μοντέλα διαφορετικά από το HEC-HMS ή ακόμη και στο HEC-HMS σε μορφή διαφορετική από ημι-κατανεμημένο και μεμονωμένων γεγονότων, όπως στην παρούσα έρευνα, θα ήταν ενδιαφέρουσα.

Μία ακόμα πρόταση για μελλοντική έρευνα αφορά στη χρήση τηλεσκοπικών δεδομένων εδαφικής υγρασίας αντί για δεδομένα εδαφικής υγρασίας που εκτιμώνται βάσει του συνολικού ύψους βροχόπτωσης κατά τις 5 μέρες που προηγούνται του πλημμυρικού επεισοδίου, τα οποία χρησιμοποιούνται στην

παρούσα έρευνα. Επίσης, θα μπορούσε να διερευνηθεί η εξέταση διαφορετικών χρονικών περιόδων μεταξύ επεισοδίων βροχόπτωσης και η εκτίμηση της επίδρασης των περιόδων αυτών στην εδαφική υγρασία για την περίοδο που προηγείται ενός πλημμυρικού επεισοδίου και ειδικότερα κατά τις 5 ημέρες πριν το πλημμυρικό επεισόδιο, όπως διευκρινίζεται στο Κεφάλαιο 9.

Περαιτέρω έρευνα θα μπορούσε επίσης να γίνει στην προτυποποίηση των κανόνων για την εκτίμηση της επίδρασης της πυρκαγιάς ως προς τη χωρική έκταση και τη σφοδρότητα, όπως εφαρμόζεται στην παρούσα έρευνα, ώστε να αυτοματοποιηθεί εύκολα και ενδεχομένως να αποτελέσει ένα ανεξάρτητο λογισμικό.

Ελλείπει λεπτομερών πληροφοριών για συγκεκριμένες συνθήκες των δασών πριν ή/και μετά την πυρκαγιά, περαιτέρω έρευνα θα μπορούσε να εστιάσει σε ασφαλείς υποθέσεις που θα μπορούσαν να γίνουν, όπως επίσης και σε συνδυαστική χρήση των διαφορετικών πηγών πληροφορίας (επιτόπιες εκτιμήσεις, δορυφορικές εικόνες, υπάρχουσες μελέτες κτλ.), ώστε να μπορούν να εξαχθούν κατά το δυνατό ακριβέστερα συμπεράσματα για την επίδραση των πυρκαγιών και να εφαρμοστεί η μεθοδολογία αποφεύγοντας σημαντικά σφάλματα.

Η αναγνώριση της βλάστησης μετά την πυρκαγιά, ώστε να εκτιμηθεί με κατά το δυνατό μεγαλύτερη ακρίβεια η δυνατότητά της για υδρολογική και περιβαλλοντική επαναφορά, αποτελεί ένα ακόμα πεδίο ενδεχόμενης μελλοντικής έρευνας. Η ακριβής εκτίμηση της βλάστησης μετά την πυρκαγιά και ενδεχόμενων μηχανισμών προσαρμογής των πληγέντων ειδών μπορεί επίσης να στηρίξει μία πιο ακριβή εκτίμηση της περιόδου κατά την οποία αναμένεται υδρολογική επαναφορά.

Εν τέλει, περαιτέρω έρευνα θα μπορούσε να γίνει στην αυτοματοποίηση της ενσωμάτωσης της προτεινόμενης μεθοδολογίας σε ένα μοντέλο βροχής-απορροής για υδρολογικές προσομοιώσεις ή ακόμη και σε ένα υδρολογικό μοντέλο που συνδέεται με υδραυλικό μοντέλο για την κατάρτιση χαρτών επικινδυνότητας πλημμύρας, όπως συμβαίνει στην πλατφόρμα FLIRE (Kochilakis *et al.*, 2016a; Kochilakis *et al.*, 2016b; Kotroni *et al.*, 2015; Papathanasiou *et al.*, 2015b; Poursanidis *et al.*, 2015a).

# CHAPTER 1: INTRODUCTION

## 1.1 Context

Floods are one of the most disastrous natural hazards that affect human societies, bringing about dire consequences, including *inter alia* loss of human lives, ecological degradation and inestimable damage costs. Thus, flood risk assessment and management become particularly important issues that humans need to deal with and to this end several methodologies and practices have been developed. Despite the profusion of such practices, floods keep affecting humans and the environment, a fact that reveals the inadequacy of existing, applied flood risk assessment and management strategies.

The assessment and management of flood risk becomes even more challenging in periurban environments, where flood impacts are magnified and thus flood risk management becomes more critical. The particularity of periurban areas lies in the fact that these areas are hybrid landscapes, in which fragmented urban and rural characteristics coexist. More specifically, periurban areas are characterized by the vicinity of areas with different, frequently changing and often conflicting land uses (*e.g.* forested areas coexist with cultivated land, pasture land, industrial zones and urban cells within a geographically limited area). This interface between different land uses contributes to the formation of a complex environment, in which complicated problems may arise in case of occurrence of a flood event.

Periurban areas are also particularly prone to another natural hazard which is interrelated with floods, *i.e.* forest fires. Large scale forest fires are also associated with tremendous impacts on humans and the environment. Particularly for periurban areas, along the zone close to the Wildland-Urban Interface (WUI), *i.e.* the transition zone between areas with intense urban development and unoccupied land, the exposure to fire danger is higher, since wildfires are more frequent; while at the same time their impact on humans, society, the economy and the environment is also magnified due to nearby human activity.

Therefore, periurban areas are prone to both natural hazards independently. However, the impact of forest fires on flood occurrence and vice versa is enormous, and hence, for efficient flood and fire risk assessment and management, emphasis needs to be placed not only to the particularities and generation mechanisms of each hazard, but also to their combined impact.

More specifically, the occurrence of a wildfire in the forested land of a periurban area results in the direct and considerable change of land cover, since local vegetation is destructed, if not destroyed completely, and the properties of upper soil layers are drastically modified. Therefore, retention and infiltration are minimized and in case of a subsequent rainfall event, runoff is significantly increased, resulting often in severe flooding.

At the same time, floods affect a potential subsequent wildfire in two, contradictory though, ways. On the one hand, frequent flood or even storm events during the wet period in a periurban area, result in increased growth of low vegetation and foliage which constitute a particularly flammable material during the dry period. On the other hand, increased rainfall during the wet period also results in increased stored wetness on trees and plants, which may inhibit a rapid fire expansion especially during the early dry period.

All the aforementioned factors that describe the interaction of floods and forest fires need to be taken into consideration appropriately and thus a realistic quantification of their combined impact becomes an issue of high priority for the accurate examination of the post-fire impact on the hydrological response and therefore for flood risk assessment and management in periurban areas.

Further to its increased vulnerability to floods, forest fires and their combined impact, the periurban environment is a “dynamic” environment, since it constantly changes in multiple ways, with its hydrological behaviour reflecting constantly the impacts of man-made interventions and natural changes. In order to interpret the behaviour of such a complicated environment, decipher its underlying mechanisms and finally achieve effective flood risk assessment and at a later stage management in periurban environments, a flexible approach needs to be adopted for its realistic representation.

Typical Mediterranean periurban areas are significantly prone to both floods and forest fires, and therefore their flood modelling necessitates the consideration of these factors. On top of that, it also needs to be noted that according to climate change scenarios for such areas, intense storms during the wet periods are expected to be succeeded by extended dry and hot periods in the upcoming years. By that way, the vulnerability to floods, forest fires and their combined action is expected to be even more intensified, thus prioritizing representative flood simulations.

## **1.2 Aim and objectives**

The primary aim of this doctoral thesis is the development of a methodological framework to theoretically estimate the dynamic evolution of hydrological parameters that affect flood risk as a function of time, following the occurrence of forest fires.

The secondary objectives of this research are listed below:

- Consideration of soil moisture conditions as an integral part of hydrological analysis,
- Quantification of the impact of fire and initial hydrological conditions on the hydrological behavior of periurban catchments,
- Development of a flexible methodology for efficient flood risk assessment in a periurban environment,
- Coupling of appropriate hydrologic and hydraulic models for enhanced flood simulation of a periurban environment and
- Incorporation of the hydrological footprint of fires and initial conditions in hydrological and hydraulic analyses in a semi-automatic way, aiming to

support near-real time flood forecasting platforms and civil protection systems.

### 1.3 Methodology

Aiming to an integrated approach towards efficient flood risk assessment in a periurban environment and at the same time the achievement of the above mentioned objectives, innovative methodologies and flexible tools need to be developed and used in combination with reliable and state-of-the-art modelling techniques. The application of these methodologies, tools and models can support flood risk assessment, and at a later stage flood risk management, both on a near real-time basis and on a planning basis. The overall approach that has been adopted in this research is described in brief in the following paragraphs.

After a thorough literature review on natural hazards, focusing on floods and forest fires, and their impacts as individual hazards, research was made on their interaction and particularly the impact of forest fires on the hydrological behaviour of a catchment. Based on the extended literature review and also after repetitive testing of properly processed relevant datasets that were retrieved from monitoring networks, an attempt to quantify the floods-fires interaction in typical Mediterranean periurban environments was made.

In order to incorporate the hydrological footprint of forest fires and initial conditions in a flood analysis, it is necessary to identify first appropriate hydrological and hydraulic models. To this end, a long list of advanced and reliable hydrological and hydraulic models was compiled and the capacities of many of these models were further investigated. Beyond the thorough literature review for each model, demo versions were tested, when available, and direct communication with model developers, as well as interaction in hydrological modelling forums for exchange of relevant experience took place during this part of the research. The hydrological model that was considered most appropriate for the current research and it was applied in order to efficiently simulate the hydrological behaviour of both urban and rural areas in a selected periurban river basin is the HEC-HMS (Hydrologic Engineering Center – Hydrologic Modeling System) model (HEC, 2009). Regarding hydraulic modelling, HEC-RAS (Hydrologic Engineering Center – River Analysis System) model has been selected as the most appropriate hydraulic model for this research (Brunner, 2010).

An innovative, coherent and robust methodology was then developed for the quantification of the impact of forest fires and initial soil moisture conditions on the hydrological response of a Mediterranean periurban catchment and its incorporation in hydrological modelling. This methodology has been developed for deterministic, physically-based, lumped or (semi-)distributed, event-based or continuous hydrological models.

More specifically, five representative hydrological parameters, *i.e.* Curve Number (CN), Initial Abstraction (IA), Standard Lag (TP), Peaking Coefficient (CP) and Muskingum K coefficient, were selected for the development of this methodology. Based on the outcomes of the extended literature review on the hydrological footprint of forest fires and using a fire severity map, an attempt was made to

quantify the change in the values of the five parameters for different initial conditions. The initial conditions were classified into initial soil moisture conditions and post-fire conditions. Particularly for this latter case, the time interval between the occurrence of a fire event and the analyzed flood events was taken into consideration. The particularities of typical Mediterranean periurban areas were also considered for the development of this methodology. Particular attention was paid on the development of the methodology in such a way so as to be easily adjustable to other areas with similar, yet not identical, hydrometeorological and geomorphological characteristics. In addition, conditions under which deviations from the proposed methodology can be observed were also investigated in detail.

The developed methodology for the quantification of initial soil moisture conditions and fire occurrence impact was incorporated in a semi-automated way in the selected hydrological model, which was a deterministic, physically-based, semi-distributed, event-based hydrological model, during its “setting-up” phase. The model was effectively calibrated and run for appropriately selected historic flood events recorded at a selected study area. Solid results from the analysis lead to the conclusion that the incorporation of the proposed methodology in a hydrological model yields accurate and representative simulations.

In order to verify the efficiency of the proposed methodology, a detailed sensitivity analysis was performed. Three sets of random values were properly selected for the five examined hydrological parameters and for these values, the performance of the hydrological model was tested using the Nash-Sutcliffe indicator. The set with the random values that yielded the best results was compared against the exact values suggested by the methodology, so as to check the proximity of the optimum values with the suggested ones.

The hydrological model was also set up and run for floods with return periods that correspond to high, medium and low probability of occurrence (*i.e.* T=5, 200 and 1000 years, respectively). The outputs of this hydrological analysis were imported in a set up hydraulic model and eventually flood hazard and flood risk maps were produced for the examined return periods for the selected study area. Given that the incorporation of the proposed methodology in a hydrological model yields accurate and representative simulations, its incorporation in a flood model chain results in the production of accurate flood hazard and flood risk maps. By that way, the developed methodology has been applied successfully for flood risk assessment, and can therefore support near-real time flood forecasting platforms and civil protection systems, as well as flood risk management on a planning basis at a later stage.

## **1.4 Innovative aspects of the research**

The methodology developed for this doctoral thesis leads to novel insights into effective post-fire flood risk assessment in the complex, easily variable and sensitive periurban Mediterranean environment. The innovative aspects of this research, are presented in the following paragraphs.

In this research, and as analyzed in Chapter 3, a clear distinction has been made between environmental and hydrological recovery. This distinction has not been

made so far in literature, where the term “*post-fire forest recovery*”, or else called “*relaxation time*” (Moody and Martin, 2001) is frequent. Both “*post-fire forest recovery*” and “*relaxation time*” refer to the so-called in this doctoral thesis “*environmental recovery*”, which concerns the canopy cover replacement and the recovery of the ecosystem services. Nevertheless, a key factor in hydrological studies, which is of particular interest and needs to be taken into consideration and should not be ignored, as is the current practice, is the (post-fire) stage when the hydrological response of a burnt catchment has recovered, for all practical (hydrological response) purposes, to its pre-fire state. This is the so-called in this research “*hydrological recovery*”, which is other than full vegetation recovery, as discussed in Section 3.3.2. Under particular conditions, analysed in this research, hydrological recovery may occur earlier than (a more complete) environmental recovery, as described above – a process that often takes several years (if at all) after a major fire event. This distinction is necessary for research on the post-fire hydrological response of a catchment, in order to avoid misinterpretations and misunderstandings.

Two additional innovations of this research include the transformation of fire severity into changes in the values of properly selected, representative hydrological parameters and thus the quantification of the impact of forest fires on the hydrological behavior of typical periurban catchments and eventually the incorporation of fire severity in hydrological modelling. The selected parameters affect all features of the simulated flood hydrographs, since they affect runoff discharge, peak volume and time to peak, and thus are parts of an integrated approach for the examination of the hydrological footprint of floods. Relevant, individual attempts to estimate the impact of forest fires on the values of some of the examined in this research parameters have also been made in the past (see also Chapter 3); however no other integrated and widely accepted approach was identified in literature.

In addition, the proposed methodology examines and quantifies the temporal evolution of fire impact in typical Mediterranean areas. The common practice (see also Chapter 3), is the examination of the fire impact only for recently burnt areas, focusing on the limited period between fire occurrence and the next growing season (e.g. Cerrelli, 2005; Higginson and Jarnecke, 2007) or the first couple of post-fire years (Cannon *et al.*, 2008; Rulli and Rosso, 2007; Inbar *et al.*, 1998; Scott and Van Wyk, 1990). However, fire impact is a phenomenon that changes dynamically in time and the proposed approach is innovative since it considers this fact and estimates not only an initial fire impact on hydrology, but also its temporal evolution and of course the period when this impact can safely be considered negligible, *i.e.* the time when hydrological recovery occurs.

Another scientific gap which has been identified through the literature review and is effectively addressed with this research is the consideration of soil moisture conditions when studying fire impact. Usually, the impacts of soil moisture and a forest fire are examined individually. However, the concurrent conditions of a recent forest fire and wet soil moisture conditions have an adverse impact on a catchment’s response, as they are associated with increased runoff volumes and peak flows and decreased times to peak. To this end, both initial conditions and



their interaction need to be co-evaluated in order to avoid underestimated catchment's responses and achieve more accurate results in flood simulations.

A major innovation of the proposed methodology, is the fact that it has been developed for typical Mediterranean periurban areas and is expressed in a generic way, so as to be easily adaptable to areas with similar hydrometeorological and geomorphological characteristics. The particular characteristics of those areas were examined in detail and the developed methodology is expressed via generalized equations that are adjusted to different case studies following specific guidelines. The methodology was then properly adjusted to a particular case study, the typical Mediterranean catchment of Rafina in Eastern Attica, as presented in detail in Chapter 7, in order to test its efficiency. For applications to other, similar areas, the temporal dimension of fire impact needs to be reexamined, taking into consideration local features such as indigenous vegetation, canopy and local climatic characteristics, vegetation development, fire-tolerance, regrowth *etc.* Particular cases when deviations from the proposed methodology may be observed and readjustment of the generic approach would be necessary are also discussed (Section 5.5).

Also, state-of-the-art tools and methods were applied for the testing of the efficiency of the methodology. In particular, a detailed sensitivity analysis, presented in Chapter 8, was performed in this research. Innovative aspects include an original code that was written in Matlab programming language for the generation of matrixes with random values for the selected hydrological parameters, the consideration in this code of Latin Hypercube Sampling (LHS), an efficient sampling method appropriate for this research, as well as an original procedure typified for the statistical analysis of the results of this research.

Finally, the proposed methodology can be easily automated and integrated in Early Warning Systems for floods and other operational systems for civil protection. As discussed in Chapter 2, such systems are very sensitive in the accuracy of their inputs. Additionally, no integrated approach for the incorporation of the combined fire and soil moisture impact on the hydrological response of a catchment supported by a Flood Early Warning System is identified in literature. Therefore, the import of more accurate information, in terms of the examined initial conditions, in these systems is another innovation that can be supported by this research.

## 1.5 Structure

The Thesis is structured as follows:

**Chapter 1** (*Introduction*) presents the context of this doctoral thesis, making a short introduction to the problems targeted with this research and the main challenges that had to be confronted. The primary aim, as well as the secondary objectives of the research are also discussed in this Chapter. Then the methodology that was undertaken in order to accomplish the purpose of this research is described in brief, it is followed by a brief presentation of the innovative aspects of the research that was performed and *Introduction* concludes with a short description of the content of all Chapters.

Chapter 2 (*Background – Natural hazards*) includes a literature review on natural hazards. The first Section includes facts and statistics for natural hazards in general, as well as a discussion on disaster management. Then, the Chapter focuses on floods and forest fires in periurban environments. Generation mechanisms, particular characteristics, impacts and risk management issues for each hazard individually are analyzed in detail in the second and third sections of Chapter 2.

Further to the significance of floods and forest fires as natural hazards that act independently, their interaction needs also to be taken into consideration in flood analyses. This interaction and more specifically the impact of forest fires on the hydrological behavior of a catchment and its assessment is analyzed in detail in Chapter 3 (*Floods-fires interaction*). A new scientific term is introduced and further discussed in this Chapter. This term is hydrological recovery, which refers to the conditions when the hydrological response of a burnt catchment has recovered to its pre-fire state and may occur a few years after a fire, as opposed to the environmental recovery, which is achieved with natural reforestation and ecosystem rebalance and is expected to occur far later than the hydrological recovery, while it may even not occur at all. The impact of floods on upcoming forest fires is also discussed in this Chapter. The Chapter *Floods-fires interaction* concludes with a Section on the existing knowledge gap in the quantification of fire impact on the hydrological behavior of a catchment, a gap that this research aims to bridge.

In order to perform a flood analysis two types of models need to be coupled: a hydrological model that will transform rainfall into runoff and a hydraulic model that will transform runoff into water levels along the river. A full list of state-of-the-art hydrological and hydraulic models, the capacities and characteristics of which are further tested, is presented in Chapter 4 (*Flood Modelling*). As mentioned above, the hydrological model that was selected for this research is the HEC-HMS model, while the selected hydraulic model is HEC-RAS. Both models are reliable, widely applied models, developed by the U.S. Army Corps of Engineers (USACE) Institute for Water Resources (IWR) and they are freely available through the website of the organization (<http://www.hec.usace.army.mil/software/>). Their selection is justified in this Chapter. The hydrographic network of the study area, as well as the subbasins and their particular geomorphological characteristics were defined and further analysed through the use of the HEC-GeoHMS module, a toolkit extent that operates in Geographic Information Systems (GIS) environment. For the geometry of the river sections another GIS extension, *i.e.* HEC-GeoRAS was used. Both modules are also developed by USACE and are freely available through the website of the organization.

Based on the extended literature review performed in the aforementioned Chapters, an innovative methodology for the appropriate selection of the values of five typical hydrological parameters, has been developed and is presented in Chapter 5 (*Methodology*). This methodology is a systematization of the interpretation of the dynamic change of initial conditions (in terms of forest fire occurrence and initial soil moisture conditions) in time into change in the values of the selected hydrological parameters and is generalized to the extent that this

is possible. The incorporation of the suggested changes in hydrological modelling is analyzed in detail in Chapter 5. This Chapter also includes a review on particularities of the first post-fire floods. Conditions under which the proposed methodology may need readjustment for the first post-fire floods are also discussed.

The study area of the proposed methodology is described in Chapter 6 (*Study area*). The methodology has been applied in Rafina catchment, a typical Mediterranean periurban area in Eastern Attica that extends over approximately 130 km<sup>2</sup>. The area has been carefully selected, in order to fulfill the requirements of an area with a typical Mediterranean climate, variable and to a certain degree conflicting land uses, for which reliable hydrometeorological and other datasets of relevance to this research are available for further analysis and exploitation. Another reason for the selection of Rafina catchment for this research is the fact that this area is particularly prone to floods, for several reasons analyzed in Chapter 6, while at the same time it has suffered from successive forest fires in the recent past. Therefore, Rafina catchment prevails as the optimal catchment for research on the forest fire impact on the hydrological behavior of typical Mediterranean periurban catchments.

Since the proposed methodology is presented in Chapter 5 in a generic way, aiming to be easily applicable in other catchment with similar hydrometeorological and geomorphological characteristics, Chapter 7 (*Adjusting the methodology to the study area*) describes the adjustment of the methodology to the study area. The fire impact of a recent fire in the area is estimated, while initial soil moisture conditions are calculated for selected rainfall events. Then, the selected hydrological model is set up for the study area and calculations are made for the estimation of the exact values of the examined hydrological parameters for variable initial conditions. Then the hydrological model is run in an event-based mode for the selected events.

Chapter 8 (*Results and discussion*) includes the results of the analysis and a relevant discussion. Initially, the results of the hydrological modelling for selected flood events when the methodology is applied and when the methodology is ignored are presented and compared against observed datasets. A detailed sensitivity analysis that serves a twofold purpose has been performed. On the one hand, the impact of each examined parameter on runoff volume, as well as the suggested by the methodology post-fire changes on the parameters were quantified and on the other hand an analysis was performed for efficiency testing of the methodology. According to this analysis, the hydrological model runs for different, properly selected values for the selected parameters. More specifically, a code was written in Matlab for the generation of three sets of random numbers that are within narrow, moderate and wide marginal limits respectively. Simulated flows for the different runs are compared against observed flows in order to identify the parameter values that correspond to the best model runs and compare these values against the values suggested by the methodology. The hydrological model is then coupled with the selected hydraulic model and the model chain runs for different design storms, taking also into consideration different initial conditions in terms of soil moisture and forest fire occurrence. The design storms selected for the coupled model runs refer to floods with low, medium and high probability

of occurrence, as suggested in EU Floods Directive 2007/60/EC and in particular floods with return periods equal to 5, 200 and 1000 years respectively. The core outputs of the model chain runs are flood hazard maps and flood risk maps for different return periods and variable initial conditions. Chapter 8 concludes with a discussion on the results of the different analyses presented above.

The conclusions of this doctoral thesis are summarized in Chapter 9 (*Conclusions*). This Chapter includes an overview of the main findings from the research, focusing on the core findings from the proposed methodological framework for the estimation of the impact of initial conditions, in terms of forest fires and soil moisture, on a catchment's hydrological behaviour, main findings from the adopted methodology for the overall implementation of the research, as well as main findings for the particular case study. A dedicated Section with all the conclusions of the research performed is foreseen in this Chapter, which eventually concludes with recommendations regarding interesting fields for further research.

In order to complete this innovative research and ensure that its outcomes will be scientifically sound and technically correct, and as also mentioned above, a thorough literature review had to be performed on numerous aspects of this research. References include scientific publications and other relevant works found in international literature and are all listed in alphabetical order in Chapter 10 (*References*).

# CHAPTER 2: BACKGROUND – NATURAL HAZARDS, FOCUSING ON FLOODS AND FOREST FIRES

## 2.1 Natural hazards

### 2.1.1 Facts and statistics about natural hazards

Natural hazards are severe and extreme natural phenomena, the occurrence of which is often associated with tremendous impacts on people (human life, health), society, economy and the environment. Due to their significant footprint, natural hazards become natural disasters upon occurrence. Natural hazards can be classified into geophysical hazards, hydrometeorological hazards and other hazards. *Geophysical hazards* are related with the geological characteristics of an area and include *inter alia* earthquakes, volcanic eruptions and lahars<sup>1</sup>, sinkholes, tsunamis, landslides and rock falls. *Hydrometeorological hazards* are primarily related with the weather and the climate of an area and include *inter alia* floods and flash floods, forest or wildland fires, droughts, avalanches, tropical cyclones, severe thunderstorms, tornadoes, hailstorms, ice storms, thermal extremes and strong winds (WMO, 2014). Natural hazards that may not be classified into either of these two categories, for example diseases, insect infestations *etc.*, may be classified as *other natural hazards*.

As mentioned above, natural disasters are associated with severe impacts on humans, society, economy and the environment both on a short-term and on a long-term basis. The most significant short-term impacts are the loss of human lives, human health problems and damages or even total destruction of properties and infrastructure. On a long-term basis, the environmental degradation and the severe deterioration of ecosystem services need to be considered, as well. The direct impact of natural disasters on humans for the period 2002-2012 on a global scale is illustrated in Figure 2.1, while indicative figures of their impact on economy for the period 1980-2012, on a global scale as well, are presented in Figure 2.2. Based on information retrieved from PreventionWeb of the United Nations Office for Disaster Risk Reduction (UNISDR) and especially for the period 2000-2011, the overall impact of natural disasters on humans and economy on a global scale is illustrated in the following figures: 1.1 million of people were killed, 2.7 billions of people were affected and total damages reached approx. 1 trillion Euros.

---

<sup>1</sup> Eruptions of (glaciated) volcanoes, which include large masses of water (from melted ice) mixed with sediment, rock and ash (Vallance and Iverson, 2015).

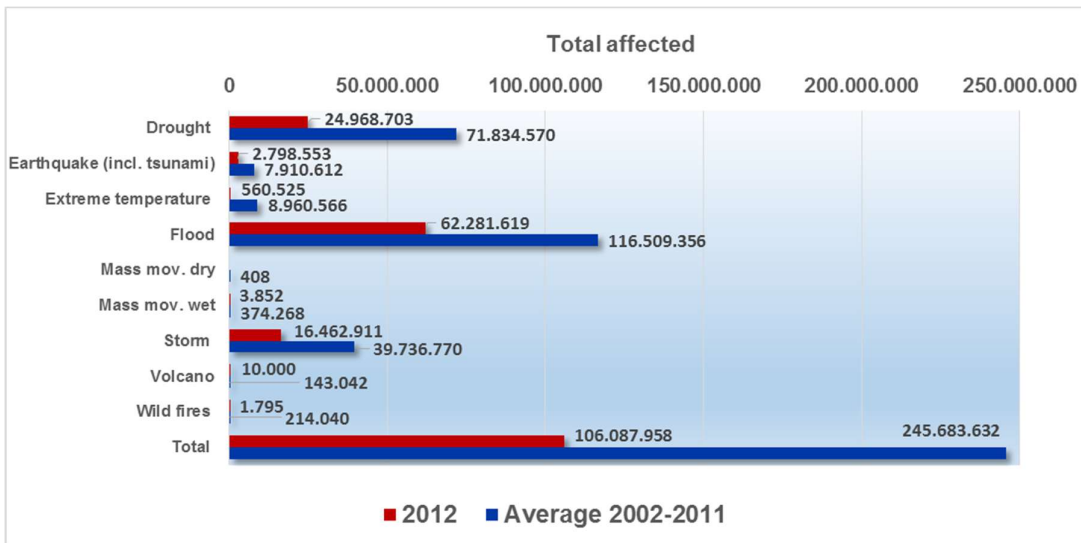
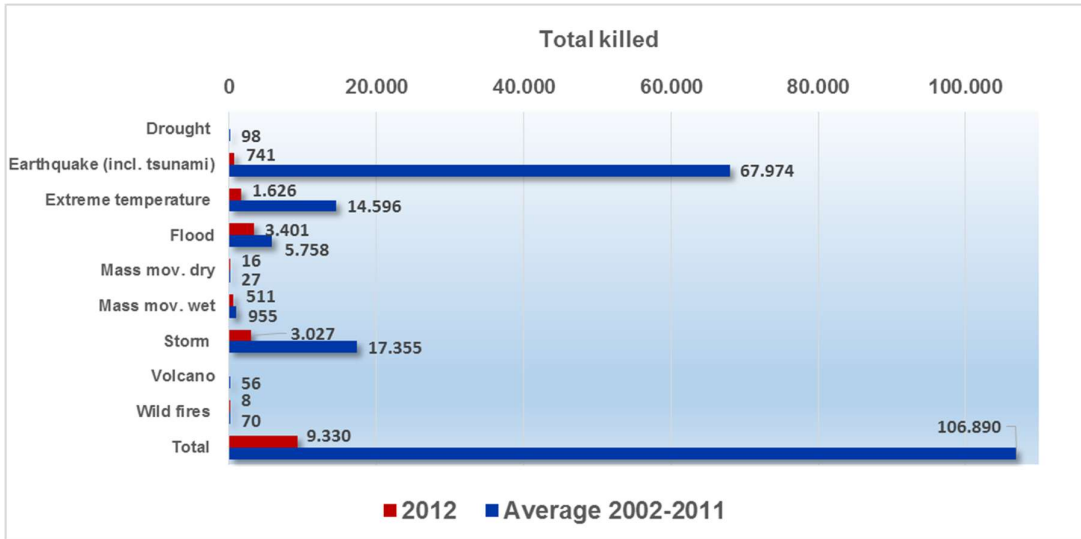


Figure 2.1. Statistics for the impact of natural disasters on humans (total killed top, total affected bottom) for the period 2002-2012 on a global scale (Source: PreventionWeb of the UNISDR).

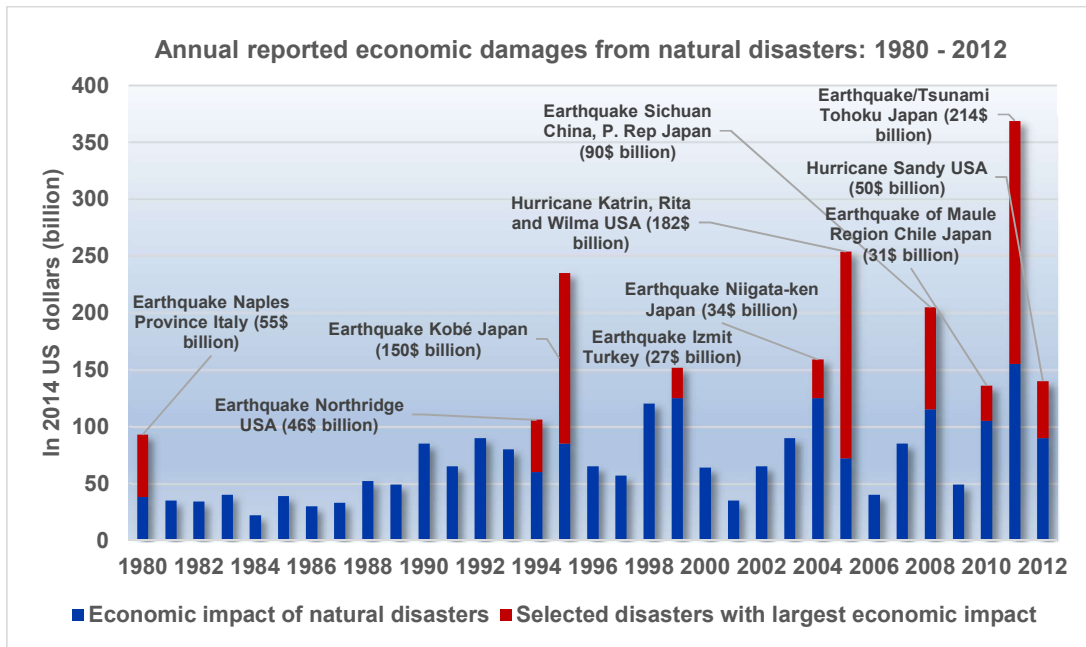


Figure 2.2. Statistics for the impact of natural disasters on the economy for the period 1980-2012 on a global scale (Source: PreventionWeb of the UNISDR).

It becomes obvious that, practically, natural hazards can occur in any part of the world. Nevertheless, some areas may be characterized as more prone to specific natural hazards in comparison to other areas, mainly due to their particular climatic, hydrometeorological, geological and topographic features, urbanization rate and particularly for diseases sanitation standards. In addition, some of these disasters are quite frequent, while others are very rare; yet, associated with more severe impacts. The frequency of occurrence of each natural hazard depends on numerous parameters, the most important of which are the area particularities as mentioned above and of course the nature of the hazard itself, which may be associated with special conditions (e.g. volcanic eruption). An indicative illustration of the geographical extent of natural disasters in 2012 is presented in Table 2.1, while a graph with the frequency of occurrence of the most significant natural disasters during the period 2002-2012 is presented in Figure 2.3.

*Table 2.1 Statistics for the geographical extent of natural disasters in 2012  
(Source: PreventionWeb of the UNISDR).*

<b>Natural disasters by number of deaths – 2012 (incl. reported missing persons)</b>			
Tropical storm “Bopha”, December		Philippines	1901
Flood, August - October		Pakistan	480
Flood, July – October		Nigeria	363
Earthquake, August		Iran Islam Rep.	306
Cold Wave, June		Peru	252
Flash Flood, July		Russia	171
Cold Wave, December		Russia	170
Flood, July		Korea Dem. P. Rep.	169
Flood, July		China, P. Rep.	151
Avalanche, April		Pakistan	135
<b>Number of reported natural disasters by country – 2012</b>		<b>Total killed and affected people by natural disasters per 100.000 inhabitants – 2012</b>	
China, P. Rep.	23	Somalia	29.840
Philippines	20	Gambia, The	23.463
United States	17	Paraguay	23.071
Indonesia	12	Chad	20.995
Afghanistan	11	Zimbabwe	14.312
India	10	Angola	14.033
Russia	8	Philippines	12.557
Japan	6	Malawi	12.509
Bangladesh	5	Guatemala	11.305
Pakistan	5	Kenya	10.065



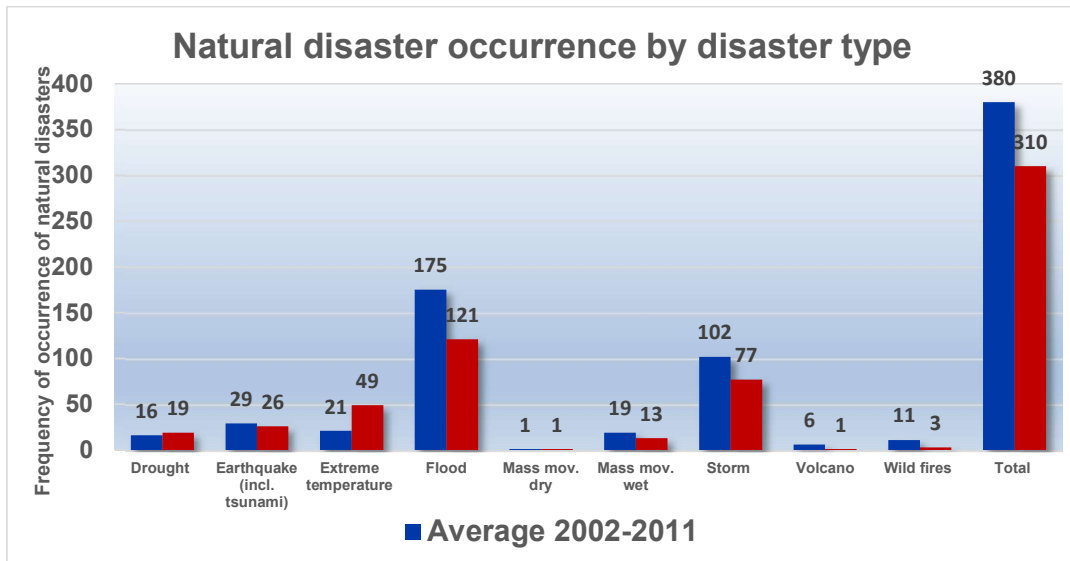


Figure 2.3. Statistics for the frequency of occurrence of significant natural disasters for the period 2002-2012 on a global scale (Source: PreventionWeb of the UNISDR).

### 2.1.2 Disaster management

The previous figures assist in illustrating in brief the dire consequences of natural disasters. However, the hydrometeorological and geological processes that determine the occurrence of natural hazards cannot be easily, if at all, managed and are not fully predictable. Hence, the reduction of the likelihood of occurrence of natural hazards becomes uncertain and to some extent problematic. At the same time, the impact of natural disasters on humans and the environment has been dramatically intensified, as a result of the population growth and expansion, which is in constant increase.

Therefore, disaster management becomes an issue of vital importance. The core components of efficient disaster management are: *Prevention and Mitigation*, *Preparedness*, *Response* and *Recovery*. The relationship between these components is rotational and is better presented through a Disaster Management Cycle. Schoupe (2008) incorporated two additional components: *Alerts* and *Post Disaster*. A comprehensive disaster management cycle is presented in Figure 2.4.

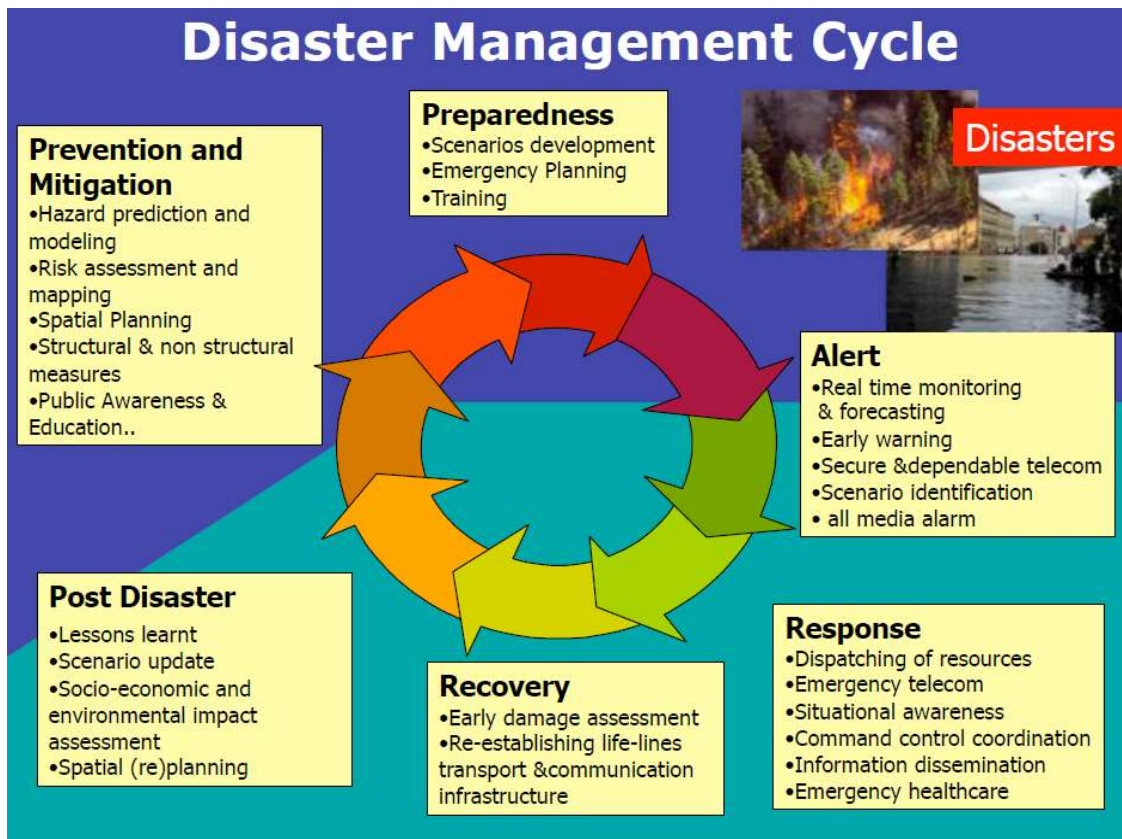


Figure 2.4. Disaster Management Cycle (Source: Schoupe, 2008).

*Prevention and Mitigation* include activities undertaken prior to a disaster. These activities include capacity building through scientific and technical progress, as well as awareness raising and education. Scientific progress will contribute to a better understanding of the generation mechanisms of natural hazards and the processes involved with their occurrence, while technical progress will enable the adoption of continuously improved engineering practices in relevant measures. Through education and public awareness people become familiar with technological achievements (e.g. issued hazard warnings) so as to fully exploit them when necessary. *Preparedness* involves activities undertaken on a central basis and also prior to a disaster. These activities support contingency planning through the development of hazard and disaster management plans and response scenarios (e.g. evacuation plans), as well as appropriate training, through which people become aware of emergency management plans and procedures and thus are prepared against natural hazards. An initiative of UNISDR has been the development of “Regional platforms for disaster risk reduction” on a global scale. Particularly for Europe, the European Forum for Disaster Risk Reduction (EFDRR) brings together regional organizations and representatives from other national platforms in Europe and facilitates discussions and exchange of experiences on disaster risk management issues (EFDRR, 2011).

*Alerts* involve real-time monitoring and accurate forecasting of conditions, primarily hydrometeorological, that may trigger a natural disaster and the issuing of early warnings. *Response* concerns real-time conditions and includes the

undertaking of necessary actions (planned during the previous phases) in order to mitigate the impacts of a hazard. These actions include issuing of alerts (usually filtered when disseminated to the public), emergency operation of hazard protection engineering works (e.g. bank strengthening, watercourse diversion to drainage networks) etc. *Recovery* refers to the early post-disaster period and includes an initial damage assessment and the re-establishment of destroyed infrastructure and public utilities. On a long-term basis, *Post disaster* refers to the re-evaluation and if necessary re-planning of the previous activities, which will be based on thorough socio-economic and environmental impact assessment.

The research performed for this research focuses on the hydrological behavior of typical Mediterranean periurban areas. As a result of climatic conditions, geomorphological and land cover properties, as well as increased urbanization rate in some cases, these areas are severely affected by two of the most significant, in terms of impact, natural hazards, *i.e.* floods and forest fires. In Sections 2.2 and 2.3, additional information for these two natural hazards is presented. A discussion on Early Warning Systems for floods is presented in Section 2.2.1.5, while Section 2.3.1.5 includes information on a particular method for fire danger management.

## **2.2 Floods**

### **2.2.1 Facts and statistics about floods**

Since the dawn of civilization, man appears to contend with floods. Legends describing severe floods that have allegedly inundated the whole surface of Earth thrive in human cultures all over the world. Typical legends presenting man striving for his life against this natural hazard, which remarkably share numerous features, stem from ancient Babylon, ancient Greece, China, Lithuania, the Norsemen in ancient Scandinavia and the Indians of South and North America (several legends are presented in Champ, 1986). Already in ancient civilizations, flooding and the protection against it are present in everyday life. This becomes evident not only through surviving legends from ancient mythology, which usually present flooding as the worst disaster of all<sup>2</sup>, but also through other official documents (e.g. construction and maintenance of flood protection works are mentioned in Hammurabi's Code), as well as through the fact that quite often historical floods constitute fundamental elements of several religions (e.g. the flood of Noah described in the Old Testament).

#### **2.2.1.1 Principal cause and generation mechanisms**

Floods are a natural hazard and are therefore triggered by a purely natural cause, *i.e.* precipitation. In many cases, floods are associated with severe precipitation, however, for the reasons presented in the following, this may not always be the case. In particular, the flooding of a certain area depends strongly on several additional factors which may worsen the impact of precipitation or even cause flooding when precipitation *per se* would not be adequate to do so.

---

<sup>2</sup> The Sumerian god Enlil punished people for being too noisy by sending them *the worst possible disaster: a flood* (Champ, 1986).

These additional factors, which eventually undertake the role of flood generation mechanisms, can be classified into natural and anthropogenic (or human-induced). The natural flood generation mechanisms are associated with hydrometeorological, geomorphological and topographic features of a catchment and include *inter alia* early and sudden snowmelt due to warm wind, clogged loamy soils, sparse or burnt vegetation, considerable rivers slopes and steep hills within a catchment (Champ, 1986). The anthropogenic flood generation mechanisms include *inter alia* urbanization and the entailed increase of impervious areas, clogging of sewer systems and improper maintenance of sewer network (Figure 2.5) and river reaches, debris discarded in rivers, improper design of or under dimensioned hydraulic works aimed to manage floods (e.g. levees, river regulations) and improper operation or even structural failure of hydraulic works aimed to manage floods (e.g. release of massive water volumes from upstream dams to the downstream areas for maximization of potential hydropower (Papathanasiou *et al.*, 2013c), not controlled spillway discharges or dam break). It becomes obvious that the aforementioned factors may be determinant of a flood event irrespective of the amount of precipitation during a given rainfall event, and for this reason the natural trigger of floods becomes precipitation and not exclusively severe precipitation.



*Figure 2.5. Clogging of sewer systems from tree leaves and litter (personal archive).*

### **2.2.1.2 Flood characteristics**

Each flood has its particular characteristics that are evaluated in order to estimate the severity of a flood event, in terms of its subsequent damages and impacts on humans and the environment. Significant flood characteristics that may serve as metrics for the estimation of flood severity are described in the following, regardless of the activated flood generation mechanisms that may cause a flood event.

One of the most important characteristics of a flood is water depth. It is estimated either along a river (flooding occurs when water depth exceeds case-specific thresholds) or over inundated areas that are normally not covered by water. It is expected that water depth varies over the whole flooded area, depending on its geomorphology and the permeability of its particular land cover types. A flood event is also characterized by its extent. Flood extent expresses the spatial extent of a floodplain and together with water depth they support the generation of flood hazard maps, as specified in EU Floods Directive (Directive 2007/60/EC). Another characteristic of a flood is its duration, *i.e.* the time from inundation to the recession of ponding water from areas that are normally not covered by water. This factor also depends strongly on geomorphology and land cover permeability and determines to a certain extent the damages caused by a flood. Floodwater velocity (both in the river and the floodplain) also characterizes a flood. Hydraulic models, described in detail in Section 4.4, are widely applied tools for a representative estimation of floodwater velocity (FEMA, 2009). Other flood characteristics include its erosional capacity, *i.e.* the capacity of moving flood water to remove soil from the ground surface (FEMA, 2009) and its alluvia storage capacity, as well as the shape, volume and growth rate of flood waves.

An additional factor that characterises a flood is flood frequency. It expresses the probable frequency of occurrence of a given flood and refers to a particular area. Flood frequency can be expressed through several ways, such as *Return Period* (T), *Annual Exceedance Probability* (AEP) and *Probable Maximum Flood* (PMF) of particular floods.

*Return Period* or else called *Recurrence Interval* (Dinicola, 1996) refers to the average time period (in years) between floods of certain extent. High, intermediate or low return periods correspond to events of low probability (extreme events), medium probability or high probability of occurrence, respectively. A flood of a particular return period may occur more than once during the given period. A typical example concerns Mississippi river, where floods of T=100 years return period occurred 4 times within 8 years (in 1943, 1944, 1947 and 1951) (Champ, 1986). Return period is widely used among hydrologists, yet it may be confusing or even misleading for the general public. To this end, the use of the less confusing term *Annual Exceedance Probability* is encouraged by several agencies, such as USGS (Holmes and Dinicola, 2010). *AEP* is the probability that a particular flood will occur in any year and is expressed as a percentage (%). For example a 1% AEP flood has 1% chance of occurring in a year; hence it is expected to occur once every 100 years. *Probable Maximum Flood* is the theoretically largest flood that can result from the combination of the most severe hydrometeorological conditions that could potential occur in a given area (FERC, 2001). This term is widely used in the design of hydraulic structures such as dams, and also as a security assessment for relevant existing structures.

As mentioned above, the aforementioned quantifiable characteristics support the estimation of the extent of damages caused by a flood and thus the estimation of its severity. In general, their values vary for different flood types, described in the following Section.

### 2.2.1.3 Flood types

Floods can be further distinguished into different types, according to their generation mechanisms, their impacts and their area of impact. Sometimes definitions of different flood types overlap and additional information is required for their classification. Each flood type is associated with different socioeconomic impact, while different areas are prone to specific flood types depending on their geomorphologic features and their hydrometeorological regime. The most common flood types are presented in the following.

A typical classification of floods includes fluvial, coastal or pluvial flooding. *Fluvial flooding* occurs when water bodies (rivers, streams, creeks or lakes) overflow their banks as a result of continuous or intensive rainfall. Particularly for rivers, fluvial flooding is also called *riverine* (FEMA, 2009) or *river flooding*, whereas for lakes the term lake flooding (French *et al.*, 2005) is also used. *Coastal flooding* occurs when extreme tidal conditions, including high tides, storm surges and tsunamis, result in the seawater intrusion in low-lying and normally dry land. *Pluvial flooding* occurs when water that comes from heavy rainfall does not enter the drainage network (usually when it has reached its capacity) or watercourse and is ponding or flowing over the ground surface instead. Pluvial flooding is also known as surface water runoff (Lester and McNally, 2012).

Floods are also distinguished into regional and flash floods, based again on their generation mechanisms and also on their impacts. Regional floods (also known as slow floods) are caused by sustained and sometimes heavy rainfall usually during the snow-melting season. Reduced infiltration due to frozen ground or saturated soil increases runoff and magnifies their impact (Perry, 2000). These floods affect medium and large size catchments, which exceed a few thousand km<sup>2</sup>. The area is inundated within a relatively long time due to the advancing of water from upstream river zones. Usually, regional floods extend over large surfaces and they have a long duration, ranging between a few days for medium scale catchments to weeks or even months for large scale catchments (Dougherty, 2011). On the other hand, flash floods occur due to rainfall activity (increased intensity and/or duration), reduced infiltration (e.g. soil clogging, urbanization and therefore increased impermeable soils) and particular geomorphology (e.g. steep slopes, dense hydrographic network). Flash floods affect small catchments (extending over a few hundred km<sup>2</sup>). They produce rapid rises in water levels and are associated with high flow velocities. On the contrary to regional floods, it may take several seconds to several hours to a rainfall to evolve into a catastrophic flash flood (Perry, 2000), while their duration is usually reduced (typically being restricted to a few hours).

As mentioned in the anthropogenic flood generation mechanisms (Section 2.2.1.1) improper design and improper operation or even destruction of hydraulic works that aim to manage floods can also result to *structural failure floods* or *overtopping floods*. They occur downstream of dams and areas protected by levees, when the hydraulic works are inadequately designed (under dimensioned), inadequately constructed or when their design capacity is exceeded. The water released after dam overtopping or levees failure carries tremendous energy and becomes a catastrophic flash flood (Perry, 2000).

Another common flood type which incorporates in its definition different flood types mentioned above is *urban flooding*. This type of flooding concerns flooding within an urban area, due to pluvial flooding (e.g. due to clogging or overflow of drainage network) or fluvial flooding (flooding of urban rivers) or more rarely due to structural failure or overtopping flooding (e.g. failure of flood protective upstream dams). Regardless of its generation mechanism, urban floods always share the characteristics of a flash flood due to the increased impermeability of the land cover and thus are particularly destructive and dangerous.

#### **2.2.1.4 Flood impacts and statistics**

The impacts of floods on humans and the environment are presented in brief in the following. Casualties constitute their most severe direct impact on humans. In classical mechanics, the kinetic energy of the water, and consequently the power of the water, increases with the square of its velocity (Eq. 2.1).

$$E_k = \frac{1}{2}mV^2 \text{ (Eq. 2.1),}$$

where:

$E_k$  = kinetic energy of a body [J],

$m$  = mass of a body [kg] ,

$V$  = velocity of a body [ $m*s^{-1}$ ].

During a flood, this velocity can reach 32 km/h and hence the power of water is sufficient to remove almost any obstacle, and carry away and ultimately drown people (Champ, 1986). In addition, floods are followed by severe socioeconomic damages. More specifically, their major social impact is their impact on human health, since stagnant waters often contain pathogens, which may trigger the evolving of contagious diseases, such as cholera and typhus, to deadly epidemics (Champ, 1986). Typical socioeconomic impacts include increased number of homeless people, destroyed crops, damages on a country's infrastructure, public utilities and other public and private works (e.g. communication systems, road network, electricity). Finally, floods are associated with severe environmental consequences, as a result of destruction of wetlands, inundation of point pollution sources such as industrial units and installations that contain large quantities of chemicals and toxic materials (e.g. pesticides and paints) etc. Evidently, the aforementioned impacts are magnified in case of frequent recurrent and devastating floods.

Flood impacts vary in space and depend on flood characteristics and flood type. In order to generalize the estimation of a flood impact, floods may be classified into different categories, based on their effect on humans and the environment and expressed in quantitative terms. A typical example is the US National Weather Service (NWS) that has defined different levels of flood severity, *i.e.* minor, moderate, major and record flooding, based on public threat posed by a flood and eventual property damage (US NWS, 2004).

It is highlighted here that water that overtops a river's banks supplies the adjacent areas with water, humidity and nutritional matters. Hence, from an ecological perspective, when these areas are rural, agricultural areas, flooding may even be beneficial. However, even in such cases and despite the moderate human activity

in such areas, flooding may become detrimental or even destructive, for example for specific cultures.

In an attempt to quantify the impact of floods, relevant information and statistics from historical floods were collected and are presented in the following. As a result of the flooding of Arno in Florence in 04/11/1333, 300 people lost their lives, while a new flooding of Arno in 1547 brought about the death to another approx. 100 people (Champ, 1986). According to a relevant study, between 1947 and 1967 173.170 people lost their lives due to direct consequences of river flooding, while in total 269.635 people lost their lives due to 18 other disasters, such as hurricanes, tornados, volcanic eruptions etc (Champ, 1986). In 1955 floods affected North India and caused the destruction of hundreds of villages, leaving tens of thousands of people homeless (Champ, 1986). In United States, damages from floods caused by hurricane Agnes in June 1972 reached 10 Million Euros, while this sum was overrun in September 1975 when damages from floods caused by the hurricane Eloise reached 13.6 Million Euros (Champ, 1986). In Australia, floods are characterized as “*the most expensive natural disaster*” (Queensland Government, 2011), with its direct costs for the period 1967-2005 averaging at approx. 254 Million Euros per year. During the period 1998 and 2002 Europe suffered from more than 100 devastating flood events, including the major floods in Danube and Elbe Rivers in the summer of 2002. As a consequence of these floods, approx. 700 people lost their lives, approx. 500.000 people were displaced, while insured economic losses exceeded  $25 \cdot 10^3$  Million Euros (EEA, 2004). Additional statistics for floods are presented in Figures 2.6 – 2.12.

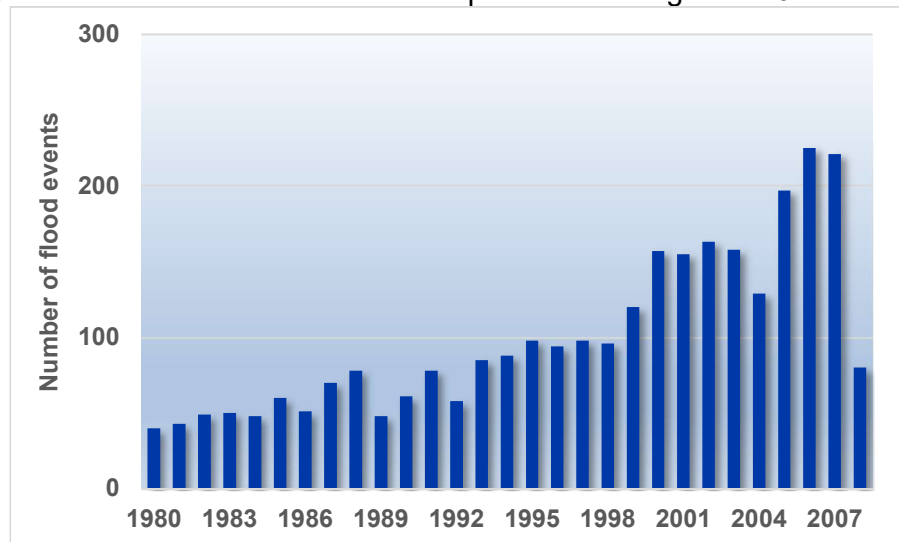
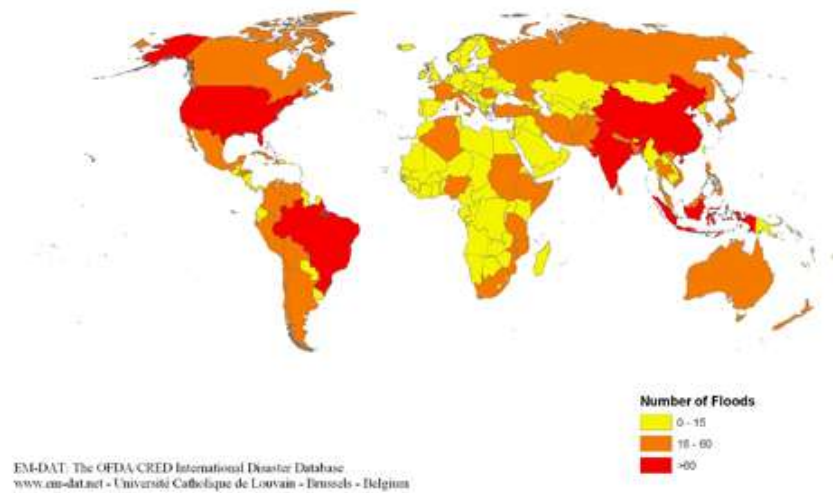


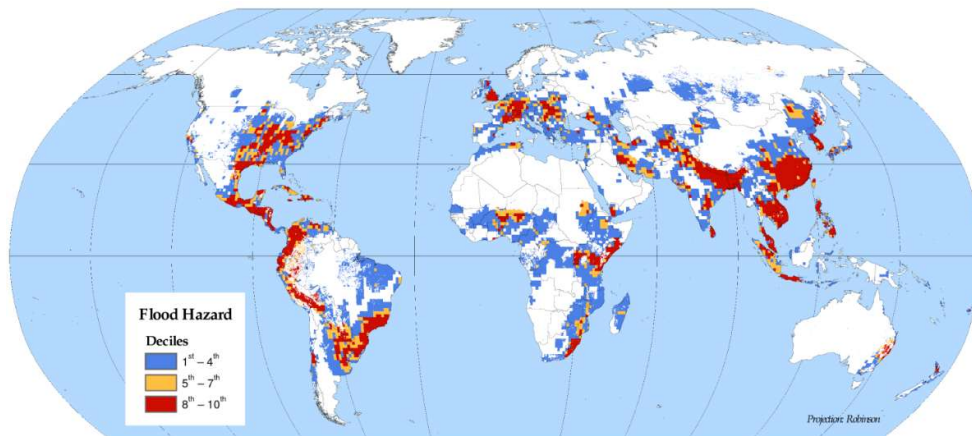
Figure 2.6. Flood events reported during the period 1980-2008 on a global scale (Source: PreventionWeb of the UNISDR).



**Number of Occurrences of Flood Disasters by Country:  
1974-2003**



*Figure 2.7. Flood disasters by country reported during the period 1974-2003 on a global scale (Source: EM-DAT: The Emergency Events Database – Université catholique de Louvain (UCL) – CRED, D. Guha-Sapir – www.emdat.be, Brussels, Belgium).*



The data set comes from the Dartmouth Flood Observatory's global listing of extreme flood events compiled from various sources for the 19-year period from 1985 – 2003. Some flooding is evident in more than one-third of the world's land area.

*Figure 2.8. Flood hazard distribution during the period 1985-2003 on a global scale (Source: Dilley et al., 2005).*

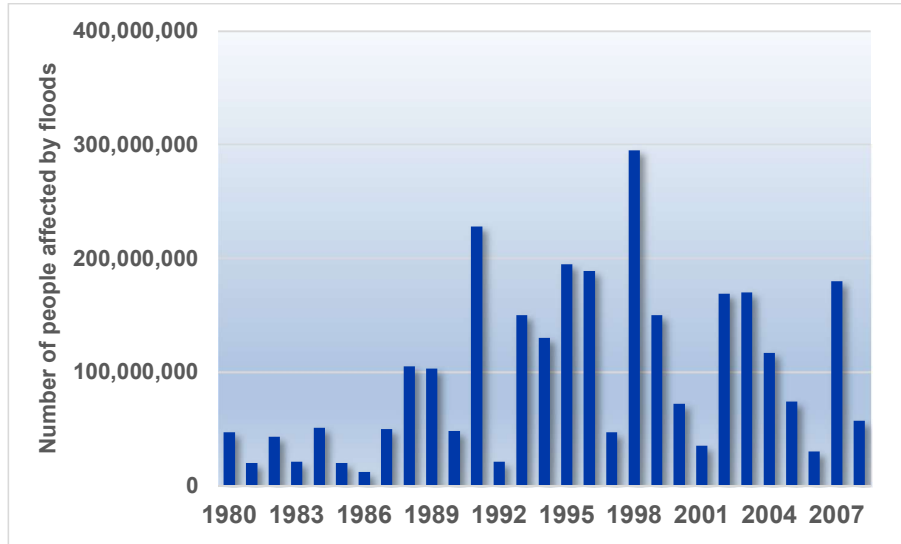


Figure 2.9. The number of people affected by floods during the period 1980-2008 on a global scale (Source: PreventionWeb of the UNISDR).

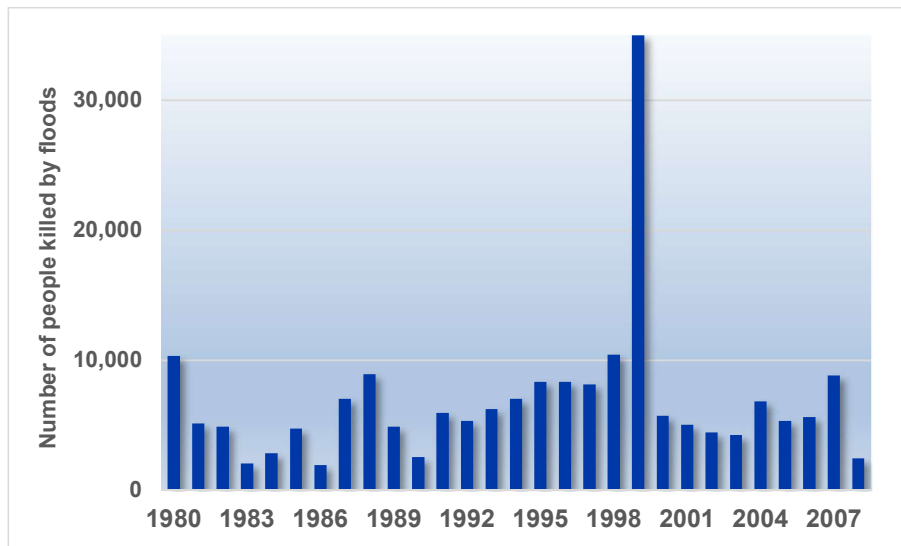


Figure 2.10. The number of people killed by floods during the period 1980-2008 on a global scale (Source: PreventionWeb of the UNISDR).

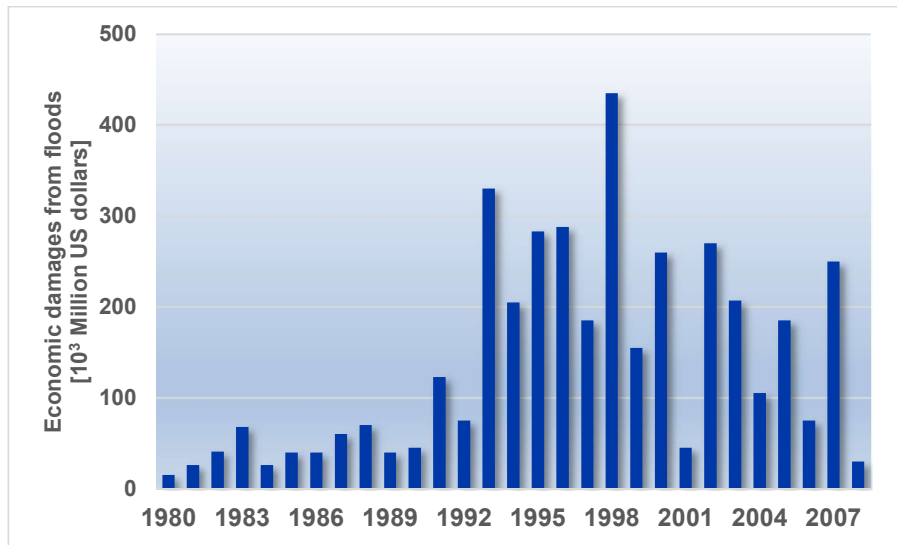


Figure 2.11. The reported economic damages (in 10<sup>3</sup> Million US dollars) from floods that occurred during the period 1980-2008 on a global scale (Source: PreventionWeb of the UNISDR).

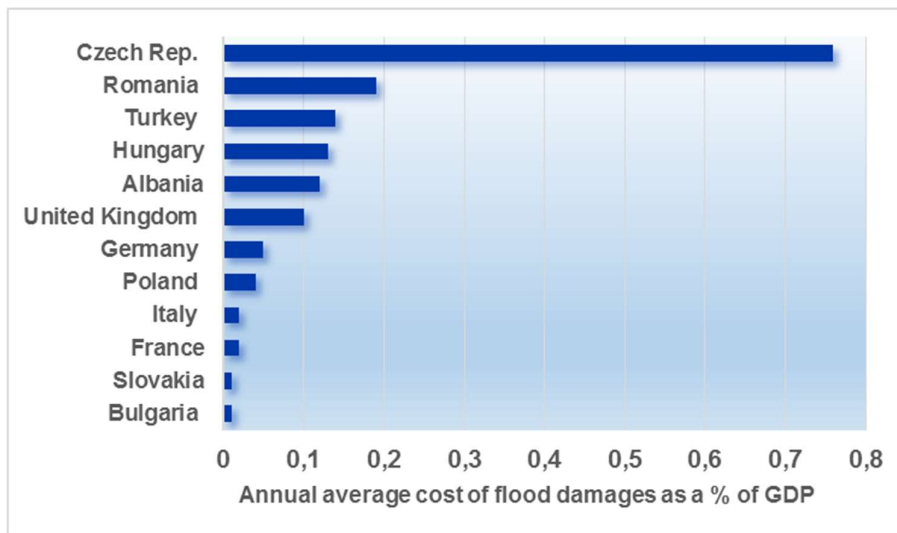


Figure 2.12. The annual average cost of flood damages as a percentage of the Gross Domestic Product (GDP) during the period 1998-2002 for the most affected EU countries (Source: EM-DAT – The International Disaster Database).

As an overall conclusion drawn from this research and illustrated in Figures 2.6 – 2.12, floods prevail as the most frequent and one of the most devastating natural hazards on a global scale.

### 2.2.1.5 Flood Early Warnings Systems

For the reasons presented in Section 2.2.1, flood risk management is now widely acknowledged as an issue of strategic importance for both socioeconomic and environmental reasons. However, despite the global wealth of experience in flood risk management and the standardization of measures and practices for its

efficient handling, this field remains still open to further research. It is noted here that different flood types have different particular characteristics and thus require different risk management strategies. In general, measures and practices for efficient flood risk management are incorporated in the components of the Disaster Management Cycle discussed in Section 2.1.2.

Flood Early Warning Systems (FEWSs) are smart systems that issue timely and accurate flood warnings when necessary and may contribute significantly in efficient flood risk management. Such systems are effective when they issue early warnings for decision makers within reasonable time, so as to provide them with sufficient time in advance to act. It needs to be considered that the operation of most of these systems relies on complicated computational methods that often require a lot of time (sometimes hours or even days) to run, thus making it challenging to keep pace with fast-changing situations (Duncan *et al.*, 2013), which is common during flash floods.

In addition, issued warnings need to be as accurate as possible. Such systems are associated with inherent uncertainty that can be propagated all the way down from system inputs (*i.e.* hydrometeorological information, weather forecasts *etc.*), to its components (*i.e.* incorporated models and other computation structures) and eventually its final outputs (*i.e.* the issued warnings).

Nowadays, modern technology and state-of-the-art tools enhance significantly the capabilities of meteorologists and hydrologists in terms of flood risk assessment (Champ, 1986). Technological achievements are widely used in remote sensing. Weather radars, satellite imagery, as well as sensors that automatically record the values and the fluctuation of hydrometeorological parameters at selected sites within a catchment constitute fundamental elements of an enhanced monitoring of a catchment's hydrometeorological regime, which is necessary for efficient FEWSs. Therefore, weather forecasts, which are core inputs in FEWSs, are issued timely and are more accurate. Additionally, powerful computers and enhanced processing software, combined with accumulated experience of modelers, enormously improve the accuracy and representativeness of simulation results. Consequently, accurate and timely weather forecasts and efficient flood modelling outputs support the issue of more precise flood warnings.

Nevertheless, the occurrence of a flood depends strongly on numerous, interrelated and difficult to foresee and manage parameters. Therefore, despite the undoubtful progress in the representativeness of inputs and outputs of FEWSs, uncertainty still exists in the issued warnings. To this end, a proper and integrated exploitation of effective techniques, datasets *etc.*, as well as the regular update of adopted methodologies and applied tools in FEWSs, become priority issues in order to further enhance the efficiency of early warnings for floods. Approaches that can be easily adopted in robust FEWSs and support their seamless operation are necessary. This research considers these elements and concludes with the development of a methodology (presented in detail in Chapter 5) for efficient post-fire hydrological modelling that can be easily incorporated in relevant FEWSs. From this perspective, FEWS are applications that may improve the accuracy of issued warnings when considering the proposed methodology.

## 2.3 Forest fires

### 2.3.1 Facts and statistics about forest fires

Similarly to floods, forest fires had always been a major hazard that affected humans and the environment. Archeological findings and, when available, written evidence reveal the occurrence of large scale fires that have severely affected the socioeconomic status of affected areas. The recorded fire events refer primarily to city fires (e.g. *the Great Fire of Rome (64 A.C.), a great fire that burnt down much of Constantinople (406 B.C.), the Great Medieval fires of London (1135 and 1212)*) and building and structure fires (e.g. *the burning of the 1<sup>st</sup> temple in Jerusalem (586 B.C.), the burning of Acropolis in Athens during the 2<sup>nd</sup> Persian invasion of Greece (480 B.C.), the burning of the temple of Artemis at Ephesus (356 B.C.)*), which were basically arsons or accidental urban fires. Information on ancient forest fires is limited, yet wildfires are recorded systematically since the early 19<sup>th</sup> century. Fire scars observed on tree rings are a common source of information for historic fires and overall past canopy disturbances (Figure 2.13).



Figure 2.13. Close up of tree ring with fire scars (Source: Laboratory of Tree-Ring Research, University of Arizona, Photo by Tom Swetnam, available at: <http://www.ltrr.arizona.edu/~sheppard/swland/scartree.html>).

#### 2.3.1.1 Forest fire ignition sources

The ignition sources of forest fires are either natural or anthropogenic. In the first category, lightning strikes seem to be the most frequent source, especially at the start of the wet period, when the biomass has dried out completely and strong winds and frequent lightning strikes, sometimes not even followed by rainfall, may occur (Heinl *et al.*, 2007). Anthropogenic induced fires may be either accidental or set in purpose (e.g. an arson or a fire set in order to induce grass regrowth for grazing animals, to clear land and remove dead biomass for the subsequent cultivation and harvesting periods *etc.*). Especially when logging activities take place, slash left on site corresponds to high fuel loads and forest fire danger is increased. Regarding the principal ignition source of forest fires in Europe, and as also discussed in Section 2.3.1.4, their overwhelming majority concerns human-induced forest fires (San-Miguel-Ayanz *et al.*, 2012).

Human-related factors, such as rural out-migration and abandonment of agricultural lands, induce changes in plant cover composition and structure (Mayor *et al.*, 2007) and increase the number of wildfires on a global scale. In addition, increased temperatures and prolonged dry periods are expected to be intensified based on climate change scenarios, thus contributing to expected increased frequency of wildfire activity (Esteves *et al.*, 2012). Given that this research focuses on typical Mediterranean areas, *i.e.* areas characterized by the Mediterranean climate, as presented in Chapter 6, the forests of which include representative species of Mediterranean vegetation, two additional reasons which increase fire occurrence in these areas need to be highlighted.

The first one is the fact that Mediterranean vegetation, includes besides several highly resilient to fire species, also numerous fire-sensitive species (Pausas *et al.*, 2008). In particular, typical Mediterranean vegetation, focusing on the Mediterranean basin, includes sclerophyllous woods, consisted chiefly of Pinus and Quercus communities and ordinarily small trees, shorter than 2.5 m, broad-leaved evergreen shrubs which on calcareous soil form widely spaced bush associations with (usually extensive) space, the so-called “*garrigues*” or “*phrygana*” and on silicious soil become closely set and taller, forming the so-called “*mâquis*”<sup>3</sup> and bushes. Mediterranean vegetation is also characterized by a considerable floristic diversity. These vegetation types may have some differences in their composition and structure, mainly attributed to soil and geographical features. However, despite their differences these shrubs and trees, which are typical for areas lying between 30° and 40° north and south latitudes, always exhibit vertical, rigid dull green leaves (Schimper, 1903; Davis *et al.*, 1996; Encyclopaedia Britannica, 2013). The representative types of Mediterranean ecosystems which are mentioned above are highly flammable, favoring thus fire ignition and as a result recurrent wildfires are an integral part of these ecosystems (Thanos and Marcou, 1991).

The second reason why Mediterranean wildfires are frequent is the sub-humid Mediterranean weather, which favors vegetative growth during the wet season and the high fuel loads produced are subjected to increased fire danger during the hot and dry summer periods (Esteves *et al.*, 2012). In Mediterranean forests extended fires occur usually during the summer time, when herbaceous vegetation is dormant or dead, in case of annual grasslands, and deciduous trees have shed their leaves. Under these circumstances, dry and easily combustible biomass fuels are accumulated and increase the vulnerability of the forests to fire. Besides, Mediterranean weather conditions also favor fire propagation during the summer.

---

<sup>3</sup> C'est avec raison qu'on le [le golfe d'Ajaccio en Corse] compare à la baie de Naples; et au moment où la goélette entrait dans le port, un maquis en feu, couvrant de fumée la Punta di Girato, rappelait le Vésuve et ajoutait à la ressemblance. (Mérimee P., 1840) / The Gulf of Ajaccio [on Corsica] is compared, with justice, with the Bay of Naples, and at the moment when the schooner entered the harbor, maquis on fire, which covered with smoke the Punta di Girato, woke up memories of Vesuvius, intensifying by that way the resemblance.

### **2.3.1.2 Fire characteristics**

In order to proceed to further analysis of given fire events it is necessary to somehow characterize the behavior of a forest fire by quantifying specific fire properties. This purpose is served by the use of specific fire science terminology. In the current research all key fire properties were further investigated and it was concluded that the most important and commonly used fire-related terms are those mentioned below.

The spatial characteristics of a fire include the *fire spatial extent* (expressed in spatial units, usually ha) and the *fire perimeter*, *i.e.* the boundary of a fire (expressed in length units). *Fire front* refers to the part of fire within which continuous flaming combustion is taking place. It is often assumed as the leading edge of the fire perimeter and is expressed in length units (NWCG, 2012). Another fire property is the *rate of fire spread*, which describes the rate of fire increase in terms of either spatial or linear dimensions and is usually expressed in m/min. The *Forward Rate Of fire Spread (FROS)* which describes the rate of spread in the heading direction is also commonly applied (Byram, 1959). The radiant heat energy released per unit time is the *Fire Radiative Power (FRP)*, a metric that is usually expressed in mW/m<sup>2</sup> and is also widely exploited in fire analyses.

Another key physical property of fire is *fire intensity*; it is a more general term that expresses the energy released during a fire and is commonly quantified through *fireline intensity* or *reaction intensity*. *Fireline intensity* (which is also referred as Byram's fire intensity (Byram, 1959) or frontal fire intensity (Santoni *et al.*, 2010) expresses the rate of energy or heat that is released per unit length of fire front, regardless of its depth. It is calculated as the numerical product of rate of fire spread, fuel consumption (the mass that is removed from fire either per unit area or as a percentage of the existing fuel load prior to the fire (NWCG, 2012)) and heat yield (the heat of combustion after correcting for various heat losses, primarily due to moisture in the fuel, also called low heat of combustion (NWCG, 2012)) at a given point on the fire perimeter and is usually expressed in kW/m. *Reaction intensity* is the rate of heat release per unit area of the flaming fire front and is expressed in units of heat energy (Kcal or Btu)/area units /time units (NWCG, 2012). An additional indicator of fire intensity is *flame length*, which is the distance between the flame tip and the midpoint of the flaming zone at the base of the flame (generally the ground surface) and is expressed in length units (NWCG, 2012).

In practice, several of these fire properties are used together to characterize a given fire event. However, during this research it was concluded that besides *fire spatial extent*, a critical fire property that can support post-fire analyses is *fire severity*. Due to its importance, this critical fire characteristic has been extensively analyzed during this research and is presented in detail in Section 2.3.1.3.

### **2.3.1.3 Fire severity**

A measure that quantifies the effects of fire on soil and overstory expressing its impact on ecosystems immediately after a fire event is fire severity (Keeley, 2009; De Santis and Chuvieco, 2007). Another term that has gained popularity in recent

years and is often used interchangeably with fire severity is burn severity (Keane *et al.*, 2012; Keeley 2009; Chuvieco *et al.*, 2005; Key, 2005; Parra and Chuvieco, 2005). This latter term addresses the same concept, combining the direct impact of fire on soil and plants after fire extinguishment and expressing post-fire ecosystem change (Veraverbeke *et al.*, 2010), and is associated with longer-term fire effects, as opposed to fire severity that expresses the more immediate fire effects (Keane *et al.*, 2012). The incorporation of ecosystem responses in the aforementioned terms may lead to confusion and thus, in order to avoid misunderstanding, fire severity and burn severity could rather be considered independent of ecosystem responses, while for more accuracy burn severity can be subdivided into *vegetation burn severity* and *soil burn severity* (Keeley, 2009). In the following, the term fire severity is used to express fire impact on aboveground and belowground organic matter.

The approaches to map fire severity include field surveys, satellite imagery processing and statistical and simulation modelling and as expected, a plethora of fire severity classifications is available in literature, each one of which being based on an inevitably limited subset of potential fire impacts. Unavoidably, the definition and measurement of fire severity indices is associated with inherent uncertainties, subjectivity, lack of standardization and potential inconsistency, which impose limitations in their use (Keane *et al.*, 2012). However, fire severity indices are undoubtedly useful, integral tools to quantify fire impact, even when they are followed by numerous assumptions. Considering the previous, the adoption of a proper, ordinal index, even if it may often needs to be case-specific, becomes critical, as also recognized in Keane *et al.* (2012).

The most widely used fire severity indices are the Normalised Difference Vegetation Index (NDVI), the Normalized Burn Ratio (NBR), the Composite Burn Index (CBI), which incorporates a complementary field sampling approach, the Relative differenced Normalized Burn Ratio (RdNBR) and the satellite-derived Differenced (or Delta) Normalized Burn Ratio (dNBR (or  $\Delta$ NBR respectively)), which is the temporal difference between pre- and post- fire NBR (Key and Benson, 2006; Keane *et al.*, 2012; Miller *et al.*, 2009). The values of each index are associated with different levels of fire severity.

Fire severity is usually classified into three to six categories (Keane *et al.*, 2012), the majority including the categories *low*, *moderate* and *high*, in many cases supplemented by the category *very high*. In general, high severity is associated with removal of the duff layer, heating of soil surface and burning of the vegetative canopy (Springer and Hawkins, 2005). These categories can be assumed as representative of the entire magnitude of fire-imposed biophysical changes in the environment. Sometimes, one more fire severity category may be identified, *i.e.* enhanced regrowth. However, when the extent of this class is limited, this class may be ignored.

### **2.3.1.4 Forest fires impacts and statistics**

Forest fires are frequently occurring natural hazards that affect forested land and are associated with dire socioeconomic consequences and particularly unfavorable environmental conditions. More specifically, forest fires pose a direct



threat on human lives. In addition to that they are often related with massive amounts of damage on properties (both public and private) and significant disruption of human activities not only in the affected area but also in the neighboring zones. However, it is the environment and the ecosystems hosted within a forest that are directly affected, and usually destroyed, during a forest fire.

A direct consequence of forest fires is the release of carbon dioxide in the air and the creation of heavy smog, which is particularly harmful to human and animal life and may even last for weeks. In the aftermath of a fire, the habitat of the environment is severely affected through deforestation, changes in species population and distribution. As documented in literature, wildfires are considered to have one of the highest environmental impacts in the Iberian Peninsula (Esteves *et al.*, 2012), while they have been also characterized as the most important single agent of geomorphological change in parts of the western USA (DeBano *et al.*, 2005).

The extent of these impacts depends strongly on geomorphological particularities and fire characteristics, the most important of which are fire severity and spatial extent of forest fire. The overall environmental footprint of forest fires is amplified in case of frequent and successive forest fires, which eventually destroy completely the habitat of the affected areas. Lands or even communities that lie in the WUI, *i.e.* in the transition zone between unoccupied land (*e.g.* forested land) and land characterized by intense human activity (*e.g.* fully urbanized areas), are exposed to increased fire danger and are thus more prone to intensified impact of forest fires (Mitsopoulos *et al.*, 2015). Typical are the recent cases of California (US) in 2003 and 2007, Greece in 2007 and Victoria State (Australia) in 2009 (Mell *et al.*, 2010; Haynes *et al.*, 2010).

It needs to be mentioned that at the same time small-scale forest fires constitute an integral, sometimes even essential, physical process of forest ecosystems, since they destroy diseased plants, harmful insects and decaying material, and they result in increased sunlight which fosters seed regeneration. In such cases the absence of fire may become equally detrimental with frequent forest fires to plant communities. Prescribed fires, which are discussed in Section 2.3.1.5, constitute a common practice for fire danger management. However, when this phenomenon occurs frequently, without control and at an extended scale, it becomes a real threat to the natural environment.

Focusing on Mediterranean areas, wildfire activity is particularly increased, especially during the last decades (Esteves *et al.*, 2012; Pausas *et al.*, 2008). According to San-Miguel-Ayanz *et al.* (2012) on average 65.000 fires occur in Europe every year, which burn approx. 5.000 km<sup>2</sup> (500.000 ha) of wildland and forested land. The 85% of the affected areas are located in the European Mediterranean region. As reported by EEA (2004), the area burnt from forest fires per year in 5 Mediterranean countries (Greece, Italy, France, Spain and Portugal) varied between 2.000 km<sup>2</sup> (200.000 ha) and 6.000 km<sup>2</sup> (600.000 ha) during the period 1980-2002, while according to WWF (2003) the total burnt area in Greece, Portugal, Italy and Spain has quadrupled since 1960.

Regarding their ignition source, analyses of relevant datasets retrieved from the European Forest Fire Information System (EFFIS) conclude that more than 95% of fires in Europe are human-induced (San-Miguel-Ayanz *et al.*, 2012). As far as frequency of occurrence of fire events is concerned, a year characterized by an increased fire activity is usually followed by several years of lower fire activity. This can be mainly attributed to the fact that fuel loads are significantly reduced after a large scale fire event. In a relevant research study by Heinl *et al.* (2007) fire activity peaks seem to be repeated roughly every 6 years. In terms of their economic impact, according to the UN Food and Agriculture Organization (FAO) Forestry Department, Mediterranean forest fires cost the region approx. 10<sup>3</sup> Million Euros each year (Kinver, 2011). Only for Spain, the annual cost of the direct impact of erosion due to fires on the environment is approx. 280 Million Euros, while the cost of rehabilitation is estimated at 3.000 Million Euros for a period of 15 to 20 years (WWF, 2003).

Additional statistics for wildfires on a global scale are presented in Figures 2.14 – 2.16, while relevant statistics particularly for the five southern EU member states (Greece, Italy, France, Spain and Portugal) are presented in Figures 2.17-2.18.

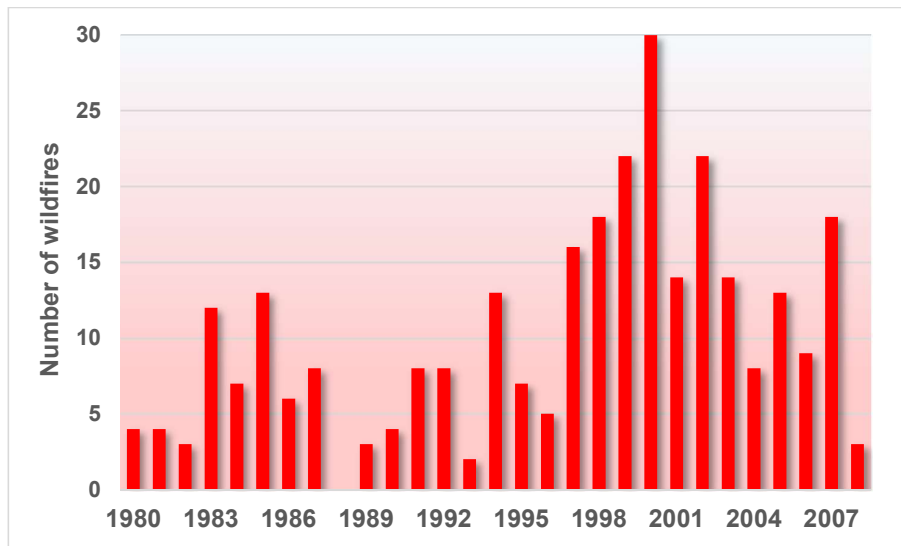


Figure 2.14. Wildfires reported during the period 1980-2008 on a global scale (Source: PreventionWeb of the UNISDR).

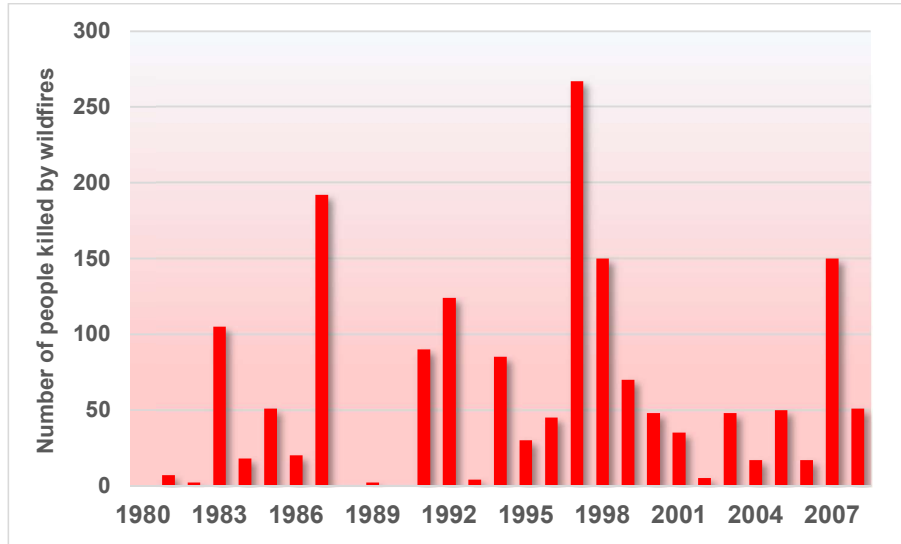


Figure 2.15. The number of people killed by wildfires during the period 1980-2008 on a global scale (Source: PreventionWeb of the UNISDR).

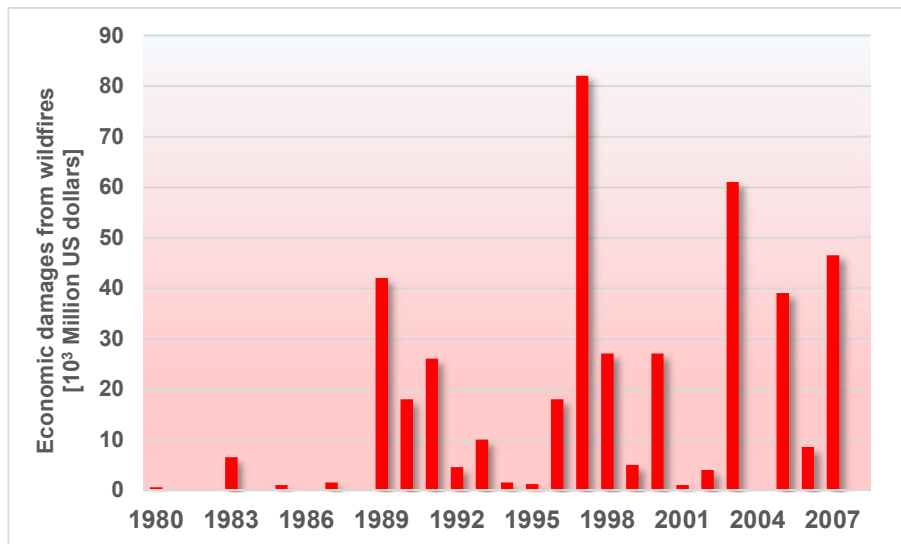


Figure 2.16. The reported economic damages (in 10<sup>3</sup> Million US dollars) from wildfires that occurred during the period 1980-2008 on a global scale (Source: PreventionWeb of the UNISDR).

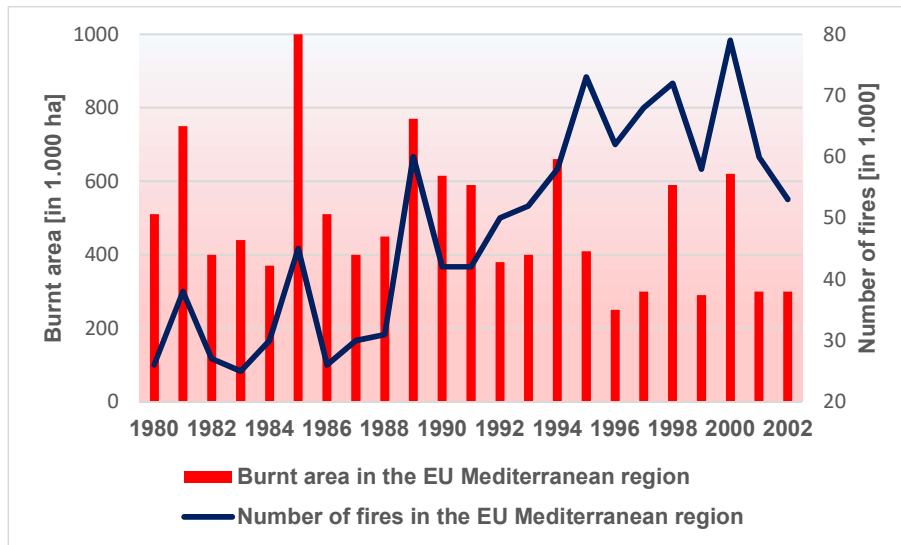


Figure 2.17. The burnt area (in ha) and the number of fires in 1.000 during the period 1980-2002 in the five Southern EU Member States (Source: EEA, 2004).

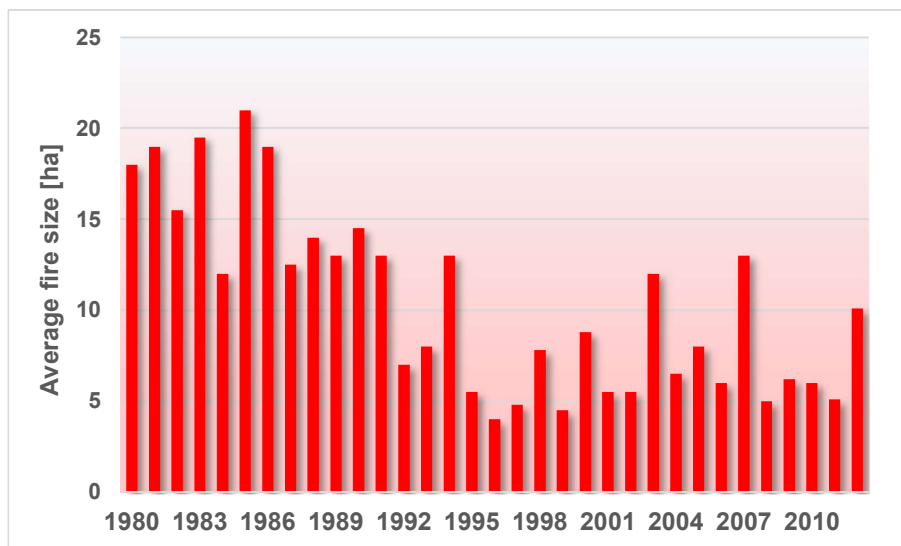


Figure 2.18. The average fire size (in ha) during the period 1980-2012 in the five Southern EU Member States (Source: JRC, 2014).

### 2.3.1.5 Prescribed fires

Fire danger management is beyond the purposes of this research, however this Chapter includes a short discussion on fire danger management for reasons of completeness. From the previous Sections, it becomes obvious that wildfires need to be properly accounted for so that appropriate fire management practices will be adopted. It needs to be highlighted that fire management practices should not be restricted to firefighting, as is the current practice in most cases nowadays, but may also include the regular application of prescribed fires.

As mentioned above, forest fires are an integral part of the physical process of forest ecosystems that under certain conditions can enhance the natural process of forest regeneration. Prescribed fires burn primarily in surface fuels, leaving a high percentage of overstory trees alive (Oliveira and Fernandes, 2009). Prescribed burning occurs on significantly smaller scales, in terms of spatial extent, intensity (related to rate and amount of energy released) and severity in comparison to wildfires, while prescribed fires are typically set during the dormant season of the vegetation, when high levels of moisture make fire control easier (Oliveira and Fernandes, 2009; Carter and Foster, 2004). Such fires modify the quantity and the structure of fuels and thus assist in preventing high-severity fires and reducing negative impacts of extended wildfires, such as increased post-fire soil erosion (Oliveira and Fernandes, 2009; Scott and Van Wyk, 1990; Esteves *et al.*, 2012).

Even though sometimes the results of prescribed fires published in literature are contrasting, a closer look may show that ineffectiveness of this practice is usually associated only with specific forest species (*e.g.* *Quercus* forests (Franklin *et al.*, 2003); combined *Quercus* and *Pinus* forests (Barton, 1999) *etc.*). In general, controlled burns, which are commonly used in fire-prone areas like the Mediterranean, are reportedly as one of the most effective practices for reducing a fire's impact, including rate of spread, fireline intensity, flame length and heat per unit of area (van Wagtendonk, 1996; Oliveira and Fernandes, 2009; Carter and Foster, 2004; Fernandes and Botelho, 2004).

## CHAPTER 3: FLOODS–FIRES INTERACTION

The tremendous impacts of floods and forest fires on humans and the environment are presented in Chapter 2. Both natural hazards and their impacts were examined for the case when each hazard acts in isolation. However, floods and forest fires interact, and consequently their impact is intensified. The current research investigates thoroughly one way of this interaction (similarly to the one-way causal effect approach), *i.e.* the impacts of forest fires on ecosystems, examined from a hydrological perspective, in an attempt to quantify it and incorporate it in hydrological modelling. These impacts are the most obvious and intense ones and are presented in Section 3.1. The forest fire impacts on typical catchment characteristics are assessed in Section 3.2, while Section 3.3 analyses in depth the term “*post-fire recovery*”. The inverse way of the floods-fires interaction, *i.e.* the impact of floods on forest fires is often underestimated; yet it is not negligible. This impact is examined in brief in Section 3.4. This Chapter concludes with the identification of the existing gap in literature regarding the quantification of the impact of forest fires on the hydrological behaviour of a catchment.

### 3.1 Impacts of forest fires on ecosystems from a hydrological perspective

As clarified above, the current research examines the impacts of wildfires on ecosystems from a hydrological perspective. More specifically, fires provoke both direct and indirect impacts on the hydrological response of affected catchments. These impacts are not uniform over time and space; they are characterized by variable temporal and spatial scales instead (Keane *et al.*, 2012). In the following, the impacts of fires on hydrological catchments are presented in brief.

#### 3.1.1 Direct impacts

The most evident direct effect of forest fires on a catchment is the change in the coverage of a catchment’s surface. A fire clears the soil surface from vegetation, litter and other barriers. Particularly for vegetated land, the vegetation cover is modified or even completely destroyed, depending on fire severity. Since land cover is a decisive feature in hydrological modelling, burnt catchments have a totally different hydrological response than catchments not affected by fire.

Another direct impact of forest fires is the alteration of the soil properties in the affected areas. The conversion of organic ground cover to soluble ash, the removal of the overhead foliage and the resulting modification of the microclimate at the affected area contribute to the alteration of the physical and chemical soil properties (Lavabre *et al.*, 1993).

Regarding the physical soil properties, prior to a fire and when high vegetation covers the soil, soil hydraulic conductivity is increased and macropore fluxes are favoured (Campo *et al.*, 2006). However, after a fire event hydraulic conductivity is expected to be significantly diminished. Relevant studies have identified a

relation between fire severity and fire impact on physical and hydraulic soil properties (Rulli and Rosso, 2007).

As far as fire-induced changes in chemical soil properties are concerned, one of the most profound such change is the development of a hydrophobic, water repellent coating over the upper soil layers. More specifically, during a fire event, very intense heating takes place, especially during high-intensity fires, and both volatile and non-volatile substances are produced. The volatile substances are evaporating soon, while the non-volatile ones affect significantly the litter and the upper soil layers. Non-volatile substances and part of vaporised water and organic compounds move downwards into the soil and towards lower temperature soil layers, where condensation on mineral soil particles takes place. This procedure results in the development of a water repellent upper soil layer of varying thickness, which is developed in parallel with the soil surface of the burnt areas, the properties of which have been studied extensively in literature (Rulli and Rosso, 2007; DeBano, 1981 and 2000). The modification in soil water repellency due to fire is presented in Figure 3.1. Before the fire, a water repellent layer is developed below the litter layer and the upper parts of the mineral soil (Figure 3.1a). During the fire, the litter and vegetation is destroyed and the hydrophobic substances move downwards, towards lower temperatures (Figure 3.1b). As a result, after the fire, a water repellent zone is developed lower in the wettable soil and parallel to the burnt soil surface (Figure 3.1c) (DeBano, 1981).

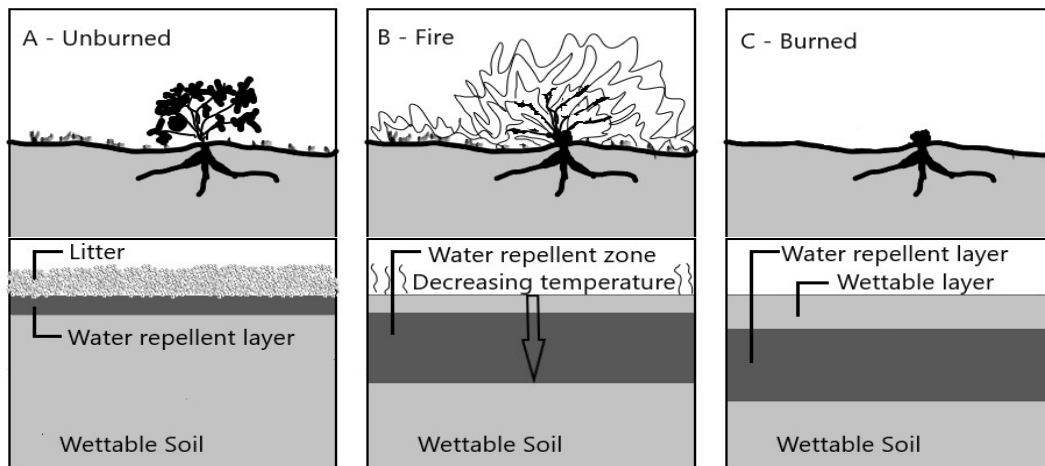


Figure 3.1. Modification in soil water repellency prior to (a), during (b) and after (c) a fire (adapted from DeBano (1981)).

Water repellency is determined in the field by means of special tests on soil (e.g. water drop penetration time (WDPT) and critical surface tension (CST)), also described in DeBano (1981). In Scott and Van Wyk (1990) repellent soils were developed to depths up to 150 mm below the surface, with decreasing frequency of repellence below 100 mm. In general, extended repellency was tracked in greater depths at locations where high fuel load conditions predominated during the fire. In the aforementioned study, the frequency of occurrence of repellency in surface layers was particular low, since sufficient level of heating in the soil surface took place.

In general, the repellent layer is not continuous over a large area (Scott and Van Wyk, 1990; DeBano, 1981). In some cases, the soil hydrophobicity is associated, albeit weakly, with fire severity, (Lewis *et al.* 2006; Robichaud, 2000), while in other cases there seems to be no correlation between the soil water repellency and fire severity (Doerr *et al.* 2006; Cannon *et al.* 2001). It is mentioned however that in some exceptional cases post-fire soil hydrophobicity may not be increased. This takes place for example when the soil affected by fire is covered with limited organic material and is fine-textured and thus less susceptible to develop water repellency (Mayor *et al.*, 2007).

### **3.1.2 Indirect impacts**

Forest fires are mainly associated with indirect impacts on the hydrological behaviour of a catchment. These indirect impacts come as a result of the aforementioned direct fire impacts and are analyzed in the following.

The change in the coverage of a catchments surface (removal of vegetative cover, litter and other barriers), which is the most evident direct fire impact, **speeds up** surface flow, since few obstacles, if any, block water flow. Particularly for the vegetation cover, as a result of its destruction or modification, canopy interception and evapotranspiration are significantly modified and the hydrological cycle is affected. In particular, the vegetation removal results in reduced interception and transpiration and increased evaporation, given the insolation and the increased wind velocities due to opening in the formerly vegetated area (Lavabre *et al.*, 1993).

Further to the aforementioned change in the soil coverage, the ash layer that is laid over the surface of the affected catchment and which is dominant especially during the first post-fire period contributes to decreased infiltration and increased runoff. Of course, it also needs to be considered that this upper layer acts to a certain extent as a protective layer to rainfall erodibility and soil detachment, especially during the first post-fire rainfall events, as also confirmed by Campo *et al.* (2006).

The alteration of physical and chemical soil properties after a fire is also associated with the indirect fire impacts presented in the following. Regarding the physical soil properties, due to decreased soil hydraulic conductivity after a fire, soil loss is increased and runoff is augmented. Changes in chemical soil properties and more specifically the development of a hydrophobic, water repellent layer is related with reduced rainfall infiltration, since it allows infiltration only up to a limited depth, *i.e.* until the wetting front that starts from the surface will reach this layer. Therefore, increased and erratic runoff is to be expected, especially in soils that have been affected by fires of high severity (Rulli and Rosso, 2007; Scott and Van Wyk, 1990; Besson *et al.*, 2001; Bolin and Ward, 1987). Increased runoff is expected even under low intensity rainfall conditions, when their duration is long. The modified infiltration rate due to the development of a water repellent layer after a fire for different soil depths, as well as its modification over time is examined in DeBano (1981). Regarding the modified infiltration rate due to the development of a water repellent layer, the research concludes that the existence of a water repellent layer makes the infiltration rate



curve sharper. As far as infiltration modification over time is concerned, the research concludes that infiltration rate in a water repellent soil increases with time, contrary to the typical decline of infiltration rate with time for wettable soils.

Forest fires also result in increased soil erosion. In general, soil erosion is a natural process that occurs as a result of the action of water, wind and/or gravity and is characterized by three main processes: detachment, transport and deposition. The presence of local disturbances (existing structures, vegetation, roots, gravels *etc.*) may induce the formation of flow preferential paths and localised erosional patterns. This natural process is intensified due to changes in land uses or land cover, which may many times be human-induced, and soil erosion is expected to be significantly increased after wildfires. Focusing on erosion due to the action of water and particularly for detachment and transport, exposed slopes are subjected to four types of erosion, *i.e.* raindrop erosion, sheet erosion, rill and gully erosion and stream and channel erosion, as presented in Figure 3.2 (IUM, 2013; NSW, Soil Erosion Factsheets).

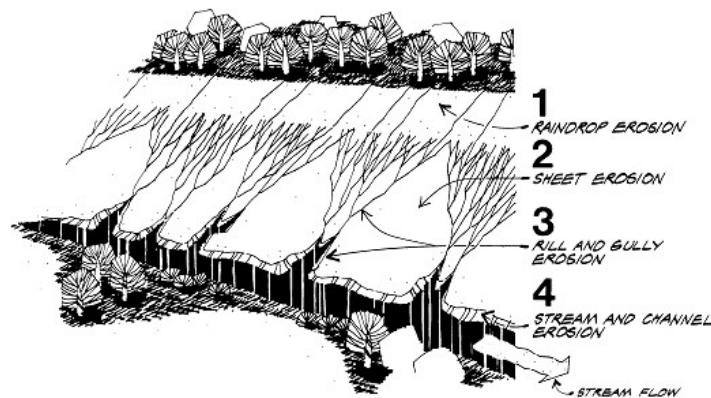


Figure 3.2. The four types of erosion that affect exposed slopes (Source: IUM, 2013).

Raindrop erosion is the effect of falling rainfall drops on the soil. Soil particles are detached due to the force of raindrops and can be transported easily by the surface flow. Sheet erosion expresses the removal of thin soil layers as a result of raindrop splash and shallow surface flow. The finest particles of the upper soil layers which contain most of the nutrients and organic matter are removed due to sheet erosion. When surface water is concentrated into rivulets, shallow drainage lines less than 30 cm are produced and rill erosion occurs. In case surface water cuts channels deeper than 30 cm through the soil, then gully erosion takes place. When the volume and the velocity of runoff is increased and particularly when water moves through dispersive subsoil, *i.e.* soil easily erodible when wet, stream and channel erosion takes place, the stream bottom and bank toe may be severely modified and large sections of the stream bank may fail (IUM, 2013; NSW-DPI, Soil Erosion Factsheets).

All these types of erosion are significantly intensified after forest fires. Esteves *et al.* (2012) clearly state that post-fire erosion is undeniably increased. The degree of fire-induced erosion depends on numerous factors, such as fire severity, fire

frequency in the affected area, topographic characteristics, soil properties, alteration in land cover, local meteorological conditions etc.

Particularly for fire severity, Inbar *et al.* (1998) state that surface erosion is significantly accelerated only in areas affected by intense fires. According to Cannon *et al.*, (2000), Bisson *et al.*, (2005) and Dragovich *et al.*, (2002) it is expected that increased fire severity is associated with increased soil erosion. Regarding topography, slope (Bisson *et al.*, 2005; Scott and Van Wyk, 1990) and to a lesser extent hillslope curvature (Bisson *et al.*, 2005) usually play a significant role in soil erosion in general and post-fire erosion in particular. In terms of slope, slopes greater than 25° are often associated with increased soil erosion and debris flow. An upper limit slope cannot be easily selected. However, relevant research has resulted that areas with very high slopes are less prone to erosion, primarily due to lower water infiltration (Pallàs *et al.*, 2004). As far as hillslope curvature is concerned, mainly concave hillslopes have been identified by several researchers as slopes of increased risk of failure (Bisson *et al.*, 2005). However, other studies conclude that slope aspect and exposure have a trivial effect on erosion (Inbar *et al.*, 1998). In addition, as analyzed above, forest fires affect soil properties (physical, chemical and mechanical) and thus alter the binding capacity of the soil particles. According to Hubbert *et al.* (2006) the structural alterations in soil properties affect erosional processes decisively. According to Scott and Van Wyk (1990), Wondzell *et al.* (2003), Bisson *et al.* (2005) and Inbar *et al.* (1998) changes in soil properties, such as detachment of soil aggregates that takes place after a high-intensity fire, trigger increased erosion. At this point, it needs to be clarified that the term fire intensity refers to the amount of energy released during a fire event, which is different from fire severity that is basically associated with the impact of fires on organic matter aboveground and belowground, as described in Section 2.3.1.3 (Keeley, 2009). In fact, there are cases where fire intensity and fire severity are negatively correlated, e.g. the case of grass and shrubland fires (Keane *et al.*, 2012). The vulnerability of a soil to erosion is particularly high especially after repeated fires, which contribute to increased soil degradation (Campo *et al.*, 2006). Post-fire erosion is also increased due to changes in the upstream contributing area (Cannon *et al.*, 2001) and severe changes in land cover and land use (Giovannini *et al.*, 2001). The extent and speed of post-fire vegetation recovery also affects soil erosion (Inbar *et al.*, 1998). Taking also into consideration the fact that forest fires are associated with increased runoff volume and velocity, it becomes clear why wildfires intensify sheet, rill, gully and stream and channel erosion.

At the same time, forest fires indirectly facilitate raindrop erosion as well. In particular, raindrop detachment is mainly affected by the characteristics of the rainfall (intensity, duration), the soil characteristics, the existing land cover (ground and canopy cover) and the surface water depth (Rulli and Rosso, 2007). A positive correlation between rainfall intensity and soil loss was identified by Campo *et al.* (2006), while soil loss was not significantly correlated with rainfall volume. However, repeated fire events result in a more degradable and thus a more sensitive to rainfall energy soil (Campo *et al.*, 2006). Furthermore, as a result of the loss of the aboveground biomass due to fire, more soil surface is exposed to rainfall and the kinetic force of precipitation on the soil surface is increased (Moody and Martin, 2001a) and therefore raindrop erosion is also increased. As

also verified in numerous relevant studies, post-fire soil erosion depends on local climate (Soto *et al.*, 1998; Cerdà *et al.*, 1995; Kutiel *et al.*, 1995; Wondzell *et al.*, 2003, Rulli and Rosso, 2007; Inbar *et al.*, 1998) and the timing of post-fire storms (Inbar *et al.*, 1998).

Since soil erosion is directly related with sedimentation, forest fires trigger increased post-fire sediment transport. As also mentioned above, as a consequence of the burning-off of all the leaves and the undergrowth, the soil is exposed and thus more vulnerable to erosion by raindrops. Therefore, an increased amount of sediment becomes available for transport by the main channels (Brown, 1972). In addition, the higher overland flow velocities that occur as a result of the destruction of forest litter and other debris on the ground, also contribute to an increase in sediment transport (Brown, 1972; Scott and Van Wyk, 1990). Furthermore, the catchment roughness and time of concentration are reduced after a forest fire. Taking also into consideration the post-fire increased channel and overland flow velocities for given amounts of rainfall, increased stream discharges and therefore increased sedimentation are expected (Brown, 1972). Relevant studies also confirm a high correlation between sediment transport and fire severity (e.g. Rulli and Rosso, 2007; Scott and Van Wyk, 1990; Bolin and Ward, 1987).

Another indirect fire impact is the inducement of debris flow. Debris flow can be initiated either from surface runoff or from soil saturation. It has a highly destructive power, it occurs without previous warning and it exerts significant loads on objects tracked in its path, thus resulting in significant damages in structures and endangering human lives. Post-fire debris flow is expected to be significantly increased (Mitsopoulos *et al.*, 2015; Scott and Van Wyk, 1990). More than 160 people were killed in Sarno (Italy) in 1998 by debris flows after a fire event (Bisson *et al.*, 2005). Particularly at recently burnt areas, debris flows generated during storm events, unlike landslide-triggered debris flows, have no identifiable initiation source and may occur even in case of limited or even absent antecedent moisture (Cannon *et al.*, 2008). In unburned areas, landsliding occurs as a result of infiltration, while in burnt area and especially within the first two years after a wildfire, debris flow is primarily resulted from the progressive entrainment of material that has been eroded from hillslopes and channels during surface runoff, even after short-recurrence interval periods (Cannon *et al.*, 2008). The most significant debris flows of this type usually occur during the first significant storm that affects the burnt area, when antecedent soil moisture is still negligible. In unburned areas, however, antecedent soil moisture conditions are quite critical for debris flow initiation. In terms of recurrence intervals of the storms that triggered debris flows, periods of less than or equal to two years seem to have as a result significant debris flows (Cannon *et al.*, 2008). Any change in rainfall characteristics during a storm event may have effect on triggered debris flow and thus it is useful to take into account the exact rainfall pattern when examining debris flows. In Cannon *et al.* (2008), debris flows seem to have occurred as a response to periods of high-intensity rainfall during the storms. Even though rainfall is the primary driver of a post-fire runoff response and therefore of the resulting debris flow, fire severity, soil properties, basin characteristics *etc.* also play a significant role in the amount of debris flow (Cannon *et al.*, 2008). For example, smaller and steeper basins are expected to

respond with debris flows in shorter time periods and after lower rainfall totals and intensities and severely affected areas are expected to yield increased debris flows.

As mentioned above, as a result of the direct impacts of fires on the soil (*i.e.* destruction of vegetation coverage and litter and modification of physical and chemical soil properties), increased and erratic runoff is to be expected, particularly in case of soil severely affected by fire. Still, increased soil erosion, sedimentation and debris flow, which are analyzed above, contribute in turn to an increase in peak flows and runoff volumes during post-fire flood events. Actually, these two consequences, *i.e.* the considerable post-fire increase in runoff volumes and peak flows, are the most evident and important impacts of forest fires on the hydrological behaviour of a catchment during post-fire flood events.

Increases in flood runoff volumes after fire events have been analyzed extensively in literature. The studies of Brown (1972), Bisson *et al.* (2005), Scott and Van Wyk (1990), Lavabre *et al.* (1993) and Beeson *et al.* (2001) are indicatively mentioned. In general, increased discharges are most of the times not associated with exceptional rainfall events (Bolin and Ward, 1987; Springer and Hawkins, 2005). Yet, they are more significant for intense events. According to Lavabre *et al.* (1993) and Scott and Van Wyk (1990), increased runoff volume after a fire event is mainly observed during “*high water days*”, while Lavabre *et al.* (1993) also states that “*low water days*” may result in no particular change in observed runoff. In addition, runoff volumes are particularly increased in areas that have steep slopes and also areas that are affected by high-severity fires (Beeson *et al.*, 2001).

Springer and Hawkins (2005), Lavabre *et al.* (1993) and Scott and Van Wyk (1990), among others, have also studied increases in peak flows after fires. Peak flow has been characterised as a sensitive parameter in describing post-fire hydrological response (Moody and Martin, 2001b). Beeson *et al.* (2001) conclude that post-fire increases in peak runoff depend strongly on rainfall characteristics, without this meaning that increased post-fire peak flows are necessarily, if at all, associated with differences in post-fire rainfall patterns (Bolin and Ward, 1987).

Inevitably, due to changes in catchment characteristics and increase in runoff volumes and peak discharges after wildfires, the shape of flood hydrographs of affected catchments is heavily modified. Generally, in the aftermath of a fire event, sharper hydrographs are to be expected. The formerly vegetated basin needs no previous saturation, given that it is coated by a hydrophobic layer, and therefore runoff response is expected to start shortly after the initiation of the rainfall. According to relevant studies performed for catchments partly affected by fire, prior to the fire, many hydrographs showed a fairly rounded peak several hours after the beginning of rainfall, which was followed by a steady recession. After the fire, it was observed that, very frequently, pronounced sharp peaks were followed by more rounded peaks, similar to the pre-fire ones. In other cases, a very sharp sole peak followed by an equally rapid recession could be observed (Brown, 1972; Lavabre *et al.*, 1993). Peak flow rate is increased with more significant rate than the direct flow, and when the pre- and post-fire runoff duration is not affected (*e.g.* in Scott and Van Wyk, 1990) a steepening of the rising limb of the hydrograph is

to be expected. In many cases the post-fire runoff duration is decreased, while runoff volume and peak discharge are increased (e.g. Springer and Hawkins, 2005; Rycroft, 1947) and this results in even more steep rising limbs.

Under particular weather conditions, wildfires and the resulting sediment yield may trigger desertification, especially in the absence of timely mitigation measures (Rulli and Rosso, 2007) or also in case of repeated fire events, which are associated with increased vulnerability to soil erosion (Campo *et al.*, 2006). Figures 3.3a-c depict the desertification due to successive destructive forest fires that have affected the Torres del Paine National Park in Chile in the last years. The most recent forest fire occurred between December 2011 and January 2012 and the pictures were taken two years later, in December 2013. Post-fire desertification risk appears to be particularly increased in typical Mediterranean drylands (Mayor *et al.*, 2007).



*Figures 3.3a-c. Desertification due to successive fire events in different parts of the Torres del Paine National Park, Chile (personal archive).*

Finally, the secondary effects of fire *per se* can be considered as a kind of indirect fire impact. More specifically, post-fire soil erosion could be mitigated when for example burnt trees fall and stabilize slopes or even when scorched trees release needles over erodible soils (Keane *et al.*, 2012). However, such effects besides occurring over long and difficult to determine time periods, usually have trivial impacts when compared to the aforementioned effects, so they could be ignored.

It is highlighted here, that as expected and as also mentioned throughout the text above, the impacts of forest fires, either direct or indirect, are more intense for catchments for which fire severity and the extent of fire are more significant. This has been verified by numerous studies which compare pre- and post-fire behaviour of catchments subjected to prescribed fires and wildfires. More specifically, the main characteristic of prescribed fires, which are presented in more detail in Section 2.3, is the considerably decreased fire severity in terms of rate and amount of energy released, in comparison to wildfires (Scott and Van Wyk, 1990). Relevant studies (Esteves *et al.*, 2012; Oliveira and Fernandes, 2009; Scott and Van Wyk, 1990) conclude that prescribed fires are associated with more moderate impacts on catchments than wildfires and therefore it can be concluded that increased fire severity is associated with more intense impacts on catchment characteristics.

### **3.2 Assessment of forest fires impacts on typical catchment characteristics**

The assessment of the impacts of forest fires on the hydrological behaviour of affected catchments has been the main research topic of numerous relevant studies that have been performed in the last decades. Some of these studies are based on observations of catchment characteristics or, when available, on measurements of parameters that represent the hydrological response of an affected catchment. Yet, in the absence of relevant information, which is usually the case, the majority of such studies include assumptions and rely on estimations of the extent to which catchment characteristics are affected by wildfires. A thorough literature review has been performed on similar studies and their outcomes, in terms of documented attempts to assess the impact of forest fires on hydrology and express it in quantifiable terms, are summarized in the following paragraphs. The impact assessment presented below concerns changes in runoff volume, peak discharges, flood return period, infiltration rate, hydraulic conductivity, soil roughness, sediment yield and soil loss, potential evapotranspiration and raindrop erodibility.

Based on literature review for the impact of forest fires on runoff volume, after a destruction of approximately 85% of a forested area from fire, 25-30% increase in runoff was observed in the following year (Lavabre *et al.*, 1993). In Bolin and Ward (1987) severely affected plots yielded 60 times higher runoff than lightly affected plots. A wildfire that affected approximately 80% of an afforested catchment in South Africa resulted in 62% and 201% increase in total and direct runoff volumes respectively during floods, while the runoff coefficient was increased by 242% and the mean weekly stream flow was increased by 12.4% in the subsequent year of the fire event (Scott and Van Wyk, 1990). In a period of 6 years after a fire event in a Mediterranean scrubland, the runoff coefficient was reduced by 45% during the first winter and by 6% during the sixth winter after the fire (Rulli and Rosso, 2007). In Campbell *et al.* (1977) stream flow was increased by 800% and runoff efficiency increased by 450% the following year of a fire. The first rainfall season that followed a fire event in Mt. Carmel in Israel resulted in increased runoff by 500 times (Inbar *et al.*, 1998). In Mediterranean areas, increased runoff varies from 11% up to 300% in large basins (Batalla, 2002),

reaching 800% in small basins (Batalla, 2002; Campbell *et al.*, 1977). As a result of a second experimental fire in catchments in Valencia, Spain, a three-fold increase in runoff rate was reported by Campo *et al.* (2006).

Similarly for peak flow, significant post-fire increase has been recorded in peak flow values of affected catchments. In a forested catchment in New Mexico that was severely affected by a fire event, post-fire peak flow was increased by two orders of magnitude one year after the fire (Bolin and Ward, 1987). A similar increase in peak flow was reported for the following two years of the Cerro Grande fire that also occurred in New Mexico in 2000 (Springer and Hawkins, 2005). In Scott and Van Wyk, (1990) the peak flow rate was increased by 290% one year after a fire event in South Africa. Particularly for Mediterranean areas, peak flow increments vary from 45% up to 600% in large basins (Batalla, 2002), reaching 5700% in small basins (Batalla, 2002; Campbell *et al.*, 1977).

Regarding reported changes in flood return periods, the T=10 year return period flood can be increased up to 100% after a fire event (Rulli and Rosso, 2007). According to Lavabre *et al.* (1993), the T=10 year return period flood changes into a T=1 year return period, at least for the first year after a fire. In the aforementioned research the T=1 year return period flood has been exceeded 3 times in the post-fire year and was induced by rainfall events that did not exceed the T=1 year return period of the 12-h rainfall. In general, Rulli and Rosso (2007) mention that the probability of occurrence of significant flood events one year after a fire event is increased by an order of magnitude.

Characteristics of typical catchments affected by fires also include infiltration rate, hydraulic conductivity and soil roughness. The outcomes of relevant literature review on the assessment of fire impact on these characteristics in quantifiable terms are presented in the following. Based on Campbell *et al.* (1977) the infiltration rate in severely affected areas after a fire event in a pine forest in Arizona was reduced by approximately 63% in comparison to unburned parts of the area. In Soulis *et al.* (2009) soil samples from two sites in the north part of Rafina catchment in Easter Attica in Greece were analysed, aiming to estimate the hydraulic conductivity of the soil prior to and after the significant fire event that affected the area in 2005. The research concluded that the hydraulic conductivity was reduced by 72% and 83% respectively at the selected sites. Another key catchment's hydraulic property is roughness coefficient. In general, post-fire Manning's roughness coefficient ( $n$ ) is expected to change significantly. Rulli and Rosso (2007) suggest that pre-fire values of  $n=0.2 \text{ m}^{-1/3}\text{s}$  in hillslopes and  $n=0.05 \text{ m}^{-1/3}\text{s}$  in channels change to the post-fire  $n=0.05 \text{ m}^{-1/3}\text{s}$  in hillslopes and  $n=0.03 \text{ m}^{-1/3}\text{s}$  in channels values respectively.

As also highlighted in Section 3.1.2, increased soil loss and sediment yield are typical expressions of fire impact on a catchment. Extended assessments of this particular impact have been tracked in literature. More specifically, a twofold increase in soil loss was observed after a second experimental fire in catchments in Valencia, Spain (Campo *et al.*, 2006). The fraction of sediments detached from raindrop erosion is also significantly increased after a fire event and according to Rulli and Rosso (2007) fires in a basin in California resulted in the post-fire fraction ranging between 0.16-0.88 ( $\text{mg}\cdot\text{m}^{-2}\cdot\text{s}^{-1}$ ) in the post-fire period, in comparison with

the pre-fire 0.045-0.44 ( $\text{mg}\cdot\text{m}^{-2}\cdot\text{s}^{-1}$ ) range. Regarding sediment yield, its post-fire annual values are expected to exceed 6 to 30 times the pre-fire ones (Rulli and Rosso, 2007). In Scott and Van Wyk (1990) a roughly four-fold increase was observed in both the mean suspended sediment yield and the bedload loss one year after a fire. In Inbar *et al.*, (1998) an increase in sediment yield by 100.000 times was observed during the first rainfall season after a fire event in Mt. Carmel in Israel. As mentioned above, successive fire events affect significantly the sediment yield of a basin. In Campo *et al.* (2006) the sediment yield was increased by two orders of magnitude after a fire event, while a subsequent fire event in the same basin resulted in an increase by three orders of magnitude. In Bolin and Ward (1987), sediment yield from severely affected plots in New Mexico was 35.4 times greater than the corresponding yields from lightly affected plots. In the same study, it was observed that sediment yield rates were considerably increased during the first couple of post-fire years, while they declined sharply afterwards.

Further to the aforementioned catchment characteristics, which are measurable (at least to a certain degree), there are several other characteristics harder to quantify. Assumptions are quite common in literature for such characteristics. In particular, one of the most difficult to quantify component of the hydrological cycle is evapotranspiration. Especially, for potential evapotranspiration assumptions are inevitable. Regarding the fire impact on a Mediterranean catchment's potential evapotranspiration, Lavabre *et al.* (1993) suggest that fire has similar effects with a 50% reduction of the potential evapotranspiration for the subsequent year of the fire. Raindrop erodibility is also hard to quantify. Even though raindrop erodibility factor ( $K_r$ ) is expected to change after a fire event, the estimation of its value remains hard. In Rulli and Rosso (2007),  $K_r$  was considered equal to  $35 (\text{Nm})^{-1}$  for the pre-fire period and equal to  $85 (\text{Nm})^{-1}$  for the post-fire period in a catchment in southern California<sup>4</sup>. Sometimes, in the absence of relevant measures, the impact of fire on certain catchment characteristics is translated to impact on other, more manageable and easier quantifiable characteristics. A typical example is presented in Rulli and Rosso (2007), where in the absence of relevant measurements, the impact of fire on soil hydraulic conductivity, *i.e.* the presence of the hydrophobic layer, was assumed equal to the post-fire reduction of the soil depth from 0.5-1 m to 0.05-0.1 m.

### 3.3 Recovery

In the aftermath of a significant forest fire event, recovery processes start taking place. Such processes are natural, but they can be accelerated through human intervention, such as reforestation activities. Post-fire forest recovery, or else called *relaxation time* (Moody and Martin, 2001a), has been examined in literature. However, research on post-fire forest recovery has been performed from scientists of different disciplines and specialties and therefore the extracted conclusions often refer to different aspects of recovery in order to serve different purposes.

As a general conclusion, following an extended literature review on the post-fire recovery phase of forests, recovery can be distinguished into *environment*

---

<sup>4</sup> Additional information on rainfall erosivity and soil erodibility is presented in Chapter 5.5.1.



*recovery* and *hydrological recovery*, based on the perspective from which this phenomenon is analysed. Characteristics of both types of recovery are presented in the following Sections, while in this research particular emphasis has been placed on hydrological recovery.

### 3.3.1 **Environmental recovery**

It can be considered that *environmental recovery* is achieved with natural reforestation and ecosystem rebalance, *i.e.* practically, when mainly the post-fire canopy cover and in a second stage the overall ecological services of an affected forest have reverted to their pre-fire conditions, at least to a considerable extent. The post-fire environmental recovery, examined from the perspective of full vegetation recovery is analysed in the following.

There are several factors that affect vegetation recovery. More specifically, vegetation recovery depends strongly on fire severity (Agee, 1993; Díaz-Delgado *et al.*, 2003; Polychronaki *et al.*, 2013; Mayor *et al.*, 2007), the type of affected vegetation (Viedma *et al.* 1997; Inbar *et al.*, 1998; Lhermitte *et al.*, 2011; Díaz-Delgado *et al.*, 2003; Veraverbeke *et al.* 2010; Mayor *et al.*, 2007), soil properties (Bisson *et al.*, 2008), post-fire meteorological conditions (Cannon *et al.*, 2008; Henry and Hope, 1998; van Leeuwen *et al.*, 2010; Mayor *et al.*, 2007), as well as on the interaction of these factors. In addition, successive and frequent burnings affect forest fuel properties and delay vegetation recovery.

Regarding the time period between fire occurrence and vegetation recovery, it needs to be noted that, in general, each species that populates an area develops its own post-fire regeneration strategy (Rulli and Rosso, 2007). Vegetation recovery, at least to a certain degree, is much more rapid in case fire-adapted sclerophyllous shrublands are affected, and may take a few years (Viedma *et al.* 1997; Pausas and Verdú, 2005); while when boreal forests are affected recovery may last for several decades (Nepstad *et al.*, 1999). Prolonged post-fire vegetation recovery, with differences between burnt and unburnt areas persisting even 6 years after a fire may also be attributed to dry periods after the fire that delay vegetation recovery (Mayor *et al.*, 2007).

Re-established vegetation after a severe fire in a typical Mediterranean forest covered 10-30% of the affected area one year after the fire, extended over 50-70% of the area in the second post-fire year (Inbar *et al.*, 1998) and reached 90% between the third and the fifth post-fire years (Viedma *et al.*, 1997). Stickney (1986) examined reforestation process for 10 years after a holocaustic fire (*i.e.* a particularly severe natural fire disturbance) in the Selkirk Range in northern Idaho, USA. Detailed information on the development of different species is provided in his research.

Regarding the recovery rate in typical Mediterranean ecosystems, in many cases, increased recovery can be observed during the first post-fire years, which is often followed by a decreased recovery rate in the following years (*e.g.* Thanos and Marcou, 1991; Trabaud *et al.*, 1985; Eccher *et al.*, 1987; Marzano *et al.*, 2012). As mentioned in Brown (1972), when several years of relatively low rainfall follow

a large scale fire event and also in the absence of livestock activities over burnt areas, the regrowth of vegetation in affected catchments is significant.

In many cases, grassy ground cover is regenerated within weeks after a fire, especially in woodland and grassland areas that in general experience lower fire severity in comparison to forest ecosystems (Carey *et al.*, 2003). In a forested catchment in New Mexico affected by fire, a relevant research concluded that 1 month after the fire grass reforestation seeds began germinating and a couple of months after the fire crown spouts from shrubs that were not killed by fire were 15-30 cm high (Bolin and Ward, 1987).

A general conclusion that can be extracted from this research is that certain types of vegetation (*e.g.* herbs and shrubs) start becoming evident even during the first post-fire growing season, while full vegetation recovery, including tree colonization, occurs some decades later. It becomes thus obvious that re-established vegetation of specific species that are dominant in Mediterranean areas, needs approximately one year after a fire event to reach a certain extent, while this re-establishment becomes even more extended in the second post-fire year and recover maturity could be reached approximately 5 years after the event. The plant cover in the first post-fire spring is also critical when examining vegetation recovery (Keeley, 2009). Indicative pictures with vegetation recovery one, two and seven months after an extended forest fire are presented in Figures 3.4-3.6.



*Figure 3.4. Vegetation recovery of Tidbinbilla Nature Reserve (Australia), one month after extended fires in 2003 (Source: Technical Report 17, Wildfires in the ACT 2003, by Carey et al., 2003).*



*Figure 3.5. Vegetation recovery of Ginini Wetlands (Australia), two months after extended fires in 2003 (Source: Technical Report 17, Wildfires in the ACT 2003, by Carey et al., 2003).*



*Figure 3.6. Resprouting of a Coast Live Oak seven months after the Grand Prix Fire, in Claremont Hills, California, 2003 (Photo by Cliff McLean, available at: [http://www.natureathand.com/Main/NAHEssays\\_StationFireRecovery.htm](http://www.natureathand.com/Main/NAHEssays_StationFireRecovery.htm), originally published in Southern Sierran, Vol. 65 No. 12, December, 2009, Angeles Chapter of the Sierra Club).*

It needs to be mentioned though, that numerous plant species that dominate fire-prone ecosystems ultimately evolve adaptation mechanisms for post-fire regeneration (Thanos and Marcou, 1991; Kruger, 1983; Trabaud, 1987; Carey *et al.*, 2003; Calvo *et al.*, 2003). Furthermore, it is already well established that such alterations in recovery dynamics and the consecutive development of new reproduction strategies affect inevitably the future forest composition (Marzano *et al.*, 2012; Buscardo *et al.*, 2011). As a result, in some cases, the direct regeneration of species affected by fire, partially fails (Rodrigo *et al.*, 2004). In other cases, increased fire severity affects post-fire vegetation properties and vegetation succession, *i.e.* colonization by different vegetation species, can be induced over time. For example Polychronaki *et al.* (2013) observed a gradual shift from low vegetation to shrublands in severely affected areas. Nevertheless, this is not always the case, as negative correlation between high fire severity and alien plant invasion in some shrublands has also been observed (*e.g.* Keeley *et al.* (2008)).

In fact, in order to assess the ecological effects of wildfires and consequently estimate the required time for *environmental recovery* fire severity and site-specific information both prior to and after the fire need to be retrieved. Considering the extended spatial distribution and often the limited accessibility of affected areas, ground truth verification is often missing (Gitas *et al.*, 2012). Therefore, satellite remote sensing becomes an essential technology for relevant research, especially for the research on vegetation recovery, while vegetation indices, with NDVI being one of the most commonly used indices, are widely employed in post-fire vegetation monitoring (Gitas *et al.*, 2012; Shoshany, 2000; Henry and Hope, 1998; Lhermitte *et al.*, 2011; Díaz-Delgado *et al.*, 2003; van Leeuwen *et al.*, 2010; Veraverbeke *et al.*, 2010; Viedma *et al.*, 1997).

### **3.3.2 Hydrological recovery**

The intensity of the impacts of forest fires on the hydrological response of a catchment also seems to vanish progressively with time (Brown, 1972; Lavabre *et al.*, 1993). Hence, *hydrological recovery* can be considered as this type of recovery that is practically achieved when the post-fire catchment hydrological characteristics are similar to the pre-fire ones and the hydrological parameters have resumed their pre-fire values. In this case, the full recovery of vegetation coverage to its pre-fire conditions is not necessary, given that the post-fire hydrological behaviour of a catchment could be similar to its pre-fire behaviour, even in the absence of the same vegetation coverage – if for example the overall hydrological behaviour has resumed its pre-fire characteristics. It is due to revegetation, which is other than full vegetation recovery, that post-fire hydrological recovery will start taking place. According to Inbar *et al.* (1998) revegetation reduced significantly runoff and sediment yield and was considered the main factor for basin recovery to pre-fire conditions in Mt. Carmel in Israel. In addition, it is obvious that hydrological recovery occurs within shorter time periods in comparison to environmental recovery. In the current research, the examination of recovery from a hydrological perspective is an issue of priority and therefore research focuses on hydrological recovery.

### 3.3.2.1 Factors that affect hydrological recovery

Hydrological recovery rate depends primarily on fire severity, vegetation coverage, post-fire precipitation rate and total amount and erosion processes that may have followed the fire event and are linked in turn with the geological, hydromorphological and geographic characteristics of the affected area.

Regarding fire severity, severely burnt catchments present a relative slow hydrological recovery rate that could exceed 4 years in contrast to less affected areas, the recovery rate of which could be even 1 year (Brown, 1972). Vegetation recovery has been analysed in Section 3.3.1, as a principal component of environmental recovery. A full vegetation recovery is not a prerequisite of the hydrological recovery, since the hydrological behaviour of an affected catchment could resume its pre-fire status even if the affected vegetation has not fully recovered. For example, seed germination takes place in average a couple of months after a fire (the timespan depends on the parameters analysed in Section 3.3.1) and the vegetation coverage of affected land starts then being recovered (see Figure 3.5). A few years later (the timespan depends again on the parameters analysed in Section 3.3.1) vegetation will grow and the catchment is expected to resume its pre-fire hydrological behaviour (in terms of infiltration, retention *etc.*). Therefore, hydrological recovery is expected to occur sooner than the full vegetation recovery. Moody and Martin (2001a) suggest that relaxation time for the regrowth of trees is expected to be even longer than the hydrological recovery, which in terms of runoff could even reach 30 years in some cases.

Similarly to environmental recovery, hydrological recovery also depends on post-fire meteorological conditions and in particular post-fire rainfall totals and intensity, given that such conditions determine the recovery of the vegetation coverage. Aiming to collect and analyse pre- and post-fire rainfall events and the corresponding hydrological response of the catchment to each event, it is necessary to classify the rainfall events in different categories, *i.e.* low rainfall rate events, intense events, medium rainfall rate events, events with long or short duration *etc.* However, due to the significant spatiotemporal distribution of rainfall, it is important to collect relevant datasets from adequate raingauges, which need also to be installed in representative locations within or around the catchment, and thus minimize over- and underestimation of rainfall depth and intensity particularly during events that are developed locally. Evidently, even when such a classification has taken place, it still remains difficult sometimes to tell whether a variation in the hydrological response may be attributed to the rainfall characteristics or to particular local conditions (*e.g.* area affected by a previous wildfire event).

The recovery rate also depends on the degree and sometimes the type of **erosion** that has occurred in an affected area. Thus, areas where sheet erosion has occurred are under a slow hydrological recovery rate, even for many years after the wildfire (Brown, 1972).

### 3.3.2.2 Temporal dimension of hydrological recovery

Analyses relevant with hydrological recovery are sometimes distinguished into: analyses of the pre-fire period, analyses of the post-fire period (that usually extends from the time of fire extinguishment to the end of spring in the subsequent year) and analyses of the transient period (a time-variant period necessary for soil restoration) (see for example Rulli and Rosso, 2007). Thorough literature review was performed at this stage in order to identify typical timespans between fire occurrence and hydrological recovery as regards different hydrological characteristics. It is difficult, not to say risky, to extract universal rules from this research; however, the issues presented below support a more comprehensive understanding of the temporal component in hydrological recovery.

The time period for the recovery of runoff rates to their pre-fire values is highly variable, as illustrated by the relevant studies presented in the following. In particular, a forested basin in New Mexico that has been affected by fire recovered its long-term average runoff 2 years after the occurrence of fire (Bolin and Ward, 1987). In Inbar *et al.* (1998) two years after a fire event in Mt. Carmel in Israel, runoff rate was decreased by 1-2 orders of magnitude in comparison with the first post-fire year. In Rulli and Rosso (2007) it is assumed that post-fire runoff matches the pre-fire one, two years after fire occurrence. Brown (1972) suggests that increased runoff is to be expected for at least the first 4 years after the occurrence of a fire event. More specifically, Brown (1972) states that in severely affected catchments of New South Wales in Australia, the recovery rate of runoff exceeds 4 years, while in less affected areas this rate could be even 1 year. A period of at least 3-4 years for the runoff recovery of forest zones in Colorado is suggested by Moody and Martin (2001a). In Mayor *et al.* (2007) annual runoff remained about two orders of magnitude higher when burnt areas were compared with unburnt, even 5 years after the fire. However, this rather abnormal persistence and unordinary for Mediterranean conditions values of runoff and sediment yield was attributed to two dry years after the fire, which delayed plant recovery. Inbar *et al.* (1998) presented some results from a study in California and indicated that approx. 30 years are necessary for runoff recovery. These 30 years for runoff recovery are also mentioned in Moody and Martin (2001a). Regarding the recovery of peak flows, according to Springer and Hawkins (2005) post-fire peak flows seem to be of the same order of magnitude with the pre-fire ones within 3 years after the Cerro Grande fire in New Mexico.

Increased sediment yield seems to persist for years after a fire. According to a research on the post-fire conditions of the affected Mt. Carmel in Israel, sediment yield was decreased by 1-2 orders of magnitude the second post-fire year, in comparison to the yield during the first post-fire year (Inbar *et al.*, 1998). Mayor *et al.* (2007) refer an increase of two orders of magnitude in sediment yield between unburnt and burnt areas, with high values persisting even 5 years after a fire. A period of 5-10 years for recovery of a burnt Mediterranean area in terms of sediment yield is suggested by Inbar *et al.* (1998), while relevant studies also presented in Inbar *et al.* (1998) concluded that 10-20 years are necessary for sediment yield recovery in California. In Moody and Martin (2001a) relaxation time for sediment yield is supposed to vary between 1 and 3 years. According to Moody

and Martin (2001a), a period of 4-5 years is necessary for the recovery of sediment transport rates of affected forested land in Colorado.

According to Campo *et al.* (2006) soil erosion is more intense for a period of 4 to 6 months after a fire in Mediterranean areas due to their particular rainfall distribution. Particularly for gully and rill erosion, the processes are pretty faster and probable to start taking place immediately after the fire event (Bisson *et al.*, 2005). In a severely affected catchment a thousand fold increase in erosion rate over the first 12 to 18 months after the fire is expected (Brown, 1972). Moody and Martin (2001a) suggest that the recovery of erosional response in affected forested zones in Colorado needs at least 3-4 years to take place, while Rulli and Rosso (2007) suggest that soil loss recovery takes 2 to 10 years in Mediterranean areas. The recovery of soil hydrophobicity also seems to last a few years. According to Robichaud (2000) soil hydrophobicity usually disappears 1 to 2 years after fire occurrence.

Shallow landslides generate debris flow and usually occur several years after a fire event (Bisson *et al.*, 2005). According to Meyer *et al.*, (2001) shallow landslides usually occur within 4-10 years after a fire, while debris flow that results from surface runoff usually occurs 1-2 years after a severe fire event. In burned areas in southwestern Colorado, debris flow started 6-10 min (*i.e.* practically instantaneously) after high-intensity convective storms of short-duration (less than 3 h), and approx. 16 h after lower-intensity frontal storms of long-duration (up to 30 h) (Cannon *et al.*, 2008). Inbar *et al.* (1998) indicated a period of approx. 7 years for debris recovery, based on the results of a study in California.

The majority of fire events in typical Mediterranean areas occur during the late summer (usually between late July and early September). The beginning of the growing season, which is typically in early spring (usually March), is critical for post-fire vegetation regrowth in these areas, especially during the first post-fire years. Therefore 7 and 19 months after the fire event, which denote the first and the second post-fire springs respectively, are critical for vegetation regrowth, as presented in Section 3.3.1. The 12, 24, 36 and 48 post-fire months correspond to the first 4 post-fire years, which, as deduced from the abovementioned statistics on hydrological recovery, can also be considered as typical benchmarks for post-fire vegetation regrowth in such areas. For these reasons, the time windows of 7, 12, 19, 24, 36 and 48 months after a fire event can be considered as typical benchmarks for post-fire vegetation regrowth and thus hydrological recovery in areas affected by successive forest fires.

### **3.4 Effect of floods on imminent forest fires**

Even though this research focuses on the other way of floods-fires interaction, *i.e.* the effect of forest fires on upcoming floods, a brief discussion on the effects of floods on imminent forest fires is presented in the following paragraphs for reasons of completeness. As presented in the following, these effect are ambiguous, difficult to quantify and could be part of another research.

In apparent self-contradiction, severe floods are many times followed by fires. On a short-term basis this happens when the lightning activity that precedes a flood

event is particularly intense and may itself set a forest to fire. Especially in urban areas, forest fires after flooding may occur due to successive short-circuits as a result of damages in the electric installations or even due to damages in gas pipes.

Focusing on periurban areas, floods are associated with forest fires in the long run. The total rainfall depth and intensity during the wet periods as well as the extent, level and duration of potential flooding affect significantly the vulnerability of an area to forest fire and its potential severity. More specifically, after a particularly wet winter the soil is saturated, the vegetation has absorbed significant amounts of water and thus forest fuels are less flammable. Therefore, in general, the occurrence of flood events during the wet periods is associated with reduced fire activity during the dry seasons. In Heinl *et al.* (2007), the highest fire activities in the southern Okavango Delta in Botswana were observed after several years with declining flood intensity.

On the other hand, increased rainfall activity and to some extent even flooding, result in increased production of biomass fuel (grass, shrubs, dead wood *etc.*) in forests, and then fire activity is expected to be more frequent. As commented in Heinl *et al.* (2007), exceptionally wet winters produce sufficient fuel for fire spreading. As a result, spring precipitation is often associated with summer fires.

### **3.5 Identification of existing gap in literature**

Numerous studies have been performed aiming to quantify the impact of forest fires on the hydrological behaviour of a catchment. In some studies relevant pre- and post-fire datasets have been analyzed, however, in many cases, no gauging or calibration has taken place in order to verify or improve suggested post-fire alterations (Cerrelli, 2005).

Another gap identified in literature is the fact that the majority of relevant studies focus on the overall post-fire hydrological response of a catchment and not on the impact of forest fires on particular, representative hydrological parameters that determine this response (*e.g.* Cannon *et al.*, 2008; Rulli and Rosso, 2007; Inbar *et al.*, 1998; Scott and Van Wyk, 1990). Only in some studies is fire impact on specific hydrological parameters examined; yet these parameters are limited (Papathanasiou *et al.*, 2012), usually restricted to the runoff Curve Number, CN (Higginson and Jarnecke, 2007; Foltz *et al.*, 2009), and they do not readily explain the post-fire CN trends (Springer and Hawkins, 2005). Fire impact on other hydrological parameters that still have a significant impact on a catchment's response, such as initial abstraction (IA), standard lag (TP) *etc.* is systematically ignored. However, an integrated approach towards efficient post-fire flood modelling necessitates the estimation of the post-fire values of all parameters that are associated with the individual aspects of flood hydrographs, *i.e.* parameters that affect runoff discharges, peak flows and times to peak.

Parallel to that, research in this field focuses on the estimation of post-fire values of hydrological parameters (usually CN, as mentioned above) for recently burnt areas, commonly referring to the period between the fire event and the beginning of the next growing season (*e.g.* Cerrelli, 2005; Higginson and Jarnecke, 2007) or the first 1-2 post-fire years (Cannon *et al.*, 2008; Rulli and Rosso, 2007; Inbar *et*



*al.*, 1998; Scott and Van Wyk, 1990). Still, as examined in Section 3.3, after a specific time period from a fire occurrence, which depends strongly, albeit not exclusively, on fire severity, *hydrological recovery* occurs and post-fire values recover to the pre-fire ones. Therefore, post-fire values need to be estimated for longer post-fire periods. This disregard of the temporal dimension of fire impact on a catchment's hydrological behavior is another gap identified in literature.

As discussed in Chapter 2, FEWS are useful tools for efficient flood risk management. In order to perform representative flood simulations and issue accurate warnings, such sensitive systems need to be updated with reliable information. As a result of the fact that only the recent forest fires are usually considered in hydrological simulations, FEWS and other operational systems for civil protection that operate in areas prone to both floods and forest fires may often issue inaccurate warnings. In practice, typical operational FEWS in fire-prone areas identified in literature either ignore the potential fire impact (*e.g.* Berni *et al.*, 2009) or, even when fire is considered, they do not account for fires-floods interaction (*e.g.* Kalabokidis *et al.*, 2005). This interaction needs to be taken into account aiming to the effective operation of FEWS.

Additionally, in studies for fire impact on a catchment, the overall hydrological conditions of the catchment are usually simplified. In particular, and as presented in Chapter 5, one of the most significant "short-term" initial hydrological conditions indicator is soil moisture. As analyzed in detail in Section 5.2, in the absence of regular and representative monitoring of a catchment's soil moisture conditions, this factor is typically assumed to be static, usually constantly wet during the rainy season and constantly dry during the dry season (Berthet *et al.*, 2009). This oversimplification however, may lead to significant errors and inefficient simulations (Brocca *et al.*, 2008; Tramblay *et al.*, 2012; Massari *et al.*, 2014; Ponziani *et al.*, 2013).

A holistic approach to post-fire flood modelling that can also support civil protection operational systems on a short-term basis and flood risk management plans in the long run is still missing in literature. Based on the aforementioned issues, such an approach necessitates the incorporation of the impact of fires in hydrological models, while the concurrent consideration of soil moisture conditions also emerges as a necessity. In literature, these factors are not only examined inefficiently (despite relevant recent works, a coherent, widely applicable and clear guidance regarding the choice of post-fire values of hydrological parameters is missing (Foltz *et al.*, 2009; Springer and Hawkins, 2005; Cerrelli, G., 2005), while soil moisture conditions are ignored or simplified), but they are also examined individually.

In addition, the wide applicability of the results of most of these studies is restricted due to variable initial conditions in terms of fire severity and soil moisture and different rainfall characteristics during each one of the analyzed rainfall-runoff events and for this reason these results can only be considered representative within their specific conditions (*e.g.* the study of Marzano *et al.* (2012) for catchments in northwest Italy, the study of Zhou *et al.* (2013) for southeast Australia, the study of Cerrelli (2005) for Montana State, the study of Springer and Hawkins (2005) for Cerro Grande fire that occurred in New Mexico in 2000, the

study of Livingston *et al.* (2005) for Los Alamos in New Mexico, the study of Inbar *et al.* (1998) for Mount Carmel in Israel *etc.*) (Papathanasiou *et al.*, 2015a).

Therefore, a need for an integrated, coherent and as generalized as possible methodological framework for the estimation of post-fire values of representative hydrological parameters that will also consider the temporal dimension of fire together with initial soil moisture conditions emerges in literature. This methodological framework needs to be widely accepted and applicable and easily incorporated in flood modelling, aiming to support also civil protection operational systems, as well as flood risk management planning in the long run. The attempt made to develop this framework during this research is presented in detail in the following Chapters.

## CHAPTER 4: FLOOD MODELLING

The environmental and socioeconomic impacts of flash floods on individuals and communities, as well as the intensification of these impacts in case a forest fire precedes a flood event, are highlighted in Chapters 2 and 3. This floods-fires interaction is critical in periurban areas, in which the existence of forests increases fire risk and the vicinity of residential areas and cultivation areas to forests (WUI) is associated with increased impact of flooding. As also mentioned in Chapter 2, the combined action of floods and fires is quite frequent in typical Mediterranean areas, since Mediterranean vegetation is highly flammable (Thanos and Marcou, 1991) and typical hydrometeorological conditions favor increased fire risk during the hot and dry summer periods (Esteves *et al.*, 2012) and flood risk during the rainy season. Therefore, a necessity to improve flood risk assessment and management, define flooding scenarios and if possible predict flood events in typical Mediterranean periurban areas emerges. This imperative need may be covered through effective and representative simulation of the hydrological processes in a periurban catchment. To this end, it is crucial to have reliable relevant datasets and exploit them through the application of appropriate modelling tools. This Chapter focuses on flood modelling that supports efficient flood risk assessment. Given that the current research focuses primarily on efficient hydrological modelling, which in turn will support hydraulic modelling, hydrological models are described in detail.

In order to perform an integrated flood study for an area with mixed rural and urban land uses it is necessary to perform a hydrologic study and then produce flood inundation maps. Therefore, a complete flood study basically requires two modelling phases, *i.e.* hydrological modelling and hydraulic modelling. The sound implementation of each modelling phase necessitates the exploitation of reliable datasets through efficient modelling tools. A short description of each modelling phase, as well as particular characteristics and further classifications of the corresponding tools required for flood modelling, *i.e.* the hydrological models and the hydraulic models, are presented in the following.

### 4.1 Hydrological modelling

The first phase of flood modelling is hydrological modelling, *i.e.* simulation of the response of a catchment to rainfall, in terms of produced runoff discharges at properly selected locations in a catchment. The mathematical equation that represents the hydrological cycle is the water balance equation, each component of which is calculated using mathematic relationships, often adapted to particular case-specific conditions. Thus, hydrological modelling is the integrated and simplified solution of a properly chosen set of such relationships, which can result in the calculation (for historic or real-time datasets) or prediction (for stochastic timeseries) of the values of specific parameters at predefined locations (*e.g.* discharge timeseries at the outlet of a watershed). Since several components of the hydrological cycle are crucial in the hydrological planning and the flood management of an area (*e.g.* an accurate calculation of stage and discharge values is critical for a representative estimation of flood extent in an area) and given the difficulty in their estimation without hydrological modelling, the

application of hydrological models has gained ground widely and during the last decades hundreds of hydrological, and in particular rainfall-runoff models, have been developed and are used extensively.

As mentioned above, hydrological modelling aims at the estimation of runoff discharges at selected locations in a catchment. To this end, rainfall is converted to runoff and the produced runoff is routed to the selected locations. In general, flood routing, which is the propagation of a flood wave in a channel, is governed by the continuity (Conservation of Mass) and the momentum equations.

In their full (not simplified) form the quasi-linear hyperbolic partial differential equations need to be solved numerically and this is computationally demanding. To this end, numerous simplified routing schemes have been developed. These simplification schemes are classified into purely empirical, linearized, hydrologic and hydraulic routing schemes (Fread, 1985).

In the following Section a description of the types of hydrological models is presented, while a review on representative and widely applied hydrological models, including the routing schemes incorporated in them is presented in Sections 4.2.1 and 4.2.2.

## 4.2 Hydrological models

Hydrological models can be classified into numerous categories, according to their particular characteristics and modelling procedures. The main categories and the corresponding types of models are briefly presented in the following.

According to its mathematical structure, a hydrological model can be classified as stochastic or deterministic. In particular, when a hydrological model uses mathematical and stochastic concepts, describes the random variation and incorporates it in the predictions of outputs, it can be characterized as a stochastic model. On the other hand, in the case of a deterministic approach, *i.e.* when all input data, parameters and processes in the model are considered free of random variation and are supposed to be known with certainty, then the model is a deterministic model (Feldman, 2000). In stochastic models the input is partly randomized, the outputs are not exactly repeatable and the probabilistic solutions are ranged. This is not the case for a deterministic model, the input in which is absolutely known and controlled, the outputs are exactly repeatable and its solutions are specific and fully defined (Gregory and Goodie, 2011).

According to the knowledge base upon which the mathematical models are built, they can be either empirical models (or black-box systems or system theoretic models) or conceptual (or process-based) models. When the knowledge base is observation of input and output and the explicit representation of the conversion process is ignored, then the model is classified as empirical. Detailed knowledge of the physical processes that explain the transformation of specific input to particular output and representation of this knowledge by means of mathematical equations allows for the development of conceptual models. When these mathematical equations represent the physics governing a phenomenon, *i.e.* streamflow and flux generation in hydrology, then the conceptual models are

characterized as physics-based (or physically-based) (El-Shaarawi and Piegorsch, 2002). Equations of conservation of mass and momentum for flow are typical equations that need to be solved in physics-based hydrologic models.

Another major feature that may classify a hydrological model concerns their spatial distribution. More specifically, a hydrological model may describe a watershed as a single aggregate entity, in which case it is characterized as lumped model, as a number of subcatchments with different properties attributed to each subcatchment, characterized in this case as a semi-distributed model, or as a number of discrete cells, each cell having different properties, being classified in this latter case as a (fully) distributed model. In order to set up a lumped model, a relative small number of parameters and variables is necessary (Refsgaard, 1997) and the spatial variations of catchment and rainfall properties (e.g. soil properties, topographic, land cover and land use characteristics, spatiotemporal distribution of rainfall) are averaged out or ignored. Inevitably, as also stated in Shultz (2007), many assumptions need to be made in a lumped modelling approach, which in the end may distort the overall hydrological behaviour of a catchment. The structure of fully distributed hydrological models makes allowances for the incorporation of the spatial variation of catchment and rainfall properties at a grid point basis, which however makes the application of these models particularly data- and time-demanding. In principle, the necessary parameters and variables for distributed models are usually two to three orders of magnitude higher than the corresponding parameters for lumped models, for the same catchment (Refsgaard, 1997). The intermediate approach, *i.e.* the semi-distributed modelling is frequently favored, in order to avoid the aforementioned drawbacks of the other two approaches. Nevertheless, it needs to be highlighted that increased spatial distribution is not necessarily related with increased model performance (Shultz, 2007; Boyle *et al.*, 2001; Smith *et al.*, 2004) and thus, available datasets, required computational time, modeler expertise and required accuracy need to be evaluated separately for each model application. Ajami *et al.* (2004) referred to an additional classification of spatial distribution in models, *i.e.* the semi-lumped models, which constitute an intermediate type between lumped and semi-distributed models and which uses the semi-distributed structure with the constraint that the parameters remain identical for all subcatchments. However, it is widely accepted that the classification of models into lumped, semi-distributed and (fully) distributed is adequate to cover all cases and no additional classification is required.

The time scale selected for a hydrological simulation is determinant of whether a steady-state or a dynamic model is more appropriate for this simulation. When it is required to perform a continuous simulation of the long-term hydrological properties of a catchment, then a steady-state (or continuous) hydrological model needs to be selected. A steady-state model performs simulations for continuous time periods, e.g. days, months, years, decades, selected according to the specific requirements and data availability of each simulation. On the other hand, when it is required to simulate the hydrological response of a catchment for a given event then it is more appropriate to apply a dynamic (or event-based) hydrological model. A dynamic model can simulate a single event (e.g. a particular flood event), regardless of its duration, which is case-specific and needs to be defined by the modeler during the setting up of the model.

Hydrological models can be further classified into groundwater, surface water or combined models according to their application field. In general, since hydrology incorporates both groundwater and surface water analysis, a hydrological model can be either a groundwater model, if it focuses on the simulation of the properties and the conditions of aquifers, a surface water model, which mainly focuses on the simulation of the rainfall-runoff procedure and flow (and/or flood) routing, or a combined model, if it includes elements for the simulation of both groundwater and surface water conditions. For example the LGSI model presented in Wanders *et al.* (2011) is a combined groundwater and surface water lumped model. However, the simulation of groundwater conditions is skipped during flood modelling, especially for event-based applications, given the limited temporal scale that is required for flood analyses.

#### **4.2.1 Review on lumped (and semi-distributed) hydrological models**

Historically, the lumped approach has been the initial approach towards the estimation of streamflow at a basin outlet. However, it has been recognized that, especially for large catchments, the application of lumped models could be considered acceptable only until more suitable spatial distributed models (either semi- or fully-distributed) would become widely available (Becker, 1992). As a result, the lumped approach has progressively been complemented and sometimes replaced by the semi-distributed approach (currently the semi-distributed approach is incorporated in most lumped models); while over time and under particular conditions (which include *inter alia* data availability, computation efficiency and modeler expertise) the application of fully distributed modelling has emerged as a robust option. Focusing on hydrological models applied for flood modelling and considering the fundamental classification of hydrological models into lumped and distributed, the models described in the following paragraphs have been identified as the most representative and widely applied ones.

##### **4.2.1.1 HEC-HMS**

**HEC-HMS (Hydrologic Engineering Center – Hydrologic Modeling System)** is a software that has been designed for the simulation of the complete hydrological processes of dendritic watershed systems. It is a product of the Hydrologic Engineering Center, an organization of the U.S Army Corps of Engineers (USACE). Hydrologic Engineering Center has developed a comprehensive list of models that can be applied for relevant simulations in the technical areas of surface and groundwater hydrology, river hydraulics, hydrologic statistics, risk analysis, sediment transport and many other related technical fields<sup>5</sup>. HEC-models are continuously being updated and new, improved versions of the models become regularly available. HEC-HMS is one of the most widely applied models that have been developed under the umbrella of HEC-models and it is also ranked among the most widely applied hydrological models on a global scale.

---

<sup>5</sup> A full list of models is available at the link: <http://www.hec.usace.army.mil/software/>

HEC-HMS can be used either in a fully lumped or in a semi-distributed mode. As described in Section 4.2, in the first case the whole catchment is considered as an integrated unit, with uniform catchment characteristics, while in the second case the catchment can be divided into a number of subcatchments. Preferably, and when applicable, the outlets of each subcatchment coincide with the locations where stream flow gauges are installed, so that the produced discharges at the outlets can be calibrated with observed measurements from flow gauges. Hydrological analysis with HEC-HMS is based on the establishment of independent submodels for the computation of the following hydrological parameters: hydrological loss, direct runoff, baseflow and channel flow routing. After the selection of the methods that will be used for those models, a meteorological model and a control specifications manager are established (Scharffenberg and Fleming, 2010). In addition, HEC-HMS can run either in a dynamic mode (for representative flood events) **or** in a continuous mode (for a defined simulation period). HEC-HMS needs to be calibrated with observed datasets (for some events in the dynamic mode or for a selected period in the continuous mode) and then validated (for the rest of the events or the rest of the simulation period, respectively) in order to produce reliable discharges at the selected locations. Regarding channel routing, HEC-HMS offers six different options (the Lag method, the traditional Muskingum method, the Muskingum-Cunge method, the Modified Puls method, the Kinematic-wave method and the Straddle Stagger method), while for surface runoff HEC-HMS provides two options (either empirical models (the typical unit hydrograph models) or a conceptual model (the kinematic-wave model of overland flow)) (Lastoria, 2008).

The main factors that have contributed to the extended application of HEC-HMS include *inter alia* the fact that this model (similarly to all HEC-models) is open source and can be freely downloaded from the website of USACE<sup>6</sup>, the software is accompanied by comprehensive documentation for its application, it is quite easy to apply and it offers a wide range of methods incorporated within the model for the simulation of the hydrological behaviour of a catchment. Another main advantage of this model is its seamless coupling with Geographic Information Systems (GIS). In particular, HEC-HMS can be coupled with the Geospatial Hydrologic Modeling Extension (HEC-GeoHMS). HEC-GeoHMS is an extension that can be incorporated in Spatial Analyst in ArcGIS (a platform for mapping and analysis of spatial information, developed by ESRI<sup>7</sup>) that allows for accurate processing and visualization of spatial catchment characteristics.

#### **4.2.1.2 TOPMODEL**

**TOPMODEL** is a continuous, semi-distributed, physically-based hydrological model designed basically for the long term simulation of hydrological processes. Similarly to most semi-distributed models, it also offers the option to model a single catchment (lumped approach). The model, originally named TOPography MODEL (Beven and Kirkby, 1979) was introduced by Kirkby and Weyman in 1974 (Kirkby and Weyman, 1974) at the School of Geography, University of Leeds and was further developed by Beven at the Lancaster University.

---

<sup>6</sup> <http://www.hec.usace.army.mil/software/hec-hms/>

<sup>7</sup> <http://www.esri.com/software/arcgis>

TOPMODEL is a variable contributing area rainfall-runoff and routing model that takes into consideration the effects of hillslope topography. Given topography information and flow patterns, the model clusters together areas of similar soil conditions and predicts slope discharge. Segmental slope discharges are then distributed to the channel network, through the appropriate routing sub-model, and routed to the outlet of the basin. As a result of this “lumping-approach” and regardless of further required validation, the computing requirements are significantly reduced. In general, the model is most appropriate for the modelling of catchments with shallow soils and moderate topography, which do not suffer from excessively long dry periods. TOPMODEL was initially developed to simulate catchment behavior under humid conditions in UK, Eastern USA and Scotland. Its updated versions improved its suitability for different conditions. The model is successfully applied over a range of small and medium sized basins. Regarding channel routing in TOPMODEL, a simple non-linear routing scheme was incorporated in the updated version of the model, which considers the average kinematic wave velocity of the channel network as spatially constant and equal to water velocities measured by tracer experiments (Beven and Kirkby, 1979). For the estimation of overland flow routing TOPMODEL includes two different mechanisms, the infiltration excess and the saturation excess (Lastoria, 2008).

The model can be downloaded for free<sup>8</sup> for academic and research purposes. Another advantage of TOPMODEL is its suitability for implementation within GIS. However, it needs to be noted that the model does not include an automatic optimization routine. Yet, its updated versions are compatible with the GLUE Freeware, a software that provides tools for calibration, sensitivity analysis, uncertainty estimation using the results of Monte Carlo simulation<sup>9</sup>. Thus, TOPMODEL offers the option to export Monte Carlo simulation results for further use with GLUE. The fact that TOPMODEL assumes steady-state conditions at a point is recognized by Ciarapica and Todini (2002) as the main disadvantage of this model, since such an assumption becomes unrealistic for cells that have a magnitude of hundreds of meters.

#### **4.2.1.3 ARNO**

**ARNO** is a continuous, semi-distributed, conceptual rainfall runoff model applied both in land-surface-atmosphere processes research and in operational flood forecasting. It was developed by Prof. Todini (University of Bologna, Department of Earth and Geo-Environmental Sciences) in 1988 within the framework of the implementation of a hydrological study for river Arno in Tuscany in Italy (Todini, 1988). Besides the aforementioned operational applications in real-time flood forecasting (ARNO is a core component of the European Flood Forecasting Operational Real-Time Systems (EFFORTS)) and research applications in catchment modelling, ARNO may also be applied as a tool for examining the impact of land uses changes (Todini, 1996; Lastoria, 2008).

---

<sup>8</sup> TOPMODEL can be downloaded for free at:

[http://www.es.lancs.ac.uk/hfdg/freeware/hfdg\\_freeware\\_top.htm](http://www.es.lancs.ac.uk/hfdg/freeware/hfdg_freeware_top.htm)

<sup>9</sup> The GLUE Freeware can be downloaded for free at:

[http://www.es.lancs.ac.uk/hfdg/freeware/hfdg\\_freeware\\_glue.htm](http://www.es.lancs.ac.uk/hfdg/freeware/hfdg_freeware_glue.htm)



The model is characterized by two main components; the most important component concerns the highly complicated soil moisture balance, while the other main component concerns the routing of runoff along the hillslopes to the drainage channels and along the channel network to the outlet of the basin. The contribution from upstream subcatchments is routed downstream by means of a concentrated-input linear parabolic model and channel routing is performed through a distributed-input linear parabolic model (Todini, 1996).

Additional modules incorporated in the model concern evapotranspiration, snowmelt and groundwater (Todini, 1996). All modules are interlinked and a detailed representation of physical phenomena is achieved through the communication of all modules. Required datasets in order to set up ARNO for a catchment include: an orographic map of the basin (the scale ranges between 1:25000 and 1:100000, depending on the actual size of the catchment), continuous historical records of precipitation, temperature and water levels at several monitoring stations within the catchment, historical records (not necessarily continuous in time) of monthly average temperature, rating curves for all the hydrometrics stations where the discharge will be simulated, geographical coordinates and elevation above mean sea-level for all monitoring stations and when possible a soil map and a land use map at a coarse scale (Todini, 1996). In general, even though ARNO cannot be directly matched with GIS and fine discretized radar images, it is simple, flexible, well-documented and it incorporates simplified calibration operations. As a result, ARNO is widely and successfully applied to operational flood forecasting systems and to modelling of medium and large catchments with different hydromorphological conditions. However, the lack of physical interpretation of model parameters, especially of those of relevance to the horizontal movement in the unsaturated zone, is the main disadvantage of ARNO, particularly with regards to GCM (General Circulation Model) applications (Ciarapica and Todini, 2002).

#### **4.2.1.4 SWAT**

**SWAT (Soil and Water Assessment Tool)** is a physically based, continuous, semi-distributed river basin scale model that quantifies the impact of land management practices in large complex watersheds, with varying soil, land use and management conditions and over long time periods. It was initially developed in the early 1990s and was the an outcome of the joint effort of US Department of Agriculture – Agricultural Research Service (USDA-ARS) and TEXAS A & M AgriLife Research, part of the Texas A & M University System. The model is regularly updated and supported by USDA-ARS and TEXAS A & M AgriLife Research.

This model simulates both the qualitative and quantitative properties of surface and groundwater and provides predictions of the environmental impact of changes in land use and land management practices. For simulations in its semi-distributed mode, SWAT allows the division of a catchment into a maximum of 100 subcatchments. For the simulation of the physical processes the model needs input for the weather, the soil properties, the topography, the vegetation and dominant land management practices occurring in the watershed. The detailed information that needs to be provided for climate and the relevant options that are

offered make this model appropriate for efficient simulations of climate change scenarios. Regarding flood routing, SWAT incorporates the Muskingum routing method, and it also offers the option for flow routing through a variable storage coefficient method (Neitsch *et al.*, 2011).

SWAT is a public domain model that can be downloaded for free<sup>10</sup>. It can also be easily connected with GIS, expanding its capabilities for spatial processing. As mentioned above, SWAT is exclusively a continuous model, on the contrary to other hydrological models that may offer the option for either continuous or event-based simulations (e.g. HEC-HMS), and thus it cannot simulate single events. As a result of the required inputs and produced outputs from SWAT, it is widely applied for assessment and control of soil erosion, non-point source pollution and regional watersheds management.

#### **4.2.1.5 Hydrological modules provided by hydraulic models**

In literature, one may find several flood models that include both a hydrological and a hydraulic component. These models simulate both procedures that are necessary for a flood analysis, *i.e.* rainfall-runoff conversion and flow routing; however, in general, they can be considered as most accurate for one of these components. The most frequent case is to find “hydrologic modules” incorporated in models characterized in principle as hydraulic models. These modules serve as hydrological models that produce the necessary runoff datasets for the hydraulic analysis. These hydraulic models are either compulsorily coupled with their corresponding hydrological module, or can be applied independently, *i.e.* coupled with any other hydrological model. In the current research these models are classified as hydraulic models (and are presented in the Section 4.4), while representative hydrological modules that are incorporated in hydraulic models are presented in Sections 4.2.1.5.1 and 4.2.1.5.2 below.

##### **4.2.1.5.1 NAM and UHM**

DHI (Dansk Hydraulisk Institut) Water & Environment is an independent, self-governing, consulting and research organization in Denmark. It was originally founded in 1964 as an offshoot of the Technical University of Denmark and has extended expertise in water-related issues. DHI has developed the MIKE series, a comprehensive suite of modelling software related to integrated water resources; urban and marine (offshore, coastal, and port) hydraulics; environmental engineering; water quality and ecology<sup>11</sup>. The full list of MIKE by DHI software is available at the official website of the organization<sup>12</sup>. MIKE by DHI is commercial software. Academic, demo versions of several DHI products are distributed by the Institute at lower prices. In this Section, two hydrological modules, *i.e.* NAM and UHM are presented.

MIKE11 (described in Section 4.4.1.2), which is a typical hydraulic model of DHI, can be coupled with any hydrological model which will provide runoff to the hydraulic model, but it also offers the possibility to simulate runoff using either

<sup>10</sup> SWAT can be downloaded for free at <http://swat.tamu.edu/software/swat-model/>.

<sup>11</sup> <http://www.stevenswater.com/software/modeling.aspx>

<sup>12</sup> <http://www.dhigroup.com>

simple empirical rainfall-runoff methods or complex fully distributed process-based modelling techniques. Simple rainfall-runoff methods include *inter alia* the application of the NAM or the UHM modules, which are typical hydrological modules, incorporated in DHI hydraulic models, such as MIKE11, and are presented below. Regardless of the selected rainfall-runoff module, channel routing is performed by MIKE11, as described in Section 4.4.1.2.

The **NAM (Nedbør-Afstrømnings-Model)** is a deterministic, lumped and conceptual rainfall-runoff modeling software appropriate for the simulation of overland flow, interflow and baseflow. It can be applied in both continuous and event-based modes. The model represents the storage capacity of a catchment as a function the water storage in each one of four mutually interrelated storages. Man-made interventions in the hydrological cycle, such as water extraction *e.g.* for irrigation, groundwater pumping *etc.* can be taken into account in the simulation. Parallel to that, NAM has a number of optional extensions (*e.g.* a snow-melt routine) which further enhance its capabilities. Its efficiency is improved by the option for auto-calibration for 9 parameters that represent the surface zone, the root zone and the ground water storages (DHI, 2007b).

An alternative to the NAM module for event-based rainfall-runoff simulation provided by MIKE11 is the **Unit Hydrograph Module (UHM)**. MIKE11 – UHM is appropriate when historic streamflow records are not available and unit hydrograph techniques for flood simulation are already well established. Several unit hydrograph models which separate the rainfall into excess rainfall (runoff) and water loss (infiltration) are incorporated in the module and the estimated final runoff of a single storm event is the output of a selected unit hydrograph model (DHI, 2007b).

#### 4.2.1.5.2 Hydrological module of SWMM

Similarly, the **Storm Water Management Model (SWMM)** (described in Section 4.4.1.3) is another typical hydraulic model that has its own hydrological component. SWMM is a combined dynamic rainfall-runoff-subsurface runoff simulation model and conveyance system hydraulics software, developed by US Environmental Protection Agency (EPA), primarily for urban areas. EPA is particularly active in the development of environmental systems, including models, databases and applications. Such systems are provided in the Registry of EPA Applications, Models and Databases<sup>13</sup> (READ). SWMM was first developed in 1971 and since then it has undergone major upgrades.

A drainage system is conceptualized in SWMM as a series of water flows between four environmental compartments. For the runoff component of SWMM, *i.e.* for the production of runoff in selected subcatchments, the atmospheric compartment, the land surface compartment and the groundwater compartment need to be modeled. The fourth compartment that needs to be modeled is the transport compartment which is necessary for its routing component, (also described in Section 4.4.1.3). Focusing on its runoff component, it is deterministic, physically-based and it can perform either event-based or continuous simulations.

---

<sup>13</sup> [http://ofmpub.epa.gov/sor\\_internet/registry/systmreg/home/overview/home.do](http://ofmpub.epa.gov/sor_internet/registry/systmreg/home/overview/home.do)

The catchment is subdivided into small and homogeneous subcatchments, which drain to user defined discharge points. Each subcatchment has uniform values for imperviousness, Manning coefficient, slope and depression storage, while the other properties of the catchment remain user-defined. Overland flow is simulated through the kinematic wave routing method and channel routing is performed by SWMM, as described in Section 4.4.1.3.

The main advantages of the hydrological module of SWMM are that it is freely available<sup>14</sup> and also it is a component of a widely used and well-documented flood model. Besides, it offers the option to include in a simulation various types of Low Impact Development (LID) practices for capture and retention of rainfall – runoff (Rossman, 2010). However, its hydrological capabilities are limited, since they primarily aim to cover the needs of a hydraulic model and hence this module does not support a detailed hydrological analysis.

## **4.2.2 Review on distributed (GIS-based) hydrological models**

The accurate representation and interaction between surface flow, base flow, groundwater conditions and spatially varied precipitation, canopy storage, infiltration and evapotranspiration is particularly difficult and demanding and to this end a distributed hydrological model for the simulation of these physical procedures is necessary. The application of 2D physics-based numerical models for the simulation of the non-linear response of watersheds to spatially varied rainfall (and infiltration) has gained popularity among hydrologists since the early 90s (Julien *et al.*, 1995). Advances in remote sensing and computer power and the proliferation of Geographic Information Systems (GIS) tools and software have strengthened the potential of distributed hydrologic modeling and have thus contributed significantly to their wide application.

### **4.2.2.1 CASC2D & GSSHA™**

**CASC2D** is a 2D physics-based, distributed rainfall-runoff model, the original version of which was a 2D overland flow routing algorithm developed and written in programming language (APL) by Prof. P. Y. Julien, from Colorado State University. This flow routing module keeps being improved, refined and updated with new technology, mainly during the implementation of several doctoral dissertations. Initially, the model was improved with the integration of the Green & Ampt infiltration component and the explicit diffusive-wave channel routing component and was converted from APL to FORTRAN by Saghafian (Julien and Saghafian, 1991; Saghafian, 1992; Julien *et al.*, 1995). The model was linked with the public-domain Geographic Resources Analysis Support System (GRASS) GIS developed by U.S. Army Construction Engineering Research Laboratories in Champaign, Illinois, a linkage which further enhanced its efficiency. As a result, the model would simulate the hydrological response of a watershed to rainfall according to the outputs of its three major components: infiltration, overland flow routing and channel routing. Regarding overland flow the model used a 2D explicit

---

<sup>14</sup> SWMM can be downloaded for free at:  
<http://www.epa.gov/nrmrl/wswrd/wq/models/swmm/#Downloads>.

finite difference, diffusive-wave formulation, while the channel flow was simulated through a 1D explicit finite volume, diffusive-wave formulation. As far as infiltration is concerned, the model, as already mentioned, used the Green and Ampt infiltration method and considered spatially varied infiltration rate.

The main advantage of the CASC2D model is its ability to simulate spatially varied surface runoff while fully utilizing raster GIS and gridded weather radar rainfall data. The model produces runoff hydrographs which are generally more accurate than either the SCS or Snyders Instantaneous Unit Hydrograph approaches with Muskingum - Cunge channel routing in HEC-1 (Julien *et al.*, 1995). Additionally, the diffusive wave formulation enables overbank flow storage and routing, while allowing for the simulation of backwater effects in the channel. However, in its initial versions, the model did not consider the infiltration capacity recovery as a result of soil moisture redistribution between successive storm events. This had a trivial effect on single storm simulations, but infiltration should be reset for multiple storm simulations. In addition, CASC2D is particularly sensitive to the appropriate selection of the size of its square grid, the typical values of which range between 100 and 200 m.

This version of the model was further enhanced with the integration of continuous simulation capabilities, numerous other improvements and bug fixes and the ability to interface with the Watershed Modeling System (WMS) graphical user interface that was developed by the Environmental Modeling Research Laboratory (EMRL), at Brigham Young University (BYU). The updated version of the model which includes WMS-specific output routines is known as **CASC2D for WMS**. For public domain use WMS is available free of charge<sup>15</sup>. Despite its capabilities, especially in sedimentation simulations, CASC2D remains a complex hydrodynamic model, particularly time- and effort-demanding to apply and for this reason it is primarily applied for academic and research purposes (Ogden and Julien, 2002).

Previous work done by Kilinc (1972) and Kilinc and Richardson (1973) at the Colorado State University concerning upland erosion and channel sediment transport was incorporated to CASC2D model by Johnson (Johnson 1997; Johnson and Julien 2000). The integration of this new module resulted in its new version **CASC2D-SED**, which additionally allowed for the simulation of overland sediment transport. Further improvements of the sediment transport algorithm over this version were performed by Rojas (Rojas, 2002). The improved CASC2D-SED can simulate better the transition between supply-limited and capacity-limited sediment transport, allows the transport by advection of suspended material even when the transport capacity can be considered as negligible and improves the simulation of sedimentation in backwater areas. The final outputs of the CASC2D-SED model are hydrographs, sedigraphs and time-series thematic grids, including rainfall rates, infiltrated volume, water depth, eroded/deposited material, sediment flux and suspended sediment. This model has been successfully coupled with precipitation forecasts from weather radar and can thus predict local flooding conditions in a watershed based on distributed rainfall data

---

<sup>15</sup> [http://www.scisoftware.com/products/wms\\_freeware/wms\\_freeware.html](http://www.scisoftware.com/products/wms_freeware/wms_freeware.html)

(Jorgeson, 1999). The source code of CASC2D-SED can be downloaded for free<sup>16</sup>.

A new reformulation and significant improvement of the model by Ogden and Julien in 2002 resulted in the development of the finite difference based **GSSHA™** (*Gridded Surface/Subsurface Hydrologic Analysis*) model, in which the simulation of the runoff mechanism is not restrained to infiltration excess. The GSSHA™ model is developed and maintained by the US Army Engineer Research and Development Center (ERDC) Hydrologic Modeling Branch, in the Coastal and Hydraulics Laboratory and its features include 2D overland flow, 1D stream flow, 1D infiltration, 2D groundwater and full coupling between the groundwater, shallow soils, streams and overland flow. It can be applied in both arid and humid environments, for both large and small scale simulations, either as an event-based or as a continuous model, where the soil surface moisture, groundwater levels, stream interactions and constituent fate are continuously simulated. Its spatially explicit nature makes GSSHA™ appropriate for analysis of inherently distributed problems, such as sediment and non-point source pollution assessment and mitigation. Finally, as a physics-based continuous hydrologic model, GSSHA™ can be used *inter alia* for the assessment of fire threat, irrigation needs and the analysis of land use change and management scenarios for flood control, sediment and pollutant transport. GSSHA™ is periodically updated and released versions can be downloaded for free<sup>17</sup>. A comprehensive list of GSSHA™ tutorials is also available on-line<sup>18</sup>.

#### **4.2.2.2 Vflo™**

Vflo™ is a physics-based, fully distributed hydrologic model developed by Vieux, Inc., and is appropriate for water management studies, flood forecasting, drainage and hydropower design, investigation of the impacts of land use changes *etc.* Two different Vflo products are available, both of which are based on a common modelling framework. These products are the *Real-time Vflo*, a software that supports real-time runoff monitoring and flash flood predictions that can exploit short-term Quantitative Precipitation Forecasts and *Desktop Vflo*, a software that supports automated catchment delineation, model setup, calibration and design functions, and includes additional modules for continuous simulation, floodplain analysis, generation of design storms and sensitivity analysis<sup>19</sup>.

Vflo™ is scalable from catchment to regional scales and as a distributed model it can efficiently use grid-based precipitation information and GIS data. In fact, the model was designed properly so as to exploit distributed rainfall information from Gauge-Adjusted Radar Rainfall (GARR). Thus, high-resolution precipitation estimates from weather radar, satellites, raingauge networks, forecasting models

---

<sup>16</sup> The source code of CASC2D-SED can be downloaded for free at:  
[http://www.engr.colostate.edu/~pierre/ce\\_old/Projects/CASC2D-SED%20Web%20site%20082506/CASC2D-SED-Download.htm](http://www.engr.colostate.edu/~pierre/ce_old/Projects/CASC2D-SED%20Web%20site%20082506/CASC2D-SED-Download.htm).

<sup>17</sup> Released versions of GSSHA™ are available at the GSSHA wiki:  
[http://www.gsshawiki.com/GSSHA\\_Download#GSSHA.E2.84.A2\\_Executable\\_Installation\\_Downloads](http://www.gsshawiki.com/GSSHA_Download#GSSHA.E2.84.A2_Executable_Installation_Downloads)

<sup>18</sup> GSSHA™ tutorials can be downloaded at: <http://www.gsshawiki.com/Tutorials:Tutorials>.

<sup>19</sup> Relevant information is provided at the official website of Vieux and Associates, Inc.:  
[www.vieuxinc.com/](http://www.vieuxinc.com/).

and combinations of these data sources can be imported and fully utilized from the model, which can also make full use of geospatial digital data sets, such as LiDAR terrain data and other digital soil, land use/land cover *etc.* digital maps. All parameters can be imported and edited manually or via ArcView grids of square cells. The governing equations for channel routing are the simplified momentum equation and the continuity equation, which comprise the kinematic wave analogy (KWA) (Vieux B. E. and Vieux J. E., 2002). Therefore, VFLO™ solves the conservation equations and the hydraulics of drainage networks and produces hydrographs, flow rates and flow depths at any location in a watershed.

A catchment can be discretized into finite elements ranging between a few hundred (in case the catchment is small) and a million (for large catchments). A simulation of a catchment for a period of a few days can be performed in seconds, depending on the size of the drainage network. Model resolution depends on the resolution of available spatial datasets (*e.g.* DEM) and the size of the basin, and is not limited by other factors (Vieux B. E. and Vieux J. E., 2002). As a physics-based model, it can be used in areas with inadequate observed flow timeseries and lack of previous modeling studies. Extensions to VFLO™ support continuous modeling and the production of inundation maps in real-time or in post analysis. Vflo™ is an efficient distributed hydrological model; yet, the fact that it is commercial software restricts its wide application for research and academic purposes.

#### **4.2.2.3 MIKE SHE**

**MIKE SHE** is a deterministic, distributed, physically-based hydrological model that has its origins in the Système Hydrologique Européen (SHE). SHE was developed in 1977 by the Danish Hydraulic Institute (DHI), the British Institute of Hydrology and SOGREAH (France) and has been widely applied for hydrological simulations (Abbott *et al.*, 1986a and 1986b). Since the mid-eighties DHI Water & Environment has further improved SHE and developed MIKE SHE, an advanced, flexible tool for hydrological simulations, which is another model of the MIKE series (discussed in Section 4.2.1.5.1 above). MIKE SHE has been successfully applied in regions of different hydrometeorological regimes, supporting both research and consultancy projects in the scientific fields of integrated catchment hydrology, floodplain management, irrigation and drought management, groundwater and wetland management, ecological evaluations *etc.* (DHI Software, 2007a).

MIKE SHE incorporates process modules for the major components of the hydrological cycle, allowing for simulations of overland, unsaturated groundwater and channel flow, evapotranspiration, as well as their interactions over a square grid-based raster system. Particularly for channel routing, MIKE SHE uses MIKE11, a dynamic 1-D modelling tool that offers options for fully dynamic, diffusive wave, kinematic wave, quasi-steady state and kinematic routing (described in Section 4.4.1.2). For overland flow, MIKE SHE uses the same 2D mesh as the groundwater component and adopts a 2D finite difference diffusive wave approach (Lastoria, 2008). Regarding applications in urban environments, MIKE SHE can be coupled with another MIKE software, *i.e.* the MOUSE sewer

model, which simulates the interaction between urban storm water and sanitary sewer networks and groundwater (DHI Software, 2007a).

One of the main advantages of MIKE SHE is its easy coupling with GIS (e.g. with ESRI's ArcView) for advanced applications. The necessary data preprocess can be performed either in GIS environment or with the MIKE SHE's built-in graphic pre-processor. Even though MIKE SHE theoretically poses no limits to the grid size, some practical limits of the model regarding number of cells, nodes, river links *etc.* need to be taken into consideration (DHI Software, 2007a). Van Der Knijff *et al.* (2010) recognize the advanced capabilities of MIKE SHE, they underline however that the model cannot be used for accurate representation of the hydrological behaviour of large river basins. Furthermore, MIKE SHE needs extensive input data for model parameterization and thus its application to ungauged catchments may become problematic (Shukla, 2011). The wider application of MIKE SHE is restricted by the fact that this model is commercial; nevertheless, similarly to other MIKE by DHI software, demo academic versions are available for free.

#### **4.2.2.4 LISFLOOD**

**LISFLOOD** is a GIS-based distributed and (to some extent) physics-based hydrological model, developed by the floods group of the Natural Hazards Project of the Joint Research Centre (JRC) of the European Commission, that simulates rainfall-runoff and channel routing processes in hydrologic catchments. It was initially developed for the hydrologic simulation of large and transnational European river basins and can be applied *inter alia* in operational flood forecasting, simulation of historic river discharges, assessment of the impact of land use change and climate change on the hydrologic response of a river basin, assessment of the effectiveness of measurements taken against flooding *etc.* (Van Der Knijff and De Roo, 2008). The model uses a combination of the PCRaster Dynamic Modelling language and the Python scripting language and its code is stable, short, easy to read and can be easily modified and adjusted to different research needs.

A special feature of the model is that it simulates both rainfall-runoff and channel routing processes in a fully distributed mode, which makes LISFLOOD differ from other models. As far as routing of water in each channel pixel is concerned, LISFLOOD offers the option for either kinematic or dynamic wave routing. Given the fact that the full dynamic wave routing is particularly data-demanding (it requires detailed channel cross-section data, which are not readily available data for most channels) routing is usually performed through the four-point implicit finite-difference solution of the kinematic wave equations. This scheme is also used for the routing of surface runoff to channel (Van Der Knijff and De Roo, 2008).

An executable version of LISFLOOD can be obtained for free<sup>20</sup>. Since the model was initially developed for the simulation of large European river basins, with the

---

<sup>20</sup> In order to obtain an executable version of LISFLOOD, an email needs to be sent to its developers at: [Ad.de-roo@jrc.ec.europa.eu](mailto:Ad.de-roo@jrc.ec.europa.eu).



aim to make the best possible use of spatial datasets with pan-European information (on soils, land cover, topography, meteorology *etc.*), it often simulates small-scale processes in a simplified way. Therefore, even though grid resolutions of 1 to 5 km have been employed in recent applications, the recommended grid resolution ranges between 10 and 100 km, while higher resolution is preferably avoided. Another characteristic of LISFLOOD is that it does not simulate deep groundwater systems and capillary forces that rise water from subsurface layers and this is why the model may prove to be inappropriate for the simulation of areas that are very dry and/or influenced by deep groundwater conditions (Van Der Knijff *et al.*, 2010). The model incorporates optional modules for the simulation of lakes and reservoirs, but man-made structures cannot be easily simulated.

#### **4.2.2.5 CHYM**

**CHYM (Cetemps Hydrological Model)** is a grid-based, physical land surface hydrological model developed by the hydrological group of the Cetemps Center of Excellence at the University of L'Aquila. The program is written in FORTRAN language and the relevant computations can run in the main UNIX platforms. The principal aim of the model was to provide a general purpose tool for flood alert mapping and hydrological risk management and to this end it was originally developed to simulate the short-term (few days) response of catchments to severe weather conditions, taking into consideration remotely sensed datasets. Therefore, its main applications are relevant with severe weather forecasting and in particular flood alerting. CHYM was initially developed for applications over the Italian area. The main characteristics of the model are presented in Coppola *et al.* (2003).

The maximum spatial resolution that can be applied in CHYM is 300 m, while its grid is built on equally spaced latlon cells. For typical catchments in central-southern Italy a few hundreds of cells per side are usually adequately to cover the area. The model simulates the standard hydrological processes, *i.e.* surface runoff, infiltration, evapotranspiration, percolation and melting. The model receives rainfall input from different heterogeneous sources (raingauges, forecasted MM5 rainfall fields, satellite rainfall estimation *etc.*) and integrates and merges the different data at each time step **using a Cellular Automata (CA)<sup>21</sup> based algorithm**. This algorithm may also be applied for rebuilding (smoothing) the drainage network. The surface overland routing and the channel routing are based on the kinematic wave approximation.

An innovative aspect of CHYM concerns the rainfall data integration. In particular, different updating rules are established for different classes of cells, on the contrary to other, typical CA applications. It is obvious that when there is sufficient availability of necessary datasets the CA method is not as efficient as other statistical methods (such as Kriging, Thiessen polygons, physically-based models *etc.*) Nevertheless, when sufficient datasets are not available for efficient statistical representation then CA method is particularly efficient. Academic

---

<sup>21</sup> CA are simple, theoretical models that can be used to study the behavior and the evolution of a complex (physical) system, applying specific rules for the interaction of its elements (cells). CA behave as self-organizing systems and constitute an important state-of-the-art tool for modelling spatially distributed processes in general (Wolfram, 1982).

institutions and non-profit organizations have free access to the source code of CHYM for any kind of scientific application.

#### 4.2.2.6 TOPKAPI

**TOPKAPI** (acronym for TOPographic Kinematic APproximation and Integration) is a physically-based hydrological model, developed by Prof. E. Todini and the hydrological research group of the University of Bologna. Although it was initially developed to operate in either lumped or fully distributed version, in the following its latter, most developed version is presented. The model can be used either as an off-line stand-alone application or as part of real-time operational flood forecasting systems. In addition, it can run either as an event-based or as a continuous model. TOPKAPI keeps being regularly improved (Liu *et al.*, 2005; Peng *et al.*, 2008), with its most recent version, TOPKAPI-X, being developed by Dr. G. Coccia on behalf of the Italian private company Idrologia & Ambiente<sup>22</sup>.

As implied by its name, the basic idea of the model is the combination of the kinematic approach with topographic characteristics of the basin, which is a lattice of square cells. Each cell is connected upstream with up to three cells, downstream with a single cell and constitutes a computational node for the physical characteristics of the model, *i.e.* the mass and the momentum balance (Ciarapica and Todini, 2002). TOPKAPI simulates subsurface, overland and channel flow and it includes components for the representation of infiltration, percolation, evapotranspiration and snowmelt. It includes also a component for lake/reservoir simulation. Calculations are performed and flow predictions are generated for any point of the channel network. The kinematic approach is adopted for channel routing in steep cells, while a hydrological parabolic routing based on the Muskingum-Cunge method is adopted when channel slope is too small (Lastoria, 2008). The kinematic approach is also adopted for overland flow routing.

The reduced execution times even for fine resolutions, both temporal (a few minutes) and spatial (typically ranging between 100 and 1000 m), and with no impact on the physical interpretation of model parameters (Ciarapica and Todini, 2002) have contributed to its wide applicability in several European countries (mainly in Italy) and in other parts of the world. Furthermore, as a result of these capabilities of TOPKAPI, the model is enrolled in EFFORTS flood forecasting system together with the semi-distributed ARNO model (described in Section 4.2.1.3). According to Melone *et al.*, the hourly timestep is the suggested temporal resolution. Particularly for applications of TOPKAPI in Mediterranean areas, Latron *et al.* (2004) highlight that a catchment response is characterized by a considerable non-linearity due to the frequent landscape heterogeneity and the seasonality of the Mediterranean climate. This non-linearity is not captured adequately, if at all, by the mathematical equations embedded in physically-based models and to this end, it is suggested that the application of such models in relevant cases should rather be preferred at least when abundant datasets for

---

<sup>22</sup> According to personal communication with model developers.

model calibration are available. The full version of TOPKAPI is commercial software, while a demo version is provided for free for academic purposes<sup>23</sup>.

#### **4.2.2.7 WATFLOOD/SPL**

**WATFLOOD** is an integrated set of computer programs applied for flood flows forecasting and long-term hydrological modelling that started being developed by Prof. N. Kouwen (University of Waterloo, Canada) in 1972 and is regularly updated since then. WATFLOOD is also applied in climate change and environmental impact studies. The programs that constitute WATFLOOD are written in FORTRAN language and the relevant computations can run either in DOS or in several UNIX platforms (Lastoria, 2008). The hydrological modelling component of WATFLOOD is the SIMPLE (SPL), which is designed for fully distributed hydrological modelling. In addition to SPL, WATFLOOD offers a range of supporting programs necessary for data processing and presentation of outputs (Lastoria, 2008).

Focusing on SPL, *i.e.* the hydrological component of WATFLOOD, it combines a physically-based routing approach and a conceptual hydrological simulation approach (Kouwen, 2010). For modelling large catchments, SPL applies the Grouped Response Unit (GRU) method, which is based on the assumption that vegetation and/or land use are the principal indicators of hydrological response (Lastoria, 2008). It is properly designed so as to receive gridded remotely sensed data, such as digital terrain data land cover maps (that may be retrieved from LANDSAT or SPOT imagery) and weather data (*e.g.* rainfall fields in ASCII files retrieved from weather radars). The physical processes simulated with SPL include interception, infiltration, evaporation, snow accumulation and ablation, interflow, baseflow, aquifer recharge and routing (both overland and channel). Regarding channel routing, the continuity equation and Manning's formula are applied. The shape of cross-section was originally assumed triangular, but in updated version of the model it is considered as rectangular with flat bottom and near vertical sides in the main channel and rectangular in the banks and is thus more realistic. As far as overland flow routing is concerned, SPL includes a mechanism for calculation of infiltration excess (Lastoria, 2008).

WATFLOOD is a flexible and not particularly sensitive to grid size distributed model that may be applied to a variety of landscapes. Its efficiency is also demonstrated by the short computational time. Indicatively, it is mentioned that it needs approx. 6 minutes to run a 1-year simulation for a 1.000.000 km<sup>2</sup> catchment with 4000 grid points and hourly temporal resolution on a 3.2 Ghz Pentium 4™ (Kouwen, 2010). The available grid sizes for simulations range between 1 and 25 km and, similarly to most distributed models, the choice of the appropriate grid size for simulations with WATFLOOD is determined by the resolution of available gridded datasets, given that cells need to match conveniently. The model can be applied for hydrological simulations of either small or large catchments, ranging between 15 and 1.700.000 km<sup>2</sup>, while it can run either as event-based model or as a continuous model, in this latter case through the chaining of up to 36 events (Lastoria, 2008). WATFLOOD is a commercial software package. Yet, for

---

<sup>23</sup> According to personal communication with model developers.

academic applications, a simplified version of WATFLOOD (WATFLOOD LITE) together with software documentation can be freely downloaded<sup>24</sup>.

### **4.2.3 Evaluation of identified hydrological models**

A coherent evaluation of the identified hydrological models presented in the previous Sections is summarized in Table 4.1, based on typical model characteristics and requirements that need to be addressed by a hydrological model.

---

<sup>24</sup> The simplified, academic version of WATFLOOD (WATFLOOD LITE) is freely available at: [http://www.civil.uwaterloo.ca/watflood/downloads/watflood\\_downloads.htm](http://www.civil.uwaterloo.ca/watflood/downloads/watflood_downloads.htm).

Table 4.1. Evaluation of the identified hydrological models.

Model / Hydrological module	Lumped / (semi-) distributed	Fully distributed	Continuous	Dynamic	Applied mainly for hydrological simulations	Wide options or hydrological parameters & routing schemes	Comprehensive documentation	Regularly updated	Easy to apply	Open source
HEC-HMS	✓		✓	✓	✓	✓	✓	✓	✓	✓
TOPMODEL	✓		✓		Basically for long-term simulations		✓		✓	✓
ARNO	✓		✓				✓		✓	
SWAT	✓		✓			✓	✓	✓	✓	✓
NAM	✓		✓	✓	Limited hydrological capabilities - designed to support hydraulic simulations		✓	✓	✓	
UHM	✓			✓	Limited hydrological capabilities - designed to support hydraulic simulations		✓	✓	✓	
Hydrological module of SWMM	✓		✓	✓	Limited hydrological capabilities - designed to support hydraulic simulations		✓	✓	✓	✓
CASC2D		✓	✓	✓	✓			✓		✓
GSSHA™		✓	✓	✓			✓	✓		✓
Vflo™		✓	✓	✓	✓	✓	✓	✓		
MIKE SHE		✓	✓	✓	✓	✓	✓	✓	✓	
LISFLOOD		✓	✓	✓		✓	✓	✓	✓	✓
CHYM		✓	✓	✓	Mainly applied for flood alert mapping & hydrological risk management				✓	✓
TOPKAPI	✓	✓	✓	✓	✓		✓	✓		
WATFLOOD / SPL		✓	Chaining of up to 36 events	✓	Basically for long-term simulations & flood flows forecasting		✓	✓		Free simplified version for academic applications

It can be concluded from this Table that HEC-HMS addresses all typical requirements from a hydrological model applied for academic purposes.

### 4.3 Hydraulic modelling

In general, hydraulic modeling involves the simulation of the behavior of a fluid flow by means of numerical modelling (*i.e.* through simulation performed on a computer) or physical modelling (*i.e.* when the geometry of a physical model is scaled in a laboratory in an appropriate way, so that its behavior can be efficiently simulated). This Section focuses on numerical hydraulic models. Considering

hydraulic modelling as the second phase of flood modelling, its aim can be summarized in the prediction of surface water elevation and other flow characteristics (e.g. channel flow velocity, sedimentation) at each cross-section that has been identified at the initial phase of model set up, with the ultimate purpose to produce flood inundation maps.

As mentioned in Section 4.1, flow routing consists in the calculation of flood propagation, which can be achieved through the application of several routing schemes. The hydraulic routing scheme is incorporated in hydraulic models and in general is more precise and computationally demanding. The hydraulic models that incorporate the fully dynamic (complete) hydraulic routing scheme, as well as their different categories are described in Section 4.4.

## 4.4 Hydraulic models

Hydraulic models and in particular those that are applied for simulations of flood inundation, can be further classified according to the number of dimensions in which the spatial domain and the flow processes that take place within it are represented (Hunter *et al.*, 2007). Therefore, even though flow in channels is fully three-dimensional, for reasons of computational efficiency and given the fact that an accurate representation of free water surface for example is many times unnecessary, one-dimensional (**1D**) simplified codes have been developed and are widely used for the simulation of channel flow. Given that such codes are most of the times oversimplified, two-dimensional (**2D**) schemes have also been developed and represent an intermediate approach between the 3D reality and its 1D simplified approximation. 2D models are based on the 2D Shallow Water Equations (or else 2D Saint-Venant equations) and provide a higher order representation of river hydraulics. However, even though 2D schemes remain simplified in comparison to the 3D reality, they are data-demanding and are associated with increased computational cost, especially for floodplain analyses. Therefore, full 2D codes are sometimes not a viable solution and to this end the so called **1D2D** approaches (Bates *et al.*, 2005) that combine the simplicity of 1D channel routing with simpler methods for spatially distributed floodplain analysis are a recent, widely applied development. 1D2D approaches include the so called **1D+** approaches (sometimes referred to as *pseudo-2D* (Evans *et al.*, 2007) or *quasi-2D* (Néelz and Pender, 2009)) and the **2D-** approaches, depending on whether they involve enhanced 1D or simplified 2D approaches for their hydraulic simulations. Particularly for 1D hydraulic models, floodplain analysis is usually supported by special tools that are either integrated within the model software (e.g. RAS Mapper in HEC-RAS, described in Section 4.4.1.1) or allow for the seamless communication of the model with GIS applications (e.g. HEC-GeoRAS, a GIS extension of HEC-RAS, also described in Section 4.4.1.1).

Another classification of hydraulic models, which is typical for the dynamic wave (complete) hydraulic models, concerns the numerical solution schemes that are applied for the full solution of Saint-Venant equations. In particular, routing in dynamic wave models may be performed with characteristic, finite difference or finite element methods (Fread, 1985). *Characteristic Methods* constitute the initial approach to numerical flood routing, in which the two partial differential equations are transformed to four ordinary differential equations before being approximated

with finite differences for the generation of solutions (Fread, 1985). In *Finite Difference Methods (FDM)*, or else called direct methods (Fread, 1985), the two partial differential equations are directly approximated by finite differences for each point on a finite grid. *Finite Element Methods (FEM)* encompass several methods for connecting numerous simple element equations over numerous finite elements. Such methods are commonly applied to 2D unsteady flow models and they are equally effective for 3D problems. FEMs were introduced by Cooley and Moin (1976) and are further analyzed in Szymkiewicz (1991).

Regardless of the method used for the solution (either simplified or full) of the Saint-Venant equations, numerical solution schemes are distinguished into explicit or implicit, depending on the finite difference scheme used in the solution of the Saint-Venant equations. In explicit schemes, the equations are solved point by point in space and time along one time line, until the evaluation of all the unknown parameters associated with that time line. This solution is then advanced to the next time line and so on, until the evaluation of all the unknown parameters of the simulated system. In implicit schemes, the Saint-Venant equations are solved simultaneously for all points along one time line and then the solution is advanced to the next time line, until the evaluation of the unknown parameters for all time lines. A description of both numerical schemes and a thorough review of relevant approaches are presented in Fread (1985). In general, it can be concluded that implicit methods are associated with less stability problems and are often independent of the size of the time and distance step, on the contrary to explicit methods (Fread, 1985).

Each type of hydrological and hydraulic model has its advantages and disadvantages and the selection of an appropriate model for a complete flood analysis depends strongly on the expected outcomes and the quality, quantity and appropriateness of the provided input data. Typical 1D and 1D2D hydraulic models are presented in the following.

#### **4.4.1 Review on 1D hydraulic models**

As mentioned above, the main advantage of 1D hydraulic models is their low computational demand. Therefore, the updating of weather and water conditions and re-running of these models takes considerably less time than the required time to update complex 2D models. As a result, 1D models emerge as a viable option for an accurate river analysis particularly for operational applications (Fread and Lewis, 1985). Besides, 1D models offer a wider range of options for advanced modelling of hydraulic structures in comparison to typical 2D models used either operationally or for research purposes (Mashriqui *et al.*, 2014). Typical, widely applied and well-proven 1D hydraulic models have been selected and are presented in the following.

##### **4.4.1.1 HEC-RAS**

**HEC-RAS (Hydrologic Engineering Center – River Analysis System)** is a software for 1D hydraulic calculations designed by the Hydrologic Engineering Center (HEC) of USACE (HEC is also presented in Section 4.2.1.1). The initial HEC-software for river hydraulics was HEC-2, which performed 1D steady flow

water analysis. HEC-RAS constitutes a significant advancement over HEC-2 in what concerns both hydraulic engineering and computer science. The first version of HEC-RAS, *i.e.* HEC-RAS 1.0, was released in July 1995. Similarly to other HEC-models, HEC-RAS is also regularly updated and its latest version (HEC-RAS 4.1) was released in January 2010 (Brunner, 2010). This model is one of the most widely applied 1D river hydraulics modelling software on a global scale.

HEC-RAS is comprised of four 1D river analysis components for steady flow water surface profile computations, unsteady flow modelling, movable boundary sediment transport computations and water quality analysis. Several hydraulic design features are included in HEC-RAS and may be incorporated in the analysis. Focusing on flow analysis, steady flow modelling results in the calculation of water surface profiles for steady and gradually varied flow at a single river reach, a dendritic system or a channel network, under subcritical, supercritical and mixed regime. The 1D unsteady flow is simulated for channel network primarily under subcritical flow regime (Brunner, 2010). The river channel and the floodplain are considered as a series of cross sections perpendicular to the direction of flow and therefore it is convenient to apply standard field surveying methods for their parameterization (Bates *et al.*, 2005). For unsteady flow, HEC-RAS solves the full, dynamic, 1D Saint-Venant equations using an implicit finite difference scheme. The numerical solution of the governing equations for defined inflow and outflow boundary conditions allows for the calculation of the cross section averaged velocity and water depth at each location (Bates *et al.*, 2005).

A new improvement incorporated HEC-RAS is its capability to perform inundation mapping of water surface profiles directly within the software. The floodplain delineation tool is called RAS Mapper and it allows the use and visualization of geospatial data in a single modelling environment with RAS simulation results (Ackerman *et al.*, 2010). Prior to this development, HEC-RAS outputs were further processed in HEC-GeoRAS (a GIS extension of HEC-RAS) in order to perform a complete floodplain analysis. In addition to its aforementioned advantages, HEC-RAS has become a quite popular model for river hydraulic modelling because it is an open access software that can be downloaded for free, similarly to all modelling tools developed by HEC<sup>25</sup>.

#### **4.4.1.2 MIKE11**

**MIKE11** is a 1-D, dynamic, river modeling software developed by the Danish Hydraulic Institute (DHI) and is widely used in flood analyses, real-time flood forecasting studies, sediment transport and river morphology studies, water quality assessments in rivers and wetlands, dam break analyses *etc.* MIKE11 includes three different modules: the rainfall-runoff module (RR), the hydrodynamic module (HD) and the updating procedure, or else flood forecasting module (FF). The RR module of MIKE11 includes *inter alia* the NAM and UHM hydrological modules described in Section 4.2.1.5.1. The FF module allows for real-time data management in terms of automating updating and correction of differences between simulated and observed hydrographs and thus supports

---

<sup>25</sup> HEC-RAS can be downloaded for free at: <http://www.hec.usace.army.mil/software/hec-ras/downloads.aspx>.



forecasting and updating. The core computational module of MIKE11 is the HD, which is applied for simulation of flow propagation along rivers and channel networks.

Focusing on the HD module, roughness coefficients for river bed and floodplain, head loss factors for hydraulic structures and parameters related to computational scheme are the main model parameters that need to be defined during the setting up phase of the model. Default values are provided for all these parameters (with the exception of roughness coefficient) and may be adopted in the absence of relevant datasets, resulting in reliable hydrodynamic simulations. The model produces water level and discharges at the computational grid point, while additional information for velocity, Froude number, hydraulic radius *etc.* may also be generated (Melone *et al.*, 2005). The simulation mode may be either unsteady or quasi steady. The HD module provides different options for channel routing, *i.e.* the fully dynamic solution to the complete non-linear 1-D Saint-Venant equations of open channel flow, the diffusive wave and kinematic wave approximations, as well as the simplified hydrological routing methods of Muskingum and Muskingum-Cunge (DHI, Software, 2007b). Overland flow is simulated through either a simplified, semi-distributed method or a 2D diffusive wave method. This latter case allows a simplified 1D2D flood modelling within the 1D MIKE11. Similarly to HEC-RAS, MIKE 11 uses an implicit finite difference scheme for the solution of the Saint-Venant equations.

Similarly to other MIKE by DHI software, MIKE 11 is a commercial modelling tool, a demo academic version of which is freely available. The RR component of MIKE11 is not sophisticated enough and thus not efficient enough for detailed hydrological analyses (Van Der Knijff *et al.*, 2010). In order to overcome this restriction, the model may be coupled with other more detailed hydrological models. The main advantages of the hydraulic model MIKE11 are, *inter alia*, its fast and robust numerical scheme, its wide range of hydrologic and flood modelling modules, its GIS add-on modules and the fact that it can be linked to other advanced hydrologic modelling tools<sup>26</sup>. In addition, MIKE 11 can simulate efficiently standard hydraulic structures, such as bridges, culverts, weirs, pumps *etc.* (DHI Software, 2007b).

#### **4.4.1.3 SWMM**

As mentioned in Section 4.2.1.5.2, SWMM is a hydraulics software that incorporates a combined dynamic rainfall-runoff-subsurface runoff simulation model and a conveyance system model. Even though SWMM has a hydrologic component (for the production of runoff discharges from rainfall events), a hydraulic component (for the routing of the produced discharges), and a water quality component (for water quality simulations), it is classified here as a hydraulic model, since it is primarily applied for its routing capabilities. It needs to be mentioned that SWMM may be used exclusively as a hydraulic model, since it offers the option for use of pre-defined hydrographs as inputs and can thus be coupled with other hydrological models. Its hydrologic module is presented in Section 4.2.1.5.2 above and its water quality module extends beyond the purpose

---

<sup>26</sup> Source: <http://gcmd.nasa.gov/records/MIKE11.html>.

of this research and its description is hence skipped. Its enhanced hydraulic module is presented in brief in the following paragraphs.

SWMM is widely used for planning, analysis and design of stormwater runoff, combined and sanitary sewers and other drainage systems, primarily in urban areas (Rossman, 2010). Recently, its application has been expanded to some non-urban areas as well; nevertheless, this model is primarily applied for urban flood simulations. As described in Section 4.2.1.5.2, the simulation of a drainage system with SWMM calls for the modelling of a *runoff component* (and the corresponding atmospheric, land surface and groundwater compartments) and a *routing component* for the transportation of runoff to catchment outfalls. Focusing on the routing component, the *transport compartment* needs to be modeled. In particular, flow can be conveyed through a network of conveyance elements which include pipes, channels, pumps, storage/treatment devices and regulators. The components of this latter compartment are modeled through *Nodes* and *Links* and flow depth is calculated in each pipe and channel for multiple time steps of a selected simulation period (described in detail in Rossman, 2010). SWMM includes the kinematic and dynamic wave flow routing algorithms and it uses an explicit finite difference scheme for the numerical solution of the 1D Saint-Venant equations. Both the overland and sewer system of SWMM are typically 1D. Therefore, regarding the spatial classification of its hydraulic component, SWMM can be considered as a 1D model, when used for either overland or sewer system simulations, or as a 1D/1D model, when these systems are coupled for a given simulation. It is also mentioned that the capacities of SWMM have recently been expanded and hence it can be applied as a 1D2D model, similar to the models presented in the following Section. As mentioned in Section 4.2.1.5.2, overland flow is simulated through the kinematic wave routing method.

As mentioned in Section 4.2.1.5.2, one of the main advantages of SWMM is the fact that it can be downloaded for free from the website of EPA<sup>27</sup>. Its wide applicability is also attributed to the fact that SWMM can handle networks of unlimited size using a wide variety of standard shapes for conduits and channels, it can model different flow regimes, including backwater effects, surcharging, reverse flow and surface ponding, and can apply dynamic, user-defined control rules for the simulation of the operation of pumps and regulators (Rossman, 2010). The advanced capabilities of SWMM address primarily the needs of a detailed urban flood modelling. However, its recent expansion to non-urban areas is promising for the wider application of this model in mixed (urban – non-urban) areas.

#### **4.4.2 Review on 1D2D hydraulic models**

In spite of the computational efficiency of 1D hydraulic models, they inevitably adopt numerous assumptions in order to simplify the 3D reality. In many applications, 2D models are preferable to 1D models, since they provide more reliable simulations. According to Cunge *et al.* (1980), a partially calibrated 2D model is in several cases preferable to a 1D model, since the former offers an approximation of that may be improved through complimentary survey. It is also

---

<sup>27</sup> <http://www.epa.gov/nrmrl/wswrd/wq/models/swmm/#Downloads>

mentioned that even in case of limited dataset availability, 2D simulations are usually proven more accurate. At this point it needs to be clarified that the choice between a 1D and a 2D model needs to be associated with the required output, the available datasets and the modeller experience. As also mentioned in Section 4.4, the 1D2D models are an intermediate approach that bridges the gap between simplified 1D and complicated 2D models. Two typical 1D2D hydraulic models are presented in the following Section.

#### **4.4.2.1 LISFLOOD-FP**

**LISFLOOD-FP** is a flood inundation model developed in 1999 in a joint effort between the University of Bristol and the EU Joint Research Centre (Bates and de Roo, 2000). Being an extension of the LISFLOOD catchment model (described in Section 4.2.2.4), LISFLOOD-FP is a raster-based flood inundation model that simulates channel and floodplain flow and is continuously upgraded (it has since been re-coded in c++), the latest version of its code (Version 2.6.2) being released in 2005. This model has been widely applied for fluvial and plain flooding simulations for both research and academic purposes.

LISFLOOD-FP is written in a dynamic GIS language, PCRaster that further facilitates the rapid development of spatiotemporal models (Bates and De Roo, 2000). It is designed to work on a regular lattice to allow easy integration with available GIS datasets. The model can dynamically simulate flood events on grids of up to  $10^6$  cells, exploiting datasets from remote sensing techniques, such as airborne laser altimetry and satellite interferometric radar. Channel flow is based on the 1D kinematic wave approximation and using an explicit finite difference scheme for its solution. Floodplain flow is two-dimensional (2D) and is modelled through the diffusion wave approximation (Bates *et al.*, 2005).

This coupled **1D2D** approach results in reliable predictions of water depths in each grid cell at each time step and sufficient simulation of flood wave dynamic propagation over fluvial, coastal and estuary floodplains. Unlike most relevant hydraulic models that require both upstream and downstream boundary conditions, LISFLOOD-FP requires only upstream inflow hydrographs. In addition, the model structure is designed in such a way that secondary processes to flood inundation, which is the main aim of LISFLOOD-FP, are either ignored or minimized, on the contrary to other models, as for example CASC2D that considers infiltration (Bates and De Roo, 2000). Besides, LISFLOOD-FP is a non-commercial research code<sup>28</sup>. However, the code of the model is limited to situations of availability of high resolution and accurate topographic data and sufficient information for the model boundary conditions.

#### **4.4.2.2 FLO2D**

**FLO-2D** is a 1D2D flood routing model, available from FLO-2D Software, Inc., for integrated river and floodplain simulations. It is characterized as a 1D2D model, since it is developed so that it exchanges 1-D channel overbank discharges with

---

<sup>28</sup>The code of LISFLOOD-FP is freely available at:  
<http://www.bris.ac.uk/geography/research/hydrology/models/lisflood/downloads/>.

2-D floodplain grid elements. This model is the evolution of a former model called MUDFLOW that was developed in 1989 by J. O'Brien for Federal Emergency Management Agency (FEMA) of the US Department of Homeland Security (FLO-2D, 2009). This combined rainfall-runoff (hydrologic) and flood routing (hydraulic) model can simulate river, alluvial fan, urban and coastal flooding since urban detail features, sediment transport, mudflow and groundwater modelling are incorporated in the software and has thus been widely used in flood mitigation design, surface and groundwater interaction studies, river overbank flooding, urban flooding and even modelling of progression of tsunami waves and ocean storm surges.

Focusing on its hydraulic component, which is the core component of FLO-2D, the model is equipped with several modules in order to achieve enhanced flood routing, including *inter alia* simulation of flow obstructions, hydraulic structures and hyper-concentrated sediment flows (mudflows), levees and levee failure. Natural, rectangular or trapezoidal cross sections may represent the channel geometry of the 1-D channel flow. The 2-D overland flow is modelled as either sheet flow or flow in multiple channels (gullies and rills) and is computed in 8 directions. The timestep used may have a variable incrementing and decrementing scheme and the array allocation, *i.e.* the grid elements, is unlimited. Regarding grid size, values between 3 m and 100 m are typical applied values in most simulations. Its flood routing scheme is based on volume conservation, which also determines its numerical stability and its computational speed. In particular, the two-dimensional flood routing is accomplished through the dynamic wave approximation to the Conservation of Momentum equation. The differential form of the governing equations is solved with an explicit finite difference numerical scheme (FLO-2D, 2009).

FLO-2D is enhanced through the incorporation of a Grid Developer System (GDS) and a MAPPER program. GDS is a pre-processor program that creates and edits the attributes of the grid system and data files, while MAPPER automates flood hazard delineation and generates detailed flood inundation and flood damage and risk maps. There are two different FLO-2D products, the FLO-2D Basic Model, which is a freely available software<sup>29</sup> and FLO-2D Pro, which is its advanced, commercial version that incorporates additional modules for sediment transport, mud and debris flow, storm drains, dam and levee breach and groundwater modelling.

#### **4.4.3 Evaluation of identified hydraulic models**

A coherent evaluation of the identified hydraulic models presented in the previous Sections is summarized in Table 4.2, based on typical model characteristics and requirements that need to be addressed by a hydraulic model.

---

<sup>29</sup> The FLO-2D Basic Model can be downloaded for free at: <http://www.flo-2d.com/download/>.

Table 4.2. Evaluation of the identified hydraulic models.

Model	1D	1D2D	Not computational demanding	Not data demanding	Simulation of standard hydraulic structures	Easily coupled with GIS & hydrol. models	Comprehensive documentation	Regularly updated	Easy to apply	Open source
HEC-RAS	✓		✓	✓	✓	✓	✓	✓	✓	✓
MIKE11	✓				✓	✓	✓	✓	✓	
SWMM	✓	✓	✓	✓	✓	✓	✓	✓	✓	✓
LISFLOOD-FP		✓			✓	✓	✓	✓	✓	✓
FLO2D		✓			✓	✓	✓	✓	✓	FLO-2D Pro is commercial

It can be concluded from this Table that both HEC-RAS and SWMM address all typical requirements from a hydraulic model applied for academic purposes.

## 4.5 Coupled hydrological – hydraulic modelling

In the paragraphs above several hydrological models that include routing methods which allow for simplified flow routing (e.g. LISFLOOD, HEC-HMS, TOPMODEL etc.) were presented. However such routing schemes are not sufficient for a detailed flood study. On the other hand and as also mentioned above, there is software that performs both rainfall-runoff and hydraulic channel routing, e.g. FLO2D, SWMM, CA2D-Todini etc. Nevertheless, such models are basically hydraulic (dynamic flood routing) models that may only be applied for simplified rainfall-runoff simulations. Besides, many hydraulic models are limited to river routing and do not contain a rainfall-runoff component at all, as for example HEC-RAS.

In order to conduct a detailed flood study, the coupling of hydrological and hydraulic models needs to take place. In general, independent hydrological and hydraulic models of the same developer offer enhanced coupling options (e.g. models under the HEC-software umbrella (HEC-HMS / HEC-RAS), the MIKE by DHI-software umbrella (MIKE11 / MIKE21), LISFLOOD / LISFLOOD-FP). A recent trend in coupled hydrological-hydraulic models is the application of platforms that support standardized data transfer and may be either “fixed”, i.e. they incorporate standard hydrological and hydraulic models already coupled or “customized”, i.e. they offer the option to couple variable datasets and different, user-defined models within their environment. The idea for integrated modelling is not new. However, recent advances in computational software, remote sensing and data process have contributed to the development of numerous and enhanced such platforms, particularly in the last decade. Indicative platforms of both types are presented in the following.

### 4.5.1 “Fixed” platforms for integrated modelling

As mentioned above, “fixed” platforms constitute an integrated environment, in which standard software and modelling tools are incorporated. Typically, within a single platform, the user may choose among a wide range of options in terms of different modules, processing and visualization tools, which enhance a simulation. Yet, the simulation software is fixed and hence there is no option to

integrate in these platforms user-defined software, nor is there any interaction between the user and the platform for model selection. “Fixed” platforms may be either commercial or free.

A typical “fixed” platform for coupled hydrological-hydraulic modelling is **MIKE FLOOD**. This integrated modelling platform developed by DHI combines two numerical hydrodynamic models, the 1-D MIKE 11 (described in Section 4.4.1.2) and the 2-D MIKE 21 for efficient urban, coastal and river flood modelling. Focusing on river flood modelling, MIKE 11 is used for the 1-D open channel modelling and MIKE 21 for the 2-D overland flow modelling. This platform utilises GIS not only for enhanced visualization, but also for automated model development and generation of flood maps. Typical outputs include water levels and flow velocities in the main channel and the floodplain and 2D and 3D flood animations (DHI, 2003). The main advantage of MIKE FLOOD is the fact that it is built on well-proven technology and simulation engines, while it also applies enhanced tools for floodplain visualization. MIKE FLOOD is a commercial platform; yet, demo academic versions may be provided for free.

Another “fixed” platform for integrated flood analysis is **KALYPSO**, an open source model system for numerical simulations in water sector, collaboratively developed by the Department for River and Coastal Engineering of Technical University of Hamburg-Harburg (TUHH) and the Björnsen Consulting Engineers (BCE) Company, Germany. KALYPSO system is modularly designed. Currently, these modules include Kalypso Hydrology, Kalypso WSPM (Water Surface Profile Module), Kalypso 1D/2D, Kalypso Flood, Kalypso Risk and Kalypso Evacuation. A KalypsoBASE framework is a structure that combines additional functionalities, such as GIS and data processing functions. The pure hydrological and hydraulic modules of KALYPSO may be used independently. However, focusing on its operation as a platform, KALYPSO Flood module offers the option for coupled hydrological and hydraulic modelling. In this module, the Kalypso WSPM and Kalypso 1D/2D modules are integrated and inundated areas, flow depths and water surface profiles are produced (TUHH, 2008). These outputs may serve as input to Kalypso Risk module for the generation of flood risk maps.

**SOBEK** is one more modelling suite for integrated water-related simulations. It has been developed by Deltares, a Dutch institute for applied research in water, subsurface and infrastructure fields and keeps being updated and further improved. Particularly for integrated hydrological-hydraulic modelling, SOBEK offers a powerful hydrodynamic 1D/2D engine, which couples the 1D SOBEK-River for channel modelling and the 2D SOBEK-Overland Flow for floodplain analysis. In Vanderkimpfen *et al.* (2009) SOBEK 1D2D and MIKE FLOOD were applied for a flood analysis in a Belgian catchment and the research concludes that these packages offer similar possibilities and the produced inundated areas and water depths are in good agreement, while some differences in flow velocities were attributed to differences in computation schemes. SOBEK is a commercial software package. Deltares also distributes educational packages at reduced price<sup>30</sup>.

---

<sup>30</sup> According to personal communication with Deltares Systems.

**InfoWorks ICM (Integrated Catchment Modelling)** is another option for coupled hydrological and hydraulic modelling. The platform is developed by Innovyze, a company that emerged from the merging of the MWH Soft and the Wallingford Software, both of which being companies that specialize in software development, particularly for water resources and environmental applications. This platform performs 1D river channel and 2D floodplain hydrodynamic simulations. Its Real-Time Control module offers the option to integrate control structures during a simulation, while it also offers the option to perform water quality and sedimentation simulations. InfoWorks ICM is compatible with ArcGIS and its performance is further improved through the incorporation in the platform of the outcomes of recent advances in hardware development (Innovyze, 2014). Similarly to all Innovyze software packages, InfoWorks ICM is a commercial product.

#### **4.5.2 “Customized” platforms for integrated modelling**

In addition to the “fixed” modelling platforms described above, numerous “customized” modelling platforms have also been developed and are widely applied. The basic concept underpinning such platforms is the development of an interface that allows the coupling of user-defined software and tools for integrated modelling. “Customized” platforms usually come with a comprehensive library of models and tools already integrated in it, while they offer at the same time tools that facilitate the integration of additional, user-defined models and tools. These platforms are usually freely available.

The **Delft-FEWS (Flood Early Warning System)** platform is a sophisticated collection of modules developed by Deltares (also mentioned in Section 4.5.1) that supports hydrological forecasting. The platform provides an open shell for managing data handling and forecasting process. Currently more than 40 commercial and well-proven software packages applied for both hydrological and hydraulic modelling, including *inter alia* HEC-HMS, TOPKAPI, HEC-RAS, MIKE 11, SOBEK and SWMM, are integrated in the system as external, independent forecasting modules<sup>31</sup>. Besides these models any other model may be incorporated in the platform, provided that an adapter for this model to the Delft-FEWS interface will be developed. Through appropriate data processing and model coupling techniques, data, models and model outputs interact and produce outputs for efficient flood forecasting. Delft-FEWS is a scalable system, *i.e.* it can run either as an independent manually driven forecasting system or as a fully automated distributed client-server application (Delft-FEWS, 2010). Its main advantage is its efficient coupling with external data sources, *e.g.* on-line hydrometeorological information, through its enhanced import modules. Delft-FEWS is available for free under licence.

Another platform that constitutes an integrated environment for model coupling is **OpenMI (Open Modelling Interface)**. It was initially developed in the framework of the implementation of the FP7 EC research project HarmonIT and further expanded through the EC LIFE ENV Programme *OpenMI-LIFE*. Currently the

---

<sup>31</sup> The complete list of models integrated in FEWS is available at:  
<http://public.deltares.nl/display/FEWSDOC/Models+linked+to+Delft-Fews>.

platform is owned and maintained by the non-profit group of international organizations and individuals *OpenMI Association*. OpenMI Standard is an interface that allows data exchange between time-dependent models at run-time. The platform enables the communication of models even in the case of different timesteps and different spatial distribution of datasets (e.g. grid size) between coupled-in models. OpenMI was developed for linking models in the environmental domain and hence it can be exploited in flood modelling. A library of relevant OpenMI-compliant softwares is already integrated in the platform, while a set of software tools facilitates the integration of new model codes. The tools for migrating and linking different models are available for free under an Open Source licence (Moore *et al.*, 2007).

**OGS (OpenGeoSys)** project is another relevant platform. OGS is an open source modelling platform that enables numerical simulations of thermo-hydro-mechanical-chemical (THMC) processes in porous media and hydrosystems, using either independent or coupled models. The platform provides a flexible numerical simulator that uses primarily the Finite Element Method (FEM) for application in energy and water research. The OGS idea has its origins in the mid-eighties. In the following decades the idea was incorporated in research schemes, expanded and further enhanced. Currently it is hosted by the Helmholtz Centre for Environmental Research (UFZ). Numerous simulation codes are integrated in OGS, while OGS also offers to the user and model developer community complete freedom to customize and further develop its existing functionalities (Kolditz *et al.*, 2012). The original code was renamed to OGS in 2009, when it became a platform freely available through the internet.

On top of these platforms, several frameworks that facilitate the communication of different sources of datasets and thus indirectly support integrated models have been developed as well. The application range of such frameworks is quite wide. A typical such framework is **DynaMind**, a software tool that can be applied for simulations of the urban environment and its infrastructure (e.g. drainage systems). It has been developed by the Unit of Environmental Engineering (IUT) of the University of Innsbruck and includes a set of basic processing and storage modules, which can be easily expanded with the integration of new modules. This framework is an open source, freely available software using the GPL license (Urich *et al.*, 2012).

## 4.6 Flood models applied in this research

It becomes obvious from the previous paragraphs, that nowadays, in order to simulate the hydrological and the hydraulic behavior of a catchment, a modeler may choose among a wide range of available and efficient hydrological and hydraulic models respectively, which may be tailored to the modeler's particular needs. Similarly, a modeler has numerous options for coupling hydrological and hydraulic models in order to perform an integrated flood study. The reliability of widely accepted models, such as those described above, is often taken for granted. In such cases, the choice of a model or a coupling platform is determined by their efficiency, which is associated with the problem investigated, the availability of datasets of acceptable quantity and quality that will be used as input or calibration data, the required output, the experience of the modeler, the ease



of access to relevant documentation and support for the application of the models and often the cost of model or platform purchase and their user-friendliness. In addition, efficiency depends strongly on the proper choice of simulation methods selected within each model and of parameter values. The choice of a model may also be submitted to constraints, which are imposed when models need to cover particular requirements of their end users, e.g. use of remotely sensed datasets and generation of results that can be incorporated in existing operational systems (Melone *et al.*, 2005).

The current research focuses on the development of a methodology for the quantification of the impact of forest fires and initial soil moisture conditions on the hydrological response of a catchment. This methodology (described in detail in Chapter 5) will be integrated in a hydrological model, which will be coupled with a proper hydraulic model and their integrated application will allow for a more accurate integrated flood analysis. The criteria mentioned above were applied for the selection of an appropriate hydrological and an appropriate hydraulic model for this study.

Following extended relevant literature review and testing of different models and coupling platforms, a coherent evaluation of the identified hydrological and hydraulic models was performed in Tables 4.1 and 4.2, respectively. HEC-HMS prevails as the most appropriate model to apply for this research, since it addresses all typical requirements from a hydrological model applied for academic purposes. Regarding the outcomes of the evaluation of the hydraulic models, both HEC-RAS and SWMM are appropriate for this research; yet, HEC-RAS is easily coupled with HEC-HMS, since both models are under the HEC models umbrella. For these reasons, the application of the HEC-HMS hydrological model and the HEC-RAS hydraulic model has been concluded for this research. The main advantages of both models, already described in Sections 4.2.1.1 and 4.4.1.1, include *inter alia* their efficiency and reliability, their extended application on a global scale, their comprehensive documentation and of course the free access to both of them. In addition, both models are particularly flexible, mainly due to their structure, which incorporates numerous simulation methods and thus offers a wide range of modelling options. These advantages, together with the appropriateness of both models for this research due to their flexibility, also described in Chapter 5 (*Methodology*), and the relevant datasets that are available, have dictated their selection.

In this research, HEC-HMS has been used in a semi-distributed, dynamic (event-based) mode, while HEC-RAS was applied for steady, mixed (subcritical, supercritical) flow. Further to these models, the GIS extensions HEC-GeoHMS and HEC-GeoRAS were also applied for the hydrological and the hydraulic simulations respectively.

## CHAPTER 5: METHODOLOGY

The accurate estimation of the initial conditions in a catchment has been recognized as an issue of significant importance when attempting a reliable hydrological simulation (Moore *et al.*, 2006), particularly for catchments with complicated geomorphology and land uses, such as typical periurban catchments. The current research examines initial conditions of a catchment from an integrated perspective. In particular, in this research the potential post-fire impact on catchment characteristics, which is the primary focus of this research, has been studied along with the initial soil moisture conditions, which are both in need of further exploration.

This Chapter, which focuses on hydrological modelling, proposes a new methodology that has been developed for the quantification of the impact of initial conditions, in terms of forest fire and soil moisture, on the hydrological response of a catchment. In addition, the post-fire impact is examined for the first time from a “temporal perspective”, which allows for the investigation of its dynamic evolution in time. For the development, testing and finalization of this methodology, successive hydrological simulations had to be performed. The methodology has been developed for deterministic, physically-based, lumped or (semi-)distributed, event-based or continuous hydrological models. Therefore, for the necessary hydrological simulations, the HEC-HMS model has been selected out of the long list of efficient hydrological models presented in Chapter 4, for the reasons presented in more detail in Section 4.6.

The conditions that determine the post-fire status of a catchment have been analyzed in detail in Chapter 3; the estimation of post-fire conditions in a catchment, as used in this methodology, is discussed in Section 5.1. The estimation of initial soil moisture conditions is discussed in Section 5.2. Guidance on the estimation of core hydrological parameters for pre-fire, normal soil moisture conditions is presented in Section 5.3, while an innovative methodology for the estimation of the same hydrological parameters under variable initial conditions, taking into consideration the temporal dimension, which eventually quantifies the impact of initial conditions on the hydrological behavior of a catchment, is presented in Section 5.4. Section 5.5 concludes with a list of particularities of the first post-fire floods that determine specific conditions under which the methodology can be applied as proposed, without needing further readjustment.

### 5.1 Estimating fire impact

The hydrological footprint of a forest fire with limited extent and/or limited intensity is often ignored and in such cases the initial conditions of the catchment are often assumed undisturbed and thus static (see for example Zhou *et al.*, 2013). Alternatively, a stochastic approach may be adopted in fire modelling, according to which the statistical properties of past fires are replicated in stochastic simulation fire models, aiming to make predictions for the impact of the analyzed fires. Inevitable assumptions need to be made in such cases (e.g. Willgoose, 2011; Esteves *et al.*, 2012), primarily for fire severity. The numerous assumptions and oversimplifications that are required from both approaches, make them

unsuitable for extended applications, particularly in operational systems, the reliability (and usefulness) of which are heavily dependent on their ability to correctly account for such changes in the catchment and propagate their impact downstream – in terms for example of changing flood risk.

The impact of a forest fire on a catchment's hydrological response depends strongly on fire extent and Fire Severity (FS), which serve as measures to quantify the effects of fire on soil and overstorey (Keeley, 2009; De Santis and Chuvieco, 2007). As analyzed in Section 2.3.1.3, several techniques have been developed to map burnt surfaces and estimate the severity of a fire event. As demonstrated in literature (Gitas *et al.*, 2012; Lhermitte *et al.*, 2011; Veraverbeke *et al.*, 2010; Viedma *et al.*, 1997) the most popular and effective FS mapping techniques are those that make use of satellite remote sensing supported by *in-situ* fieldwork complemented with statistical and simulation modelling.

Both, the spatial extent and the temporal evolution of FS are critical elements for the quantification of hydrological footprint of forest fires and have been incorporated in the methodology presented in this Chapter, as described in the following.

### **5.1.1 Examining fire impact from a spatial perspective**

Clearly, FS is not uniform over the whole area that has been affected by fire, with different patches of land affected by different FS. In general, according to Keane *et al.* (2012), the exact definition and estimation of FS is associated with inherent uncertainties, subjectivity and lack of standardization. Yet, several reliable FS *indices* exist in literature, most of which can be calculated from satellite imagery (Key and Benson, 2006; Keane *et al.*, 2012; Miller *et al.*, 2009).

In this research, a FS map has been produced for the study area based on satellite images. More specifically, two Landsat TM images, the first one for the period prior to an examined fire event and the second one for the period shortly after the fire event were radiometrically and geometrically corrected so that the quality of the satellite data would be enhanced. Thorough literature review was performed at this part of the research, in order to identify and adopt the most appropriate fire severity index for this research out of the most widely used indices presented in Section 2.3.1.3. Given that the proposed methodology refers to historic fire events and hence fieldwork is not an option, and also after considering issues of satellite imagery availability and representativeness, the Differenced (or Delta) Normalized Burn Ratio (dNBR (or  $\Delta$ NBR respectively)) index has been selected as most appropriate for the production of a FS map for the current research. To this end, the bands 4 and 7 of the Landsat TM images were linked for the calculation of two indices of Normalized Burn Ratio (NBR), *i.e.*  $NBR_{PRE-FIRE}$  and  $NBR_{POST-FIRE}$  for the pre- and post-fire images respectively.

The DNBR was then estimated from the subtraction of the NBR maps and the values of DNBR were classified into distinct classes, which correspond to different FS levels. Initially, the FS levels included very high, high, moderate, low severity, unburnt areas and areas with enhanced vegetation regrowth. The analyzed satellite image was imported in ArcGIS 9.3 and was further analyzed in ArcMap,

in Geographic Information System (GIS) environment. At a first stage, the burnt area of the study area was isolated. At this stage and aiming to achieve a more detailed representation of FS conditions, FS levels were restricted to five, namely very high FS (i), high FS (ii), moderate FS (iii), low FS (iv) and no severity (referring to unburnt land), since areas with enhanced regrowth were not identified in the affected land within the boundaries of the study area.

The results of this analysis for the study area are presented in more detail in Section 7.1. The clipped FS map of the study area was further analyzed in GIS for the identification of the exact spatial extent of each FS class within each subbasin of the study area. For the application of the methodology, presented in Section 5.3, the percentages of the affected area within each FS class were used for the estimation of weighted hydrological parameters for each subbasin.

### **5.1.2 Examining fire impact from a temporal perspective**

A major challenge in this research has been the incorporation of the temporal variation of post-fire hydrological behavior in hydrological modelling. In literature, the temporal dimension of this impact is thoroughly examined from an **ecological perspective**, *i.e.* extended research has been performed on post-fire vegetation recovery and natural reforestation researches focus either on the early regeneration stages of vegetation, which is usually restricted to the first one or two post-fire years (Thanos *et al.*, 1989; Oliveira and Fernandes, 2009; Bolin and Ward, 1987; Cannon *et al.*, 2008; Rulli and Rosso, 2007; Scott and Van Wyk, 1990; Inbar *et al.*, 1998) or on the period several years after the fire (Polychronaki *et al.*, 2013; Nepstad *et al.*, 1999; Thanos and Marcou, 1991; Eccher *et al.*, 1987; Mayor *et al.*, 2007), when forest regrowth has occurred, vegetation density is increased and ecosystems are almost reset to their initial status (Gitas *et al.*, 2012; Marzano *et al.*, 2012; Veraverbeke *et al.* 2010; Lhermitte *et al.* 2011; Le Hou rou, 1987; Trabaud *et al.*, 1985; Viedma *et al.* 1997). However, as also discussed in Chapter 3, limited research has been performed so far on how a forest fire's impact changes in time and when it can be assumed that the catchment has reverted to its pre-fire conditions from a hydrological perspective (Willgoose 2011; Esteves *et al.*, 2012; Mayor *et al.*, 2007; Springer and Hawkins, 2005). The fact that post-fire hydrological recovery depends strongly on site-specific parameters, such as dominant vegetation, soil, topography and slope properties, geographical characteristics, local meteorological conditions and FS in the affected area (Gitas *et al.*, 2012; Esteves *et al.*, 2012) is a main reason for this limited research.

One of the innovative elements of this research is the fact that FS and hydrological recovery (in terms of vegetation regrowth and not necessarily full vegetation recovery, as clarified in Sections 3.3.1 and 3.3.2) have been examined not only from a spatial perspective, but also from a temporal perspective. More specifically, time periods of variable duration and different hydrological impact, directly associated with the status of vegetation regrowth, were identified within each severity class. The duration of each time period has been defined based on extended literature review on the conditions of typical Mediterranean vegetation, in terms of annual changes in foliage, post-fire regrowth *etc.* (presented in detail in Chapter 3 and including *inter alia* the findings of Carey *et al.*, 2003; Inbar *et al.*,

1998 *etc.*), while the characteristic, transitional periods that can be identified in post-fire vegetation regrowth and are related with hydrological recovery (analyzed in Section 3.3.2.2) were also taken into consideration for this research.

More specifically, when examining revegetation in typical Mediterranean areas, as well as in repeatedly burnt Mediterranean forests, mainly covered by evergreen broadleaved shrublands, conifers (mainly Aleppo pine) and sclerophyllous forest types known as *garrigues* or *mâquis* (Inbar *et al.*, 1998; Davis *et al.*, 1996), the plant cover during the first post-fire springs becomes critical (Keeley, 2009). Viedma *et al.* (1997) mention that vegetation recovery in these areas usually needs a few years to occur. In relevant studies, re-established vegetation one year after a severe fire event in a typical Mediterranean forest covered 10-30% of the affected area, in the second post-fire year it extended over 50-70% of the area (Inbar *et al.*, 1998), reaching eventually 90% between the third and the fifth post-fire years (Viedma *et al.*, 1997). In addition grasses, forbs, and more fire-tolerant low vegetation need approximately one year after a fire event to regrow, while other, less fire-tolerant species of low vegetation may need three or four years to regrow. This vegetation cover, even though it cannot be considered as indicative of ecological recovery, needs yet to be considered when studying hydrological recovery. When available, earth observation data validated by field observations of the vegetation cover can support the study of the temporal perspective of fire impact.

Based on these findings a general rule that was adopted for the study of the temporal perspective of fire impact was the assumption of a sharply descending hydrological impact with time for each FS class. In the proposed methodology, which is developed for areas covered by successively burnt Mediterranean forests, it is considered that hydrological recovery takes place 4 years after the fire, with the first 2 years being more critical (Brown, 1972; Moody and Martin, 2001a; Springer and Hawkins, 2005; Inbar *et al.*, 1998; Rulli and Rosso, 2007; Robichaud, 2000). In an attempt to associate FS with the temporal evolution of hydrological recovery, it is assumed that in order to reach hydrological recovery, areas affected by low or moderate severity need approx. 2 years, areas affected by high FS need approx. 3 years and areas affected by very high FS need approx. 4 years. For all these reasons and also for the reasons presented in Section 3.3.2.2, the time windows of 7, 12, 19, 24, 36 and 48 months after a fire event have been used in this research, as transitional periods in hydrological recovery.

These considerations are often case-specific and may need to be readjusted for different areas. In order to verify them for the study area of this research (presented in Chapter 6), relevant datasets from satellite imagery, cross-validated with *in-situ* observations of the vegetation cover, were studied (Eftychidis and Varela, 2013). The considerations on the temporal evolution of the hydrological recovery mentioned above are consistent with the outcomes of this study and in accordance with the findings from literature review.

It needs to be clarified that, as also defined in Section 3.3.2, this *hydrological recovery* needs not to be confused with the full *environmental recovery*, which, especially in severely affected areas, can only take place after the replacement of the canopy cover, *i.e.* many years after the fire event, if at all.

## 5.2 Estimating initial soil moisture

A reliable estimation of initial Soil Moisture (SM) conditions in a catchment necessitates the regular monitoring of its hydrometeorological conditions. Preferably, a dense network of SM sensors is installed in appropriate locations over the catchment and properly selected depths in the soil, so that representative measurements of the catchment's SM conditions are ensured. However, regular monitoring is rarely practiced and such historic datasets are usually unavailable. It becomes thus a standard practice to assume that initial SM conditions are static (e.g. constantly wet during the rainy season and constantly dry during the dry season) (Berthet *et al.*, 2009). Undoubtedly, this assumption is an oversimplification and may induce significant errors undermining the robustness of the simulations (Brocca *et al.*, 2008; Trambly *et al.*, 2012; Massari *et al.*, 2014). Correctly identifying initial SM conditions is also critical for (automated) early warning systems, which depend strongly on the availability and accuracy of SM datasets in order to perform representative flood simulations and in turn issue accurate warnings. However, generalizations and simplifications in such systems are inevitable (Ponziani *et al.*, 2013).

A recent trend in estimating a catchment's SM conditions is the use of updated SM information from satellite images, such as the Advanced Scatterometer (ASCAT) products (Trambly *et al.*, 2012). SM-related satellite products can be used either as stand-alone SM datasets in the absence of relevant *in-situ* measurements (Chen *et al.*, 2014; Wanders *et al.*, 2012) or validated and/or calibrated with ground SM measurements, when available (Dorigo *et al.*, 2015; Su *et al.*, 2013; Albergel *et al.*, 2013). However, the exclusive use of remotely sensed datasets remains controversial, since validation of satellite data with ground truth SM measurements is not straightforward due to differences in spatial resolution, observation depths and measurement uncertainties (Brocca *et al.*, 2011), while at the same time relevant *in-situ* measurements are usually not available (Matgen *et al.*, 2012; Brocca *et al.*, 2010; Massari *et al.*, 2014, Wanders *et al.*, 2012). Hence, it can be concluded from literature that despite the significant progress that has been made in the estimation of SM conditions, the incorporation of reliable SM estimations in semi-automatic hydrological systems, such as those needed for example for flood forecasting, remains challenging.

In the current research and given the frequent absence of long historic SM datasets, the estimation of initial SM conditions has been based on the so-called Antecedent Moisture Conditions (AMC) as identified in the SCS Curve Number method (USDA-SCS, 1985; USDA-NRCS, 2004b). According to this method, initial SM conditions depend on the total rainfall depth of the five (5) days preceding a flood event. Based on this total rainfall depth and on whether the season is dormant or growing, three different AMC classes are distinguished: *dry*, *normal* and *wet*. The marginal values for the classification of the antecedent conditions in each class, which have also been adopted in this research, are listed in Table 5.1. In this Table, the corresponding values presented in a relevant table in Chow *et al.* (1988) have been converted from inches to millimeters and rounded to the closest integral number.

Table 5.1. Different classes of Antecedent Moisture Conditions.

AMC	Total rainfall depth of the previous 5 days [mm]	
	Dormant Season	Growing Season
I (dry)	< 13	< 36
II (normal)	13÷28	36÷53
III (wet)	> 28	> 53

The validity of this Table for large basins has been questioned, since its applicability was generalized even though its development was based on limited data and it does not account for regional differences or scale effects (Ponce and Hawkins, 1996). Nonetheless, for small river basins, similar to the river basin studied in this research, the AMC are represented well when they follow the values of this Table.

### 5.3 Hydrological modelling – selected simulation methods and hydrological parameters

In order to quantify the impact of initial conditions, in terms of forest fire and SM, on the hydrological response of a catchment and examine its evolution in time, appropriate simulation methods need to be applied and representative hydrological parameters need to be examined. The estimation of the hydrological losses, the design of a catchment Unit Hydrograph and the calculation of channel routing are core components of hydrological simulations which are strongly affected by the fire impact on a catchment and its initial soil moisture conditions. During this research, widely applied simulation methods for each one of these hydrological modelling components, as incorporated in flexible and typical hydrological models (in this case HEC-HMS and more specifically the version HEC-HMS 3.5 (Scharffenberg and Fleming, 2010)), have been selected and the representative hydrological parameters necessary for application of these simulation methods have been thoroughly investigated.

The selection of the simulation methods was based on required input and available datasets, considering the fact that model efficiency depends strongly on the selected methods (see also Section 4.6). Regarding hydrological parameters, the basic criteria for their selection have been their representativeness, their sensitivity in initial conditions and their wide applicability in hydrological studies. Their selection has also been determined by the accumulated experience gained from the use of these parameters as calibration parameters in numerous applications. This experience has been recorded in relevant scientific publications (Papathanasiou *et al.*, 2012; Bariamis *et al.*, 2014; Papathanasiou *et al.*, 2013e) and has supported the implementation of several graduate and post-graduate theses that have been performed in the Laboratory of the Hydrology and Water Resources Management (Alonistioti, 2011; Kassela, 2011; Pagana, 2012; Bariamis, 2013).

Eventually, five typical hydrological parameters that depend strongly on catchment characteristics and its initial conditions have been selected and

thoroughly examined. These five parameters are: the Curve Number (CN), the initial abstraction (IA), the standard lag (TP), the peaking coefficient (CP), and the K Muskingum coefficient. CN and IA are used in the estimation of the hydrological losses, TP and CP are used in the design of the Unit Hydrograph and K is used in the Muskingum channel routing method. CN and IA are very sensitive calibration parameters, since they significantly affect simulation results, while TP, CP and K affect to a smaller extent simulation results, remaining however significant enough not to be ignored (as justified in Chapter 8). The simulation methods that were selected including a detailed presentation of the selected hydrological parameters are presented in Section 5.3.1.

### **5.3.1 Hydrological loss method**

Hydrological losses are estimated on a subbasin basis and include infiltration, subsurface loss, retention *etc.* All these processes and their interaction are simulated in an integrated way in HEC-HMS through a “loss method” that needs to be defined for every subbasin. HEC-HMS 3.5 offers twelve different hydrological loss methods for estimating the actual infiltration, which are designated for either event-based or continuous simulations. These methods include *inter alia* deficit constant loss method (either gridded or lumped), exponential loss method, Green and Ampt loss method (either gridded or lumped) and SCS Curve Number loss method (either gridded or lumped). Required input for each method and available datasets were examined and eventually, the SCS Curve Number loss method (lumped version) was selected, for reasons of wide applicability, representativeness and simplicity, as well. The option to use a different method for each subbasin is also available; however, considering the available datasets as well as the inherent uncertainty in those methods, a common method was applied in all subbasins.

The **SCS Curve Number method** was selected in order to account for hydrological losses in the hydrological model. This method was developed by the US Department of Agriculture Natural Resources Conservations Service (NRCS), formerly the Soil Conservation Service (SCS), for the estimation of runoff and peak flow during a flood event. The method is described in detail in USDA-SCS (1985), first published in 1954 and revised several times ever since (USDA-NRCS, 1986; USDA-NRCS, 2004b). According to this method, CN is the SCS Curve Number and can be estimated from relevant Tables, based on the land cover type and treatment, the dominant hydrologic conditions and the hydrologic soil group, as presented below.

The method seems to perform best at agricultural sites, for which it was originally developed, fairly at range sites and poorly at forest sites, while it is also recommended for use in urban areas (Mishra and Singh, 2003). In general, it is a simple, widely applied, empirical method that has been tested and has proved its efficiency in time, with its main disadvantage being the fact that it does not incorporate time in its calculations, it is particularly sensitive to one parameter (CN), which unavoidably depends on a limited number of other parameters, while it also ignores the impact of rainfall intensity and its temporal distribution on runoff (Mishra and Singh, 2003, Ponce and Hawkins, 1996).



In HEC-HMS, the *runoff Curve Number (CN)*, the *initial abstraction (Ia)* and the *percentage of impervious areas* need to be defined for the estimation of hydrological loss based on the SCS CN method (HEC, 2009). The current study focuses on CN and IA and examines thoroughly the impact of initial conditions on both parameters, as described in Sections 5.3.1.1 and 5.3.1.2 respectively. The percentage of imperviousness expresses the percentage of the directly connected impervious areas in the subbasin. This parameter can either be adjusted to CN or can be calculated separately. In this research imperviousness has been considered in the estimation of a composite CN for each subbasin and has been thus set to zero in the hydrological loss method.

### **5.3.1.1 Estimating CN for pre-fire and normal SM conditions**

CN quantifies the impact of a subbasin's soil properties and land uses on its hydrological response. As mentioned in Section 5.3.1, in order to determine the **runoff Curve Number (CN)** the land cover type and treatment, the dominant hydrologic conditions and the hydrologic soil group need to be determined first.

Regarding land cover type, it is usually determined from land cover maps. Treatment includes mechanical practices (e.g. contouring and terracing) and management practices (e.g. crop rotations and reduced or no tillage) and needs to be defined for cultivated agricultural lands.

Regarding the hydrologic conditions, they can be estimated from the density of plant and residue cover on sample areas and they are classified as poor, fair or good, with *good hydrologic condition* denoting that the soil has a low runoff potential for the specific cover type, treatment and hydrologic soil group. Regarding the hydrologic soil group, soils are classified into 4 types: A, B, C and D, according to their minimum infiltration rate, obtained for bare soil after prolonged wetting, as presented in detail in USDA-NRCS (1986) and USDA-NRCS (2009).

### **5.3.1.2 Estimating IA for pre-fire and normal SM conditions**

**Initial abstraction, IA**, indicates the amount of precipitation that needs to fall before surface excess, *i.e.* direct runoff, starts and mainly includes interception, initial infiltration, surface depression storage and evapotranspiration (USDA-NRCS, 1986). In the SCS method, infiltration volume during a storm is recalculated at the end of each time interval and incremental precipitation is then computed. In HEC-HMS model, when choosing the SCS-CN method for the estimation of the hydrological losses, the definition of IA is optional. A blank IA field is automatically filled in with the value  $IA = 0.2 * S$ , where S is the potential retention calculated directly from the CN value.

However, this generalized equation is based on datasets from agricultural watersheds in the United States and should be adopted with caution in other applications. For example, in more urbanized areas initial abstraction may be totally different, and in particular IA could be significantly decreased due to numerous impervious areas or it could even be increased in case of existence of surface depressions that store runoff on impervious areas (USDA-NRCS, 1986).

In general, IA is a very sensitive calibration parameter (Papathanasiou *et al.*, 2015a; Shi *et al.*, 2009; Bariamis *et al.*, 2014) and thus its reliable estimation is of paramount importance for an efficient simulation.

To this end, numerous studies have been performed for the estimation of initial abstraction ratio, *i.e.* IA/S, and several of them have concluded that the value of 0.2 for this ratio is particularly high, affecting thus modelling efficiency (Shi *et al.*, 2009; Beck *et al.*, 2009; Mishra *et al.*, 2003; Mishra and Singh, 1999; Baltas *et al.*, 2007). More specifically, according to Mishra and Singh (2003) increased values of initial abstraction ratio are associated with decreased efficiency in a versatile SCS-CN model, while Woodward *et al.* (2003) and Jiang (2001) suggest a ratio equal to 0.05 in order to calculate runoff.

It is suggested that IA is not considered necessarily as equal to  $0.2 \cdot S$  and, when available, relevant datasets need to be examined so as to define its marginal values. In the absence of such datasets, general guidelines verified in literature for study areas similar to the examined areas, as those mentioned above, could be followed.

### **5.3.2 Transform Method**

Transform methods are estimated on a subbasin basis and refer to the transform of excess precipitation into surface runoff. Typically, Unit Hydrographs (UHs) are used as transform methods. The UH represents the response of a catchment to a given rainfall, *i.e.* the runoff discharge after a rainfall with effective rainfall depth equal to 10 mm, uniformly distributed in space over the whole catchment and with a uniform rate over a unit time period. UHs are specific for every catchment and for different time lengths which correspond to the duration of effective rainfall. When the response of a catchment to a given rainfall is estimated, then its response to rainfall with other characteristics may be estimated as well, through the use of the ordinates of a UH (the abscissas being the time).

An assortment of different transform methods are incorporated in HEC-HMS. These include *inter alia* the SCS UH, the Snyder UH, the Clark UH, the Modified Clark (ModClark) UH and User-Specified UH. Different methods were tested (the SCS UH, User-Specified UH, the Snyder UH), however both SCS UH and User-Specified UH provided poor results (Papathanasiou *et al.*, 2013e; Bariamis 2013). The **Snyder UH method** was finally selected as transform method due to its wide applicability, its representativeness and its simplicity. Snyder has been the first to develop a synthetic UH based on studies on catchments in Appalachian Highlands (Snyder, 1938). According to Snyder method, the Lag Time (or Standard Lag, TP), the peak flow, the time base of hydrograph and the UH widths at the time that correspond to the 50% and 75% of the peak time, need to be determined in order to estimate a catchments UH for a given time length. These five parameters are calculated based on Equations 5.1-5.5.

$$TP = 0.752 * Ct * (L * Lc)^{0.3} \text{ (Eq. 5.1),}$$

$$Q_p = 2.78 * A * \frac{CP}{TP} \text{ (Eq. 5.2),}$$

$$T_b = 3 + \frac{TP}{8} \text{ (Eq. 5.3),}$$

$$W_{50} = \frac{2.14}{\left(\frac{Q_p}{A}\right)^{1.08}} \text{ (Eq. 5.4),}$$

$$W_{75} = \frac{1.22}{\left(\frac{Q_p}{A}\right)^{1.08}} \text{ (Eq. 5.5),}$$

where:

TP: Standard Lag [hr],

Ct: coefficient that represents the topographic and soil characteristics of a catchment and typically ranges between 1.8 and 2.2,

L: length of the main channel [km],

Lc: length of the channel between the centroid of the catchment and its outlet [km],

Qp: peak flow [m<sup>3</sup>/sec],

CP: Peaking Coefficient (described in detail in Section 5.3.2.2) that normally ranges between 0.4 and 0.8,

A: the drainage area [km<sup>2</sup>],

Tb: time base of the hydrograph,

W<sub>50</sub>: UH width at the time that corresponds to the 50% of the peak time and

W<sub>75</sub>: UH width at the time that corresponds to the 75% of the peak time

In HEC-HMS, the input parameters for the application of this method are the *Standard Lag* (TP) and the *Peaking Coefficient* (CP), presented in detail in the following Sections.

### **5.3.3.1 Estimating TP for pre-fire and normal SM conditions**

**Standard Lag (TP)** is the time interval between the centroid of precipitation mass and the peak of the unit hydrograph. Several relationship have been developed for the estimation of Lag Time in other UH methods, such as the SCS UH method, which suggests Equation 5.6 for Lag Time (Elliott *et al.*, 2005).

$$TP = L^{0.8} * \frac{(S+1)^{0.7}}{1900 * Y^{0.5}} (S + 1) \text{ (Eq. 5.6),}$$

where:

L: the hydraulic length of the catchment [ft],

S: the potential max soil moisture retention in the catchment [in] and

Y: the catchment slope [%],

However, particularly in Snyder method, Standard Lag can be determined from Equation 5.1. The length of the main channel and the length of the channel between the centroid of the catchment and its outlet need to be estimated, while at the same time sufficient information on topographic and soil properties per catchment subbasins needs to be available so as to estimate Ct. Usually, such information is not available and inevitably several assumptions need to be made

for the estimation of TP. For this reason, practical and sometimes empirical methods have been developed. A practical rule to estimate TP is to consider it as a percentage of time of concentration (HEC, 2009), which can usually be calculated more easily.

### **5.3.3.2 Estimating CP for pre-fire and normal SM conditions**

The **Peaking Coefficient (CP)** in the Snyder UH method is a dimensionless descriptor of the shape of a UH, the value of which quantifies the steepness of the hydrograph. Its typical values range between 0.4 and 0.8, with the lower values denoting steep-rising hydrographs (HEC, 2009; McEnroe and Zhao, 1999). In a detailed study on 19 small rural gauged catchments in Kansas, McEnroe and Zhao (1999) verified that CP ranged from 0.46 to 0.77, with mean value equal to 0.62 and standard deviation equal to 0.10. In other studies, recommended CP average values are 0.6 for the Appalachian Highlands, 0.8 for central Texas and central Nebraska and 0.9 for Southern California (Viessman and Lewis, 1995).

In the SCS UH method, CP is considered constantly equal to 0.75, while for ungauged rural catchments a CP equal to 0.62 is recommended as input to the Snyder UH method (McEnroe and Zhao, 1999). In practice, CP is estimated empirically and typically ranges between 0.4 and 0.7, as described above.

### **5.3.3 Routing Method**

As analyzed in Chapter 4, flood routing is the propagation of flood wave in a channel. Routing methods are estimated on a reach basis. Due to complexities in routing estimation, simplified routing schemes have been developed and are widely applied.

The options that HEC-HMS offers for simplified flood routing are described in Section 4.2.1.1. In this research, the **Muskingum Method** has been selected for flood routing. The main criteria for this selection have been its minimal data requirements, its representativeness and its wide applicability, as demonstrated in numerous published works (e.g. Chow *et al.*, 1988; O'Sullivan *et al.*, 2012; Gill, 1978).

This method is based on the simple storage – discharge relationship of Equation 4.3, which expresses the continuity equation. For its application, the *Muskingum K* and *Muskingum X coefficients* and the number of *time increments  $\Delta t$*  need to be defined. Muskingum K coefficient has been selected as calibration parameter for the methodology developed in this research and is described in more detail in Section 5.3.3.1.

*Muskingum X coefficient* (or else called Storage Routing) represents storage in channel per routing time step, *i.e.* it expresses the attenuation that can be achieved through routing and is dimensionless. The values of X range from 0 to 0.5, where 0 denotes maximum attenuation and 0.5 denotes no attenuation. Muskingum X values range from 0 to 0.3 for natural streams, with mean value being 0.2 (Chow *et al.*, 1988; Johnson, 1999), while values between 0.4 and 0.5

are most appropriate for streams with little or no floodplain (Johnson, 1999), *i.e.* smooth, uniform channelized streams. Usually,  $X$  takes intermediate values, with 0.2 and 0.25 being in most cases appropriate (Chow *et al.*, 1988; HEC, 2009). The impact of Muskingum  $K$  and  $X$  coefficients on routed hydrographs is illustrated in Figure 5.1.

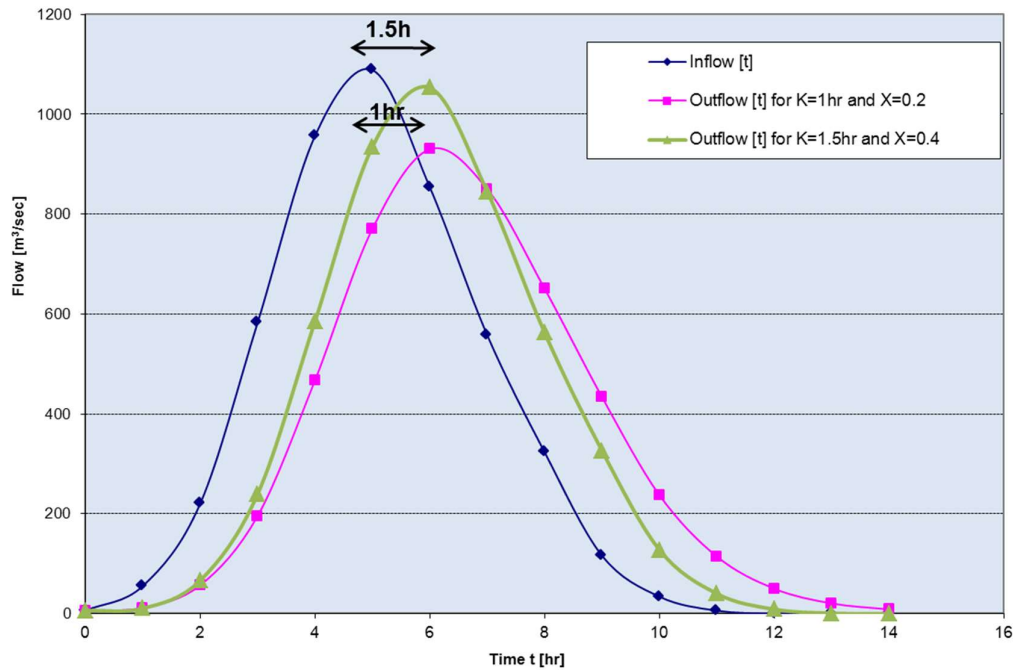


Figure 5.1. The impact of  $K$  and  $X$  on routed hydrographs.

Time increment  $\Delta t$  has to be less or approximately equal to the time the wave needs to travel through the reach. Several criteria have been developed that need to be fulfilled by time increment  $\Delta t$  for a successful application of the Muskingum method. In general, time increment  $\Delta t$  ranges between 5 minutes and one day (Elbashir, 2011), while minimum time increments result in good routing hydrographs (Garbrecht and Brunner, 1991). Sometimes, for the application of the Muskingum method it is necessary to define the *number of subreaches* instead of the time increment  $\Delta t$ . The division of the reach length by the product of wave velocity and the time increment  $\Delta t$  provides a reliable estimation of the value of the *number of subreaches* (HEC, 2009). Increased number of subreaches denotes decreased attenuation.

In HEC-HMS, for the application of the Muskingum method it is necessary to determine the values of *Muskingum  $K$*  and  *$X$  coefficients* and the number of subreaches. In the proposed methodology, a constant value for the attenuation (Muskingum  $X$  coefficient) and a constant number of subreaches in each subbasin were considered and were not altered, regardless of dominant wet or dry conditions and burnt or unburnt subbasins. The rules applied for the estimation of Muskingum  $K$  coefficient for pre-fire and normal SM conditions are presented in the following.

### 5.3.3.1 Estimating K for pre-fire and normal SM conditions

The **Muskingum K coefficient** represents the ratio of storage to discharge for the channel and takes dimensions of time (hours). It expresses the travel time of the wave through the channel reach and in the absence of relevant reliable datasets the value of K can be estimated as the average travel time of the peak flow through the reach (Chow et al., 1988; O'Sullivan *et al.*, 2012). Therefore, Muskingum K coefficient can be determined by the ratio of the mean velocity to the length of the reach. In the absence of velocity measurements, channel velocity can be determined either empirically (using simplified rules-of-thumb for water movement) or through performing a simple open-channel flow calculation using Manning's equation. Assumed velocities can be verified through hydraulic simulations.

To estimate initial values for K, an analysis that includes either observed upstream and downstream hydrographs or geometrical and resistance properties of channels (O'Sullivan *et al.*, 2012) has to be performed. Observed hydrographs are usually not available and therefore K is more often estimated by channel properties, still when available. For reasons of simplification, Muskingum K coefficient for channels is often assumed to be constant throughout the range flow (Chow *et al.*, 1988), even if in practice this is not always the case.

## 5.4 Estimating the temporal evolution of the selected hydrological parameters for variable initial conditions

The values of the five examined parameters for pre-fire and normal SM conditions are estimated as indicated in the previous paragraphs. For **pre-fire and variable SM conditions** (either wet or dry), the values of the parameters can be estimated through a pre-fire calibration process. This procedure will result in the extraction of a set of rules that directly associate pre-fire values for normal conditions with pre-fire values for wet and dry conditions.

Particularly for CN, according to the SCS methodology, besides soil type and land uses (described above) CN values depend strongly on initial SM conditions. As presented in Section 5.2, the SCS Curve Number method assumes that the total rainfall depth of the five days preceding a flood event is representative of the catchment's SM conditions and assists their classification as wet, dry or normal, as presented in Table 5.1. Different classes are associated with different CN values. Based on the SCS method, CN values provided in relevant, widely used Tables (USDA-NRCS, 2004a; USDA-NRCS, 1986) correspond to *normal conditions*, *i.e.* CN<sub>II</sub>, while for wet (CN<sub>I</sub>) and dry (CN<sub>III</sub>) conditions the following transformations are suggested:

$$CN_I = \frac{4.2 * CN_{II}}{10 - 0.058 * CN_{II}} \text{ (Eq. 5.7)}$$

$$CN_{III} = \frac{23 * CN_{II}}{10 + 0.13 * CN_{II}} \text{ (Eq. 5.8)}$$

However, the application of Equations 5.7 and 5.8 is often associated with poor results in CN estimation, and more specifically with underestimated CN for wet

conditions (CN<sub>I</sub>) and overestimated CN for dry conditions (CN<sub>III</sub>) (Mishra and Singh, 2002; Huang *et al.*, 2006; Gao *et al.*, 2012). For this reason, these Equations were not applied in this research.

Also, as mentioned in Section 5.3.3.1 the assumption that Muskingum K coefficient for channels is constant throughout the range flow is usual, mainly for reasons of simplification (Chow *et al.*, 1988). However, this parameter depends on initial conditions in terms of both initial SM and fire impact and therefore its value needs to change under variable initial conditions. Focusing on the impact of SM, during wet conditions, when discharge is increased, the wave velocity in a given river section is increased and thus the travel time of the peak flow is decreased.

The values of the examined hydrological parameters are expected to be significantly affected for **post-fire conditions**, especially for areas that have been affected severely by fire. As stated in Chapter 3, numerous studies have been performed in order to translate the fire impact into changes in the hydrological response of a catchment. However, as discussed in Section 3.5, most of these studies refer to a limited post-fire time-window (*i.e.* the first 1-2 post-fire years), they are case-specific and thus can only be considered representative within their specific conditions and also they examine post-fire impact from an ecological perspective, focusing on vegetation recovery and natural reforestation (Oliveira and Fernandes, 2009; Thanos *et al.*, 1989; Bolin and Ward, 1987). At the same time, the majority of these studies focuses on the examination of changes in post-fire CN values, while limited research has been performed on the estimation of fire impact on IA, TP, CP and K. Usually this impact is ignored and average values of these parameters are estimated instead (*e.g.* Viessman and Lewis, (1995; McEnroe and Zhao, 1999).

Regarding the post-fire recovery rate of a catchment, as mentioned in Section 3.3.1, in typical Mediterranean ecosystems, increased recovery is often observed during the first post-fire years, and is usually followed by a decreased recovery rate (*e.g.* Thanos and Marcou, 1991; Trabaud *et al.*, 1985; Eccher *et al.*, 1987 Marzano *et al.*, 2012). A persisting fire impact on a catchment's hydrological response during the first three post-fire years was reported by Mayor *et al.* (2006), which was however attributed to a 2-year post-fire dry period.

For this reason, a sharply descending impact of fire with time has been considered in the suggested changes in the values of the examined hydrological parameters. Given that post-fire vegetation regrowth determines the post-fire values of the examined hydrological parameters, this logical assumption is verified. Therefore, the logarithmic profile of the characteristic time-windows in post-fire vegetation development can be directly associated with a dynamic post-fire evolution of hydrological parameters in time with regards to their pre-fire values, with changes following a logarithmic profile (Papathanasiou *et al.*, 2015a).

In this context, the Equations 5.9a-e and 5.10a-e presented below are proposed for the estimation of the post-fire evolution in time of the examined hydrological parameters for normal SM conditions.

$$CN_{pf,FS}(t) = CN_{af} + h_{CN,FS}(t) \quad (\text{Eq. 5.9a})$$

$$IA_{pf,FS}(t) = IA_{af} + h_{IA,FS}(t) \quad (\text{Eq. 5.9b})$$

$$TP_{pf,FS}(t) = h_{TP,FS}(t) * TP_{af} \quad (\text{Eq. 5.9c})$$

$$CP_{pf,FS}(t) = \text{MAX}[(CP_{af} + h_{CP,FS}(t)), p] \quad (\text{Eq. 5.9d})$$

$$K_{pf,FS}(t) = h_{K,FS}(t) * K_{af} \quad (\text{Eq. 5.9e})$$

where:

$$h_{CN,FS}(t) = a_{CN,FS} * \ln(t) + b_{CN,FS} \quad (\text{Eq. 5.10a})$$

$$h_{IA,FS}(t) = a_{IA,FS} * \ln(t) + b_{IA,FS} \quad (\text{Eq. 5.10b})$$

$$h_{TP,FS}(t) = a_{TP,FS} * \ln(t) + b_{TP,FS} \quad (\text{Eq. 5.10c})$$

$$h_{CP,FS}(t) = a_{CP,FS} * \ln(t) + b_{CP,FS} \quad (\text{Eq. 5.10d})$$

$$h_{K,FS}(t) = a_{K,FS} * \ln(t) + b_{K,FS} \quad (\text{Eq. 5.10e})$$

and where:

index pf: corresponds to post-fire conditions,

index af: corresponds to pre-fire (ante-fire) conditions,

index FS: indicates FS that depends on the % of the affected area within each FS class,

t: time after fire event [months] and

a, b: parameters that depend on FS and boundary conditions for the estimation of the post-fire values of each parameter

Equations 5.9a-e are expressed as presented above for reasons of compatibility and therefore quantitative control with relevant findings in literature. For example, post-fire changes in CN are usually discrete (e.g. Higginson and Jarnecke, 2007) and for this reason post-fire CN values are proposed to be estimated as the sum of the corresponding pre-fire values and a discrete change in these values (Eq. 5.9a). At the same time, post-fire TP values are typically expressed as a percentage of the corresponding pre-fire values (e.g. Elliott *et al.*, 2005), similar to the expression proposed for the estimation of post-fire TP values in Equation 5.9c. Regarding CP, Equation 5.9d is expressed as presented above in order to set an upper threshold in TP post-fire values, as described in Section 5.3.3.2.

In order to estimate the parameters a and b in Equations 5.10a-e above, it is necessary to define the boundary conditions of each FS class. The upper boundary conditions are represented by the values of h for different FS for  $t_{upper}$  (i.e. the first post-fire period), while the lower boundary conditions are represented by the values of h for different FS for  $t_{lower}$  (i.e. the period just prior to hydrological recovery). Given that the research performed so far on the estimation of h for different FS is limited, a co-evaluation of threshold values identified in literature, calibration results and, when relevant, particular conditions and restrictions, needs to take place for each case study.

Thus, in order to estimate the post-fire values of the five examined hydrological parameters for normal SM conditions,  $t_{upper}$  and  $t_{lower}$ , as well as the corresponding values of h for all parameters and different FS classes need to be determined first. Based on these boundary conditions, Equations 5.10a-e can be applied for the estimation of a and b parameters and Equations 5.9a-e can be applied for the eventual estimation of the post-fire values of all five hydrological parameters.



As far as post-fire values of these hydrological parameters for wet and dry SM conditions are concerned, rules mentioned above that associate normal pre-fire SM conditions with wet and dry pre-fire SM conditions, can be applied for the estimation of values for wet and dry post-fire SM conditions in relation to the values for normal post-fire SM conditions, estimated from Equations 5.9a-e and 5.10a-e. A generic equation that expresses the relation between parameter values for normal, wet and dry SM conditions is Eq. 5.11.

$$X_{af,dry/wet} = c * X_{af,normal} + d, \text{ (Eq. 5.11),}$$

where:

X: a hydrological parameter and

c, d: coefficients that depend on case-specific conditions.

Based on the percentage of the affected area within each FS class (as estimated from the GIS analysis mentioned in Section 5.1.1) and the suggested parameter values for each severity class (as estimated from Equations 5.9a-e), a composite, weighted parameter value for each subbasin is estimated and this value is imported in the hydrological model for the necessary simulations.

## **5.5 The 1<sup>st</sup> post-fire flood: a particular situation**

The methodology for incorporating post-fire hydrological footprint in hydrological simulations presented above has been developed for typical Mediterranean periurban catchments that are affected by successive fire events. However, under particular conditions, deviations from the proposed methodology could be observed especially during the first post-fire floods and necessary readjustments need to be made in this methodology in order to apply it. The particular conditions under which the first post-fire floods do not comply strictly with all the rules of the proposed methodology as expressed in previous Sections, posing thus potential restrictions in its wide applicability, are discussed below. These conditions include intense rainfall events during the first post-fire period, particular geomorphological features, extended livestock activities (especially during the first post-fire period) and burnt areas that are not successively affected by forest fires. Additional features for each of these conditions are presented in detail in the following.

### **5.5.1 Particularly erosive rainfall**

Particularly intense rainfall events during the first post-fire period can restrict the wide applicability of the proposed methodology, since rainfall is a key driver of soil erosion (Panagos *et al.*, 2015). More specifically, the occurrence of successive low-rainfall events during the post-fire period favors vegetation regrowth (Brown, 1972). At the same time, as discussed in Section 3.3.1, during the first post-fire years increased vegetation recovery rate is typical in Mediterranean ecosystems (Thanos and Marcou, 1991; Trabaud *et al.*, 1985; Eccher *et al.*, 1987; Marzano *et al.*, 2012). When rainfall events during the first post-fire months are characterized by high erosivity, as discussed in the following, then the upper soil layers are significantly affected by intense soil erosion, losing nutrients and organic matter and having reduced infiltration rates and retention capacity (Panagos *et al.*, 2015; Ferreira and Panagopoulos, 2012), all of which are critical for vegetation regrowth. As a result, vegetation regrowth and the consequent hydrological recovery are

delayed and more intense post-fire floods (in terms of volume, peak flows and time to peak) are to be expected.

A typical metric used to quantify this erosivity is the “*Rainfall Erosivity Factor*” (R-factor) (Eq. 5.13 and 5.14), or else called “*Rainfall-Runoff Erosivity Factor*” (Park *et al.*, 2011), used in the Revised Universal Soil Loss Equation (RUSLE) (Eq. 5.12). This factor represents the rainfall erosive force and intensity in a normal year (Goldman *et al.*, 1986) and can be estimated as the sum of the product of total energy and maximum 30-min storm intensity ( $EI_{30}$ ) for all storms in the area during an average year (Brown and Foster, 1987). It is usually estimated as a multi-annual average index and describes rainfall impact on sheet and rill erosion (discussed in Section 3.1.2), ignoring runoff erosive forces due to rainfall movement over frozen soils, snow movement and snowmelt (Panagos *et al.*, 2015). Mean values for R-factor in Europe are  $722 \text{ MJ*mm*ha}^{-1}\text{h}^{-1}\text{yr}^{-1}$ , with the highest values, exceeding  $1000 \text{ MJ*mm*ha}^{-1}\text{h}^{-1}\text{yr}^{-1}$ , being typical in Mediterranean areas (Panagos *et al.*, 2015).

$$A = R * K * LS * C * P \quad (\text{Eq. 5.12}),$$

$$R = \frac{1}{n} \sum_{j=1}^n \sum_{k=1}^{m_j} (\sum_{r=1}^0 (e_r * v_r) * I_{30})_k \quad (\text{Eq. 5.13}),$$

$$e_r = 0.29 * [1 - 0.72 \exp(-0.05 * i_r)] \quad (\text{Eq. 5.14})$$

where

A: average soil loss [ $\text{t*ha}^{-1}\text{yr}^{-1}$ ],

R: rainfall erosivity factor [ $\text{MJ*mm*ha}^{-1}\text{h}^{-1}$ ]

K: soil erodibility factor [ $\text{t*h*MJ}^{-1}\text{mm}^{-1}$ ],

LS: slope length-steepness factor [dimensionless],

C: cover (crop/vegetation) management factor [dimensionless],

P: support practice factor (contour farming, cross slope *etc.*) [dimensionless],

n: number of years covered by the data records,

m<sub>j</sub>: number of erosive events of a given year j,

k: number of a single event,

e<sub>r</sub>: unit rainfall energy [ $\text{MJ*ha}^{-1}\text{mm}^{-1}$ ],

v<sub>r</sub>: rainfall volume during a time period r [mm],

I<sub>30</sub>: max rainfall intensity during a 30-min period of the rainfall event [ $\text{mm*h}^{-1}$ ],

i<sub>r</sub>: rainfall intensity during the time interval [ $\text{mm*h}^{-1}$ ]

Therefore, when the time periods used for an analysis of a post-fire impact on hydrology include particularly wet and intense storm events, the methodology needs to be readjusted, considering extended post-fire recovery periods, *i.e.* prolonged both  $t_{\text{upper}}$  and  $t_{\text{lower}}$ , and increased post-fire changes in the values of the selected parameters, *i.e.* increased  $h_{\text{CN,FS}}(t)$ ,  $h_{\text{IA,FS}}(t)$ ,  $h_{\text{TP,FS}}(t)$ ,  $h_{\text{CP,FS}}(t)$  and  $h_{\text{K,FS}}(t)$ , respectively.

### **5.5.2 Particular geomorphological features**

Other conditions that may restrict the wide applicability of the suggested methodology and are strongly associated with rainfall erosivity, concern particular

geomorphological features. When the upper soil layers of a catchment are particularly sensitive, they are more prone to landslides, sediment erosion, transport and sedimentation. In general, “sensitive soils” are those that have texture close to that of fine sand ( $100\ \mu$ ), while clays are more coherent and less easily dislodged (Roose, 1996). As mentioned above and discussed in detail in Section 3.1.2, soil erosion, which is particularly intensified after severe forest fires (Esteves *et al.*, 2012; Inbar *et al.*, 1998; Cannon *et al.*, 2000; Bisson *et al.*, 2005; Dragovich *et al.*, 2002) is directly related with decreased soil fertility and increased post-fire runoff (Ferreira and Panagopoulos, 2012). As a result, vegetation regrowth can be irreversibly affected (Fig. 5.2), especially during the first post-fire period, delaying in turn the hydrological recovery of the affected catchment and making it more prone to severe post-fire floods regarding volume, peak flows and time to peak.



*Figure 5.2 Debris flow generated from a catchment near Glenwood Springs, Colorado burnt in 2002 (Source: Cannon *et al.*, 2003).*

The factors that make an area susceptible to landslides and intense soil erosion and sedimentation without actually triggering it, also known as “predisposing factors” include geological formation, slope gradient, land cover, soil physical properties, relative relief and drainage patterns (Zhu *et al.*, 2014). In literature “predisposing factors” are also called “causative factors” (Donati and Turrini, 2002), “causal factors” (Carrara *et al.*, 1995), “intrinsic factors” (Atkinson and Massari, 1998), “conditioning factors” (Zêzere *et al.*, 1999), “preparatory factors” (Ermini *et al.*, 2005) or “quasi-static factors” (Xu *et al.*, 2012). When certain predisposing factors are followed by triggering factors, the most important of which are intensive rainfall, rapid snowmelt, change in water level, earthquakes and in particular cases volcanic eruption (Zêzere *et al.*, 1999), then landslides and soil loss occurs. A rough approximation to vulnerability to landslides and soil loss

can be performed through appropriate landslide susceptibility maps and soil loss maps, respectively, that are developed for large scale areas (e.g. Fig. 5.3 and 5.4), while detailed geological profiles and hydromorphological features need to be examined so as to make a more accurate estimation of the susceptibility of an area to landslides and soil loss.

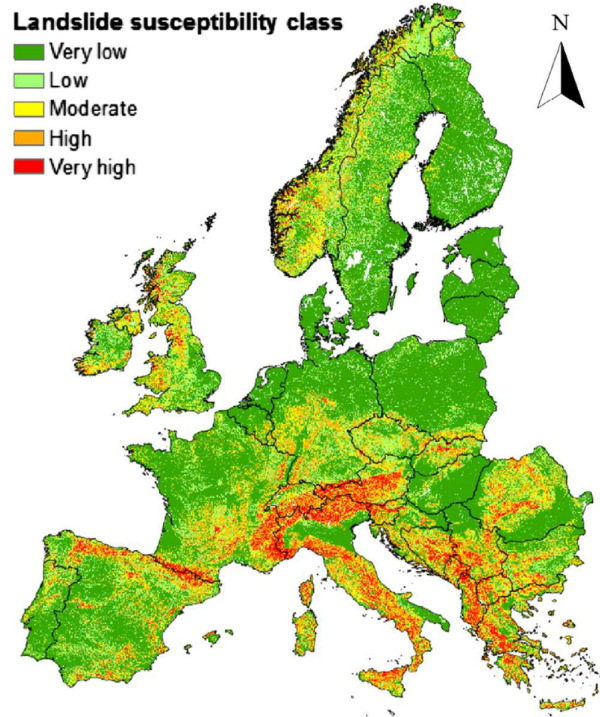


Figure 5.3 European Landslide Susceptibility Map (Source: Günther et al., 2014).

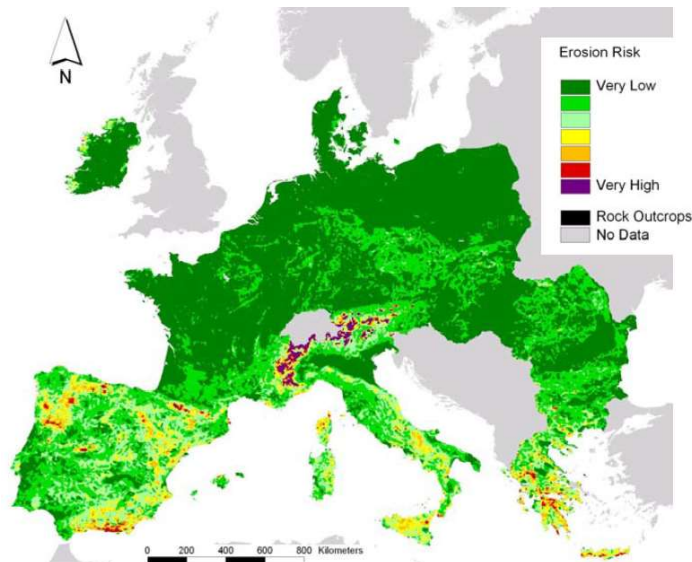


Figure 5.4. Actual soil erosion risk map for Europe, based on the USLE approach (Source: Grimm et al., 2002).

The methodology presented above is suggested for typical Mediterranean soils that are particularly erodible and susceptible to landslides, as verified from Figures 5.3 and 5.4. For application in less erodible soils, the elements of the methodology need to be readjusted accordingly, considering shorter post-fire recovery periods, *i.e.* short  $t_{upper}$  and  $t_{lower}$  and decreased post-fire changes in the values of the selected parameters, *i.e.* decreased  $h_{CN,FS}(t)$ ,  $h_{IA,FS}(t)$ ,  $h_{TP,FS}(t)$ ,  $h_{CP,FS}(t)$  and  $h_{K,FS}(t)$ , respectively. It needs also to be highlighted that when particular geomorphological features are dominant, the methodology needs to be periodically readjusted (*e.g.* on a 3-year basis) due to alterations in river cross-sections.

### **5.5.3 Extended livestock activities**

Extended livestock activities, especially during the first post-fire period, contribute to further soil degradation and may also necessitate the readjustment of the proposed methodology. According to Brown (1972), the livestock activities over an affected area expose the upper soil layers, which become thus more vulnerable to the erosive force of rainfall and wind. Therefore, livestock activities, particularly when followed by intense rainfall events, influence strongly post-fire recovery rate and are associated with increased post-fire runoff volumes and peak discharges and minimized times to peak.

In particular, overgrazing is a long term practice that causes loss of soil nutrients and organic matter as a result of the removal of vegetation cover. Consequently, this practice is directly associated with soil degradation (Salvati and Carlucci, 2015), *i.e.* soil fertility decline and thus overall low agricultural productivity. Overgrazing, similarly to over-cultivation, delays vegetation regrowth and hydrological recovery, while it is also related with deforestation and desertification. Desertification due to overgrazing is typical in Mediterranean-type landscapes (Arianoutsou-Faraggitaki, 1984).

The methodology presented in this Chapter is suggested for areas that are not characterized by extended livestock activities. For its application in such areas, the methodology needs to be readjusted, considering extended post-fire recovery periods (due to the aforementioned delay in hydrological recovery caused by overgrazing) and also increased changes in the post-fire values of the examined hydrological parameters, *i.e.* prolonged  $t_{upper}$  and  $t_{lower}$  and increased  $h_{CN,FS}(t)$ ,  $h_{IA,FS}(t)$ ,  $h_{TP,FS}(t)$ ,  $h_{CP,FS}(t)$  and  $h_{K,FS}(t)$ .

### **5.5.4 Successively burnt forest land**

As discussed in detail in Chapter 3, plant species that are dominant in fire-prone ecosystems, as the Mediterranean, evolve adaptation mechanisms for post-fire regeneration when successively affected by fires (Thanos and Marcou, 1991; Kruger, 1983; Trabaud, 1987; Carey *et al.*, 2003; Calvo *et al.*, 2003). The future forest composition is thus affected by both alterations in recovery dynamics and the consecutive development of new reproduction strategies (Marzano *et al.*, 2012; Buscardo *et al.*, 2011). Sometimes, vegetation succession can be observed in areas affected by high severity forest fires, which are then colonized by different and often more fire-tolerant vegetation species (*e.g.* Polychronaki *et al.*, 2013).

The proposed methodology concerns areas that are successively burnt in the recent past and their vegetation species have developed adaptation mechanisms, becoming thus more fire-tolerant.

However, when the burnt area has not been affected by successive forest fires in the recent past and is covered by dense forested land, potential modifications in the proposed methodology could be required. More specifically, in the absence of development of adaptation mechanisms from the affected species after successive and frequent burnings, a more intense and a longer-lasting fire impact is expected during the first post-fire period. Therefore, a delay in vegetation regrowth, which is associated with more intense flood events and a delay in hydrological recovery is to be expected. In this case, as also discussed in Sections 5.5.1 and 5.5.3, prolonged  $t_{upper}$  and  $t_{lower}$  and increased  $h_{CN,FS}(t)$ ,  $h_{IA,FS}(t)$ ,  $h_{TP,FS}(t)$ ,  $h_{CP,FS}(t)$  and  $h_{K,FS}(t)$  need to be foreseen in the proposed methodology.

## CHAPTER 6: STUDY AREA

The methodology for the quantification of fire impact and its integration in flood modelling, described in Chapter 5, has been tested on a typical Mediterranean periurban area in Greece. More specifically, the study area of this methodology is Rafina catchment, an area that extends over approx. 123 km<sup>2</sup>, located in Eastern Attica region. The exact location of the area is presented in Figures 6.1a, b and c. Additional information on the geomorphologic characteristics, the hydrometeorological regime and prevailing land uses in the study area is provided in the following.



Figure 6.1. Zooming in the study area: in the red square in Figures 6.1a (upper left) and 6.1b (upper right) and highlighted in blue font in Figure 6.1c (lower middle).

## 6.1 Geomorphological and hydrogeological properties

The study area extends geographically east of Hymettus Mountain and south of Penteli Mountain to the coastline of Evoikos Gulf. Geologically, Rafina catchment belongs to the Attico-Cycladic Massif. The dominant geological structure of the south part of the study area is Neogene and Quaternary clastic deposits, which fill up the degradations and tectonic grabens of the area and consist of marly limestones, marls, clays, sandstones, conglomerates and other coarse, unconsolidated sediments (Jacobshagen, 1986; Katsikatsos, 1992). Lignite layers in the northern and eastern parts of the Spata have been verified by borehole owners who proceeded to deep drillings in the area (Stamatis *et al.*, 2006). According to Marinou (1955), the thickness of the lignite-bearing layers west of Rafina is approx. 6 m. A fault system controls tectonically the area. In this system east-northeast and west-northwest directions are dominant, followed by smaller displacement faults with northwest-southwest directions. As a result of the northwest-southeast faulting, the Mesogea tectonic graben has been formed. The southwest part of the study area is tectonically controlled by the Hymettus mountain marble massif (Stamatis *et al.*, 2006). Rafina marbles are also dominant at the south part of Rafina city. A simplified geological map of the south eastern part of the study area is presented in Figure 6.2.

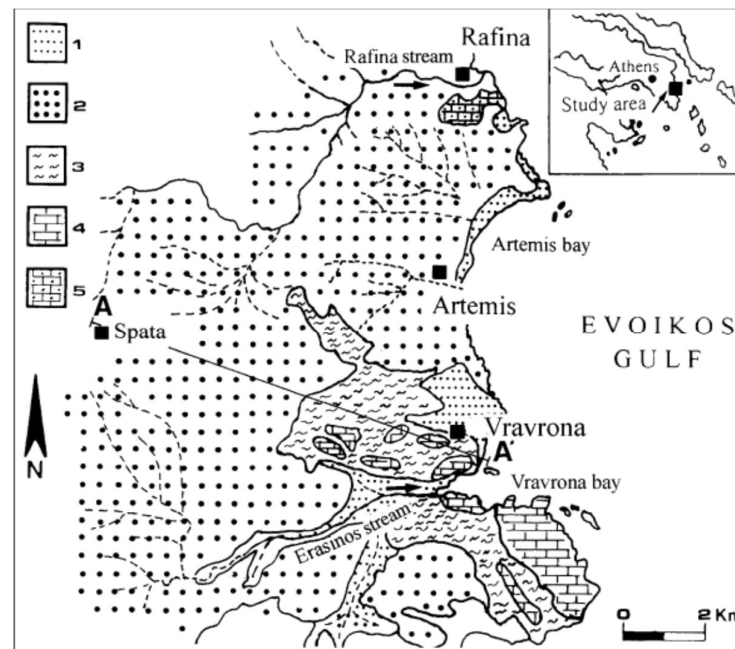


Figure 6.2. The geological structures of the south eastern part of the study area: (1) Holocene deposits, (2) Neogene formations, carbonates, marls, conglomerates, sands, etc., (3) schists and phyllites, (4) carbonates of Upper Cretaceous, (5) Rafina marbles, Mesozoic; A–A', hydrogeological section (Source: Stamatis *et al.*, 2006).

The geological formations that are dominant in the study area are characterized by different hydrogeological properties. According to Stamatis *et al.* (2006), independent or semi-independent hydrogeological units in the area have been



created due to the particular geological and geomorphological conditions, the lithostratigraphical diversity and the complicated tectonics described above. A schematic hydrogeological section in the area between Spata and Vravra, showing the development and the structure of a phreatic aquifer within the hard rocks of the metamorphic basement and the unconsolidated Neogene formations is presented in Figure 6.3. Schists and phyllites, which have similar hydrogeological properties with hard rocks, have been developed among them. These rocks are particularly impermeable, as their fracture system is blocked by the fine-grained material, gradually produced by their weathering. This limited permeability of formations, especially at the south part of the study area, is directly associated with increased surface runoff (Stamatis *et al.*, 2006). Schists that are dominant in the north part of the study area (Soulis *et al.*, 2007) show high permeability due to their intense karstification and fracture porosity (Stamatis *et al.*, 2006).

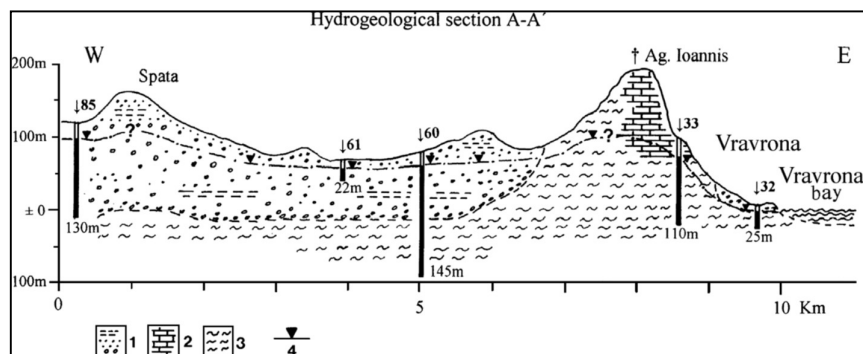


Figure 6.3. Hydrogeological section between Spata and Vravra (see cross section A-A' in Figure 6.2) (1: Neogene deposits, 2: Carbonates, 3: Schists and phyllites, 4: Level of ground water) (Source: Stamatis *et al.*, 2006).

The mean altitude of the area is approx. 225 m, with the maximum value being 920 m and the minimum 0 m. Ground slopes range from 0% to 37.8%, with its mean value estimated to be 7.5% (Papathanasiou *et al.*, 2013e). Steep slopes, *i.e.* slopes that exceed 30%, exist mainly at the upstream areas of the catchment and are clustered at its north part, where slopes range between 0.5% and 127% and mean slope is estimated to be 36% (Soulis *et al.*, 2007). A detailed 5m X 5m DSM (Digital Surface Model) of the area, as produced based on datasets kindly provided by the National Cadastre & Mapping Agency S.A., is presented in Figure 6.4.

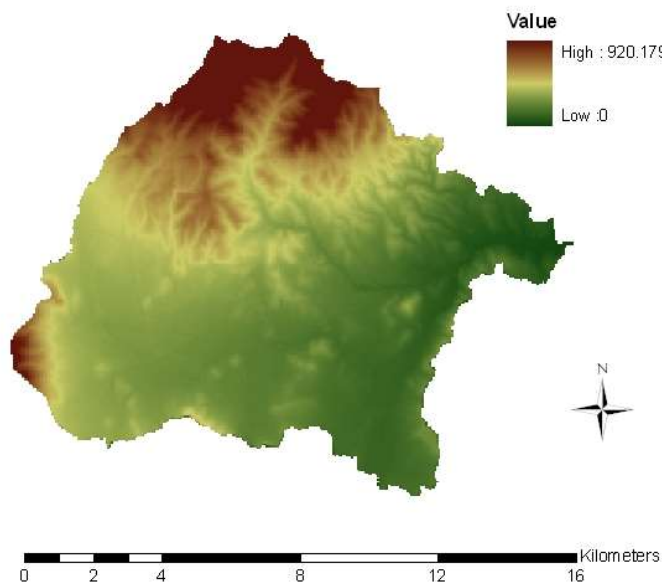


Figure 6.4. The 5m X 5m DSM of the study area.

## 6.2 Hydrometeorological regime and monitoring

### 6.2.1 Hydrometeorological characteristics

In terms of **climate**, the study area has a typical subtropical Mediterranean climate with prolonged hot and dry summers and considerably mild and wet winters (Papathanasiou *et al.*, 2013a). According to Köppen (Köppen, 1901) and as verified in the updated world map of the Köppen-Geiger climate classification by Kottek *et al.* (2006), the greater area is classified to the Csa classification scheme. The area is surrounded by sea at its east, while mountains delineate its southwestern and northwestern borders from the Metropolitan Athens area. The surrounding of the area by high mountains and its vicinity to the sea regulate the existing meteorological conditions over the area.

The typical Mediterranean climate of the greater Attica area, in which the study area belongs, is characterized by high variability of precipitation. According to Soulis *et al.* (2007), the distribution of precipitation follows the characteristics of the dry areas in Greece, with their greatest amount being recorded during the wet period as heavy storms, usually short and intense. Based on datasets available at the website of the Hellenic National Meteorological Service (HNMS, 2015), the mean annual precipitation of the area is approx. 400 mm, with snowfall being rare and most of the intense rainfall events occurring mainly between September and March. The mean monthly temperature is approximately 27 °C during the summer months and 11 °C during the winter, with the mean min monthly temperature being approximately 7.5 °C during the winter and the mean max monthly temperature being approximately 30.5 °C during the summer (HNMS, 2015). Regarding ET, the mean reference ET ranges between 1 mm/d (for January) and 7 mm/d (for July) (Soulis *et al.*, 2009), while Mariolakos and Lekkas (1974) state that for the

period 1950-60 the mean evapotranspiration was 344 mm, reaching 64% of the total precipitation during this period.

In terms of its hydrological regime, the upstream parts of the area have a quite dense river network, where watercourses reach up to the 5<sup>th</sup> class according to Strahler hydrographic network classification (Strahler, 1952). Based on historical hydrometeorological data recorded for the area (mainly from the Hydrological Observatory of Athens, as described below), the response of the catchment to the frequent short and intense storms is direct and base flow along the main watercourse is not negligible in late winter and early spring. Yet, several tributaries to the main watercourse are ephemeral streams, dry for most of the year.

### **6.2.2 Hydrometeorological monitoring**

The hydrometeorological regime of the study area is regularly monitored by a dense network of fully equipped, automatic hydrometeorological stations that cover adequately, in terms of representativeness, the greater area of Athens, an area that extends over approximately 700 km<sup>2</sup>. More specifically, two independent networks operate in the area. The Hydrological Observatory of Athens (HOA, [www.hoa.ntua.gr](http://www.hoa.ntua.gr)), which is operated by the Centre for Hydrology and Informatics (CHI) of the School of Civil Engineers of the National Technical University of Athens (NTUA) and an additional meteorological network operated by the National Observatory of Athens (NOA) (NOA, 2012). All stations meet strict monitoring surveying criteria that are set by the World Meteorological Organization (WMO) (World Meteorological Organization, 1983), as well as specific criteria regarding their ground elevation, distance from high and/or bulk buildings, trees, structures *etc.* and security and ease of access issues (Papathanasiou *et al.*, 2013a). Recorded hydrometeorological parameters include *inter alia* water levels, rainfall, temperature, relative humidity, evaporation, air pressure, solar radiation, sunshine duration, wind direction and velocity.

Within the study area and close to its boundaries, HOA operates currently two fully equipped meteorological stations, two stand-alone raingauges and four streamflow gauges, while NOA operates two additional fully equipped meteorological stations. Both networks have long and reliable historic timeseries and record hydrometeorological information in 10 min temporal resolution. The exact locations of HOA and NOA stations used in this research are presented in Figure 6.5.

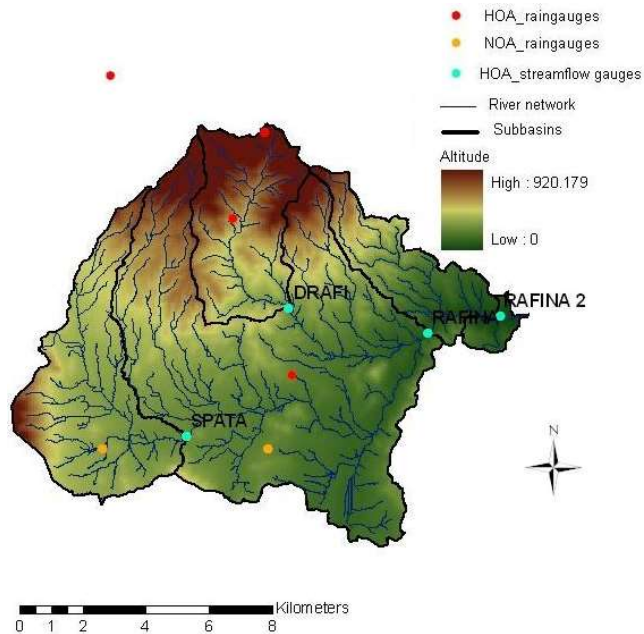


Figure 6.5. The locations of meteorological and flow measurement stations used in this research.

### 6.3 Land cover and land uses

Rafina catchment is a typical periurban area with mixed land cover, characterized by a mosaic of different and to a certain extent conflicting land uses. The **land cover** of the area is represented by a typical wildland urban intermix, in which scattered settlements, built up areas and roads occupy approx. 20% and coexist with typical Mediterranean forests and scrublands in approx. 30% of the area and agricultural areas and grasslands in approx. 50% of the area. The forests and scrublands are located mainly at the upstream parts of the study area, while urban settlements are located downstream. Along the main watercourse of Rafina stream and its major tributaries, there are naturally occurring belts of riparian vegetation.

A hybrid land use-land cover map that has been developed for the study area by the Foundation for Research and Technology Hellas (FORTH) during the implementation of the FLIRE Project (Papathanasiou *et al.*, 2013b) is presented in Figure 6.6. This map has been created after the analysis of Landsat 8 satellite images, ALOS AVNIR & PRISM datasets, and color VHR aerial photos from the National Cadastre & Mapping Agency S.A., Hellenic Mapping & Cadastral Organization (HEMCO), combining vector data from the URBAN ATLAS dataset of the European Environment Agency (EEA) for 2010. Additional information on dominant land cover-land use is provided in the following Sections.

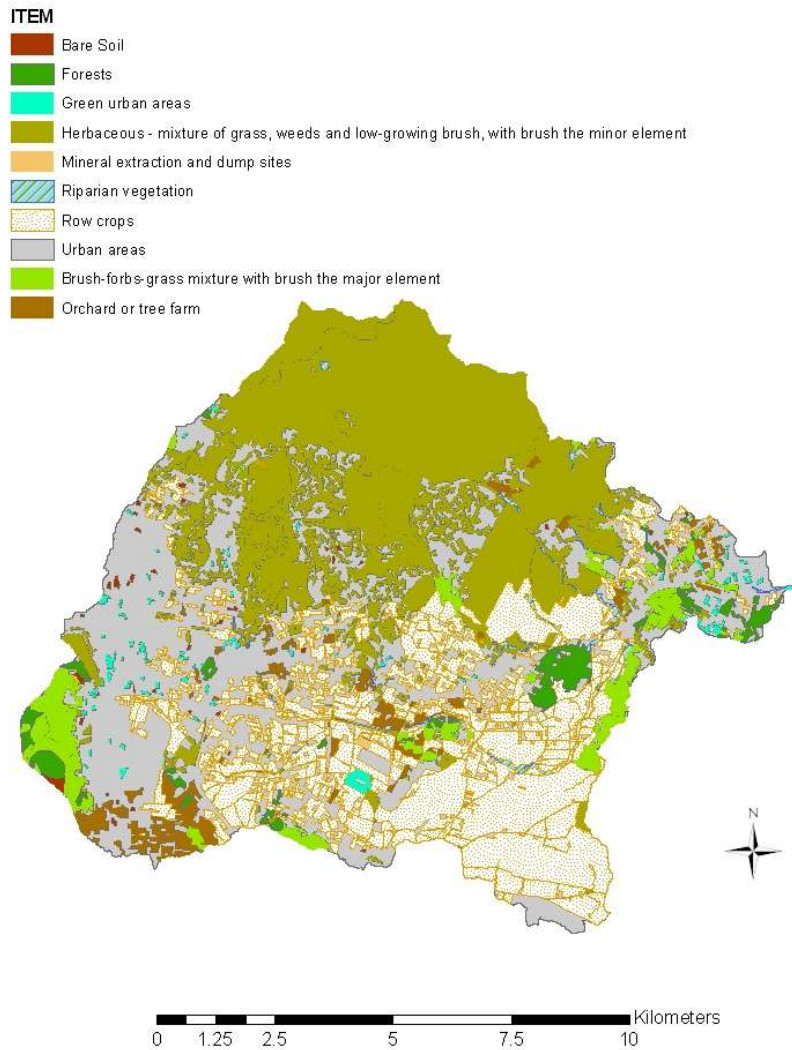


Figure 6.6. A hybrid land use-land cover map of the study area.

### 6.3.1 Forested land

The scrublands are dominated by evergreen-broadleaved low, medium and high sclerophyllous scrubs, while indigenous forest vegetation is mainly represented by evergreen conifers (primarily Aleppo pines). The fuel types in the study area according to the PROMETHEUS fuel classification scheme (Giakoumakis *et al.*, 2002) are presented in Figure 6.7 and explained in Table 6.1.

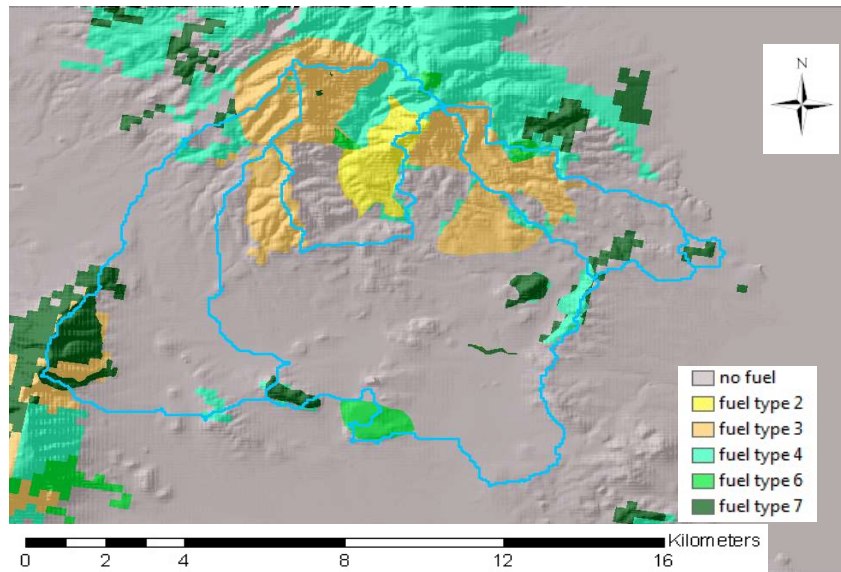


Figure 6.7. Fuel mapping for the study area (Source: Eftychidis and Varela, 2013)

Table 6.1. PROMETHEUS fuel categories in the study area

Prometheus Fuel Types	Fuel description
2	Surface fuels (shrub cover >60%, tree cover <50%)
3	Medium height shrubs (shrub cover >60%, tree cover <50%)
4	Tall shrubs (shrub cover >60%, tree cover <50%)
6	Tree stands with medium surface fuels (shrub cover >30%)
7	Tree stands with heavy surface fuels (shrub cover >30%)

As discussed in Section 6.4, the forested land of the study area has been repeatedly burnt during the last decades. These successive extended wildfires have seriously impaired the forest vegetation, decreased the soil protective capacity and in many regions blocked the regeneration of parts of the affected land and vegetation regrowth. More specifically, successive fires have resulted in the transformation of large areas from conifer stands to scrublands, with few chances for high forest recover. In addition, the risk of desertification in certain formerly forested parts of the study area has increased considerably. On top of these, the burnt land is constantly in a post-fire natural regeneration process and as a result a continuous forest fuel bed keeps being formed after the fires. This fuel bed favors fast propagation of subsequent fires contributing to even profounder degradation of the forest vegetation.

### 6.3.2 Urban areas and demographic data

Rafina catchment includes several municipalities and settlements of Eastern Attica. According to the recent *Kallikratis scheme* (Greek Law 3852/2010), the

study area includes: the Municipality of Rafina – Pikermi, parts of the Municipalities of Penteli, Pallini, Peania and Spata – Artemida, as well as a very limited part of the Municipality of Marathonas. The boundaries of the study area and the borders of its neighbouring municipalities (as retrieved from [www.geodata.gov.gr](http://www.geodata.gov.gr)), are presented in Figure 6.8.

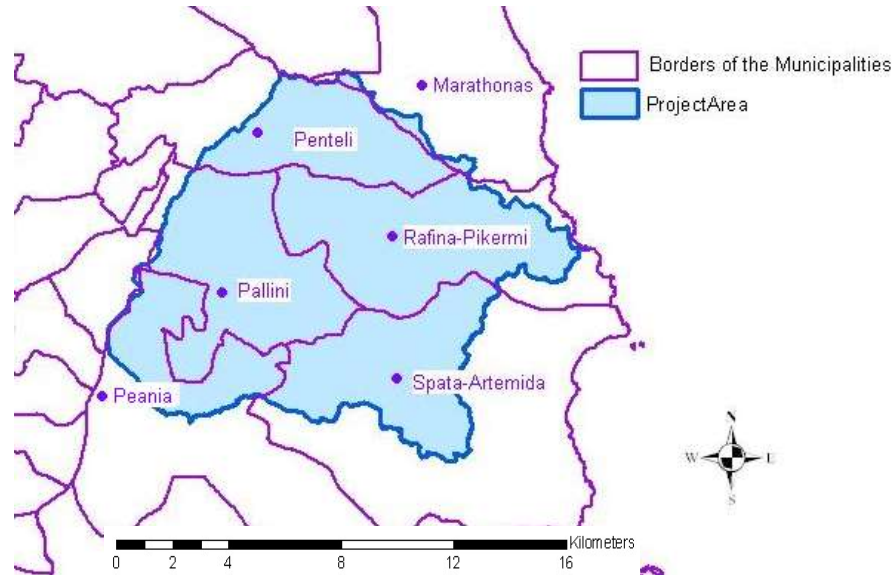


Figure 6.8. The Municipalities included in the study area.

The urbanization rate of the area has increased significantly, especially during the last 30 years. According to the latest population censuses for the area, as available from the Hellenic Statistical Authority, population increase in Pikermi community was estimated up to 419.36% from 1971 to 2007, while for Drafi and Rafina communities population increase for the period between 1971 and 2001 was estimated up to 79.27% and 8.30% respectively.

One of the main factors that have contributed to the constantly increasing urbanization rate of the study area is the construction of large-scale public works in this area, which increase in turn private building activity in the neighbouring settlements and Municipalities (Papathanasiou *et al*, 2009). The most important, recent public works in the area are the new Athens International Airport (AIA) Eleftherios Venizelos in Spata (Figure 6.9a), the Attiki Odos motorway (Figure 6.9b), which connects the southeast Attica area with the rest of the Prefecture and the business centre of Athens and the developing Rafina port (Figure 6.9c), which is considered as one of the 12 major ports of national importance, taking complementary, yet essential role next to the port of Piraeus (Papathanasiou *et al.*, 2013d).



Figure 6.9. The three large-scale public works in the study area: The AIA (Source: [www.ana-mpa.gr](http://www.ana-mpa.gr)) in Figure 6.9a, at the upper left, Rafina port (Source: [www.irafina.gr](http://www.irafina.gr)) in Figure 6.9b, at the upper right and the airport junction of Attiki Odos motorway (Source: <http://en.aodos.gr/>) in Figure 6.9c, at the lower middle.

Particularly for the Attiki Odos motorway, it is mentioned that during its construction and targeting the safe circulation of the vehicles, it was sometimes inevitable to intervene with the environment. A frequent construction work was the deviation of rivers that crossed the motorway. One such intervention has been the deviation of a stream from the basin of Vrilissia (a neighbouring basin to the study area) to the Spata subbasin of Rafina catchment, affecting thus the hydrology of the study area. This additional subcatchment that contributes to the main watercourse of Rafina stream has been considered during the hydrological modelling of the study, as discussed in Section 7.3.1.

### 6.3.3 Industrial units

**Industrial activity** is limited in the study area; yet, several industrial units are clustered in the southwest regions of the area, close to Spata, and a couple of industries are located at the outskirts of Rafina city. The locations of industrial units in Rafina catchment, as isolated from the list of industrial units in the Attica river basin (included in the RBMP of Attica – Phase A, 2012), are presented in Figure 6.10.



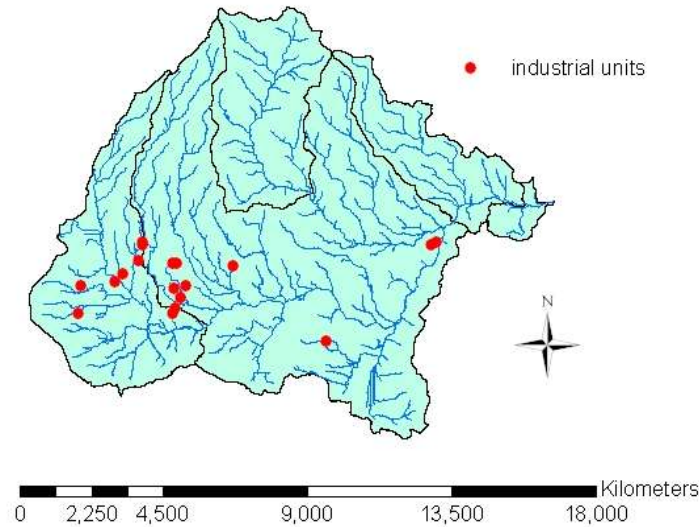


Figure 6.10. Locations of industrial units in the study area.

## 6.4 Vulnerability to floods and forest fires

Several factors have contributed to the selection of this particular area as an appropriate study area for this research. One of these reasons is the fact that, as analysed in Section 6.2.2, this area is covered by a dense monitoring network of fully equipped, state-of-the-art hydrometeorological stations. Such measurements are critical to support the development of a methodology for the quantification of fire impact on hydrology. Further to that, due to the reasons presented in the following, this area is particularly prone to both flash floods and forest fires and therefore research on post-fire hydrological modelling becomes an issue of high priority.

More specifically, the study area is prone to floods due to its particular hydrological and geomorphological conditions. The geological structure *per se* of the basin, as described in Section 6.1, allows for deep losses of surface water at the downstream areas to be ignored. The mixture of downstream impermeable soils, steep upstream slopes and flat downstream areas and dense upstream hydrographic network contributes to quick drainage of the catchment and thus the increased vulnerability of the downstream areas, which are the most densely populated ones, to flash floods, especially during storms and heavy rainfall events.

Further to this, the unprecedented urban development of the area, as described in Section 6.3.2, was not followed by the necessary readjustment, *i.e.* redesign and when necessary expansion of existing hydraulic infrastructure so that flooding water would be safely released to the catchment outlet, which is the sea. On the contrary, existing hydraulic works already inadequate to release floods (Papathanasiou *et al.*, 2009) had to bear the burden of conveying excessive flows. As a result of this urbanization pressure over the study area, the downstream, mostly flat, areas of Rafina catchment become particularly vulnerable to flooding.

A recent flood event that affected the study area occurred on the 22<sup>nd</sup> of February 2013. Based on recorded datasets from HOA hydrometeorological network (Papathanasiou *et al.*, 2013a), the duration of the rainfall event was approx. 9 hours, while the most intense rainfall was recorded at the upstream of the study area and more specifically at Penteli station, where total rainfall reached 95.6 mm. During this event, significant damages were recorded at Spata region and Rafina region. In Spata, the large volume of water destroyed the protective barriers of a bridge in the main avenue of the area, landslides occurred, a big tree broke and traffic was interrupted. A flow gauge of HOA installed on the bridge was completely destroyed. In Rafina, the volume of water was too big to be safely conveyed to the sea, *i.e.* the outlet of the catchment. Water level exceeded 3 m at the area approx. 350 m upstream the outlet and adjacent houses and structures suffered from extended damages (Papathanasiou *et al.*, 2013d). The severity of the event is illustrated in the following pictures, taken from inhabitants of the area.



*Figure 6.11. Pictures depicting the floodplain and the damages caused in private properties in the area of Rafina during the flood event of 22/02/2013 (personal archive).*

At the same time, the particular vegetative land cover of the study area, in which evergreen-broadleaved sclerophyllous scrubs and evergreen conifers are dominant, is highly flammable and prone to forest fires, especially during the

summer and the dry season. As also discussed in Section 6.3.1, the forested land of the Rafina catchment that has suffered extended and successive fires in the last decades is constantly in a post-fire natural regeneration process. Therefore, a particularly flammable forest fuel bed that is formed after the fires, when regeneration starts, contributes to increased vulnerability of the already affected forested land to new forest fires. As a result, large scale forest fires are quite frequent in the greater geographic region.

The intense population growth during the last decades, as described above, was also followed by no or very limited improvement of the fire-fighting infrastructure. On top of this, extended forested land in the area is owned by Land Development Cooperatives, which press for land use change and conversion of forests to urban zones, especially since the value of this land has increased. The flammable vegetation, combined with inadequate fire prevention culture, urbanization pressure and increase of value of the forested land of Eastern Attica has led to disastrous conflagrations in the area in recent years.

During the period 1991-2004, the percentage of burnt land in Eastern Attica reached the highest percentage of land affected by forest fires on a national basis<sup>32</sup>. According to data provided by the Union of Local Authorities of Attica Region (*geodata.gov.gr/*) 114 fires were recorded in the Municipalities surrounding the study area between 1999 and 2009, most of which affected the Municipality of Nea Makri-Marathon. This area is the most critical for fires entering the study area, since the prevailing north-west winds in the region can easily lead the flames towards South and West, in Rafina catchment and in this case even a small fire can affect a great percentage of the area.

The forest fires that affected the greater area of Rafina catchment during the period 2000-2012 based on the European Forest Fire Information System (EFFIS) database (<http://forest.jrc.ec.europa.eu/effis/>), are presented in Figure 6.12.

---

<sup>32</sup>Personal communication with Dr. Xanthopoulos Gavriil (Institute of Mediterranean Forest Ecosystems and Forest Products Technology, Laboratory of Forest Ecosystems and Fire Protection).

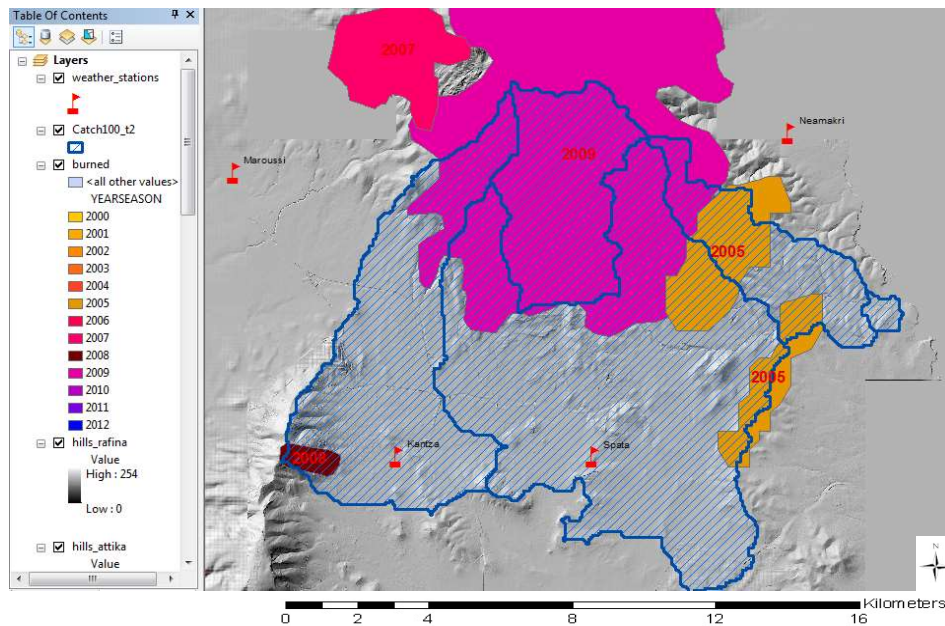


Figure 6.12. Forest fires in the greater area of Rafina catchment for the period 2000-2012 (Source: Eftychidis and Varela, 2013).

The most recent devastating forest fires that occurred within the boundaries of the study area are the fires of the years 2005 (two parallel forest fires on July 28<sup>th</sup>) and 2009 (on August 21<sup>st</sup>). The total burnt area after the fires of 2005 reached approximately 10 km<sup>2</sup> (1,000 hectares), as shown in Figure 6.12 extended mainly in the study area and during the event more than 160 homes and other structures suffered damages or were completely destroyed. The fire of 2009 burnt approx. 210 km<sup>2</sup> (21,000 hectares) of pine forest, olive groves, shrub land and farmland, affected 15 municipalities and communities and destroyed 60 homes, damaging another 150 (Eftychidis and Varela, 2013).

Focusing on the affected land within the boundaries of the study area, this fire affected approximately 30.9 km<sup>2</sup> (3,090 hectares) of the total 123 km<sup>2</sup> of the catchment (*i.e.* approximately 25% of the catchment), burning the majority of the forested land. According to estimations of the Centre for the Assessment of Natural Hazards and Proactive Planning of the School of Rural and Surveying Engineering of NTUA, as published in 2009 in an on-line article on post-fire floods<sup>33</sup>, 92% of the forested land of Valanaris catchment (the catchment of a main tributary of Rafina stream) has been affected from the recent forest fires. The percentage of burnt land in other subcatchments that contribute to the main watercourse of Rafina stream (Megalo Rema) was also high, with the subcatchments of Palios Mylos being affected by 30%, Ntaou Pentelis by 37%, Aghia Paraskevi by 60%, Rema Pallinis (together with Rema Viglas and Rema Marizas) by 43% and Rema Anthousas by 38%.

Furthermore, the climatic conditions during the last years in terms of water potential for the most common forest species in Eastern Attica are getting worse (Xanthopoulos and Caballero, 2007). The water stress of forest vegetation

<sup>33</sup> <http://tvxs.gr/news/ελλάδα/δαμόκλειος-σπάθη-για-την-αττική-οι-πλημμύρες-μετά-τις-πυρκαγιές>

species that are tracked in the study area as estimated for the years 2003-2007 is presented in Table 6.2. These conditions are expected to become even worse according to climate change scenarios. In addition, as mentioned in Chapter 1, climate change scenarios are characterized by extended dry and hot periods and intense storms and therefore are associated with even greater fire and flood risk.

*Table 6.2. Water stress of vegetation species dominant in the forested areas of Rafina catchment (Source: Xanthopoulos and Caballero, 2007).*

Water potential [bar]					
Vegetation species	August 5 <sup>th</sup> , 2003	August 4 <sup>th</sup> , 2004	August 7 <sup>th</sup> , 2005	August 23 <sup>rd</sup> , 2006	August 9 <sup>th</sup> , 2007
<i>Pinus halepensis</i>	-7.3	-6.5	-9.0	-23.7	-21.0
<i>Quercus coccifera</i>	-19.0	-20.0	-14.5	-28.5	-34.5
<i>Cistus creticus</i>	-20.5	-43.6	-26.0	-61.0	-45.0

The spatial arrangement of different land cover mentioned in Section 6.3, *i.e.* the fact that forested land and scrublands are located in the upstream areas, while the downstream areas host the urban zones, renders the downstream, urbanized areas particularly **prone to floods**, especially **after forest fires**, and highlights the importance of managing both floods and fires in a combined and integrated way.

As a result of the extended and successive forest fires that have affected the greater area of Rafina catchment and taking into consideration its particular geomorphology, as described in Section 6.1, the study area is susceptible to landslides and is covered by erodible soils (Marinos *et al.*, 1995). In the aftermath of forest fires and especially during the first post-fire floods, the soil erosion and sedimentation is particularly intense, resulting in changes in the geometry of river cross sections. The deposited sediment minimizes the effective capacity of the sections to carry and convey flood water, which overflows river sections and results in the flooding of the surrounding area.

## 6.5 First post-fire floods in the study area

As discussed in Chapter 5, some deviations from the proposed methodology could be observed under particular conditions during the first post-fire floods, which would necessitate the readjustment of the methodology. These conditions include particularly erosive rainfall, erodible soil and susceptibility to landslides, extended livestock activities and successively burnt forest land.

Based on a detailed study for the estimation of rainfall erosivity across Europe (Panagos *et al.*, 2015), Rafina catchment (red square in Figure 6.13) is not characterized by particularly high rainfall erosivity. On top of this, the almost 2-year period of low rainfall rates after the fire of summer of 2009 in Rafina

catchment, as verified by the event cloud of HOA in Figure 6.14<sup>34</sup>, seems to have contributed to the increased post-fire recovery of the burnt area. Consequently, the methodology needs no readjustment so as to consider intense rainfall erosivity during the first post-fire floods and can be applied in Rafina catchment as suggested.

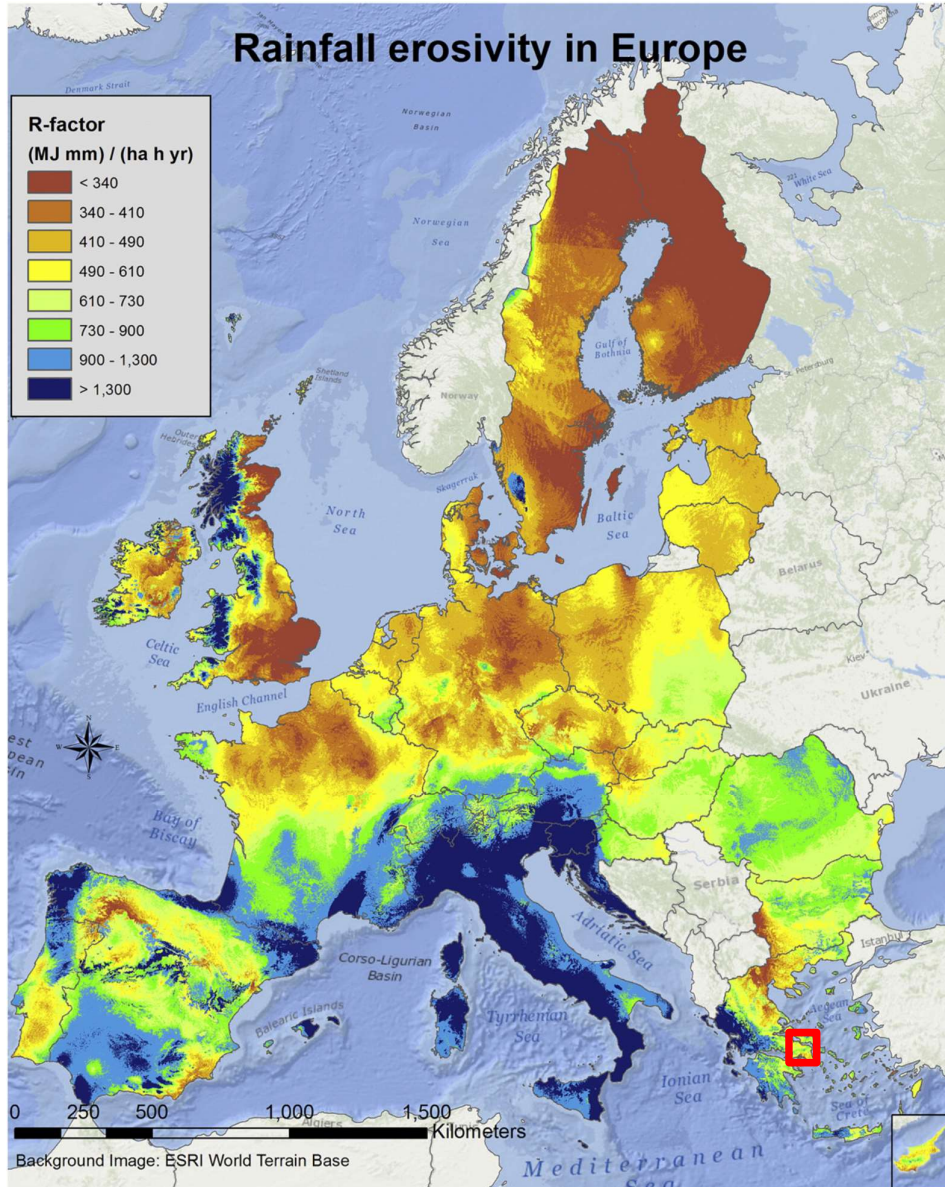


Figure 6.13. Rainfall erosivity map of Europe (adapted from: Panagos et al., 2015).

<sup>34</sup> Rainfall events observed by HOA since March 2005 are presented in this Figure, where the size of the font in the event cloud is proportional to the magnitude of the rainfall event.

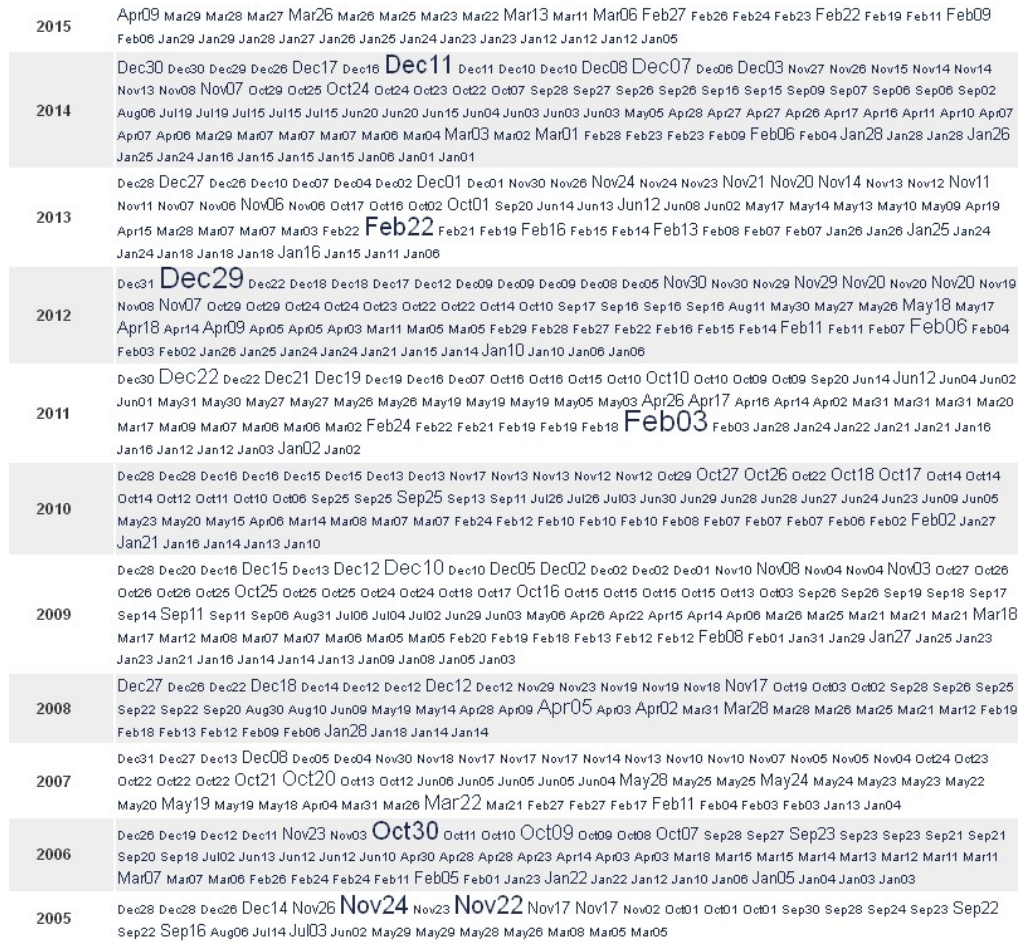


Figure 6.14. The event cloud of HOA, where the size of the font is proportional to the magnitude of the event (Source: [www.hoa.ntua.gr](http://www.hoa.ntua.gr)).

Given that the methodology presented in Chapter 5 has been developed for erodible soils, susceptible to landslides, both of which are particular geomorphological features of the study area as discussed in Section 6.4, no modifications in the methodology are suggested for application in the study area. It is also noted that no livestock activities are undertaken in recent years in this typical Mediterranean area. Additionally, as discussed in Sections 6.3 and 6.4, the study area has suffered from successive forest fires, which have affected significantly its vegetation, during the recent years. To sum up, the proposed methodology needs no readjustment and modifications for application in Rafina catchment.

## CHAPTER 7: ADJUSTING THE METHODOLOGY TO THE STUDY AREA

### 7.1 Estimating fire impact

In this research, a historic fire event that affected severely the study area in 2009 has been studied and fire severity maps for the study area have been produced based on satellite images. The necessary procedure is graphically represented in Figure 7.1 and discussed in detail below.

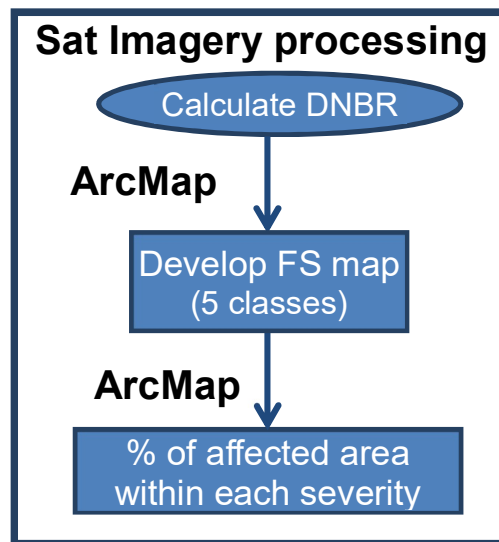


*Figure 7.1. The procedure to estimate fire impact according to the suggested methodology.*

As described in Section 5.1.1 radiometrically and geometrically corrected satellite imagery can be used for the development of a fire severity map for the area. In particular, two Landsat TM thematic mapper images of the greater region of the study area, which referred to the period prior to and shortly after the fire event of August 2009 were properly processed and used for the calculation of the two NBR indices,  $NBR_{PRE-FIRE}$  and  $NBR_{POST-FIRE}$  for the pre- and post-fire images respectively. The results of this analysis are presented in Figures 7.2a and 7.2b.



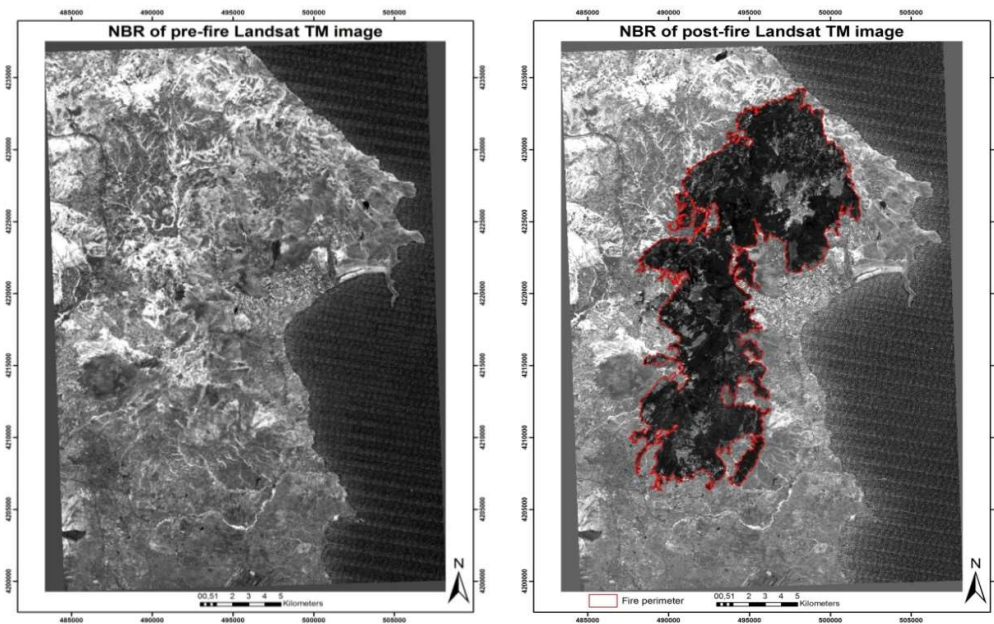


Figure 7.2. Landsat TM images of  $NBR_{PRE-FIRE}$  (Figure 7.2a on the left) and  $NBR_{POST-FIRE}$  (Figure 7.2b on the left) (Source: Mitsopoulos, 2013).

From the subtraction of the two NBR maps, the DNBR was estimated and its values were classified into six distinct classes, which correspond to six fire severity classes. These classes are low, moderate, high and very high severity, unburnt areas and areas with enhanced vegetation regrowth. The DNBR map and the fire severity classes within the boundaries of the greater area affected by this fire event are presented in Figure 7.3.

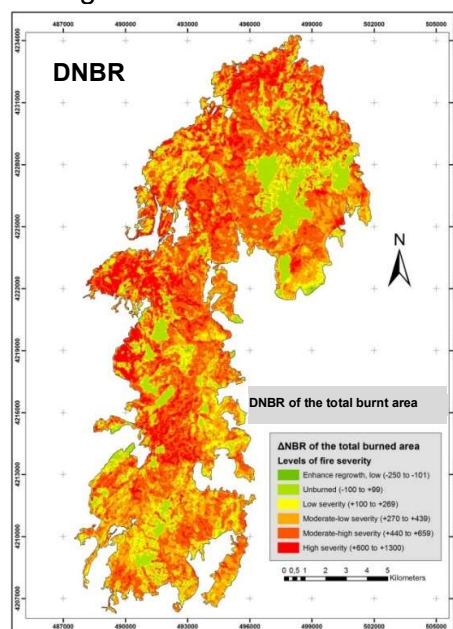
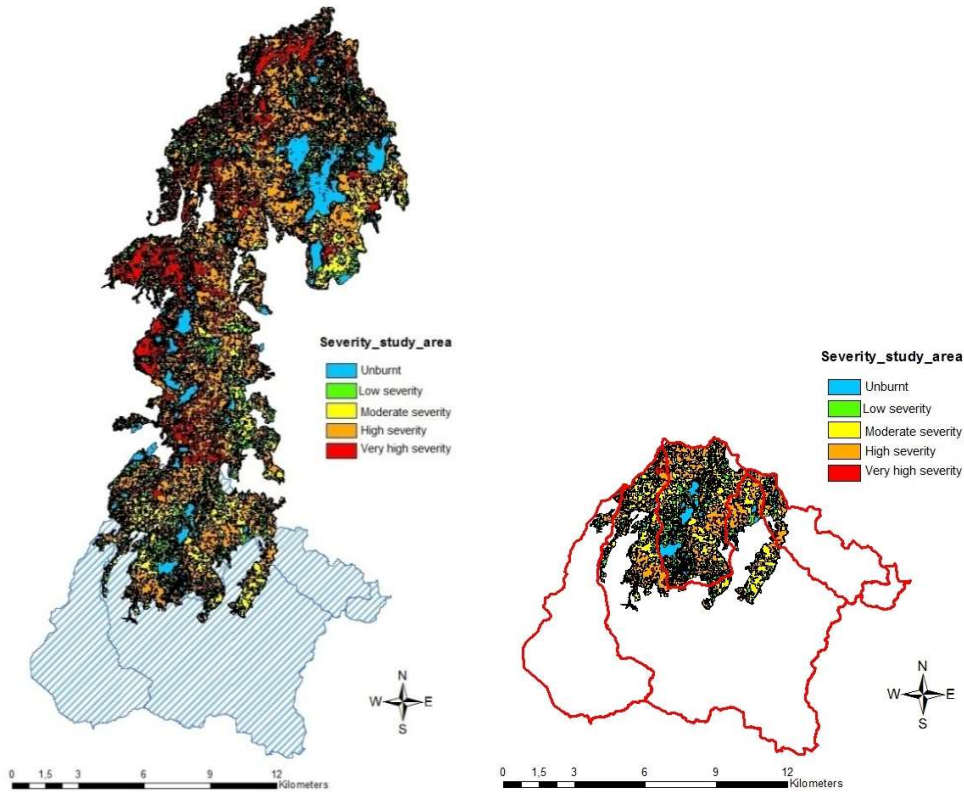


Figure 7.3. The DNBR map and the fire severity classes of the greater area affected by the fire event of August 2009.

An analysis in GIS environment is then performed, as described in Section 5.2.1, in order to clip the affected area within the boundaries of the study area out of the total area affected by fire. The total area affected and the study area are presented in Figure 7.4a, while the clipped area and the subbasins of the study area (the creation of which is discussed in Section 7.3.1) are presented in Figure 7.4b. Areas with enhanced regrowth were particularly limited in the affected area and absent within the boundaries of the study area and thus the fire severity classes were restricted to five, namely low, moderate, high and very high fire severity and unburnt land.



*Figure 7.4. The different fire severity classes from the fire event of 2009 at the total affected area (Figure 7.4a on the left) and in the study area (Figure 7.4b on the right).*

Additional analysis of the clipped fire severity map of the study area in GIS environment resulted in the calculation of the spatial extent of each fire severity class within each subbasin. The spatial extent retrieved from this analysis, expressed both in spatial units [km<sup>2</sup>] and as a percentage of the total area of each subbasin, is presented in Tables 7.1-7.3.

*Table 7.1 The total area [km<sup>2</sup>], total burnt area [km<sup>2</sup>] and % of burnt area of each subbasin of the study area.*

	Total area [km <sup>2</sup> ]	Burnt area [km <sup>2</sup> ]	% of burnt area
Drafi (W15460)	17.54	14.746	84.07
Rafina big (W15020)	68.45	13.49	19.71
Rafina small (W16340)	11.44	2.098	18.34
Spata (W17990)	23.68	0.57	2.41
Urban (W16890)	1.91	0	0.00
<b>Total</b>	<b>123.02</b>	<b>30.904</b>	<b>25.12</b>

*Table 7.2 The area [km<sup>2</sup>] of each subbasin of the study area affected by different severity.*

	Very high FS [km <sup>2</sup> ]	High FS [km <sup>2</sup> ]	Moderate FS [km <sup>2</sup> ]	Low FS [km <sup>2</sup> ]	Enhanced regrowth [km <sup>2</sup> ]
Drafi (W15460)	0.346	4.88	6.36	3.16	0.001
Rafina big (W15020)	0.42	4.51	6.19	2.37	0
Rafina small (W16340)	0.038	0.9	0.75	0.41	0
Spata (W17990)	0.02	0.16	0.21	0.18	0
Urban (W16890)	0	0	0	0	0
<b>Total</b>	<b>0.824</b>	<b>10.45</b>	<b>13.51</b>	<b>6.12</b>	<b>0.001</b>

*Table 7.3 The area [%] of each subbasin of the study area affected by different severity.*

	Very high FS [%]	High FS [%]	Moderate FS [%]	Low FS [%]	Enhanced regrowth [%]
Drafi (W15460)	1.97	27.82	36.26	18.02	0.01
Rafina big (W15020)	0.61	6.59	9.04	3.46	0.00
Rafina small (W16340)	0.33	7.87	6.56	3.58	0.00
Spata (W17990)	0.08	0.68	0.89	0.76	0.00
Urban (W16890)	0.00	0.00	0.00	0.00	0.00
<b>Total</b>	<b>0.67</b>	<b>8.49</b>	<b>10.98</b>	<b>4.97</b>	<b>0.00</b>

## 7.2 Estimating initial soil moisture conditions for selected rainfall events

As discussed in Section 6.2.1, the study area is located in Eastern Attica and has a typical Mediterranean climate. Therefore, the period between September and February can be considered as the “dormant season” and the period between March and August can be considered as the “growing season”. Three distinctive rainfall events have been selected for further analysis.

All of the examined events occurred after the fire event of August 2009. They were properly selected so that each one corresponds to different SM conditions and distant post-fire periods. The type of AMC for each one of the simulated events,

as estimated based on total rainfall of the 5 days preceding each event as recorded at Agios Nikolaos station and using the marginal values for the distinction of classes presented in Table 5.1, is presented in the following Table.

*Table 7.4. AMC for each one of the examined flood events.*

Flood event	Total rainfall depth of previous 5 days [mm]	AMC
10-11/12/2009	19	II (normal)
03/02/2011	0.6	I (dry)
22/02/2013	62	III (wet)

More specifically, the first examined event (10-11/12/2009) occurred approx. 5 months after the fire event of 2009 and corresponds to normal SM conditions, the second event (03-04/02/2011) occurred 17 months after the fire event of 2009 and corresponds to dry SM conditions and the third event (22/02/2013) occurred 42 months after the fire event of 2009 and corresponds to wet SM conditions.

### **7.3 Setting up the hydrological model for the study area**

The software that has been used for the hydrologic simulation is the deterministic, physically-based HEC-HMS hydrological model and especially the version HEC-HMS 3.5 (Scharffenberg and Fleming, 2010), in semi-distributed and event-based mode. Details on the general features of HEC-HMS are discussed in Section 4.2.1.1. The processing of geospatial information that is necessary for hydrological simulations was performed using the GIS extension HEC-GeoHMS and especially the versions HEC-GeoHMS 5.0 and ArcGIS 9.3 (Fleming and Doan, 2010). The setting up of both HEC-GeoHMS and HEC-HMS is presented in the following.

#### **7.3.1 Setting up HEC-GeoHMS**

In general, HEC-GeoHMS serves in visualizing spatial information, editing watershed features, performing spatial analysis, delineating subbasins and streams, developing inputs for hydrologic models and extracting necessary hydrological information for the catchment (Fleming and Doan, 2010). In this research, the version 5.0 of HEC-GeoHMS was used for the creation of background map files and the basin model file that are then imported in HEC-HMS. The basin model files include geospatial and hydromorphological information on the subbasins selected to discretize the catchment and the physical characteristics of the corresponding streams.

The initial input for this analysis is the 5m X 5m DSM of the area described in Section 6.1. The coordination system adopted was EGSA87. In order to create the basin model file, 6 independent modules, *i.e. Terrain Preprocessing, HMS Project Setup, Basin Processing, Basin Characteristics, Hydrologic Parameters and HMS*, were run in a step-by-step way in ArcGIS.

The final stream and subbasin delineation was performed through the *Terrain Preprocessing* module. Particularly for the stream definition, a threshold of 5000 cells was set. The downstream outlet of the catchment, which is the sea in this study area, and the area upstream the outlet is defined through the *HMS Project Setup* module. Then, the *Basin Processing* module is used to revise the catchment delineations. In this research, each subbasin is defined so that its outlet corresponds to a location where a HOA stream flowgauge is installed (Papathanasiou *et al.*, 2013a), while the outlet of the most downstream subbasin corresponds to the catchment outlet, *i.e.* the location where the river drains to the sea. When necessary, multiple subbasins were merged into one. Through this procedure, the catchment is divided into 5 subbasins (four upstream the stream flowgauges and one upstream the outlet to the sea).

Topographic characteristics of streams and subbasins which are used in the estimation of hydrological parameters and include *inter alia* river length and slope, basin slope and centroid and longest flow path, are estimated through the *Basin Characteristics* module. Hydrological parameters are defined exclusively in HEC-HMS, so the attribution of river and subbasin names was the sole procedure performed through the *Hydrologic Parameters* module, in sequence from upstream to downstream. The final output of HEC-GeoHMS and core input to HEC-HMS, which is an HMS basin schematic, which depicts the connectivity of the catchment elements, is created through the *HMS* module. The export file includes a *Background Shape File* that carries geographic information and a *Basin Model File*, which contains the hydrologic parameters.

This analysis results in the delineation of the catchment of the study area, which is 123.01 km<sup>2</sup>. It needs to be mentioned that even though the geospatial analysis resulted in the creation of five subbasins, six subbasins were finally used in the current research. More specifically, one additional subbasin, the neighbouring basin of Vrillissia, which is located beyond the boundaries of the catchment, deviates to Rafina catchment and more specifically to the Spata subbasin, due to regulations for the Attiki Odos motorway, as discussed in Section 6.3.2. The hydrographic network of the catchment and its six subbasins mentioned above are presented in Figure 7.5, while Table 7.5 is populated with typical features of each subbasin. The boundaries of the neighbouring subbasin of Vrillissia are indicated schematically with the red line.

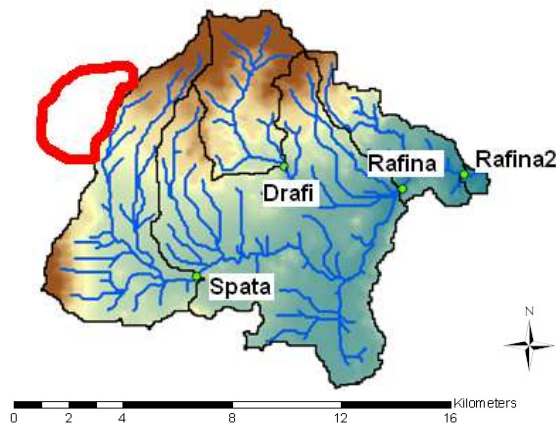


Figure 7.5. The subbasins of the study area and its hydrographic network, as drawn on its DSM.

Table 7.5. Name, ID and area covered by each subbasin of the catchment.

Subbasin name	Subbasin ID	Area [km <sup>2</sup> ]
Drafi	W15460	17.54
Spata	W17990	23.68
Rafina	W15020	68.45
Rafina2	W16340	11.44
Urban	W16890	1.90
Vrilissia subbasin	Sub-1	8.90
<b>Total catchment area (excluding Vrilissia subbasin)</b>		<b>123.01</b>

### 7.3.2 Setting up HEC-HMS

The geographic file with the study area, its subbasins and their properties, which has been created in GIS environment through HEC-GeoHMS, is then imported in HEC-HMS, in order to perform hydrological simulations. For the analysis, a *Basin Model*, a *Meteorological Model*, a *Control Specification Manager* and a *Time-Series Data Manager* need to be defined. The *Basin Model* includes all hydrological parameters that are defined in this research according to the suggested methodology and are presented below.

The *Meteorological Model* prepares meteorological boundary conditions for each subbasin. In this research, the *Gage Weight* method has been selected to define the *Meteorological Model*, with gauge weights calculated in GIS environment using Thiessen polygons. In particular, based on raingauge locations, the catchment is discretized into polygons of variable weight, which corresponds to the impact area of each raingauge. These polygons-areas are the so called Thiessen polygons. The total rainfall in each subbasin per event is the sum of the rainfall recorded by the representative (non-zero weighted) for the subbasin stations, when distributed proportionally to their weight. The impact of stations with weights below a threshold of 0.01 has been ignored. The weight of these stations was considered equal to zero and was summed to the weight of an adjacent station with increased weight and thus representativeness. The Thiessen weights of the six most representative raingauges (four HOA stations and two NOA stations) that are operating in the study area for all subbasins are presented in Table 7.6.

Table 7.6. The Thiessen weights for every raingauge and each subbasin.

	Drafi	Spata	Rafina	Rafina2	Urban	Subbasin-1
<b>Pikermi (HOA)</b>	0.077	-	0.411	0.664	1.000	-
<b>Penteli (HOA)</b>	-	-	-	-	-	1.000
<b>Ag. Nikolaos (HOA)</b>	0.676	0.131	0.208	0.204	-	-
<b>Diavasi Balas (HOA)</b>	0.247	-	0.013	0.132	-	-
<b>Kantza (NOA)</b>	-	0.869	0.079	-	-	-
<b>Spata (NOA)</b>	-	-	0.289	-	-	-
<b>Total</b>	<b>1.000</b>	<b>1.000</b>	<b>1.000</b>	<b>1.000</b>	<b>1.000</b>	<b>1.000</b>

The simulation time-window, which includes the duration of and the time interval required for the simulation, are defined in the *Control Specifications Manager*. Finally, the *Time-Series Data Manager*, which includes precipitation and, when available, discharge recordings is defined. Relevant input is imported for each gauge (raingauge in [mm] and stream flowgauge in [m<sup>3</sup>/sec], respectively) at a 10-min time interval.

The HEC-HMS simplified schematic of the study area is presented in Figure 7.6.

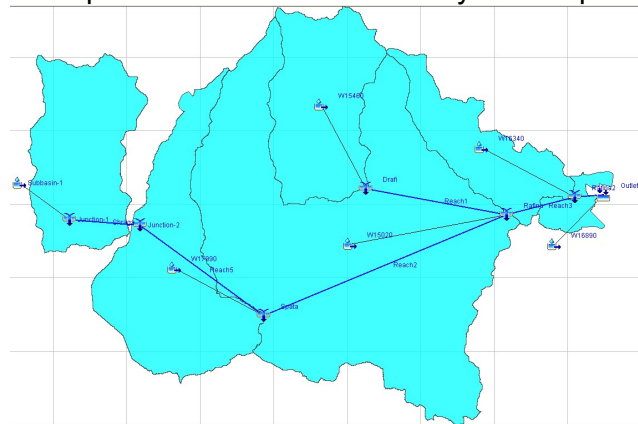


Figure 7.6. The HEC-HMS simplified schematic of the study area.

The model was set up and run for historical (pre-fire) events. For model calibration HEC-HMS was applied for several pre-fire flood events for which “observed” discharges were available at specific locations and in particular at subbasin outlets. For these events simulated discharges were compared against the “observed” discharges in an attempt to estimate as accurate as possible the model parameter values that result in the best fit between simulated and “observed” values. “Observed” discharges correspond to measurements of water levels from flowgauges at subbasin outlets, which were converted to discharges according to an empirical methodology developed for this particular study and presented in brief in the following.

More specifically, in the absence of abundant observed water levels and discharges during historical flood events, stage-discharge rating curves were developed based on historical observations of water levels and flows for all locations where flowgauges are installed. Given that historical datasets were only available for low stages these rating curves were used to transform measured water levels into discharges for low water levels. For high water levels, the Manning's equation (Eq. 7.1) was used to transform water levels into discharges, while for intermediate water levels linear interpolation between the marginal values of rating curves and the Manning equation was performed. The classification of water levels as low, intermediate and high was made properly for each location, using different marginal values. Aiming to an enhanced model calibration, all available *in-situ* flow velocity measurements were gathered, properly processed with observed water levels and converted to flow discharges, providing by that way an additional, reliable source of discharge information for the sites where the measurements were taken. By that way, the flows recorded by flowgauges on a 10-min basis were transformed to discharges and imported in the selected hydrological model (HEC-HMS) as "observed flows" so as to be compared against simulated flows.

$$Q = \frac{1}{n} * A * R_h^{2/3} * S^{1/2} \text{ (Eq. 7.1),}$$

where:

Q: discharge [m<sup>3</sup>/sec],

n: Manning's roughness coefficient [dimensionless],

A: the cross sectional area of flow [m<sup>2</sup>],

R<sub>h</sub>: the hydraulic radius [m],

S: the slope of the linear hydraulic loss [dimensionless].

## 7.4 Estimating parameter values for variable initial conditions

As discussed in Section 7.2, the selected rainfall events correspond to different initial conditions in terms of SM and also refer to different post-fire time periods. Therefore, in order to run the HEC-HMS model for these events, the corresponding values of the five examined hydrological parameters need to be estimated, according to the methodology presented in Chapter 5.

First of all, the values of the five selected hydrological parameters for pre-fire and normal SM conditions were estimated for CN, IA, TP, CP and K according to the procedure described in Sections 5.3.1.1, 5.3.1.2, 5.3.2.1, 5.3.2.2 and 5.3.3.1, respectively. Then the values of these parameters for variable conditions were estimated according to the proposed methodology, as described in the following paragraphs. The procedure is illustrated in Figure 7.7.



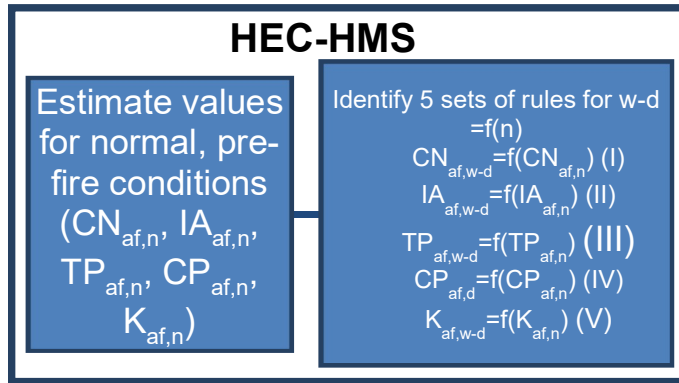


Figure 7.7. The procedure to estimate the values of the examined parameters for variable conditions.

### 7.4.1 Estimating CN for variable initial conditions

Theoretically, CN values range between 0÷100 and in many studies this full range for CN values is used (e.g. Higginson and Jarnecke, 2007). Nonetheless, other relevant studies, which have been validated by experience, have shown that CN values are more likely to range between 40÷98, with few exceptions, while the validity of SCS tables needs to be further investigated beyond the marginal values 30÷98 (Ponce and Hawkins, 1996; USDA-NRCS 1986). Therefore, in the current research, both a lower threshold of CN=35 and an upper threshold of 98 were set.

Assuming fair hydrologic conditions and soil type B as representative of the study area, initial values for CN for pre-fire normal SM conditions were estimated for all the subbasins of the catchment. The hybrid land use - land cover map that was developed for the study area based on satellite images and in-situ verification (Figure 6.6), was used as a reference for cover type and treatment and supported the estimation of these CN values.

The hydrological model was then calibrated for pre-fire conditions and different SM conditions using historical rainfall recordings and available flow measurements. More specifically, extended trial and error testing was carried out for the estimation of CN values for all types of SM conditions, using the difference between simulated discharges and observed discharges, when available, as a metric of simulations' performance. Flood events with normal, wet and dry initial soil moisture conditions were selected, different CN values were applied to subbasins and simulated results were compared against observed discharges. The calibration process resulted in the adoption of the values of c and d (Eq. 5.11) presented in Table 7.7, that associate CN for normal with CN for wet and dry SM conditions for the study area.

For post-fire normal SM conditions CN is estimated from Eq. 5.9a and 5.10a, given that  $t_{upper}$ ,  $t_{lower}$  and the corresponding  $h_{CN,FS}$  for these periods are known. The first post-fire period, *i.e.*  $t_{upper}$  is the time-window 0-7 months. A detailed research was performed by Higginson and Jarnecke (2007) on changes in post-fire CN values during the first post-fire period (*i.e.*  $h_{CN,FS,t_{upper}}$ ), and this research is considered representative for normal SM conditions. In that research, the temporal dimension of post-fire impact was ignored and FS was classified into

three (3) classes (low, moderate and high). Higginson and Jarnecke eventually proposed an increase in post-fire CN by 5, 10 and 15 units in case of low, moderate and high FS, respectively. These changes are also applied in this research. Proportionally, an increase by 20 units is proposed for areas affected by very high FS, *i.e.*  $h_{CN,FS=i,t_{upper}=0+7m} = 20$  for very high FS (a class that had not been considered in the research of Higginson and Jarnecke (2007)). The values of  $h_{CN,FS,t_{upper}}$  for different FS classes are summarized in Table 7.8.

$t_{lower}$ , which is the period just prior to hydrological recovery, does not necessarily refer to the same time-window for all FS classes. It is expected that severely affected areas need more time to recover when compared against areas affected by low FS. Given that CN values for low and moderate FS usually differ slightly between each other, as is the case in this research as well,  $t_{lower}$  for these two FS classes can be safely considered identical. Therefore, based on the selection of the time windows of 7, 12, 19, 24, 36 and 48 months after a fire event as transitional periods in hydrological recovery, as justified in Section 5.1.2,  $t_{lower}$  for FS=i is considered 36-48 months, for FS=ii it is considered 24-36 months and for FS=iii and iv it is considered 19-24 months.

As discussed in Chapter 5, changes in CN follow a logarithmic profile in time and as such they become less significant in time, until eventually hydrological recovery occurs and post-fire CN regains its pre-fire value. For this reason,  $h_{CN,FS,t_{lower}}$  is low, as hydrological recovery will be re-established soon. This is especially true for areas affected by less intense FS. The changes in post-fire CN just prior to hydrological recovery, *i.e.* of  $h_{CN,t_{lower}}$  are also summarized in Table 7.8.

Using these marginal values of  $h_{CN,FS,t_{upper}}$  and  $h_{CN,FS,t_{lower}}$  for given  $t_{upper}$  and  $t_{lower}$ , the values of  $a_{CN,FS}$  and  $b_{CN,FS}$  (Eq. 5.10a) for different FS classes are estimated and summarized in Table 7.9.

Following the Equation 5.9a, post-fire CN for normal conditions becomes:

$$CN_{pf,FS=i}(t) = CN_{af} + (-8.31 * \ln(t) + 36.17) \quad (\text{Eq. 7.2a})$$

$$CN_{pf,FS=ii}(t) = CN_{af} + (-7.33 * \ln(t) + 29.26) \quad (\text{Eq. 7.2b})$$

$$CN_{pf,FS=iii}(t) = CN_{af} + (-6.50 * \ln(t) + 22.63) \quad (\text{Eq. 7.2c})$$

$$CN_{pf,FS=i}(t) = CN_{af} + (-3.25 * \ln(t) + 11.32) \quad (\text{Eq. 7.2d})$$

The aforementioned changes in post-fire CN values are combined with the values of Table 7.7 for CN under different SM conditions and suggested alterations in CN values for post-fire dry conditions are presented in Eq. 7.3a-d, while suggested alterations in CN values for post-fire wet conditions are presented in Eq. 7.3e-h.

$$CN_{pf,dry,FS=i}(t) = [CN_{af} + (-8.31 * \ln(t) + 36.17)] - 7 \quad (\text{Eq. 7.3a})$$

$$CN_{pf,dry,FS=ii}(t) = [CN_{af} + (-7.33 * \ln(t) + 29.26)] - 7 \quad (\text{Eq. 7.3b})$$

$$CN_{pf,dry,FS=iii}(t) = [CN_{af} + (-6.50 * \ln(t) + 22.63)] - 7 \quad (\text{Eq. 7.3c})$$

$$CN_{pf,dry,FS=iv}(t) = [CN_{af} + (-3.25 * \ln(t) + 11.32)] - 7 \quad (\text{Eq. 7.3d})$$

$$CN_{pf,wet,FS=i}(t) = [CN_{af} + (-8.31 * \ln(t) + 36.17)] + 7 \quad (\text{Eq. 7.3e})$$

$$CN_{pf,wet,FS=ii}(t) = [CN_{af} + (-7.33 * \ln(t) + 29.26)] + 7 \quad (\text{Eq. 7.3f})$$

$$CN_{pf,wet,FS=} (t) = [CN_{af} + (-6.50 * \ln(t) + 22.63)] + 7 \quad (\text{Eq. 7.3g})$$

$$CN_{pf,wet,FS=iv}(t) = [CN_{af} + (-3.25 * \ln(t) + 11.32)] + 7 \quad (\text{Eq. 7.3h})$$

#### **7.4.2 Estimating IA for variable initial conditions**

As mentioned in Section 5.3.1.2, the initial abstraction ratio is not necessarily equal to 0.2, as assumed in the SCS-CN method and case-specific studies may be necessary for its more accurate estimation. To this end, extended literature review was performed for the estimation of IA for each subbasin under pre-fire and normal SM conditions. This ratio was thoroughly examined for an experimental basin in Eastern Attica, which is part of the selected study area, by Baltas *et al.* (2007) and the research concluded that representative values for the experimental basin range between 0.014 and 0.037. In a relevant research in the study area, Papathanasiou *et al.* (2012) suggest that initial abstraction ratio values between 0.01 and 0.037 for different subbasins result in representative simulations. In this research an upper threshold of 0.05 has been set to initial abstraction ratio.

In the current research it was found that low (or default) initial abstraction ratio values result in significant underestimation of IA. The rule of 0.05 as an upper threshold for initial abstraction ratio has been applied and different values of IA for different initial conditions (*i.e.* for wet and dry SM conditions and for burnt and not-burnt soils) were estimated for the study area. Available historic rainfall and discharge measurements were used for the calibration of the hydrological model for pre-fire normal conditions and the estimation of IA for pre-fire wet and dry SM conditions, based on IA for normal SM conditions. The values of *c* and *d* (Eq. 5.11) that associate IA for normal with IA for wet and dry SM conditions in this research are presented in Table 7.7.

In order to estimate IA for post-fire normal SM conditions,  $t_{upper}$ ,  $t_{lower}$  and the corresponding  $h_{IA,FS}$  need to be estimated first (Eq. 5.9b and 5.10b). The first post-fire period, *i.e.*  $t_{upper}$  is the time-window 0-7 months. However, even though the fire has a significant impact on post-fire IA values (Elliott *et al.*, 2005; Papathanasiou *et al.*, 2012) and it is expected that this impact is sharply decreased with time (since IA is directly related with vegetation regrowth, the fire impact on which is also sharply decreasing in time), there are no generalized guidelines that support the estimation of IA during the first post-fire period, *i.e.* the estimation of  $h_{IA,FS,t_{upper}=0-7m}$ . The assumption of the upper threshold of 0.05 on initial abstraction ratio for this catchment and of the sharply descending fire-impact on IA, were used for the estimation of post-fire changes in IA for different FS classes for  $t_{upper}$ , as presented in Table 7.8.

Similarly with CN,  $t_{lower}$  for FS=i is considered 36-48 months, for FS=ii it is considered 24-36 months and for FS=iii and iv it is considered 19-24 months. Just prior to hydrological recovery, changes in IA are expected to be low and for this reason  $h_{IA,FS,t_{lower}}$  is set to -1 for all FS. Post-fire changes in IA for different FS classes for  $t_{lower}$  are also summarized in Table 7.8.

Using these marginal values of  $h_{IA,FS,t_{upper}}$  and  $h_{IA,FS,t_{lower}}$  for given  $t_{upper}$  and  $t_{lower}$ , the values of  $a_{IA,FS}$  and  $b_{IA,FS}$  (Eq. 5.10b) for different FS classes are estimated and summarized in Table 7.9.

Following the Equations 5.9b, post-fire IA for normal conditions becomes:

$$IA_{pf,FS=i}(t) = IA_{af} + (4.67 * \ln(t) - 19.10) \quad (\text{Eq. 7.4a})$$

$$IA_{pf,FS=ii}(t) = IA_{af} + (4.27 * \ln(t) - 16.32) \quad (\text{Eq. 7.4b})$$

$$IA_{pf,FS=iii}(t) = IA_{af} + (4.06 * \ln(t) - 13.90) \quad (\text{Eq. 7.4c})$$

$$IA_{pf,FS=iv}(t) = IA_{af} + (2.44 * \ln(t) - 8.74) \quad (\text{Eq. 7.4d})$$

These post-fire changes are combined with the values of Table 7.7 for IA under different SM conditions, and suggested alterations in IA for post-fire dry conditions are presented in Eq. 7.5a-d, while suggested alterations in CN values for post-fire wet conditions are presented in Eq. 7.5e-h.

$$IA_{pf,dry,FS=i}(t) = [IA_{af} + (4.67 * \ln(t) - 19.10)] + 3 \quad (\text{Eq. 7.5a})$$

$$IA_{pf,dry,FS=ii}(t) = [IA_{af} + (4.27 * \ln(t) - 16.32)] + 3 \quad (\text{Eq. 7.5b})$$

$$IA_{pf,dry,FS=iii}(t) = [IA_{af} + (4.06 * \ln(t) - 13.90)] + 3 \quad (\text{Eq. 7.5c})$$

$$IA_{pf,dry,FS=iv}(t) = [IA_{af} + (2.44 * \ln(t) - 8.74)] + 3 \quad (\text{Eq. 7.5d})$$

$$IA_{pf,wet,FS=i}(t) = [IA_{af} + (4.67 * \ln(t) - 19.10)] - 3 \quad (\text{Eq. 7.5e})$$

$$IA_{pf,wet,FS=ii}(t) = [IA_{af} + (4.27 * \ln(t) - 16.32)] - 3 \quad (\text{Eq. 7.5f})$$

$$IA_{pf,wet,FS=iii}(t) = [IA_{af} + (4.06 * \ln(t) - 13.90)] - 3 \quad (\text{Eq. 7.5g})$$

$$IA_{pf,wet,FS=iv}(t) = [IA_{af} + (2.44 * \ln(t) - 8.74)] - 3 \quad (\text{Eq. 7.5h})$$

### **7.4.3 Estimating TP for variable initial conditions**

Based on the procedure described in Section 5.3.2.1 TP values for pre-fire normal SM conditions were estimated. These values were verified through the calibration process discussed in Section 7.4.1, which resulted in the estimation of the values of c and d (Eq. 5.11) presented in Table 7.7, that associate TP for pre-fire normal SM with TP for pre-fire wet and dry SM conditions.

For post-fire normal SM conditions TP is estimated from Eq. 5.9c and 5.10c, given  $t_{upper}$ ,  $t_{lower}$  and the corresponding  $h_{CN,FS}$  for these periods. As in previous cases,  $t_{upper}$  is the time-window 0-7 months. Regarding fire impact on TP, in Elliott *et al.* (2005) the mean post-fire lag time for burnt catchments in Colorado was estimated to be reduced by 40% in comparison to the corresponding pre-fire values, with the exact value depending on the extent of the burnt area. Cydzik and Hogue (2009) undertook a relevant study and concluded that post-fire lag time in San Bernardino County, California, was reduced by 30% when compared with its pre-fire value, with TP remaining low during the first three post-fire years. Papathanasiou *et al.* (2012) suggest a 40% reduction in post-fire lag time for totally burnt land in typical Mediterranean areas. In the current research, post-fire Standard Lag is assumed to be reduced by 40% and this reduction is attributed to areas affected by very high FS and for the period 0÷7 months after the fire

occurrence. The 40% reduction of TP is proportionally decreased for longer post-fire periods and less intense fire impact.

Similarly with CN and IA,  $t_{lower}$  for FS=i is considered 36-48 months, for FS=ii it is considered 24-36 months and for FS=iii and iv it is considered 19-24 months. For  $t_{lower}$ , *i.e.* the period just prior to hydrological recovery, when TP is expected to recover to its pre-fire condition, changes in TP are expected to be significantly low, with  $h_{TP,FS,t_{lower}}$  tending to 1, especially in areas affected by low and moderate FS. The values of  $h_{TP,FS,t_{upper}}$  and  $h_{TP,FS,t_{lower}}$  for different FS classes used in this research are presented in Table 7.8.

Using these marginal values of  $h_{TP,FS,t_{upper}}$  and  $h_{TP,FS,t_{lower}}$  for given  $t_{upper}$  and  $t_{lower}$ , the values of  $a_{CN,FS}$  and  $b_{CN,FS}$  (Eq. 5.10c) for different FS classes are estimated and summarized in Table 7.9.

Following the Equation 5.9c, post-fire TP for normal conditions becomes:

$$TP_{pf,FS=i}(t) = (0.16 * \ln(t) + 0.30) * TP_{af} \quad (\text{Eq. 7.6a})$$

$$TP_{pf,FS=ii}(t) = (0.12 * \ln(t) + 0.46) * TP_{af} \quad (\text{Eq. 7.6b})$$

$$TP_{pf,FS=i}(t) = (0.12 * \ln(t) + 0.56) * TP_{af} \quad (\text{Eq. 7.6c})$$

$$TP_{pf,FS=iv}(t) = (0.06 * \ln(t) + 0.79) * TP_{af} \quad (\text{Eq. 7.6d})$$

The values of Table 7.7 for TP under different SM conditions are combined with these post-fire changes and suggested alterations in TP for post-fire dry conditions are presented in Eq. 7.7a-d, while suggested alterations in TP values for post-fire wet conditions are presented in Eq. 7.7e-h.

$$TP_{pf,dry,FS=i}(t) = [(0.16 * \ln(t) + 0.30) * TP_{af}] + 0.05 \quad (\text{Eq. 7.7a})$$

$$TP_{pf,dry,FS=ii}(t) = [(0.12 * \ln(t) + 0.46) * TP_{af}] + 0.05 \quad (\text{Eq. 7.7b})$$

$$TP_{pf,dry,FS=i}(t) = [(0.12 * \ln(t) + 0.56) * TP_{af}] + 0.05 \quad (\text{Eq. 7.7c})$$

$$TP_{pf,dry,FS=iv}(t) = [(0.06 * \ln(t) + 0.79) * TP_{af}] + 0.05 \quad (\text{Eq. 7.7d})$$

$$TP_{pf,wet,FS=i}(t) = [(0.16 * \ln(t) + 0.30) * TP_{af}] - 0.05 \quad (\text{Eq. 7.7e})$$

$$TP_{pf,wet,FS=ii}(t) = [(0.12 * \ln(t) + 0.46) * TP_{af}] - 0.05 \quad (\text{Eq. 7.7f})$$

$$TP_{pf,wet,FS=i}(t) = [(0.12 * \ln(t) + 0.56) * TP_{af}] - 0.05 \quad (\text{Eq. 7.7g})$$

$$TP_{pf,wet,FS=iv}(t) = [(0.06 * \ln(t) + 0.79) * TP_{af}] - 0.05 \quad (\text{Eq. 7.7h})$$

#### **7.4.4 Estimating CP for variable initial conditions**

As discussed in Section 5.3.2.2 typical CP values range between 0.4 and 0.7, with lower values assigned to steep-rising hydrographs (HEC, 2009; McEnroe and Zhao, 1999). CP is estimated for pre-fire normal SM conditions using these marginal values and the selected values were verified through the calibration process discussed in Section 7.4.1. For wet SM conditions the rising limb of hydrographs is expected to be steeper and thus the corresponding CP values are decreased, with respect to CP values for normal or dry SM conditions. For adverse conditions, CP is set to its lower value, *i.e.* 0.4, for pre-fire wet SM conditions. The aforementioned calibration process, co-evaluated with the setting

of an upper threshold of 0.7 for dry conditions, resulted in the estimation of a rule that associates pre-fire CP values for normal SM conditions with pre-fire CP values for dry SM conditions. This rule is presented in Eq. 7.8a. Therefore,

$$CP_{af,dry} = MIN(CP_{af,normal} + 0.05, 0.7) \quad (\text{Eq. 7.8a})$$

$$CP_{af,wet} = 0.4 \quad (\text{Eq. 7.8b})$$

$t_{upper}$ ,  $t_{lower}$  and the corresponding  $h_{CP,FS}$  for these periods need to be defined so as to estimate CP for post-fire normal SM conditions. Again,  $t_{upper}$  is the time-window 0-7 months. A steep rising limb of hydrographs is also expected for burnt areas and therefore decreased CP values can be considered for burnt areas, in comparison to the corresponding values for areas not affected by fire. The marginal value 0.4 is also considered representative for normal SM conditions, when referring to recently burnt areas affected by severe fire (*i.e.* for FS=i and ii). These rules are summarized in the following:

$$CP_{pf,normal,FS=i,t_{upper}=0\div7m} = CP_{pf,normal,FS=ii,t_{upper}=0\div7m} = 0.4 \quad (\text{for FS=i and ii}).$$

McEnroe and Zhao (1999) argue that there is no strong correlation between CP values and catchment characteristics, while on the contrary CP values are more correlated with rainfall depth. Therefore, CP can be considered more sensitive to initial SM conditions than to FS and as such, changes in post-fire CP values are expected to be limited. The changes in CP for all other conditions and for different FS classes for  $t_{upper}$  are summarized in Table 7.8.

Given the limited impact of fire on CP, when compared with the impact of fire on CN, IA and to a lesser extent TP, post-fire CP values are expected to recover to their pre-fire values sooner than CN, IA and TP values. For this reason,  $t_{lower}$  for FS=i is considered 24-36 months, for FS=ii it is considered 19-24 months and for FS=iii and iv it is considered 12-19 months. Accordingly, post-fire changes in CP for different FS classes for  $t_{lower}$  are expected to remain low, as presented in Table 7.8 for this study.

Using the values of  $h_{CP,FS,t_{upper}}$  and  $h_{CP,FS,t_{lower}}$  for given  $t_{upper}$  and  $t_{lower}$ , the values of  $a_{CP,FS}$  and  $b_{CP,FS}$  (Eq. 5.10d) for different FS classes are estimated and summarized in Table 7.9.

The role of the parameter  $p$  in Equation 5.9d is the maintenance of a lower threshold in CP, which in this study is 0.4. Following the Equation 5.9d, post-fire CP for normal conditions for different FS becomes:

$$CP_{pf,FS=i}(t) = MAX[(CP_{af} + 0.05 * \ln(t) - 0.24), 0.4] \quad (\text{Eq. 7.9a})$$

$$CP_{pf,FS=ii}(t) = MAX[(CP_{af} + 0.06 * \ln(t) - 0.22), 0.4] \quad (\text{Eq. 7.9b})$$

$$CP_{pf,FS=iii}(t) = MAX[(CP_{af} + 0.04 * \ln(t) - 0.14), 0.4] \quad (\text{Eq. 7.9c})$$

$$CP_{pf,FS=i}(t) = MAX[(CP_{af} + 0.03 * \ln(t) - 0.10), 0.4] \quad (\text{Eq. 7.9d})$$

CP is considered constantly equal to 0.4 for all post-fire wet SM conditions, regardless of fire impact. Therefore,

$$CP_{pf,wet,FS}(t) = 0.4 \quad (\text{Eq. 7.10})$$

Regarding post-fire dry SM conditions, Eq. 7.9a-d are combined with Eq. 7.8a and suggested alterations in CP are presented in Eq. 7.11a-d.

$$CP_{pf,dry,FS=i}(t) = MIN(MAX[(CP_{af} + 0.05 * ln(t) - 0.24), 0.4] + 0.05, 0.7) \quad (\text{Eq. 7.11a})$$

$$CP_{pf,dry,FS=ii}(t) = MIN(MAX[(CP_{af} + 0.06 * ln(t) - 0.22), 0.4] + 0.05, 0.7) \quad (\text{Eq. 7.11b})$$

$$CP_{pf,dry,FS=iii}(t) = MIN(MAX[(CP_{af} + 0.04 * ln(t) - 0.14), 0.4] + 0.05, 0.7) \quad (\text{Eq. 7.11c})$$

$$CP_{pf,dry,FS=i}(t) = MIN(MAX[(CP_{af} + 0.03 * ln(t) - 0.10), 0.4] + 0.05, 0.7) \quad (\text{Eq. 7.11d})$$

#### **7.4.5 Estimating K for variable initial conditions**

K can be estimated for pre-fire normal conditions based on Section 5.3.3.1. Regarding K for variable initial SM conditions, even though their impact on K is not very strong, it still needs not to be neglected. In particular, under wet SM conditions discharge is increased resulting in increased wave velocity in a given river section, which in turn contributes in decreased travel times of the peak flow. For the exact estimation of K for pre-fire wet and dry SM conditions the aforementioned calibration process resulted in the estimation of the values of c and d (Eq. 5.11) presented in Table 7.7, that associate K for pre-fire normal SM with K for pre-fire wet and dry SM conditions.

For post-fire normal SM conditions K is estimated from Eq. 5.9e and 5.10e, given  $t_{upper}$ ,  $t_{lower}$  and the corresponding  $h_{K,FS}$  for these periods.  $t_{upper}$  is the time-window 0-7 months. Regarding the impact of fire on K, it is expected to be similar with the impact of wet SM conditions on K, yet less intense. In particular, in the aftermath of a fire, discharge is increased (as presented in detail in Chapter 3), the wave velocity in a given river section is also increased and therefore the wave travel time through the channel is decreased. However, wave velocity is more strongly correlated to initial SM conditions than to a potential fire impact, since fire has an indirect impact on it. Therefore, a reduced post-fire decrease in the wave travel time is to be expected, especially for low and moderate FS. For this reason, classes of low and moderate FS (FS=iii and iv) could be merged without affecting the value of K.

Additionally, due to the indirect impact of fire on K it is expected that this impact will attenuate sooner in comparison to the fire impact on CN, IA and TP, as is the case with CP (Section 7.4.4). In this research,  $t_{lower}$  for FS=i is considered 24-36 months, for FS=ii it is considered 19-24 months and for FS=iii and iv it is considered 12-19 months. Also, given the low post-fire change in K for  $t_{lower}$ ,  $h_{K,FS,t_{lower}}$  is considered stable and equal to 0.95 for all FS classes. The values of  $h_{K,FS,t_{upper}}$  and  $h_{K,FS,t_{lower}}$  for different FS classes are summarized in Table 7.8.

Using these marginal values of  $h_{K,FS,t_{upper}}$  and  $h_{K,FS,t_{lower}}$  for given  $t_{upper}$  and  $t_{lower}$ , the values of  $a_{K,FS}$  and  $b_{K,FS}$  (Eq. 5.10e) for different FS are estimated and presented in Table 7.9.

Following the Equation 5.9e, post-fire K for normal conditions becomes:

$$K_{pf,FS=i}(t) = (0.12 * \ln(t) + 0.51) * K_{af} \text{ (Eq. 7.12a)}$$

$$K_{pf,FS=ii}(t) = (0.12 * \ln(t) + 0.56) * K_{af} \text{ (Eq. 7.12b)}$$

$$K_{pf,FS=iii}(t) = K_{pf,FS=iv}(t) = (0.10 * \ln(t) + 0.66) * K_{af} \text{ (Eq. 7.12c)}$$

The values of Table 7.7 for K under different SM conditions are combined with these post-fire changes and suggested alterations in K for post-fire dry conditions are presented in Eq. 7.13a-c, while suggested alterations in K for post-fire wet conditions are presented in Eq. 7.13d-f.

$$K_{pf,dry,FS=i}(t) = 1.3 * [(0.12 * \ln(t) + 0.51) * K_{af}] \text{ (Eq. 7.13a)}$$

$$K_{pf,dry,FS=ii}(t) = 1.3 * [(0.12 * \ln(t) + 0.56) * K_{af}] \text{ (Eq. 7.13b)}$$

$$K_{pf,dry,FS=iii}(t) = K_{pf,dry,FS=iv}(t) = 1.3 * [(0.10 * \ln(t) + 0.66) * K_{af}] \text{ (Eq. 7.13c)}$$

$$K_{pf,wet,FS=i}(t) = 0.7 * [(0.12 * \ln(t) + 0.51) * K_{af}] \text{ (Eq. 7.13d)}$$

$$K_{pf,wet,FS=ii}(t) = 0.7 * [(0.12 * \ln(t) + 0.56) * K_{af}] \text{ (Eq. 7.13e)}$$

$$K_{pf,wet,FS=iii}(t) = K_{pf,wet,FS=iv}(t) = 0.7 * [(0.10 * \ln(t) + 0.66) * K_{af}] \text{ (Eq. 7.13f)}$$

To account for adverse conditions, it can be further assumed that K remains constant for intensely urbanized zones. In this research these rules-equations were not followed for the tunnel and reaches that had a length less than 2 km (*i.e.* Reach 4), in which cases K was not altered.

*Table 7.7. The values of c and d for different SM conditions for CN, IA, TP, CP and K.*

Parameter	CN <sub>dry</sub>	CN <sub>wet</sub>	IA <sub>dry</sub>	IA <sub>wet</sub>	TP <sub>dry</sub>	TP <sub>wet</sub>	K <sub>dry</sub>	K <sub>wet</sub>
c	1	1	1	1	1	1	1.3	0.7
d	-7	7	3	-3	0.05	-0.05	0	0

*Table 7.8. The values of  $h_{CN,FS,t_{upper}}$  and  $h_{CN,FS,t_{lower}}$ ,  $h_{IA,FS,t_{upper}}$  and  $h_{IA,FS,t_{lower}}$ ,  $h_{TP,FS,t_{upper}}$  and  $h_{TP,FS,t_{lower}}$ ,  $h_{CP,FS,t_{upper}}$  and  $h_{CP,FS,t_{lower}}$  and  $h_{K,FS,t_{upper}}$  and  $h_{K,FS,t_{lower}}$  for different FS classes.*

		FS class			
		i	ii	iii	iv
Parameters	$h_{CN,FS,t_{upper}}$	20	15	10	5
	$h_{CN,FS,t_{lower}}$	4	3	2	1
	$h_{IA,FS,t_{upper}}$	-10	-8	-6	-4
	$h_{IA,FS,t_{lower}}$	-1			
	$h_{TP,FS,t_{upper}}$	0.6	0.7	0.8	0.9
	$h_{TP,FS,t_{lower}}$	0.9	0.9	0.95	0.97
	$h_{CP,FS,t_{upper}}$	-0.1	-0.08	-0.06	-0.04
	$h_{CP,FS,t_{lower}}$	-0.04	-0.04	-0.02	-0.01
	$h_{K,FS,t_{upper}}$	0.75	0.80	0.85	
	$h_{K,FS,t_{lower}}$	0.95			



Table 7.9 The values of  $a_{CN,FS}$  and  $b_{CN,FS}$ ,  $a_{IA,FS}$  and  $b_{IA,FS}$ ,  $a_{TP,FS}$  and  $b_{TP,FS}$ ,  $a_{CP,FS}$  and  $b_{CP,FS}$  and  $a_{K,FS}$  and  $b_{K,FS}$  for different FS classes.

		FS class			
		i	ii	iii	iv
Parameters	$a_{CN,FS}$	-8.31	-7.33	-6.50	-3.25
	$b_{CN,FS}$	36.17	29.26	22.63	11.32
	$a_{IA,FS}$	4.67	4.27	4.06	2.44
	$b_{IA,FS}$	-19.10	-16.32	-13.90	-8.74
	$a_{TP,FS}$	0.16	0.12	0.12	0.06
	$b_{TP,FS}$	0.30	0.46	0.56	0.79
	$a_{CP,FS}$	0.05	0.06	0.04	0.03
	$b_{CP,FS}$	-0.24	-0.22	-0.14	-0.10
	$a_{K,FS}$	0.12	0.12	0.10	
	$b_{K,FS}$	0.51	0.56	0.66	

Graphs with the proposed post-fire changes in the values of the five examined parameters for normal SM conditions are presented in Figure 7.8.

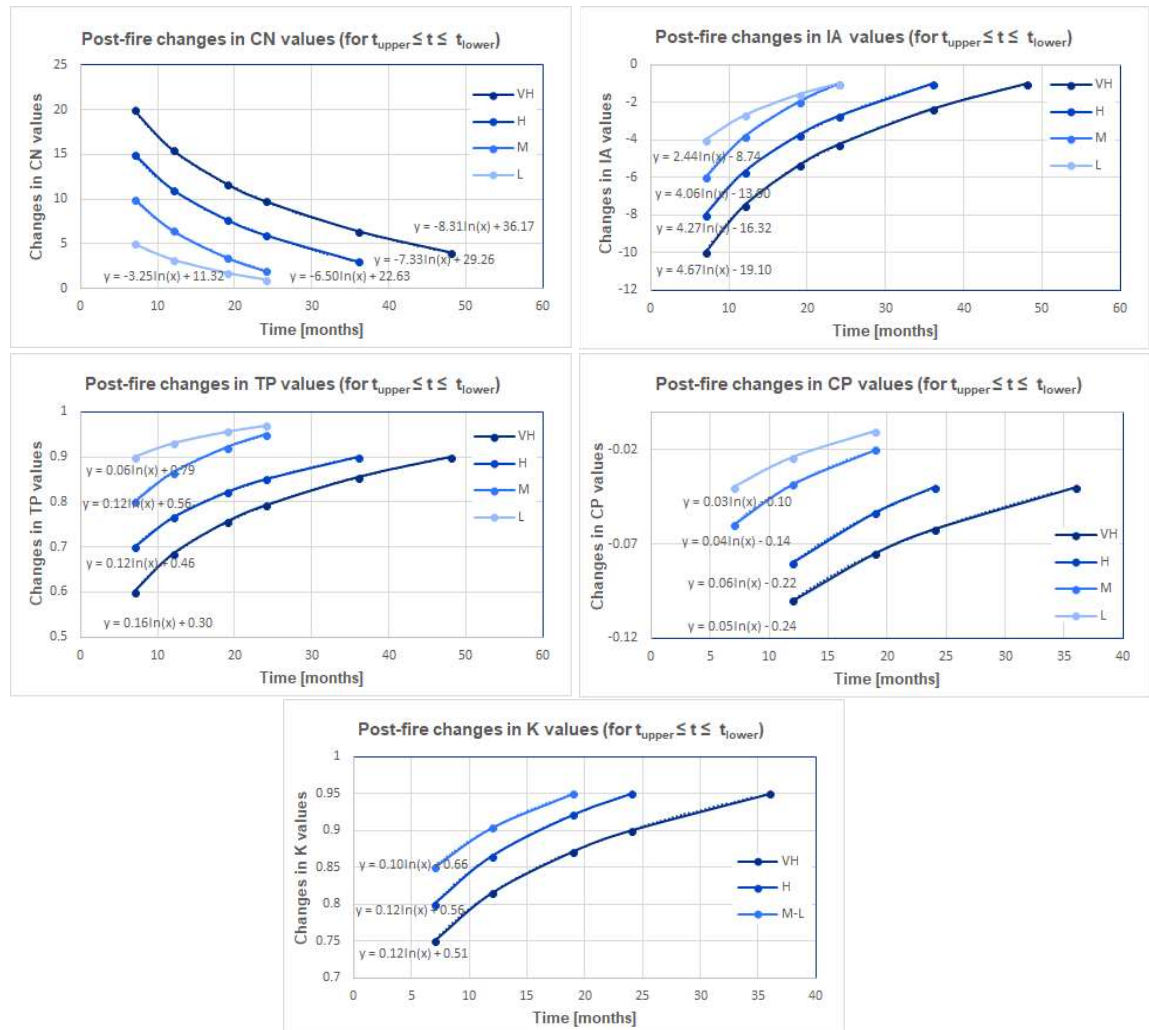


Figure 7.8. The proposed post-fire changes in the values of the five examined parameters for normal SM conditions.

## 7.5 Running the hydrological model for the study area

In order to run the hydrological model for a given rainfall event and a specific post-fire period, which is determined from the time period between the fire occurrence and the date of the rainfall event, and as suggested in the proposed methodology (Section 5.4), one composite weighted value for each one of the five examined hydrological parameters for each subbasin (for CN, IA, TP and CP) and each reach (for K) need to be imported in the model. These weighted parameters will depend on the percentage of the affected area within each FS class (as estimated from the GIS analysis presented in Section 7.1).

To this end, the composite weighted values are estimated co-evaluating the suggested values for all parameters and all FS classes (following the procedure described in Section 7.4) together with the corresponding percentage of affected area in each FS class (as presented in Table 7.3).

In this research, this procedure is followed for all three examined rainfall events and for the relevant each time post-fire periods. The final composite weighted values of the five hydrological parameters for the three examined events (which correspond to different initial SM conditions) and for all subbasins and reaches are presented in Table 7.10.

After the import of all necessary datasets for the hydrological analysis, HEC-HMS ran for each flood event and the corresponding results from each run are presented and further analyzed in detail in Chapter 8.

Table 7.10. The final values of CN, IA, TP, CP and K for each event and each subbasin and reach of Rafina catchment.

		<b>DRY (03/02/2011)</b>	<b>NORMAL (10-11/12/2009)</b>	<b>WET (22/02/2013)</b>
<b>CN</b>	Drafi	39	53	48
	Rafina big	44	53	57
	Rafina small	44	53	57
	Spata	36	43	50
	Urban	51	58	65
	Sub1	56	63	70
<b>la</b>	Drafi	15	7	11
	Rafina big	16	12	11
	Rafina small	15	11	10
	Spata	18	15	12
	Urban	13	10	7
	Sub1	11	8	5
<b>TP</b>	Drafi	0.54	0.42	0.49
	Rafina big	0.88	0.8	0.8
	Rafina small	0.78	0.71	0.7
	Spata	0.8	0.75	0.7
	Urban	0.3	0.3	0.3
	Sub1	0.4	0.4	0.4
<b>Cp</b>	Drafi	0.52	0.43	0.4
	Rafina big	0.47	0.42	
	Rafina small	0.47	0.42	
	Spata	0.47	0.42	
	Urban	0.4	0.4	
	Sub1	0.4	0.4	
<b>K</b>	Reach 1	0.85	0.57	0.50
	Reach 2	1.67	1.24	0.91
	Reach 3	1.19	0.89	0.65
	Reach 5	1.30	0.99	0.7
	Reach 4	0.25	0.25	0.25
	Shragga	0.55	0.55	0.55

## CHAPTER 8: RESULTS AND DISCUSSION

The methodology presented in Chapter 5 was adjusted to the study area for three flood events, used for the validation of the proposed methodology, as discussed in Chapter 7 and the values of the five parameters studied in this research, *i.e.* CN, IA, TP, CP and K, were estimated and imported in the already set up and calibrated HEC-HMS. Each simulated flood event corresponds to different initial SM conditions and different post-fire time period after the fire event of August 2009. In particular, the flood event of 10-11/12/2009 corresponds to normal SM conditions and occurred shortly after fire occurrence, when the fire impact in all FS classes was increased, the flood event of 03/02/2011 corresponds to dry SM conditions and occurred several months after fire occurrence, when the fire impact in most FS classes was moderate and the flood event of 22/02/2013 corresponds to wet SM conditions and occurred after a long post-fire period, when the fire impact in all FS classes was expected to have vanished.

### 8.1 Application of the methodology

HEC-HMS simulated the flows at the outlets of each subbasin for all selected events. An in-depth analysis of (limited) observed and recorded water levels and velocities (when available) was performed for comparison purposes. All available velocity measurements and flow observations and recordings were analyzed according to the empirical methodology developed for this research and discussed in Section 7.3.2 and, when possible, “observed discharges” were calculated and compared against simulated discharges. Additional simulations were also performed for the case when the suggested methodology is not applied.

Indicative results of these simulations, used for the validation of the proposed methodology, are presented in Figures 8.1-8.3.

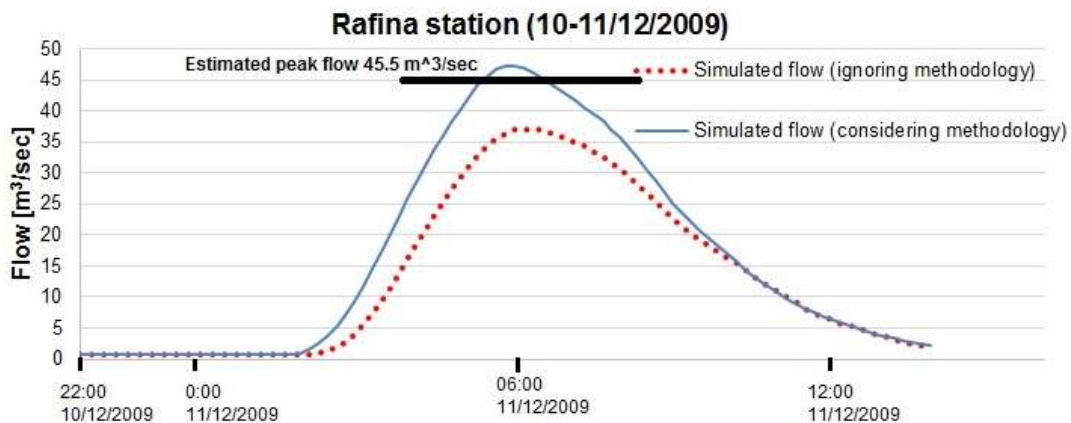


Figure 8.1. Simulated flows when applying and when ignoring the methodology and estimated peak flow for the flood event of 10-11/12/2009 (Rafina station).

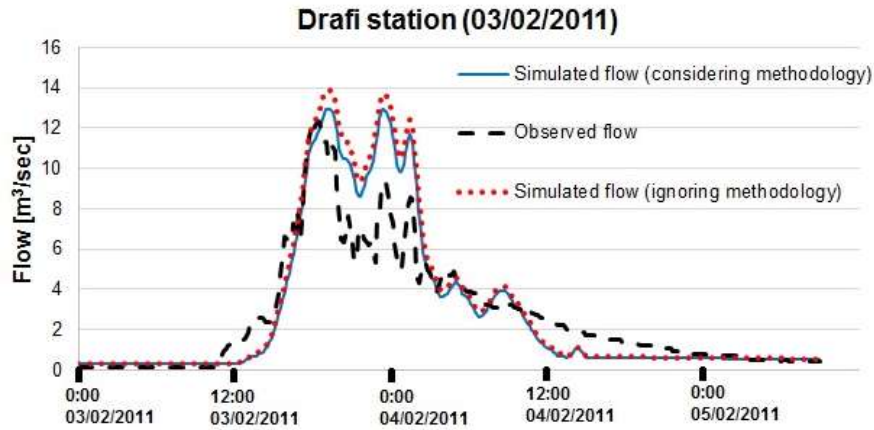


Figure 8.2. Observed and simulated flows when applying and when ignoring the methodology for the flood event of 03/02/2011 (**Drafi station**).

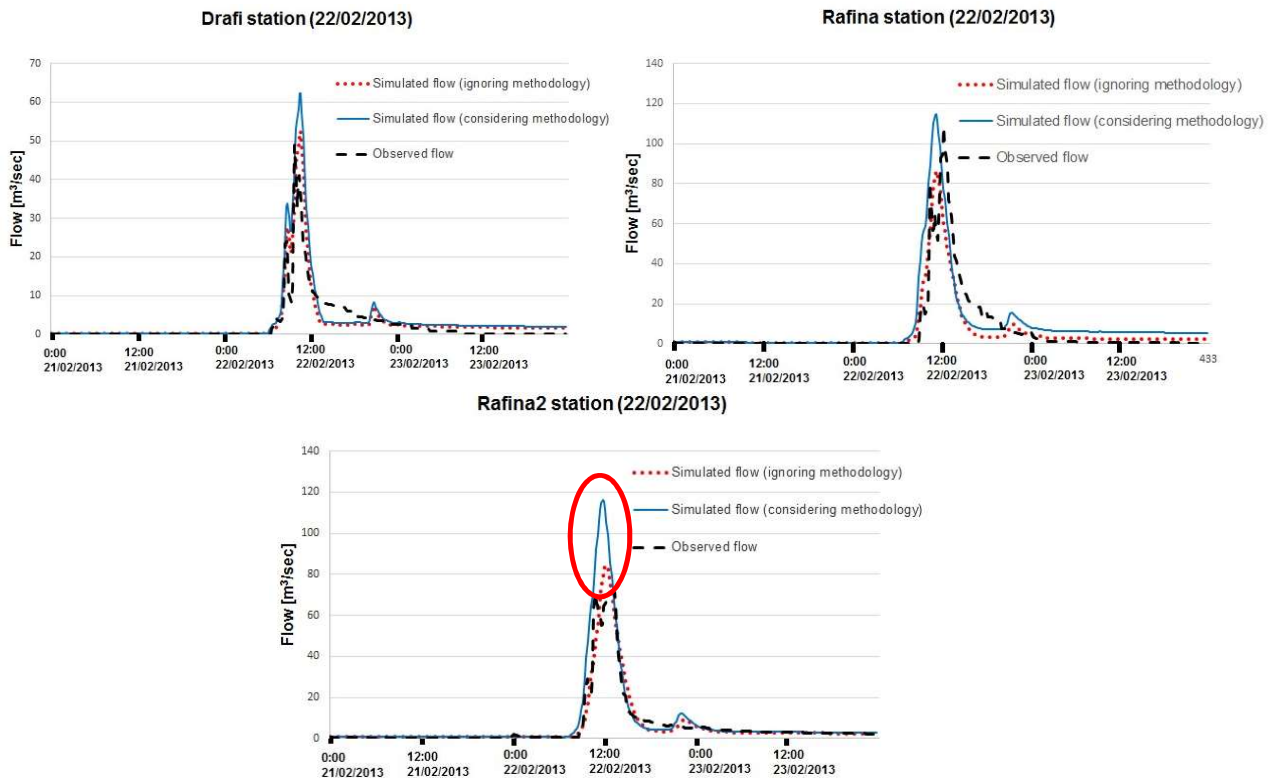


Figure 8.3. Observed and simulated flows when applying and when ignoring the methodology for the flood event of 22/02/2013 for **Drafi** (top left), **Rafina** (top right) and **Rafina2** (bottom) stations.

As discussed in Section 7.3.2, HEC-HMS was calibrated for historical events. Focusing on the event of **10-11/12/2009**, it needs to be noted that the forest fire occurred 4 months prior to the flood event and as a result the river cross sections downstream Drafi had been significantly altered. Particularly for Rafina station, where a HOA streamflow gauge was installed, the pedestals of the bridge that carried the gauge were undermined and the riverbed was modified: both of its

sides were eroded and debris was deposited in the middle of the cross section, where the streamflow gauge targets. Hence, the water levels that were recorded during this event cannot be accurately translated into flows. *In situ* estimations of the exact geometry of this cross section during this event were performed and flood traces were tracked on the bridge shortly after the event. Based on these, the event peak flow is estimated to have reached 45.5 m<sup>3</sup>/s.

Particularly for the flood event of **22/02/2013**, flow velocity measurements are available for the sites where Drafi and Rafina stations are installed and these measurements are used for the estimation of observed flows for this event. During this event, the bridge where Rafina-2 station is installed was flashed-over by the flow and for this reason the flows at that location are only presented for comparison purposes and cannot be further exploited. The flooding of the area is verified by testimonies and photographs from local residents, as presented in Figure 6.11.

It can be concluded from Figures 8.1, 8.2 and 8.3 that for all examined flood events, in case of the application of the methodology, the simulated peak flows, runoff volumes and times to peak match well to the corresponding values derived from observed datasets, when available. As expected, simulation results when the methodology is not applied and especially for adverse conditions (wet SM conditions and flood events after a recent forest fire) are poor when compared against the corresponding results when the methodology is applied.

Focusing on the flood event of **22/02/2013**, when the bridge where Rafina-2 station is installed was flashed-over by the flow, the water level reached the height of the sensor (~2.7 m) and flows close to this water level cannot be considered representative, since there can be no simulation of the conditions after the overcoming of this value. However, as verified in Figure 8.3, there seems to be an excellent matching at Rafina-2 station between the simulated flows when the methodology is considered and the corresponding observed flows, both prior to and after the flooding of the bridge. A significant underestimation in simulated flows is observed when the methodology is not applied. Therefore, even though simulation results cannot be further exploited for this station, it is clear that the proposed methodology yields very good results even in this case.

Different efficiency criteria, also called objective functions (OF) (Gupta *et al.*, 1998), used to measure performance of hydrological models and reported in literature were examined. Such criteria provide an objective assessment of the “closeness” of simulated values (usually discharges) to observed measurements (Krause *et al.*, 2005). Typical such criteria in literature include the Nash-Sutcliffe efficiency index NS, the Nash-Sutcliffe efficiency index with logarithmic values ln(NS), the coefficient of determination  $r^2$ , the index of agreement d, modified forms of NS and d, the Mean Absolute Percentage Error MAPE, also known as Mean Absolute Percentage Deviation MAPD, the Normalized Mean Squared Error NMSE, the Average Relative Variance ARV, the Root Mean Squared Error RMSE, the Peak Difference PDIFF and numerous others (Nash and Sutcliffe, 1970; Krause *et al.*, 2005; Wagener and Kollat, 2007; Gupta *et al.*, 1998; Brocca *et al.*, 2010; Brocca *et al.*, 2013). NS (Equation 8.1) was finally selected as most appropriate, representative and efficient for this hydrological application. NS

efficiencies range between  $-\infty$  and 1, with optimum model efficiency being achieved when  $NS=1$ , which indicates a perfect match between observed and simulated values.

$$NS = 1 - \frac{\sum_{i=1}^n (O_i - S_i)^2}{\sum_{i=1}^n (O_i - \bar{O})^2} \quad (\text{Eq. 8.1})$$

Relevant information is summarized in Table 8.1, where NS efficiency indicator is estimated when the methodology is applied and simulated peak flows and runoff volumes for each examined flood event for Rafina and Drafi are compared against the corresponding observed peak flows and runoff volumes when the methodology is not applied. Particularly for the flood event of 10-11/12/2009, a certified technician from NTUA proceeded to two flow measurements during the event. These flow measurements are compared against the corresponding simulated flows from HEC-HMS (when methodology is applied and when methodology is ignored) and are also presented in Table 8.1.

Table 8.1. Comparative analysis of simulated and observed runoff volumes and peak and other discharges for three flood events.

Simulated vs Observed figures	Flood Event					
	22/02/2013	03/02/2011	10-11/12/2009			
	Rafina	Drafi	Rafina			
$Q_{peak,sim}$ [m <sup>3</sup> /sec] (methodology considered)	113.0	12.9	47.3			
$Q_{peak,sim}$ [m <sup>3</sup> /sec] (methodology not applied)	86.1	13.9	37.1			
$Q_{peak,obs}$ [m <sup>3</sup> /sec]	108.5	12.26	45.5			
Difference between $Q_{peak,sim}$ (methodology considered) & $Q_{peak,obs}$ [%]	3.98	4.96	3.81			
Difference between $Q_{peak,sim}$ (methodology not applied) & $Q_{peak,obs}$ [%]	-26.0	12	-22.6			
$V_{runoff,sim}$ [10 <sup>3</sup> m <sup>3</sup> ] (methodology considered)	1607	561	$Q_{sim}$ [cms] (11/12/2009-12:10) (methodology considered)	6.3	$Q_{sim}$ [cms] (11/12/2009-13:15) (methodology considered)	3.7
$V_{runoff,sim}$ [10 <sup>3</sup> m <sup>3</sup> ] (methodology not applied)	1216	605	$Q_{sim}$ [m <sup>3</sup> /sec] (11/12/2009-12:10) (methodology not applied)	6.3	$Q_{sim}$ [m <sup>3</sup> /sec] (11/12/2009-13:15) (methodology not applied)	3.2
$V_{runoff,obs}$ [10 <sup>3</sup> m <sup>3</sup> ]	1547	535	$Q_{meas}$ [cms] (11/12/2009-12:10)	6.02	$Q_{meas}$ [cms] (11/12/2009-13:15)	4
Difference between $V_{runoff,sim}$ (methodology considered) & $V_{runoff,obs}$ [%]	3.73	4.6	Difference between $Q_{sim}$ & $Q_{meas}$ [%] (methodology considered)	4.44	Difference between $Q_{sim}$ & $Q_{meas}$ [%] (methodology considered)	-8.1
Difference between $V_{runoff,sim}$ (methodology not applied) & $V_{runoff,obs}$ [%]	-27.18	11.6	Difference between $Q_{sim}$ & $Q_{meas}$ [%] (methodology not applied)	4.44	Difference between $Q_{sim}$ & $Q_{meas}$ [%] (methodology not applied)	-25
Nash-Sutcliffe efficiency (methodology considered)	0.61	0.68				



As quantified in Table 8.1, for the examined rainfall events, the absolute mean relative difference [%] between simulated and observed peak discharges is 4.25% when the methodology is applied, while it reaches 20.2%, when the methodology is not applied. The absolute mean relative difference [%] between simulated and observed runoff volumes is less than 4.2% when the methodology is applied, reaching 19.4% when the methodology is not applied. In addition, the absolute mean relative difference [%] between simulated and available measured flows (in the absence of discharge timeseries) is 6.3% when the methodology is applied and 14.7% when the methodology is ignored. It can hence be safely concluded that the application of the proposed methodology for the estimation of the values of CN, IA, TP, CP and K, renders the simulations of the hydrological behaviour of the examined catchment accurate and representative.

The hydrological impact of changes in initial conditions, in terms of fire occurrence and initial SM, on the subsequent changes in the values of five properly selected hydrological parameters is examined in this research. Overall, the results of the application of the proposed methodology, as presented above, indicate that each descriptor of initial conditions affects the values of these parameters to a different extent and for a variable time period. In general and as expected, the hydrological footprint of forest fires is more intense than the footprint of SM during the first post-fire years. Yet, as a result of the sharply descending impact of fire with time, which is verified by the solid results of the methodology, SM significantly affects the values of the examined parameters at later stages, thus becoming the dominant descriptor of initial conditions when time for hydrological recovery is approaching. It is clarified, that in this research hydrological recovery has been examined based on runoff data, considering peak flows, runoff volumes and times to peak.

As also discussed in Section 5.2, in numerous studies and for reasons of simplification, SM is usually considered to be constantly normal (AMC type II in Table 5.1), or in some cases and for adverse conditions it is considered as constantly wet (AMC type III in Table 5.1) during the rainy season (Berthet *et al.*, 2009). Similarly, the consideration of initial SM conditions is omitted in studies that have been performed in the past for the study area during the implementation of graduate and post-graduate theses (Alonistioti, 2011; Kassela, 2011; Pagana, 2012; Bariamis, 2013). The fact that this assumption may undermine the robustness and the accuracy of hydrological simulation, also commented in Brocca *et al.* (2008), Trambly *et al.* (2012) and Massari *et al.* (2013), is verified as well by the results of the hydrological analysis presented above, where the consideration of three different SM conditions yields results, which are more than satisfactory.

## 8.2 Sensitivity analyses

At this stage of the research a detailed sensitivity analysis, which involves two independent analyses was performed. Initially, a sensitivity analysis was performed in order to quantify the impact of each examined hydrological parameter on simulated runoff volumes. Then, an innovative sensitivity analysis was performed aiming to test the efficiency of the proposed methodology. These analyses are described in detail in Sections 8.2.1 and 8.2.2 respectively.

### 8.2.1 Quantification of the impact of each parameter on runoff volume

The analysis presented in this Chapter has been performed in order to estimate the impact of each one of the five examined hydrological parameters on runoff volumes. To this end, the value of each parameter has been altered by 50%, while keeping every time the values of the other four parameters unchanged. The hydrological model ran for each set of parameter values and the corresponding change in runoff volume was estimated. This analysis was performed for two flood events and the impact of each parameter on runoff volume is summarized in Table 8.2.

Table 8.2. The quantification of the impact of each parameter on runoff volume.

22/02/2013			03/02/2011		
Parameter	Relative change [%] in parameter	Relative change [%] in runoff volume	Parameter	Relative change [%] in parameter	Relative change [%] in runoff volume
CN	50	11.57	CN	50	11.9
IA		12.32	IA		9.10
TP		2.90	TP		0.36
K		0.19	CP		0.89
			K		0.89

It is noted that for adverse conditions and as clarified in the proposed methodology (Section 7.4.4), when applying the methodology for wet conditions CP is considered stable and equal to 0.4, which is its lower limit. Therefore, no change (reduction) has been considered in CP for the wet event (22/02/2013).

Then, aiming to quantify how main model parameter values change after a fire, the relative post-fire change between the parameter values proposed by the methodology and a standard set of parameter values for normal SM conditions and when no recent forest fire has occurred, was estimated for each subbasin and for the three different SM conditions. An average post-fire change in parameter values for all subbasins was estimated and is presented in Figure 8.4.

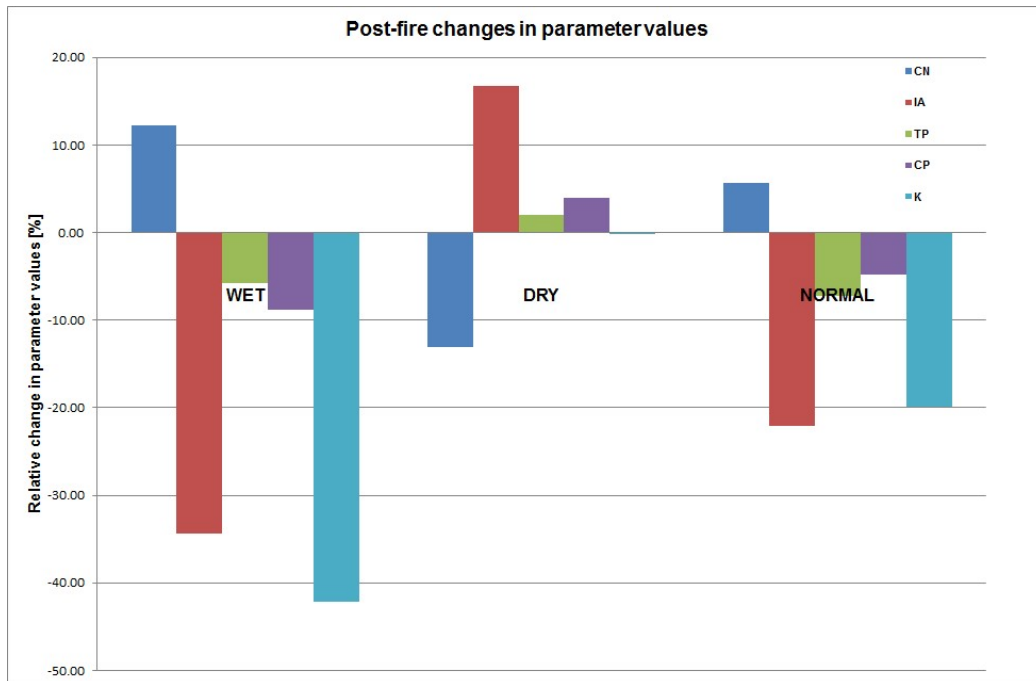


Figure 8.4. The relative change [%] in all parameter values after a fire event, when applying the proposed methodology.

The results of the hydrological analysis and the sensitivity analysis for the quantification of the impact of each examined parameter on runoff volume suggest that CN and IA have a stronger hydrological impact than the other three examined hydrological parameters, *i.e.* TP, CP and K. More specifically, as quantified in Table 8.2, both CN and IA are particularly sensitive hydrological parameters, since changes in their values have a more intense impact on runoff volume than relevant changes in the values of TP, CP and K. As visualized in Figure 8.4, post-fire changes in K are also intense; yet, the impact of K on runoff volume when compared against the impact of the other parameters on runoff volume is trivial, as presented in Table 8.2. To this end, the attribution of representative and accurate values to CN and IA becomes an issue of paramount importance in order to achieve efficient hydrological simulations.

At the same time, the parameters CN, IA and TP, which are associated in the proposed methodology with more severe post-fire changes and longer lasting post-fire impact (up to 48 months, on the contrary to the maximum of 36 months for CP and K), are more sensitive to fire impact and their post-fire values need to be estimated with caution. However, even though post-fire changes in CP and K under variable SM conditions are less intense, they still remain important enough so as not to be underestimated.

## 8.2.2 Efficiency testing of the proposed methodology

In order to test the efficiency of the proposed methodology, *i.e.* the convergence of parameter values given by the application of the proposed methodology and parameter values for best simulations (in terms of best convergence between simulated and observed discharges), a detailed sensitivity analysis has been

performed, following the procedure described below. In this analysis, the values of the five examined hydrological parameters were tested for all six subbasins of the study area (in total 30 values).

More specifically, random sampling was performed for the values of these 30 parameters. For reasons of representativeness, it has been assumed that the random parameters follow a uniform distribution, so as to have equal probabilities of occurrence, rather than a normal distribution, in which the probabilities of occurrence follow the normal distribution curve bell and numbers closer to mean values are thus more likely to be selected. Extended literature review was performed at this stage of this research and concluded that a sampling approach that ensures the representativeness of the ensemble of random values in terms of real variability is Latin Hypercube Sampling (LHS) (McKay *et al.*, 1979; Iman and Conover, 1980; McKay M.D., 1992; van Griensven *et al.*, 2006).

In particular, LHS is a statistical method that adopts a stratified sampling approach, by subdividing the distribution of each parameter into N intervals, with equal probability of occurrence (1/N for each). When parameter values are generated using this approach, then for each parameter each interval is sampled only once. By that way, efficient estimation of output statistics is achieved, since sampling results are non-overlapping (van Griensven *et al.*, 2006; Tolson and Shoemaker, 2008). For these reasons, LHS was considered more appropriate for this application and it was finally applied.

For the application of LHS to all 30 parameters, an original programming code was developed in Matlab7.11.0 (version R2010b), that resulted in the production of 1000 sampled values for each parameter. The code includes three different subroutines that run independently. Each subroutine is properly adjusted so as to be applied to one of the 3 examined initial SM conditions (*i.e.* wet, normal and dry). For this adjustment, the three subroutines differed between each other in the marginal values selected for each initial SM condition mode, for each subbasin and hydrological parameter.

The running of this code results in the generation of three matrixes (one for each subroutine – initial SM conditions mode) with 1000 rows and 20 columns each. Rows correspond to sampled parameter values and columns to parameters; therefore, each row corresponds to one full set of sampled values for each parameter and each subbasin. Then, HEC-HMS ran in batch mode for each set of parameter values, for all initial SM conditions (in total 3000 runs), with each run resulting in simulated discharges at subbasin outlets. It is noted that for adverse conditions, TP and CP of the two core urban subbasins (W16890 and Sub-1) are considered stable, as indicated by the green columns.

The goodness of fit of simulated versus observed discharges, used for validation purposes, was quantified using the NS efficiency. NS was calculated for the locations (subbasin outlets) for which observed discharges are available and for all SM conditions. Columns with 1000 values (one for each run for each SM conditions mode) were produced for these locations and organized in .xlsx files. Given that 1000 values are not easily manageable; the upper 10% of these values was isolated for further analysis. Then, the exact values of the hydrological

parameter that correspond to these 100 best runs were identified for these locations. Statistical analysis was performed for these 100 values, the average values of which for each parameter were compared against the values suggested by the methodology for these parameters and for the given subbasin and SM conditions. Indicative results are presented in the following Tables.

*Table 8.3. Suggested parameter values from the methodology and average parameter values of the best 100 runs of HEC-HMS, for dry SM conditions in Drafi and Rafina-big subbasins.*

Subbasin	Parameter	Suggested from methodology	Av. of best 100 runs	Relative difference [%]
<b>Drafi (W15460)</b>	CN	39	37	<b>5.1</b>
	IA	15	14	<b>6.67</b>
	TP	0.54	0.54	<b>0</b>
	CP	0.52	0.52	<b>0</b>
	K	0.86	0.85	<b>1.16</b>
<b>Rafina-big (W15020)</b>	CN	44	42	<b>4.5</b>
	IA	16	17	<b>-6.3</b>
	TP	0.88	0.87	<b>1.1</b>
	CP	0.47	0.45	<b>4.3</b>
	K	1.67	1.67	<b>0</b>

*Table 8.4. Suggested parameter values from the methodology and average parameter values of the best 100 runs of HEC-HMS, for wet SM conditions in Drafi, Rafina big and Rafina small subbasins.*

Subbasin	Parameter	Suggested from methodology	Av. of best 100 runs	Relative difference [%]
<b>Drafi (W15460)</b>	CN	48	47	<b>2.1</b>
	IA	11	12	<b>-9.1</b>
	TP	0.49	0.49	<b>0</b>
	CP	0.4	0.4	<b>0</b>
	K	0.50	0.49	<b>2</b>
<b>Rafina-big (W15020)</b>	CN	57	57	<b>0</b>
	IA	11	12	<b>-9.1</b>
	TP	0.80	0.79	<b>1.3</b>
	CP	0.4	0.4	<b>0</b>
	K	0.91	0.92	<b>-1.1</b>
<b>Rafina-small (W16340)</b>	CN	57	57	<b>0</b>
	IA	10	10	<b>0</b>
	TP	0.70	0.69	<b>1.4</b>
	CP	0.4	0.4	<b>0</b>
	K	0.65	0.65	<b>0</b>

The marginal values originally selected for each one of the total 30 parameter and for all three SM conditions, were within limits that make sense for the study area,

given its hydromorphology and geomorphology, targeting a more realistic approach. For a more generalized approach, different marginal values for wider limits were also tested. To this end, changes had to be made in all subroutines of the original programming code in Matlab, so that sampling areas would be wider. This procedure was followed for both **moderate limits** (wide limits that exceed the originally selected limits) and **wide limits** (even wider limits that include all values of the parameters acceptable in literature). Therefore, new 1000x30 matrixes for each SM conditions mode and for both moderate and wide limits were generated. Indicative results from this additional analysis are presented in the following Tables.

*Table 8.5. Suggested parameter values from the methodology and average parameter values of the best 100 runs of HEC-HMS, for dry SM conditions in Rafina-big subbasins, for moderate limits.*

Subbasin	Parameter	Suggested from methodology	Av. of best 100 runs	Relative difference [%]
Rafina-big (W15020)	CN	44	38	13.6
	IA	16	16	0
	TP	0.88	0.72	18.2
	CP	0.47	0.53	-12.8
	K	1.67	1.30	22.2

*Table 8.6. Suggested parameter values from the methodology and average parameter values of the best 100 runs of HEC-HMS, for wet SM conditions in Rafina big and Rafina small subbasins, for moderate limits.*

Subbasin	Parameter	Suggested from methodology	Av. of best 100 runs	Relative difference [%]
Rafina-big (W15020)	CN	57	57	0
	IA	11	12	-9.1
	TP	0.80	0.63	21.25
	CP	0.4	0.4	0
	K	0.91	0.72	20.9
Rafina-small (W16340)	CN	57	61	-7.0
	IA	10	11	-10
	TP	0.70	0.55	21.4
	CP	0.4	0.4	0
	K	0.65	0.78	-20

Table 8.7. Suggested parameter values from the methodology and average parameter values of the best 100 runs of HEC-HMS, for dry SM conditions in Drafi and Rafina-big subbasins, for wide limits.

Subbasin	Parameter	Suggested from methodology	Av. of best 100 runs	Relative difference [%]
Drafi (W15460)	CN	39	38	2.56
	IA	15	14	6.67
	TP	0.54	0.64	-18.5
	CP	0.52	0.60	-15.4
	K	0.86	1.05	-22.1
Rafina-big (W15020)	CN	44	42	4.5
	IA	16	14	12.5
	TP	0.88	0.66	25
	CP	0.47	0.60	-27.7
	K	1.67	1.10	34.1

Table 8.8. Suggested parameter values from the methodology and average parameter values of the best 100 runs of HEC-HMS, for wet SM conditions in Rafina big subbasin, for wide limits.

Subbasin	Parameter	Suggested from methodology	Av. of best 100 runs	Relative difference [%]
Rafina-big (W15020)	CN	57	49	14.0
	IA	11	14	-27.3
	TP	0.80	0.66	17.5
	CP	0.4	0.58	-45
	K	0.91	1.16	-27.5

Regarding the results of the sensitivity analysis, as quantified in Tables 8.3 – 8.8, it becomes evident that the relative difference between the values of the parameters suggested by the methodology and the average values from the 100 best runs of HEC-HMS for values sampled with LHS is small. This is particularly true for the **narrow limits** for the marginal values selected for the sampled parameters (Tables 8.3 and 8.4), as expected, given that these limits are more representative for this case study. In this case, the mean absolute relative difference for dry conditions for Drafi subbasin is 2.6% and for Rafina-big subbasin is 3.2%, while the mean absolute relative difference for wet conditions for Drafi subbasin is 2.6%, for Rafina-big subbasin is 2.3% and for Rafina-small subbasin is 0.3%. These small differences remain trivial when translated into differences in values of parameters of significance for flooding, such as flow discharge, runoff volume, flood extent *etc.* It is also highlighted that in several cases, the value suggested from the methodology coincides (0% relative difference) with the average value of the best model runs.

As far as the results of the analysis for moderate limits for the marginal values are concerned (Tables 8.5 and 8.6), the mean absolute relative difference for dry conditions for Rafina-big subbasin is 13.4%, while the mean absolute relative

difference for wet conditions for Rafina-big subbasin is 10.3% and for Rafina-small subbasin is 11.7%. Again, in several cases for the moderate limits, the value suggested from the methodology coincides (0% relative difference) with the average value of the best model runs.

The results of the analysis for wide limits for the marginal values (Tables 8.7 and 8.8), show greater relative differences; yet, even in that case, the differences are for no reason significant enough so as to restrict the applicability of the proposed methodology. More specifically, the mean absolute relative difference for dry conditions for Drafi subbasin is 13.0% and for Rafina-big subbasin is 20.8%, while the mean absolute relative difference for wet conditions for Rafina-big subbasin is 26.3%. Of course, wide limits were only tested for reasons of comparison with the other set of limits, in the framework of a more generalized approach, as discussed in Section 8.2. In practice, when examining a particular case study, the particularities of which are known, limits do not need to exceed the narrow ones. As a general comment, it becomes evident from Tables 8.3 – 8.8 that the estimated mean absolute relative difference for all three cases of limits for marginal values is low, considering the slight deviation in the parameter values *per se*.

### **8.3 Flood Mapping**

As discussed in detail in Chapter 4, in order to produce flood maps, which are critical elements of flood risk management, it is necessary to run a model chain that consists of a hydrological model for the hydrological simulations that transform rainfall to runoff and a hydraulic model for the hydraulic simulations that transform runoff discharges to water levels. Appropriate software either incorporated in or compatible with hydraulic models, can support the generation of floodplains from water levels along the river for a given rainfall event. The hydraulic modelling performed in this research for the production of flood maps after the incorporation of the methodology proposed in Chapter 5 in the hydrological model HEC-HMS, as well as the procedure followed for flood mapping, which is compliant with the generic procedure discussed in EXCIMAP (2007), is described in the following.

#### **8.3.1 Hydraulic modelling**

Out of the long list of efficient hydraulic models that has been compiled and is presented in Section 4.4, the HEC-RAS model was selected for the hydraulic simulations in this research, for the reasons presented in more detail in Section 4.6.

Prior to the setting up and running of HEC-RAS, the GIS extension HEC-GeoRAS and especially the version HEC-GeoRAS 4.3 (Ackerman, 2011) ran in GIS environment and in particular using ArcGIS 9.3. Initially, the basic layers were created through the RAS Geometry menu. These layers include the stream centerline (and concern its editing, digitization and the assignment of river and reach names to the stream network), the main channel banks (and concern its editing and digitization), the flowpath centerlines (and concern the assignment of left, channel or right line type to the flow paths) and the cross-sectional cut lines



(which were automatically generated at specified intervals and widths). Then, the Stream Centerline attributes (topology, lengths/stations) and XS Cut Lines attributes (river/reach names, stationing and elevations) were assigned to the corresponding layers. By that way, an .sdf data file, which is exportable to HEC-RAS was created.

The geometric information included in this file was imported in HEC-RAS and more specifically the version 4.1 of HEC-RAS (Brunner, 2010), so as to perform the hydraulic analysis. A new project was then created for each subbasin and using the “Cross Section Editor” a value for Manning’s roughness coefficient,  $n$ , was assigned to each reach. Table 8.9 summarizes the Manning’s roughness coefficients attributed to the reaches of all subbasins. The same value of  $n$  was used for the riverbed and the river banks of each subbasin.

*Table 8.9 Manning’s roughness coefficients for the riverbed and the river banks of all subbasins of Rafina catchment.*

Subbasin	Drafi	Spata	Rafina	Rafina2	Urban
<b>Manning’s roughness coefficient, <math>n</math></b>	0.05	0.03	0.04	0.035	0.03

HEC-RAS was set up and run for steady flow analysis. Therefore, for adverse conditions, and as far as hydrological-hydraulic coupling is concerned, the peak flows of the hydrographs produced from HEC-HMS for the outlets of all subbasins were imported in HEC-RAS. Mixed subcritical and supercritical flow regime was selected as more representative for this research. Normal depth upstream and downstream was selected for boundary conditions.

HEC-RAS ran for different design floods and variable initial conditions in terms of SM and forest fire, as discussed in Section 3.3.2. The hydraulic analysis resulted in the transformation of flows into water levels along river reaches. HEC-RAS outputs include cross-section profiles, perspective plots and data tables.

### **8.3.2 Flood hazard mapping**

After the coupled running of the hydrological-hydraulic model chain, flood hazard maps can be produced. Flood hazard maps are maps on which the boundaries of the floodplain and thus the flood hazard areas along the river are delineated and they are produced for design floods that correspond to different levels of probability of occurrence. In this research, flood hazard maps are produced for floods with low, medium and high probability of occurrence, similarly to the requirements for flood hazard mapping as expressed in the EU Floods Directive (Directive 2007/60/EC). The selected return periods for flood hazard mapping are  $T=5$  years (for high probability of occurrence),  $T=200$  year (for medium probability of occurrence) and  $T=1000$  years (for low probability of occurrence). The design storms for these return periods for each subbasin were estimated and imported as rainfall input in HEC-HMS.

As far as initial conditions are concerned, flood maps are produced for normal SM and recently burnt (less than 7 months post-fire period) conditions and for wet and no longer affected by the latest fire (more than 36 months post-fire period)

conditions. The reason for the selection of these conditions is that the first one (normal SM and recently burnt land) represents typical post-fire conditions, while the latter (wet SM and land no longer affected by the latest fire) corresponds to the worst case for current conditions in the area.

A typical procedure in order to produce flood hazard maps is to use the RAS Mapping option of HEC-GeoRAS. According to this procedure, an .sdf output file from HEC-RAS that includes information on the water levels for all cross sections is imported in HEC-GeoRAS (in GIS environment) and converted to .xml file. The DSM and additional layers that include hydraulic information are imported in GIS, new layers with topographic information (e.g. a new layer for cross sections and another one for boundary inundation) are created and water surface for each cross-section is generated. A comparison between DSM and water surface results in floodplain delineation.

Another option in recent versions of HEC-RAS is to use RAS Mapper in HEC-RAS environment (also mentioned in Section 4.4.1.1) and import the necessary topographic information so as to produce the floodplain without using GIS. In this research, the flood model chain ran for the design storms and initial conditions mentioned above and a code in python developed during the implementation of the FLIRE Project (Papathanasiou *et al.*, 2013b; Kochilakis *et al.*, 2016a) was applied for the production of the corresponding floodplains, *i.e.* the flood hazard maps. Flood hazard maps produced for normal SM, recently burnt conditions and T=5, 200 and 1000 years and wet SM, no longer affected by fire conditions and T=5, 200 and 1000 years are presented in Figures 8.5 and 8.6, where the boundary of the study area is marked with the red line.

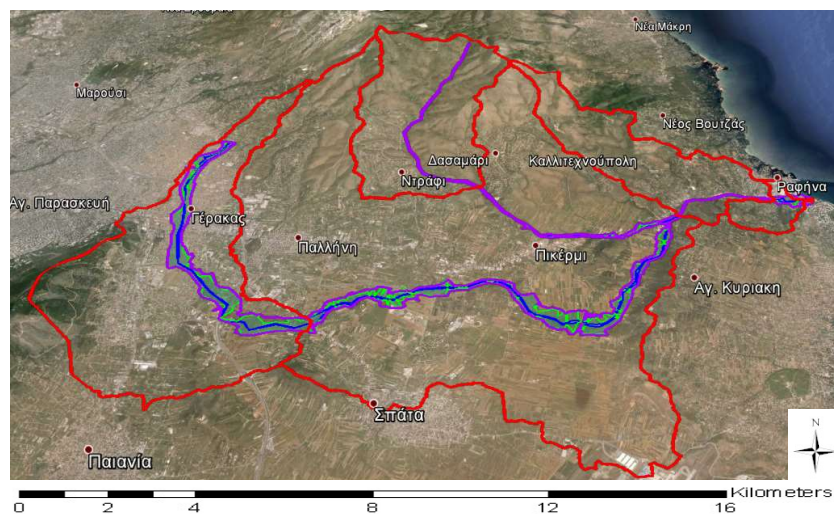


Figure 8.5. A Google Earth map with the flood hazard maps for T=5 years (blue line), T=200 years (green line) and T=1000 years (purple line) for normal SM, recently burnt conditions.

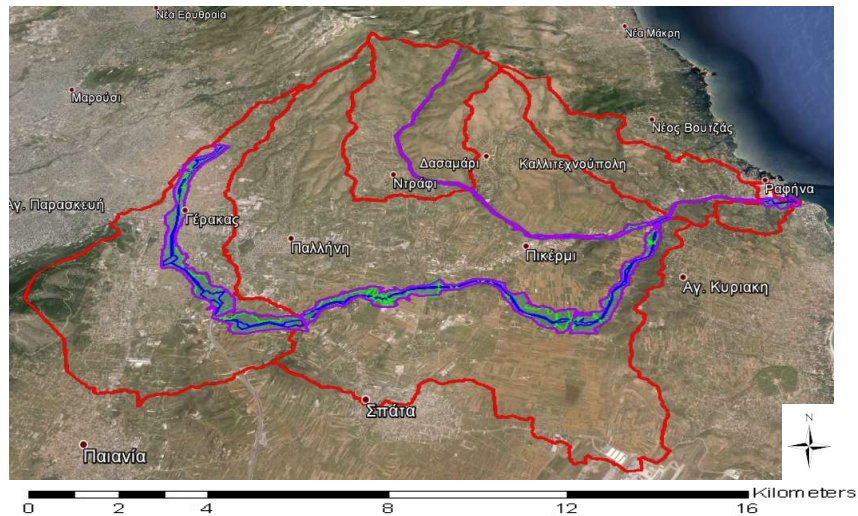


Figure 8.6. A Google Earth map with the flood hazard maps for  $T=5$  years (blue line),  $T=200$  years (green line) and  $T=1000$  years (purple line) for wet SM, unburnt conditions.

### 8.3.3 Flood risk mapping

Flood risk maps were also produced for the study area for different scenarios that correspond to flood events of low, medium and high probability. Flood risk maps include information on the probability of occurrence of a flood event and the potential adverse consequences of this flood event on humans, the environment and the economic activity associated with the event (Directive 2007/60/EC). In this research, the potential adverse consequences associated with the examined flood scenarios are expressed through a normalized index that incorporates elements of socioeconomic and environmental interest.

More specifically, a static flood vulnerability map was developed using normalized values of five properly selected socioeconomic and environmental parameters, the values of which were normalized to a scale between 1 and 5. These parameters include population density, key customers, *i.e.* important buildings, structures and services such as hospitals, schools and public services, property values and road network (socioeconomic parameters) and pollution sources, *i.e.* industrial areas (environmental parameters). A similar approach has been applied in the study area for the implementation of the FLIRE Project (Papathanasiou *et al.*, 2013b).

Population density refers to population within the boundaries of the Municipalities, as available from population census of 2011<sup>35</sup>, while property values are retrieved from relevant information for each Municipality, as available for 2007 from the Greek Ministry of Finance<sup>36</sup>.

After the normalization of these parameters according to a 1-5 scale, respective layers for each parameter were created in GIS environment. Buffer zones of 100,

<sup>35</sup> Source: <http://www.geodata.gov.gr/geodata/>.

<sup>36</sup> Source: [http://www.gsis.gr/gsis/info/gsis\\_site/Services/Polites/Antikeimenikes.html](http://www.gsis.gr/gsis/info/gsis_site/Services/Polites/Antikeimenikes.html).

300, 500, 700 and 1000 m were set around the key customers and the pollution sources layers, while buffer zones of 50, 100, 300, 500 and 700 m were set around the road network layer. A different, properly selected weight was attributed to each layer, following environmental and socioeconomic criteria. A layer for floodplain is also considered even though for the static map this layer has zero values. These weights are summarized in Table 8.10. The static flood vulnerability map was created by superimposing each layer on the others, considering also its particular weight. The final static flood vulnerability map is presented in Figure 8.7.

*Table 8.10 The weights attributed to each layer of the static flood vulnerability map.*

Layer	Population density	Key customers	Property values	Road network	Pollution sources	Floodplain
Weight	0.17	0.17	0.14	0.12	0.15	0.25

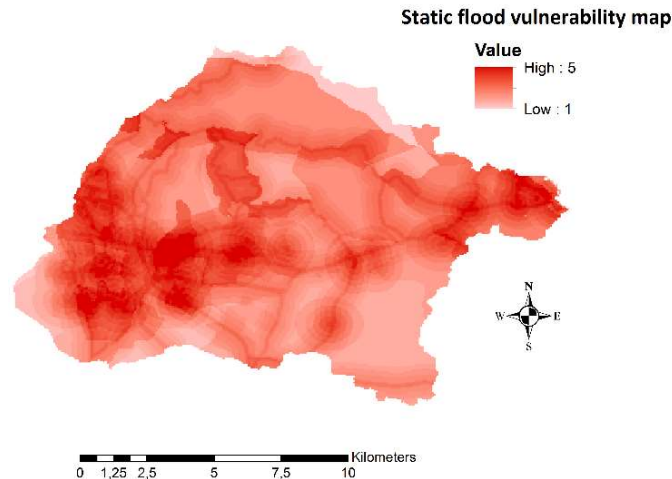


*Figure 8.7. The static flood vulnerability map of Rafina catchment.*

The flood hazard maps that were produced as discussed in Section 8.3.2 were then imposed over the static flood vulnerability map in GIS environment, as illustrated in Figure 8.8 and by that way six flood risk maps (for the three flood interval periods and the two different initial conditions considered in flood hazard mapping) were produced. For adverse conditions, a buffer zone was set around the floodplain layer. This buffer zone was different for each flood hazard map and was calculated according to the maximum floodplain width. The half distance of the maximum floodplain width was the buffer zone for each flood hazard map (for normal and recently burnt conditions: 125 m for T=5 years, 225 m for T=200 years and 325 m for T=1000 years and for wet and no longer affected by recent fire conditions: 150 m for T=5 years, 300 m for T=200 years and 335 m for T=1000 years). The flood risk maps for T=5, 200 and 1000 years for both normal and recently burnt conditions and wet and no longer affected by recent fire conditions are presented in Figure 8.9.

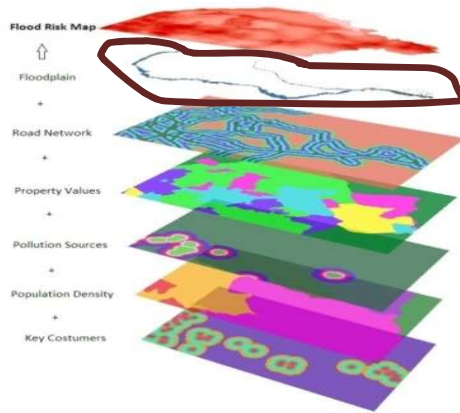


Figure 8.8. The different layers used in the production of the flood risk maps.

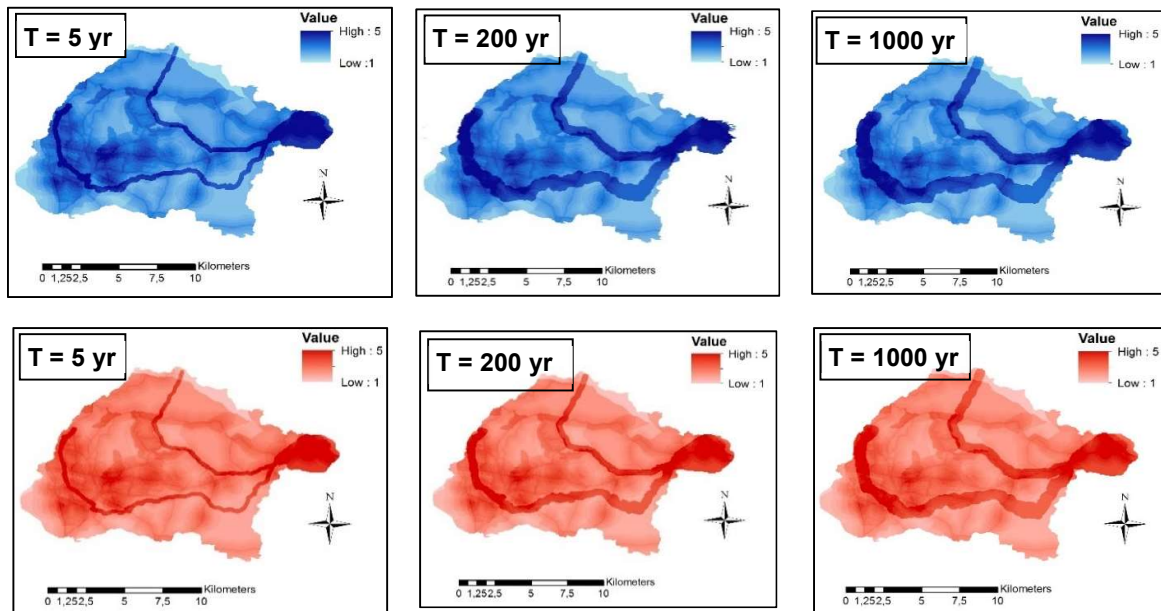


Figure 8.9. Flood risk maps for  $T=5$ , 200 and 1000 years for wet and no longer affected by recent fire conditions (upper row) and for normal and recently burnt conditions (lower row).

As verified by the analysis presented in Section 8.1, summarized in Table 8.1 and illustrated in Figures 8.1, 8.2 and 8.3, simulation results when the methodology is applied are significantly improved when compared against the corresponding results when the methodology is not applied. The analysis concluded that this is especially true for adverse conditions, *i.e.* for wet SM conditions and flood events after a recent forest fire. More specifically, when the methodology is applied, the simulated peak flows, runoff volumes and times to peak match well to the corresponding values derived from observed datasets, when available. As also discussed in this Section, simulated flows may be significantly underestimated when the methodology is ignored, with obvious negative effects for downstream flood estimation.

The outcomes of the sensitivity analyses presented in detail in Section 8.2, as summarized in Tables 8.2 – 8.8 and illustrated in Figure 8.4, also strengthen the statement that the application of the proposed methodology for the estimation of values of CN, IA, TP, CP and K, renders the simulations of the hydrological behavior of the examined catchment more accurate and representative.

Therefore the incorporation of the proposed methodology in flood assessment, *i.e.* the consideration of initial conditions, both in terms of fire occurrence and SM in a flood model chain, yields more accurate and representative simulations and hence results in the production of more accurate flood hazard and corresponding flood risk maps.

Importantly, the proposed methodology can significantly improve the accuracy of near-real time FEWS and civil protection platforms. This is because, as discussed in detail in Section 3.5, FEWS need to be up to date with reliable information in order to perform representative flood simulations and issue accurate warnings. In practice, typical operational FEWS in fire-prone areas either ignore the potential fire impact (*e.g.* Berni *et al.*, 2009) or, even when fire is considered, they do not account for fires-floods interaction (*e.g.* Kalabokidis *et al.*, 2005) and as such, they become less reliable whenever a fire event occurs in the area in which they are deployed. Hence, the incorporation of the proposed methodology in such systems can support more reliable flood simulations and issuing of more accurate warnings – that actually take into account the changes in the catchment's response that occur after fire events.

One such system is the FLIRE DSS that has been developed for the study area (Kochilakis *et al.*, 2016a; Kochilakis *et al.*, 2016b; Kotroni *et al.*, 2015; Papathanasiou *et al.*, 2015b; Poursanidis *et al.*, 2015a; Poursanidis *et al.*, 2015b; Poursanidis *et al.*, 2015c; Poursanidis *et al.*, 2015d; Papathanasiou C., 2015). So far, the flood model chain of the system is set up using only a limited part of the proposed methodology. The automatic integration of the complete methodology in the FLIRE platform would be particularly interesting and would verify the value and usability of the methodology in the undesirable case of a future fire event in the area.

## CHAPTER 9: CONCLUSIONS

The overall aim of this research is to support flood risk assessment under post-fire conditions for typical Mediterranean periurban catchments, taking also into consideration initial soil moisture conditions. To this end, a methodological framework to theoretically estimate the dynamic evolution of representative hydrological parameters as a function of time, following the occurrence of forest fires, has been developed and applied in a Mediterranean periurban area in Eastern Attica. The results of the analysis verify the efficiency of the developed methodology in determining flood risk in a representative way. Efficient flood risk assessment can in turn support flood risk management in the long run. This Chapter summarizes the main findings of the research, regarding the proposed methodological framework, the adopted methodology for the implementation of this research and the case study, conclusions drawn during its implementation, as well as recommendations for further research.

### 9.1 Conclusions

Both floods and forest fires are natural hazards, and therefore their generation mechanisms are strongly associated with imponderable factors. Yet, if appropriate measures and practices for threatened areas are adopted in advance, then their impact on humans and the environment will be definitely reduced or even eliminated to the greatest extent possible, while under particular circumstances their probability of occurrence will also be reduced.

An integrated approach towards efficient hydrological modelling involves the calibration of properly selected hydrological parameters, which are associated with all features of flood hydrographs (*i.e.* runoff volumes, peak discharges and times to peak). This research concludes that the calibration of CN, IA, TP, CP and K, which are typical parameters, included in the vast majority of modelling structures, yields optimum simulation results, on the contrary to current calibration practice which usually involves the calibration of some of these parameters, and more frequently CN and IA. TP, CP and K are definitely less sensitive calibration parameters than CN and IA since they have a less intense impact on runoff volume; however, they still need to be properly calibrated for more representative hydrological simulations (Papathanasiou *et al.*, 2015a).

During this research, a gap has been identified in literature regarding the estimation of the hydrological footprint of a forest fire on a typical Mediterranean ecosystem and its incorporation in hydrological modelling. In the absence of an integrated methodology for this estimation, the post-fire hydrological footprint was eventually either ignored or only examined for a limited period (the first post-fire period) and for specific case studies with particularities. The comprehensive methodology developed for this dissertation, allows for the dynamic estimation of this footprint in time, without restricting its application to particular case studies and considering also the fact that some time after fire occurrence, hydrological recovery occurs. The research concludes that the post-fire impact is very intense during the first post-fire period, while it is sharply decreasing with time, until

hydrological recovery occurs and the post-fire hydrological footprint vanishes (Papathanasiou *et al.*, 2015a).

The research also concludes that post-fire impact is not the same on all examined hydrological parameters. As discussed in Chapter 8, CN and IA are more sensitive parameters to fire impact than TP and CP and to a lesser extent K and are thus associated with more severe post-fire changes and longer lasting post-fire impact. Post-fire changes in K may in some cases be intense, as presented in Figure 8.4; however changes in K do not affect significantly the hydrological simulations, as verified by Table 8.2. Hence, it is of paramount importance to attribute representative and accurate values to CN and IA for representative post-fire simulations. At the same time, the post-fire changes in TP, CP and K under variable SM conditions, whilst less intense and especially for CP and K temporally shorter, still remain important and need to be properly assessed.

The current research also highlights the importance of considering initial SM conditions, even in the application of an event-based hydrological model. Standard practice is the consideration of SM conditions when applying continuous rainfall-runoff models, so as to simulate in a representative way the complex interaction between rainfall and SM and result in efficient modelling results (Massari *et al.*, 2014, Camici *et al.* 2011). In event-based models, which need reduced parameterization so as to be easily applied and with low computational effort, SM is usually ignored or considered stable (either continuously normal or continuously wet for adverse conditions). The methodology proposed in this research suggests the incorporation of SM conditions in event-based models as well, and concludes that the co-evaluation of SM with post-fire conditions yields optimum simulation results, as verified from the results presented in Chapter 8.

In general, the post-fire impact is more intense on all examined parameters than the impact of initial SM during the first post-fire years. For this reason, fire occurrence can be characterized as the dominant descriptor of initial conditions during this period. However, given that fire impact is sharply descending with time, several months after fire (their number depending on FS, the examined parameters and hydrometeorological and geomorphological particularities of the case study, as analysed in detail in previous Chapters) hydrological recovery is approaching. Then, the impact of SM becomes increasingly important and eventually SM replaces fire-impact and becomes the dominant descriptor of initial conditions from that period and on, determining the changes in the values of the examined parameters.

A sensitivity analysis was performed in this research for the efficiency testing of the proposed methodology. During this analysis, the parameter values retrieved from a smart random sampling and which are associated with the optimum hydrological simulations were compared against the parameter values retrieved from the application of the proposed methodology. Attention had to be paid on the selection of appropriate limits for the marginal values of the parameters from which sampling would be performed in order to achieve representative random sampling. It can be concluded that the optimum limits are case-specific, since they need to make sense for the particular hydromorphology and geomorphology of the study area and thus need to be carefully set for every case study.



In order to apply the proposed methodology to other areas, the key factor that needs to be reexamined is the temporal dimension of the impact of forest fires in those areas, considering indigenous vegetation, canopy and local climatic characteristics as well as other particularities during the first post-fire period, which determine vegetation development, fire-tolerance, regrowth *etc.*, as analyzed in detail in Section 5.5. By that way, case-specific particularities can be considered and incorporated in a properly adjusted methodology.

For efficient hydrological simulations, the prevailing conditions in the complex and dynamically changing typical periurban Mediterranean environment need to be represented in a simple, though realistic way. In addition, a generalized (not localized) and flexible approach, as discussed above, needs to be adopted, so that case-specific particularities do not restrict its applicability. The co-evaluation of findings from literature and case-specific features further supports representative simulations.

## 9.2 Overview of main findings

The main findings of this research include main findings of the methodology and main findings for the particular case study that was examined. Regarding the main findings of the methodology, they can be classified into findings from the proposed methodological framework for the estimation of the hydrological footprint of initial conditions (described in Chapter 5) and findings from the methodology *per se* that has been adopted for the implementation of the research. An overview of these findings is presented in the following paragraphs.

### 9.1.1 Main findings of the methodology

The main findings of the proposed methodological framework for the estimation of the hydrological footprint of initial conditions and its incorporation in hydrological modelling are listed below:

- Both descriptors of initial conditions examined in this research, *i.e.* forest fires and SM, affect the values of properly selected hydrological parameters to a different extent and for a variable time period.
  - CN and IA are more sensitive calibration parameters in hydrological modelling than TP, CP and K, since they have a stronger hydrological impact.
  - CN and IA are more sensitive parameters to forest fire and SM impact than TP, CP and K.
  - Post-fire changes in K are in some cases more intense than post-fire changes in TP and CP.
  - K has the minimum impact on runoff volume in comparison with the impact of all the other examined parameters.
  - For CN, IA and TP, the post-fire impact remains 48 months for very high FS, 36 months for high FS and 24 months for moderate and low FS.

- For CP, the post-fire impact remains 36 months for very high FS, 24 months for high FS and 19 months for moderate and low FS.
- For K, low and moderate FS classes can be merged. The post-fire impact remains 36 months for very high FS, 24 months for high FS and 19 months for moderate (and low) FS.
- For an integrated approach towards efficient hydrological modelling, it is necessary to identify and calibrate appropriate, representative parameters that are associated with all aspects of flood hydrographs, *i.e.* parameters that affect runoff discharges, peak flows and times to peak (such as CN, IA, TP, CP and K), instead of confining the calibration exclusively to the typically used parameters (usually CN and IA).
- The hydrological footprint of forest fires is more intense than the impact of SM on a catchment's hydrological response during the first post-fire years.
- The impact of forest fires on the hydrological behavior of a catchment is sharply descending with time. In typical Mediterranean areas and for fire conditions similar to those prevailing in the study area, this impact can be considered negligible beyond 48 months.
- SM is the dominant descriptor of initial conditions at later stages, when time for hydrological recovery is approaching, since at these stages the impact of SM on the values of the examined parameters is more intense.
- The assumption that SM can be considered as constantly normal, or constantly wet for adverse conditions during the rainy season, while in some cases it may also be ignored (as discussed in Section 8.4) undermines the robustness and the accuracy of hydrological simulations.
- The consideration of three different SM conditions, *i.e.* wet, normal and dry conditions in hydrological simulations, yields optimum results, when compared against simulations that do not consider this variation in SM conditions.
- The changes in parameter values for variable initial conditions suggested from the proposed methodology result in improved hydrological simulations in comparison with the simulations when the methodology is not applied.

The main findings of the methodology *per se* adopted in this research for efficient flood risk assessment under variable initial conditions are listed below:

- An efficient way to perform a sensitivity analysis for testing the accuracy of parameter values for hydrological modelling suggested by a methodology is the comparison of those values with parameter values retrieved from LHS and yield optimum hydrological simulations.
- The optimum limits for the marginal values of examined hydrological parameters that need to be set for the random sampling in the sensitivity analysis are case-specific, since the particular characteristics of the study area needs to be considered.

- When initial conditions, in terms of both fire occurrence and SM are considered in hydrological and hydraulic modelling, then more accurate flood hazard and respectively flood risk maps are produced.

### **9.1.2 Main findings for the case study**

The main findings of the methodology adopted in this research for Rafina catchment are listed below:

- The geological structure of the study area, its downstream impermeable soils, steep upstream slopes and flat downstream areas and its dense upstream hydrographic network contribute to the quick drainage of the catchment. The area is also characterized by unprecedented urban development, while the existing hydraulic works are inadequate to release floods. As a result, the area is particularly vulnerable to floods.
- The particular vegetative land cover of the study area is highly flammable. At the same time, the recent intense population growth has not been followed by a relevant improvement of the fire-fighting infrastructure, while owners of extended forested land in the area press for conversion of forests to urban zones. Therefore, the forested areas of Rafina catchment are particularly prone to forest fires, especially during the summer and dry season.
- The hydrometeorological and geomorphological features of Rafina catchment together with its vulnerability to both flash floods and forest fires, contribute to its characterization as a typical Mediterranean area.
- Further to that, the area is characterized by mixed and to some extent conflicting land cover and land uses. Forests in the upstream parts are succeeded by cultivated land, industrial zones and urban cells with constantly increasing urbanization rate at the downstream areas. Due to these characteristics Rafina catchment can also be characterized as a typical periurban area.
- In order to apply the methodology as suggested and not readjust it so that the first post-fire floods are simulated in a more representative way, some additional conditions need to be fulfilled for the case study. Further to the particular geomorphological features for which this methodology was developed and are all fulfilled by Rafina catchment, these conditions also include not particularly erosive rainfalls during the first post-fire period, limited livestock activities and successively burnt forest land. A detailed analysis of the study area presented in Chapter 8 concluded that Rafina catchment also fulfills these additional conditions and can thus be safely considered an ideal case study for this research.
- Another characteristic that renders the area an ideal case study for this research is its regular monitoring by reliable hydrometeorological networks. The Hydrological Observatory of Athens (HOA) and the National Observatory of Athens (NOA) operate within the boundaries of the catchment reliable, state-of-art gauges that monitor on a real-time basis its hydrometeorological regime. Such historical as well as real-time

measurements are necessary for representative hydrological simulations and were critical for the implementation of this research.

- As a result of the successive forest fires that have affected the study area during the last decades, the particular plant species that are dominant in this flood prone area have evolved adaptation mechanisms for post-fire regeneration. The forest composition has thus changed in comparison to its former composition, and it includes now more fire-tolerant species. Therefore, hydrological recovery to the pre-fire status after a new forest fire is expected to occur sooner than hydrological recovery of an area that has been less affected by fires.
- Standard practice in hydrological simulations performed for the study area in the past was the omission of SM conditions during the setting up of the hydrological models and their consideration as constantly normal for reasons of simplicity (Alonistioti, 2011; Kassela, 2011; Pagana, 2012; Bariamis, 2013). However, the consideration of three different states of SM conditions (wet, normal and dry) that was adopted in this research yields more reliable hydrological simulations for Rafina catchment, as verified in Chapter 8, and is suggested to be incorporated in all future hydrological simulations.
- Given the vulnerability of the study area to floods, which is intensified by the fact that the area is also vulnerable to forest fires, another natural hazard that has adverse effects on flood vulnerability, its fortification with a modern and reliable FEWS emerges as a necessity. Such a platform will be an efficient tool for relevant authorities, which will support real-time flood risk management.
- Numerous studies for flood risk assessment and management have been implemented during the last decades for Rafina catchment (e.g. Machairas Design Office, 1984; HYDROTEK *et al.*, 1996; HYDROTEK *et al.*, 1997; METER Consulting Engineers, 1998a and 1998b; HYDROEXIGIANTIKI Consulting Engineers *et al.*, 1999a and 1999b; HYDROEXIGIANTIKI Consulting Engineers *et al.*, 2008), usually including several suggestions for structural works (sometimes large-scale works) that could be constructed in the area. So far, as mentioned above and verified by the flood hazard and flood risk maps produced for the study area and presented in Chapter 8, the catchment and more specifically its most urbanized areas are particularly vulnerable to floods and therefore the inefficient flood risk management on a planning basis in Rafina catchment prevails.

### 9.3 Further research

The methodology presented in detail in Chapter 5 of in this research, has been developed for typical Mediterranean periurban areas, with particularities during the first post-fire period as presented in Section 5.5. The methodology has been expressed in a generic way and then it has been tested on a specific case study that fulfills the conditions so as to be characterized typical Mediterranean periurban area and of course prone to both natural hazards examined in this research (*i.e.* floods and forest fires), as well as their interaction. More specifically,

it has been applied using detailed datasets for the fire of August of 2009 and post-fire flood events in Rafina catchment.

For further research, the methodology could be tested to other case studies, with similar characteristics, in terms of land use/land cover properties, urbanization rate, hydrometeorological, geomorphological features *etc.* In such applications, the methodology will be replicated with the spatial extent and severity of the studied fire events being determined first and followed by properly selected changes in marginal values of the examined parameters, when necessary.

Similarly, further research could focus on the expansion of the applicability of this methodology to other areas, which are of course typical Mediterranean periurban ones, yet they do not share the specific particularities during the first post-fire period. The testing of the methodology to other, different case studies, also involves the determination of the spatial extent and severity of the studied fire events; however the other parts of the proposed methodology may need major readjustment. More specifically, this readjustment could concern not only the selection of appropriate marginal values for the examined parameters, but also the potential expression of different equations that associate pre-fire with post-fire values, vegetation-specific  $t_{upper}$  and  $t_{lower}$  values (which depict the recovery rate and the duration of hydrological recovery) *etc.* For example when forests are not affected by successive forest fires, then dominant vegetation may have not developed adaptation mechanisms and thus hydrological recovery might occur later, if at all, and/or following a different rate.

As clarified in Chapter 5, the methodology proposed in this research has been developed for deterministic, physically-based, lumped or (semi-)distributed, event-based or continuous hydrological models. It has then been applied in the deterministic, physically-based HEC-HMS hydrological model, which ran in semi-distributed and event-based mode. It would be interesting to incorporate the proposed methodology in deterministic, physically-based models, set up in lumped and event-based or continuous mode or semi-distributed and continuous mode. Thus, incorporated either in hydrological models other than HEC-HMS or even in HEC-HMS which would be in that case set up in a mode other than semi-distributed and event-based.

Another recommendation for further research concerns the use of remotely sensed SM datasets instead of estimated SM using the total rainfall during the 5 previous days, which is used in this research. As discussed in Chapter 5, reliable SM datasets could be retrieved from dense networks of SM sensors installed in appropriate locations over an examined catchment and properly selected depths in the soil. Another recent trend in this field concerns the use of SM datasets retrieved from satellite imagery, such as the Advanced Scatterometer (ASCAT) products (Massari *et al.*, 2014; Trambly *et al.*, 2012), used either as stand-alone datasets (Chen *et al.*, 2014; Wanders *et al.*, 2012) or after being calibrated with ground SM measurements (Dorigo *et al.*, 2014; Su *et al.*, 2013; Albergel *et al.*, 2013). Potential drawbacks of these techniques are analyzed in Section 5.2. Yet, as intensive progress is being made in this field, both sources of information and particularly datasets retrieved from satellite are expected to become increasingly reliable, even when high resolution datasets are required. Therefore, the testing

of the proposed methodology after being properly adjusted so as to use remotely sensed SM, would be scientifically interesting.

Research could also be made in the examination of the impact of inter-event time period on the estimation of SM conditions. Inter-Event Time Definition (IETD) represents the minimum time period between rainfall events that are considered independent. The importance of IETD in the accuracy of flood modelling has been acknowledged in literature (Aryal *et al.*, 2007). Yet, its selection is usually case-specific. Hijoka *et al.* (2006) use IETD equally to 8 hours for an urban catchment in Japan and Raimondi and Becciu (2015) suggest IETD 10 hours for the design of flood control detention facilities. Merz *et al.* (2006) conclude that IETD between 3 and 6 hours is appropriate for a range of different catchments in Austria, Adams *et al.* (1986) suggest IETD between 1 and 6 hours for typical urban catchments in Canada and this upper threshold is also suggested in Chen and Adams (2006) for another urban catchment in Canada. The IETD used in this research is 6 hours. Further research could focus on examining different IETD and estimating their impact on SM for the period preceding a flood event and more specifically the 5 days preceding a flood event.

One of the core components of the proposed methodology in Chapter 5, which needs to be estimated during the first steps of its application, is the estimation of fire impact from a spatial and qualitative perspective. The procedure suggested for this estimation is described in detail in Section 5.1.1, while the application of this procedure to the study area is described in detail in Section 7.1. This procedure involves standard satellite imagery processing and a standard GIS analysis. Therefore, the rules for the implementation of this explicit procedure for the estimation of fire impact in terms of its spatial extend and severity, as applied in this research, could be standardized, so as to be easily automated and potentially constitute a stand-alone software.

Sometimes certain pre- and/or post-fire forest conditions are not available, restricting thus the estimation of the impact of a specific forest fire. In the absence of detailed information for these conditions, further research could focus on safe assumptions that could be made, as well as combined use of different sources of this information (*in-situ* estimations, satellite imagery, existing studies *etc.*), so as to extract as accurate as possible conclusions on fire effect and proceed to the application of the methodology avoiding significant errors.

Another field for further research concerns the recognition of post-fire vegetation, so as to estimate as accurately as possible the potential of the affected vegetation for hydrological recovery and of course environmental recovery. As discussed in Section 3.3.1, nowadays remote sensing techniques, involving primarily satellite imagery processing, support the estimation of post-fire vegetation species (Gitas *et al.*, 2012; Shoshany, 2000; Henry and Hope, 1998; Lhermitte *et al.*, 2011; Díaz-Delgado *et al.*, 2003; van Leeuwen *et al.*, 2010; Veraverbeke *et al.*, 2010; Viedma *et al.*, 1997). Progress that is being made in this domain can support a more accurate estimation of post-fire vegetation and potential adaptation mechanisms of affected species and thus support more accurate estimation of the period when hydrological recovery is expected ( $t_{lower}$ ).

Finally, a recommendation for further research concerns the automation of the incorporation of the proposed methodology in a rainfall-runoff model for hydrological simulations or even in a hydrological – hydraulic model chain for the production of flood hazard maps, as is for example the FLIRE platform (Kochilakis *et al.*, 2016a; Kochilakis *et al.*, 2016b; Kotroni *et al.*, 2015; Papathanasiou *et al.*, 2015b; Poursanidis *et al.*, 2015a). Coding in an appropriate programming language could enable the automatic application of the methodology and thus the performance of accurate simulations and the production of representative flood maps. Especially when the model, or the model chain receive forecasted rainfall as input and support FEWSs, these systems become more robust, since they can issue more accurate warnings.

## 9.4 Epilogue

The methodology developed in the framework of implementation of this research constitutes a robust framework for improved hydrological simulations and therefore improved flood risk assessment and mitigation in Mediterranean periurban areas both on a near-real time basis and in the long run. In particular, this methodology can be automated and incorporated in early warning platforms for floods and operational systems for civil protection that use regularly updated information on initial SM conditions and forest fire occurrence, and support their efficient operation through the issuing of more precise flood warnings.

This methodology supports the production of more representative flood hazard and floods risk maps on an operational basis, since both SM and fire occurrence are taken into consideration through an innovative and holistic approach. At the same time, the proposed methodology can support the design of long-term and efficient flood risk management plans according to the requirements of EU Floods Directive 2007/60/EC, where adverse initial conditions (*i.e.* wet SM conditions following a recent forest fire) can also be considered for the generation of flood hazard and flood risk maps.

To sum up, the methodological framework developed for this research for the estimation of the dynamical changes in time of five representative hydrological parameters under variable initial conditions, in terms of forest fire occurrence and SM conditions, serves the overall purpose of this research, *i.e.* the accurate flood risk assessment in typical Mediterranean periurban areas under post-fire conditions. Finally, the fact that the presented methodology has been developed using state-of-art tools, modern technologies and comprehensive analyses and exploiting well documented relevant knowledge and experience, together with its easy adjustability and thus applicability to other areas, support its robustness and its suitability for further applications (Papathanasiou *et al.*, 2015a).

## CHAPTER 10: REFERENCES

- Abbott, M.B., Bathurst, J.C., Cunge, J.A., O'Connell, P.E. and Rasmussen, J., (1986a), *An introduction to the European Hydrological System – Système Hydrologique Européen, "SHE", 1: History and philosophy of a physically-based, distributed modelling system*, Journal of Hydrology, Vol. 87, No 1-2, pp. 45-59.
- Abbott, M.B., Bathurst, J.C., Cunge, J.A., O'Connell, P.E. and Rasmussen, J., (1986b), *An introduction to the European Hydrological System – Système Hydrologique Européen, "SHE", 2: Structure of a physically-based, distributed modelling system*, Journal of Hydrology, Vol. 87, No 1-2, pp. 61-77.
- Ackerman, C.T., (2011), *HEC-GeoRAS – GIS Tools for Support of HEC-RAS using ArcGIS, User's Manual, Version 4.3.93*, US Army Corps of Engineers, Hydrologic Engineering Center (HEC), CPD-83, 244p.
- Ackerman, C.T., Jensen, M.R. and Brunner, G.W., (2010), *Geospatial capabilities of HEC-RAS for model development and mapping*, Proceedings of the 2<sup>nd</sup> Joint Federal Interagency Conference, June 27<sup>th</sup> – July 1<sup>st</sup> 2010 Las Vegas, NV.
- Adams, B., Fraser, H., Howard, C., and Sami Hanafy, M., (1986), *Meteorological Data Analysis for Drainage System Design*, Journal of Environmental Engineering, Vol. 112, No 5, pp. 827–848.
- Agee, J.K., (1993), *Fire ecology of Pacific Northwest forests*, Island Press, Washington DC, USA.
- Ajami, N.K. Gupta, H., Wagener, T. and Sorooshian, S., (2004), *Calibration of a semi-distributed hydrologic model for streamflow estimation along a river system*, Journal of Hydrology, Vol. 298, pp. 112-135.
- Albergel, C., Dorigo, W., Balsamo, G., Muñoz-Sabater, J., De Rosnay, P., Isaksen, L., Brocca, L., De Jeu, R. and Wagner, W., (2013), *Monitoring multi-decadal satellite earth observation of soil moisture products through land surface reanalyses*, Remote Sensing of Environment, Vol. 138, pp. 77-89.
- Alonistioti, D., (2011), *Investigation of forest fire impact on the hydrological response of river basins in Eastern Attica region*, Master Thesis, Inter-Departmental Postgraduate Course Water Resources Science and Technology, National Technical University of Athens (in Greek).
- Arianoutsou-Faraggitaki, M., (1985), *Desertification by overgrazing in Greece: The case of Lesbos island*, Journal of Arid Environments, Vol. 9, pp. 237-242.
- Aryal, R.K., Furumai, H., Nakajima, F. and Jinadasa, HKPK, (2007), *The role of inter-event time definition and recovery of initial/depression loss for the accuracy in quantitative simulations of highway runoff*, Urban Water Journal, Vol. 4, No 1, pp. 53-58.
- Atkinson, P.M. and Massari, R., (1998), *Generalized linear modeling of landslide susceptibility in the Central Apennines, Italy*, Computers and Geosciences., Vol. 24, No 4, pp. 373–385.



- Baltas, E.A., Dervos, N.A. and Mimikou, M.A., (2007), *Technical note: Determination of the SCS initial abstraction ratio in an experimental watershed in Greece*, Hydrology and Earth System Sciences, Vol. 11, pp. 1825-1829.
- Bariamis, G., (2013), *Sensitivity analysis of parameters of HEC-HMS hydrological model and application in Rafina catchment*, Master Thesis, Inter-Departmental Postgraduate Course Water Resources Science and Technology, National Technical University of Athens (in Greek).
- Bariamis, G., Papathanasiou, C., Baltas, E. and Mimikou, M., (2014), *Hydrological simulation and sensitivity analysis of the Rafina basin*, Proc. 12<sup>th</sup> International Conference on Protection and Restoration of the Environment, 29<sup>th</sup> June – 3<sup>rd</sup> July 2014, Skiathos, Greece.
- Barton, A.M., (1999), *Pines versus oaks: effects of fire on the composition of Madrean forests in Arizona*, Forest Ecology and Management, Vol. 120, No 1-3, pp. 143-156.
- Batalla, R.J., (2002), *Hydrological implications of forest fires: an overview*, In Pardini, G., Pinto, J., (Eds.), *Fire, Landscape and Biodiversity*, Diversitas, Universitat de Girona, pp. 99-116.
- Bates P., Horritt M., Wilson M. and Hunter N., (2005), *LISFLOOD-FP – User manual and technical note, Code release 2.6.2*, University of Bristol, 22<sup>nd</sup> June 2005.
- Bates, P.D. and De Roo, A.P.J., (2000), *A simple raster-based model for flood inundation simulation*, Journal of Hydrology, Vol. 236, pp. 54-77.
- Beck, H.E., De Jeu, R.A.M., Schellekens, J., Van Dijk, A.I.J.M. and Bruijnzeel, L.A., (2009), *Improving Curve Number based storm runoff estimates using soil moisture proxies*, IEEE Journal of Selected Topics in Applied Earth Observations and Remote Sensing, Vol. 2, pp. 250–259.
- Becker, A., (1992), *Criteria for a hydrologically sound structuring of large scale land surface process models*, In: *Advances in Theoretical Hydrology: A Tribute to James Dooge*, Part B – Chapter 7, Ed. O’Kane, J. P., Elsevier, Amsterdam, pp. 97-111.
- Beeson P.C., Martens S.N. and Breshears D.D., (2001), *Simulating overland flow following wildfire: mapping vulnerability to landscape disturbance*, Hydrological Processes, Vol. 15, pp. 2917-2930.
- Berni, N., Pandolfo, C., Ponziani, F., Stelluti, M. and Viterbo, A., (2009), *Umbria region forecasting / decision support for hydraulic risk mitigation purposes*, Proc. of the 10<sup>th</sup> International Conference on Computing and Control in the Water Industry, 1-3 September 2000, Sheffield, UK, pp. 289-291.
- Berthet, L., Andréassian V., Perrin C. and Javelle P., (2009), *How crucial is it to account for the antecedent moisture conditions in flood forecasting? Comparison of event-based and continuous approaches on 178 catchments*, Hydrology and Earth System Sciences, Vol. 13, pp. 819-831.
- Beven K.J. and Kirkby M.J., (1979), *A physically based, variable contributing area model of basin hydrology*, Hydrological Sciences – Bulletin des Science Hydrologiques, Vol. 24, pp. 43-69.

- Bisson, M., Favalli, M., Fornaciai, A., Mazzarini, F., Isola, I., Zanchetta, G. and Pareschi, M.T., (2005), *A rapid method to assess fire-related debris flow hazard in the Mediterranean region: An example from Sicily (southern Italy)*, International Journal of Applied Earth Observation and Geoinformation, Vol. 7, pp. 217-231.
- Bisson, M., Fornaciai, A., Coli, A., Mazzarini, F. and Pareschi, M.T., (2008), *The Vegetation Resilience After Fire (VRAF) index: development, implementation and an illustration from central Italy*, International Journal of Applied Earth Observation and Geoinformation, Vol. 10, No 3, pp. 312–329.
- Bolin, S.B. and Ward, T.J., (1987), *Recovery of a New Mexico drainage from a forest fire*, Forest Hydrology and Watershed Management, Proceedings of the Vancouver Symposium, August 1987, IASH-AISH, Vol. 167, pp. 191-198.
- Boyle, D. P., Gupta, H. V., Sorooshian, S., Koren, V., Zhang, Z. and Smith, M., (2001), *Toward improved streamflow forecasts: Value of semidistributed modeling*, Water Resources Research, Vol. 37, No 11, pp. 2749-2759.
- Brocca, L., Liersch, S., Melone, F., Moramarco, T. and Volk, M., (2013), *Application of a model-based rainfall-runoff database as efficient tool for flood risk management*, Hydrology and Earth System Sciences, Vol. 17, pp. 3159-3169.
- Brocca, L., Hasenauer, S., Lacava, T., Melone, F., Moramarco, T., Wagner, W., Dorigo, W., Matgen, P., Martínez-Fernández, J., Llorens, P., Latron, J., Martin, C. and Bitteli, M., (2011), *Soil moisture estimation through ASCAT and AMSR-E sensors: An intercomparison and validation study across Europe*, Remote Sensing of Environment, Vol. 115, pp. 3390–3408.
- Brocca, L., Melone, F., Moramarco, T., Wagner, W., Naeimi, V., Bartalis, Z. and Hasenauer, S., (2010), *Improving runoff prediction through the assimilation of the ASCAT soil moisture product*, Hydrology and Earth System Sciences, Vol. 14, pp. 1881-1893.
- Brocca, L., Melone, F. and Moramarco, T., (2008), *On the estimation of antecedent wetness conditions in rainfall-runoff modelling*, Hydrological Processes, Vol. 22, pp. 629-642. Brocca L., Melone F., Moramarco T., Wagner W., Naeimi V., Bartalis Z. and Hasenauer S., (2010), *Improving runoff prediction through the assimilation of the ASCAT soil moisture product*, Hydrology and Earth System Sciences, Vol. 14, pp. 1881-1893.
- Brown J.A.H., (1972), *Hydrologic effects of a bushfire in a catchment in south-eastern New South Wales*, Journal of Hydrology, Vol. 15, pp. 77-96.
- Brown, L.C. and Foster, G.R., (1987), *Storm erosivity using idealized intensity distributions*, Transactions of the ASCE, Vol. 30, No 2, pp. 379–386.
- Brunner, G.W., (2010), *HEC-RAS – River Analysis System, Hydraulic Reference Manual, Version 4.1*, US Army Corps of Engineers, Hydrologic Engineering Center (HEC), CPD-69, 417p.
- Buscardo, E., Freitas, H., Pereira, J.S. and De Angelis, P., (2011), *Common environmental factors explain both ectomycorrhizal species diversity and pine regeneration variability in a post-fire Mediterranean forest*, Mycorrhiza, Vol. 21, pp. 549-558.

- Byram, G.M., (1959), *Combustion of forest fuels*, Chapter 3 in Davis, K.P. Ed. *Forest fire: Control and use*, New York, McGraw Hill, pp. 61-89.
- Calvo, L., Santalla S., Marcos, E., Valbuena, L., Tárrega, R. and Luis, E., (2003), *Regeneration after wildfire in communities dominated by Pinus pinaster, an obligate seeder, and in others dominated by Quercus pyrenaica, a typical resprouter*, *Forest Ecology and Management*, Vol. 184, No 1-3, pp. 209-223.
- Camici, S., Tarpanelli, A., Brocca, L., Melone, F. and Moramarco, T., (2011), *Design soil moisture estimation by comparing continuous and storm-based rainfall-runoff modeling*, *Water Resources Research*, Vol. 47, No 5, pp. W05527, doi :10.1029/2010WR009298, 2011.
- Campbell, R.E., Baker, M.B., Ffolliott, P.F. and Larson, F.R., (1977), *Wildfire effects on a ponderosa pine ecosystem: an Arizona case study*, USDA Forest Service, Rocky Mountain Forest and Range Experiment Station Forest Service, Research Paper RM-191, Fort Collins, Colorado.
- Campo, J., Andreu, V., Gimeno-García, E., González, O. and Rubio, J.L., (2006), *Occurrence of soil erosion after repeated experimental fires in a Mediterranean environment*, *Geomorphology*, Vol. 82, pp. 376-387.
- Cannon, S.H. and Reneau, S.L., (2000), *Conditions for generation of fire-related debris flows, Capulin Canyon, New Mexico*, *Earth Surface Processes and Landforms*, Vol. 25, pp. 1103-1121.
- Cannon, S.H., Kirkham, R.M. and Parise, M., (2001), *Wildfire-related debris-flow initiation processes, Storm King Mountain, Colorado*, *Geomorphology*, Vol. 30, pp. 171-188.
- Cannon, S., Gartner, J., Holland-Sears A., Thurston B. and Gleason A., (2003), *Debris-flow response of basins burned by the 2002 coal seam and missionary ridge fires, Colorado*, in Boyer, D.D., Santi, P.M., and Rogers, W.P., eds., *Engineering Geology in Colorado-Contributions, Trends, and Case Histories*: Association of Engineering Geologists Special Publication 14, Colorado Geological Survey Special Publication 55, in CD-ROM.
- Cannon, S.H., Gartner, J.E., Wilson, R.C., Bowers, J.C. and Laber, J.L., (2008), *Storm rainfall conditions for floods and debris flows from recently burned areas in southwestern Colorado and southern California*, *Geomorphology*, Vol. 96, pp. 250-269.
- Carey, A., Evans, M., Hann, P., Lintermans, M., MacDonald, T., Oram, P., Sharp, S., Shorthouse, D. and Webb, N., (2003), *Technical Report 17, Wildfires in the ACT 2003: Report on initial impacts on natural ecosystems*, Environment ACT, Canberra.
- Carter, M.C. and Foster, C.D., (2004), *Prescribed burning and productivity in southern pine forests: a review*, *Forest Ecology and Management*, Vol. 191, No 1-3, pp. 93-109.
- Cerdà, A., Imeson, A.C. and Calvo, A., (1995), *Fire and aspect induced differences on the erodibility and hydrology of soils at La Costera, Valencia, southeast Spain*, *CATENA*, Vol. 24, No. 4, pp. 289-304.

- Carrara, A., Cardinali, M., Guzzetti, F. and Reichenbach, P., (1995). GIS-based techniques for mapping landslide hazard. In: Carrara, A., Guzzetti, F. (Eds.), *Geographical Information Systems in Assessing Natural Hazards*. Kluwer Academic Publishers, Dordrecht, The Netherlands, pp. 135–175.
- Cerrelli, G.A., (2005), *FIRE HYDRO: A simplified method for predicting peak discharges to assist in the design of flood protection measures for western wildfires*, In: Moglen G.E. (Eds.), *Proceedings: 2005 Watershed Management Conference-Managing Watersheds for Human and Natural Impacts: Engineering, Ecological, and Economic Challenges*, 19-22 July 2005, Williamsburg, VA. Alexandria, American Society of Civil Engineers, pp. 935-941.
- Champ, C., (1986), *Der Planet Erde – Überschwemmungen*, Time-Life Bücher, Amsterdam, Authorized German language edition, 3rd German printing (in German).
- Chen, J. and Adams, B.J., (2006), *A derived probability distribution approach to stormwater quality model*, *Advances in Water Resources*, Vol. 30, No 1, pp. 80-100.
- Chen, T., De Jeu, R.A.M., Liu, Y.Y., Van Der Werf, G.R. and Dolman, A.J., (2014), *Using satellite based soil moisture to quantify the water driven variability in NDVI: A case study over mainland Australia*, *Remote Sensing of Environment*, Col. 140, pp. 330-338.
- Chow, V.T., Maidment, D.R. and Mays, L.W., (1988), *Applied Hydrology*, 1<sup>st</sup> Printing 1988, McGraw Hill International Editions, Civil Engineering Series.
- Chuvieco, E., Riaño, D., Danson, F.M., Bowyer, P. and Martín, M.P., (2005), *Use of canopy reflectance models to simulate burn severity levels*, In De la Riva, J., Pérez-Cabello, F. and Chuvieco, E. (Eds.), *Proceedings of the 5th International Workshop on Remote Sensing and GIS Applications to Forest Fire Management: Fire Effects Assessment* (pp. 233–238), Paris, Universidad de Zaragoza, GOF-C-GOLD, EARSeL.
- Ciarapica, L. and Todini, E., (2002), *TOPKAPI: a model for the representation of the rainfall-runoff process at different scales*, *Hydrological Processes*, Vol. 16, pp. 207-229.
- Coppola, E., Verdecchia, M., Tomassetti, B. and Visconti, G., (2003), *CHYM: A Grid based Hydrological Model*, International Symposium on Remote Sensing of Environment, Honolulu, Hawaii, November 2003.
- Cooley, R.L. and Moin, S.A., (1976), *Finite element solution of Saint-Venant equations*, *Journal of the Hydraulics Division*, Vol. 102, No 6, pp. 759-775.
- Cunge, J.A., Holly, F.M. and Verwey, A., (1980), *Practical aspects of computational river hydraulics*, Pitman Advances Publishing Program, London, UK, 420p.
- Cydzik, K. and Hogue, T.S., (2009), *Modeling postfire response and recovery using the Hydrologic Engineering Center Hydrologic Modeling System (HEC-HMS)*, *Journal of the American Water Resources Association*, Vol. 45, No 3, pp. 702-714. doi: 10.1111/j.1752-1688.2009.00317.x.

- Davis, G.W., Richardson, D.M., Keeley, J.E. and Hobbs, R.J., (1996), *Mediterranean-Type Ecosystems: The Influence of Biodiversity on their Functioning*, Chapter 7 in: *Functional Roles of Biodiversity: A Global Perspective*, Edited by Mooney, H.A., Cushman, J.H., Medina, E., Sala O.E. and Schulz, E.D., SCOPE, Published by John Wiley & Sons Ltd.
- DeBano, L.F., (1981), *Water repellent soils: a state of the art*, USDA Forest Service, Pacific Southwest Forest and Range Experiment Station, General Technical Report PSW-46.
- DeBano, L.F., (2000), *The role of fire and soil heating on water repellency in wildland environments: a review*, Journal of Hydrology, Vol. 231-232, pp. 195-206.
- DeBano, L.F., Neary, D.G. and Ffolliott, P.F., (2005), *Soil physical properties*, In: Neary, D.G., Ryan, K.C. and DeBano, L.F. (Eds.), *Wildland Fire in Ecosystems. Effects of Fire on Soil and Water*, General Technical Report RMRS-GTR-42-Volume 4: Rocky Mountain Research Station, 250, USDA Forest Service.
- Delft-FEWS, (2010), *Software Delft-FEWS description*, Deltares Innovative solutions for water and subsurface issues.
- De Santis, A., Chuvieco, E., (2007), *Burn severity estimation from remotely sensed data: Performance of simulation versus empirical models*, Remote Sensing of Environment, Vol. 108, No 4, pp. 422–435.
- DHI Software, (2007a), *MIKE SHE User manual, Volume 1: User Guide*, DHI Water and Environment, Edition 2007, 396p.
- DHI Software, (2007b), *MIKE11: A modelling system for rivers and channels – User Guide*, DHI Water and Environment, Edition 2004, 460p.
- DHI Software, (2003), *MIKE FLOOD 1D-2D Modelling – User Manual*, DHI Water and Environment, Edition 2003, 63p.
- Díaz-Delgado, R., Lloret, F. and Pons, X., (2003), *Influence of fire severity on plant regeneration by means of remote sensing*, International Journal of Remote Sensing, Vol. 24, pp. 1751-1763.
- Dilley, M., Chen, R.S., Deichmann, U., Lerner-Lam, A.L. and Arnold, M., (2005), *Natural Disaster Hotspots: A global risk analysis*, Washington, D.C.: World Bank, 148p., © World Bank. <https://openknowledge.worldbank.org/handle/10986/7376>, License: CC BY 3.0 IGO.
- Dinicola, K., (1996), *The “100-Year Flood”*, United States Geological Survey, Fact Sheet 229-96, 2p.
- Directive 2007/60/EC of the European Parliament and of the Council of 23 October 2007 on the assessment and management of flood risks (Text with EEA relevance), 6.11.2007 Official Journal of the European Union, L288/27 - L288/34.
- Doerr, S.H., Shakesby, R.A., Blake, W.H., Chafer, C.J., Humphreys G.S. and Wallbrink P.J., (2006), *Effects of differing wildfire severities on soil wettability*

*and implications for hydrological response*, Journal of Hydrology, Vol. 319, No. 1-4, pp. 295-311.

- Donati, L., and Turrini, M.C., (2002), *An objective method to rank the importance of the factors predisposing to landslides with the GIS methodology: application to an area of the Apennines (Valnerina, Prugia, Italy)*, Engineering Geology., Vol. 63, No 3-4, pp. 277-289.
- Dorigo, W.A., Gruber, A., De Jeu, R.A.M., Wagner, W., Stacke, T., Loew, A., Albergel, C., Brocca, L., Chung, D., Parinussa, R.M. and Kidd, R., (2015), *Evaluation of the ESA CCI soil moisture product using ground-based observations*, Remote Sensing of Environment, Vol. 162, pp. 380-395.
- Dougherty, T., (2011), *Anatomy of a flood*, 1st Ed., Capstone Press, 48p.
- Dragovich, D. and Morris, R., (2002), *Fire intensity, slopewash and bio-transfer of sediment in eucalypt forest, Australia*, Earth Surface Processes and Landforms, Vol. 27, pp. 309-1319.
- Duncan, A., Keedwell, E., Djordjevic, S. and Dragan, S., (2013), *Machine learning-based early warnings system for urban flood management*, Proc. ICFR 2013: International Conference on Flood Resilience: Experiences in Asia and Europe, University of Exeter, UK, 5-7 September 2013.
- Eccher, A., Fusaro, E. and Pelleri, F., (1987), *Résultats de l' expérimentation italienne sur les principales procenances de pins de la section halepensis dix ans après la plantation*, Forêt Méditerranéenne, Vol. 9, No 1, pp. 5-14 (in French).
- EEA, (2004), *Mapping the impacts of recent natural disaster and technological accidents in Europe*, Environmental Issue report, No 35, Copenhagen: European Environment Agency, 48p.
- EFDRR, (2011), *European Forum for Disaster Risk Reduction*, United Nations Office for Disaster Risk Reduction – Regional office for Europe, 17p.
- Eftychidis G. and Varela V., (2013), *Technical Report on forest fuel map*, Technical report for Action A2: "Identification of the current status of the study area" of the FLIRE Project (LIFE11 ENV GR 975).
- Elbashir, S., (2011), *Flood routing in natural channels using Muskingum methods*, Dissertation submitted in partial fulfilment of the requirements of the DIT's (Dublin Institute of Technology) Master of Engineering Computation, School of Civil and Building Services Engineering.
- Elliott, J.G., Smith, M.E., Friedel, M.J., Stevens, M.R., Bossong, C.R., Litke, D.W., Parker, R.S., Costello, C., Wagner, J., Char, S.J., Bauer, M.A. and Wilds, S.R., (2005), *Analysis and mapping of post-fire hydrologic hazards for the 2002 Hayman, Coal Seam, and Missionary Ridge wildfires, Colorado*, U.S. Geological Survey Scientific Investigations Report 2004-5300, 104 p.
- El-Shaarawi, A.H. and Piegorisch, W.W., (2002), *Encyclopedia of Environmetrics – Volume 1*, Ed. John Wiley and Sons Ltd, Chichester, 585p.
- Encyclopaedia Britannica, (2013), updated on-line version of Encyclopaedia Britannica, (Available at:

<http://www.britannica.com/EBchecked/topic/372721/Mediterranean-vegetation>).

- Ermini, L., Catani, F. and Casagli, N., (2005), *Artificial Neural Network applied to landslide susceptibility assessment*, *Geomorphology*, Vol. 66, pp. 327–343.
- Esteves, T.C.J., Kirkby, M.J., Shakesby, R.A., Ferreira, A.J.D., Soares, J.A.A., Irvine, B.J., Ferreira, C.S.S., Coelho, C.O.A., Bento, C.P.M. and Carreiras, M.A., (2012), *Mitigating land degradation caused by wildfire: Application of the PESERA model to fire-affected sites in central Portugal*, *Geoderma*, Vol. 191, pp. 40-50.
- EXCIMAP, (2007), *Handbook on good practices for flood mapping in Europe*, European exchange circle on flood mapping, Document prepared for EC and endorsed by Water Directors, 29-30 November 2007, 60p.
- Ferreira, V. and Panagopoulos, T., (2012), *Predicting risk of soil erosion at the Alqueva dam watershed*, Proc. of the 8<sup>th</sup> WSEAS International Conference on Energy, Environment, Ecosystems and Sustainable Development (EEESD '12), Recent Researches in Environment, Energy Systems and Sustainability, University of the Algarve, Faro, Portugal, 2-4 May 2012, pp. 99-104.
- FEMA, (2009), *Protecting Manufactured Homes from Floods and Other Hazards – A Multi-Hazard Foundation and Installation Guide*, Federal Emergency Management Agency, P-85, 2<sup>ND</sup> Ed., 266p.
- Evans, E.P., Wicks, J.M., Whitlow, C.D. and Ramsbottom, D. M., (2007), *The evolution of a river modelling system*, Proceedings. of the Institution of Civil Engineers – Water Management, Vol. 160, No 1, pp. 3-13.
- Feldman, A.D., (2000), *Hydrologic Modeling System – HEC-HMS – Technical Reference Manual*, US Army Corps of Engineers, Hydrologic Engineering Center (HEC), CPD-74B, 158p.
- FERC, (2001), *Engineering guidelines for the evaluation of hydropower projects*, Federal Energy Regulatory Commission, Chapter 8 – Determination of the Probable Maximum Flood.
- Fernandes, P. and Botelho, H., (2004), *Analysis of the prescribed burning practice in the pine forest of northwestern Portugal*, *Journal of Environmental Management*, Vol. 70, No 1, pp. 15-26.
- Fleming, M.J. and Doan, J.H., (2010), *HEC-GeoHMS- Geospatial Hydrologic Modeling Extension, User's Manual, Version 5.0*, US Army Corps of Engineers, Hydrologic Engineering Center (HEC), CPD-77, 197p.
- FLO-2D, (2009), *Reference Manual, Basic Model – Version 2009*.
- Foltz, R.B., Robichaud, P.R., Rhee, H., (2009), *A synthesis of postfire road treatments for BAER teams: methods, treatment effectiveness, and decision making tools for rehabilitation*, General Technical Report RMRS-GTR-228, Fort Collins, CO: U.S. Department of Agriculture, Forest Service, Rocky Mountain Research Station, 152p.
- Franklin, S.B., Robertson, P.A. and Fralish. J.S., (2003), *Prescribed burning effects on upland Quercus forest structure and function*, *Forest Ecology and Management*, Vol. 184, No 1-3, pp. 315-335.

- Fread, D.L., (1985), *Channel Routing*, In “Hydrological Forecasting, Chapter 14, Ed. M. G. Anderson and T. P. Burts, John Wiley and Sons, New York, pp. 437-503.
- Fread, D.L. and Lewis, J.M., (1985), *Real-time hydrodynamic modelling of coastal rivers*, Proceeding of the Symposium: Applications of real-time oceanographic circulation modeling, Ed. B. B. Parker, Marine Technology Society, Washington D.C., pp. 269-284.
- French, R.H., Miller, J.J. and Dettling C.R., (2005), *Estimating playa lake flooding: Edwards Air Force Base, California, USA*, Journal of Hydrology, Vol. 306, No 1-4, pp. 146-160.
- Gao G.Y., Fu B.J., Lü Y.H., Liu Y., Wang S. and Zhou J., (2012), *Coupling the modified SCS-CN and RUSLE models to simulate hydrological effects of restoring vegetation in the Loess Plateau of China*, Hydrology and Earth System Sciences, Vol. 16, pp. 2347-2364.
- Garbrecht, J. and Brunner, G.W., (1991), *A Muskingum – Cunge channel flow routing method for drainage networks*, Technical Paper No 135, US Army Corps of Engineers, Hydrologic Engineering Center, AD-A247 020.
- Giakoumakis N. M., Gitas I. Z. and San-Miguel J., (2002), *Object-oriented classification modelling for fuel type mapping in the Mediterranean, using LANDSAT TM and IKONOS imagery- preliminary results*, Proc. Of the 4<sup>th</sup> International Conference on Forest Fire Research & Wildland Fire Safety, p. 66, Ed. Millpress, Rotterdam.
- Gill, M.A., (1978), *Flood routing by the Muskingum Method*, Journal of Hydrology, Vol. 36, pp. 353-363.
- Gitas, I., Mitri, G., Veraverbeke, S. and Polychronaki, A., (2012), *Advances in Remote Sensing of Post-Fire Vegetation Recovery Monitoring – A Review*, Chapter 7 in *Remote Sensing of Biomass – Principles and Applications*, Edited by Fatoyinbo, T., Published by InTech, doi: 10.5772/20571.
- Giovannini, G., Vallejo, R., Lucchesi, S., Bautista, S., Ciompi, S. and Llovet, J., (2001), *Effects of land use and eventual fire on soil erodibility in dry Mediterranean conditions*, Forest Ecology and Management, Vol. 147, pp. 15-23.
- Goldman, S.J., Jackson, K., Bursztynsky, T.A., (1986). *Erosion and Sediment Control Handbook*, Mc-Graw Hill, New York, 449p.
- Greek Law 3852/2010, *New Architecture of Local Government and Decentralized Administration – Kallikratis Programme*, Greek Official Gazette (FEK) A, Volume 1, No 87, 7 June 2010 (in Greek).
- Gregory, K.J. and Goodie, A.S., (2011), *The SAGE Handbook of Geomorphology*, First published 2011, SAGE Publications Ltd, pp. 648.
- Grimm, M., Jones, R. and Montanarella, L., (2002), *Soil Erosion Risk in Europe*, European Commission, Directorate General, Joint Research Centre, Institute for Environment and Sustainability, European Soil Bureau, 38p.
- Günther, A., Van Den Eeckhaut, M., Malet, J.P., Reichenbach, P., and Hervás, J., (2014), *Climate-physiographically differentiated Pan-European landslide*



*susceptibility assessment using spatial multi-criteria evaluation and transnational landslide information*, *Geomorphology*, Vol. 224, pp. 69-85, <https://doi.org/10.1016/j.geomorph.2014.07.011>.

- Gupta, H.V., Sorooshian, S. and Yapo, P.O., (1998), *Toward improved calibration of hydrologic models: Multiple and noncommensurable measures of information*, *Water Resources Research*, Vol. 34, No 4, pp. 751-763.
- Haynes, K., Handmer, J., McAneney, J., Tibbits, A. and Coates, L., (2010), *Australian bushfire fatalities 1900–2008: Exploring trends in relation to the ‘Prepare, stay and defend or leave early’ policy*, *Environmental Science and Policy*, Vol. 13, No 3, pp. 185–194.
- HEC – Hydrologic Engineering Center, (2009), *Hydrologic Modeling System HEC-HMS, User’s Manual, Version 3.4*, U.S. Army Corps of Engineers, Davis CA.
- Heinl, M., Frost, P., Vanderpost, C. and Sliva, J., (2007), *Fire activity on drylands and floodplains in the southern Okavango Delta, Botswana*, *Journal of Arid Environments*, Vol. 68, pp. 77-87.
- Hellenic National Meteorological Service (HNMS), (2015), Datasets available at the website of HNMS ([www.hnms.gr](http://www.hnms.gr)).
- Henry, M.C. and Hope, A.S., (1998), *Monitoring post-burn recovery of chaparral vegetation in southern California using multi-temporal satellite data*, *International Journal of Remote Sensing*, Vol. 19, No 16, pp. 3097-3107.
- Higginson, B. and Jarnecke, J., (2007), *Salt Creek BAER-2007 Burned Area Emergency Response*, Provo, UT: Unita National Forest, Hydrology Specialist Report, 11 p.
- Hijioka, Y., Nakajima, F. and Furumai, H., (2001), *Modified models of wash-off from roofs and roads for non-point pollution analysis during first flush phenomena*, *Urban Drainage Modelling*, Proc. of the Specialty Symposium of the World Water and Environment Resources Congress, 20<sup>th</sup>-24<sup>th</sup> of May 2001, ASCE, pp.275–286.
- Holmes, R.R. and Dinicola, K., (2010), *100-Year Flood – It’s all about chances*, United States Geological Survey, General Information Product 106, 4p.
- Huang M., Gallichand J., Wang Z. and Goulet M., (2006), *A modification to the Soil Conservation Service curve number method for steep slopes in the Loess Plateau of China*, *Hydrological Processes*, Vol. 20, pp. 579-589.
- Hubbert, K.R., Preisler, H.K., Wohlgemuth, P.M., Graham, R.C. and Narog, M.G., (2006), *Prescribed burning effects on soil physical properties and soil water repellency in a steep chaparral watershed, southern California, USA*, *Geoderma*, Vol. 130, No 3-4, pp. 284–298.
- Hunter N.M., Bates P.D., Horritt M.S. and Wilson M.D., (2007), *Simple spatially-distributed models for predicting flood inundation: A review*, *Geomorphology*, Vol. 90, pp. 208-225.
- HYDROEXIGIANTIKI Consulting Engineers, Machairas Design Office Ltd., HYDOR NOTARAS Ltd., (1999a), *Design Study of Rafina Stream - General Arrangement of suggested works*, EYDAP S.A. (in Greek).

- HYDROEXIGIANTIKI Consulting Engineers, Machairas Design Office, HYDOR-NOTARAS Ltd., ENVECO S.A., (1999b), *Siting prior authorization Design Study*, EYDAP S.A. (in Greek).
- HYDROEXIGIANTIKI Consulting Engineers, Machairas Design Office, HYDOR-NOTARAS Ltd., (2008), *Design of River Defenses along the Rafina Stream – Hydrology: Mathematic simulation of the hydrological catchment of Rafina Stream, Region of Attica*, Directorate of Hydraulic Works (D10) (in Greek).
- HYDROTEK Hydraulic Studies Ltd., ENM Consulting Engineers, ADK Consulting Engineers S.A., (1996), *Preliminary Design Study of Rainwater Drainage in Rafina Catchment*, EYDAP S.A. (in Greek).
- HYDROTEK Hydraulic Studies Ltd., ENM Consulting Engineers, ADK Consulting Engineers S.A., (1997), *Final Design Study of Rainwater Drainage in Rafina Catchment*, EYDAP S.A. (in Greek).
- Iman, R.L. and Conover, W.J., (1980), *Small sample sensitivity analysis techniques for computer models, with an application to risk assessment*, Communications in Statistics – Theory and Methods, Vol. 9, No 17, pp. 1749-1842.
- Inbar, M., Tamir, M. and Wittenberg, L., (1998), *Runoff and erosion processes after a forest fire in Mount Carmel, a Mediterranean area*, Geomorphology, Vol. 24, pp. 17-33.
- Innovyze, (2014), Software and Services Catalog 2014, Innovating for Sustainable Infrastructure, 92p.
- IUM (Illinois Urban Manual), (2013), *An Erosion and Sediment Control Best Management Practice Manual*, Association of Illinois Soil and Water Conservation Districts, p.144.
- Jacobshagen V., (1986), *Geologie von Griechenland*, Beiträge zur regionalen Geologie der Erde, Gebrüder Borntraeger, Berlin (in German).
- Johnson, B.E., (1997), *Development of a storm-event based two-dimensional upland erosion model*, Ph.D. Dissertation, Colorado State University, Fort Collins, Colorado, USA.
- Johnson, B.E. and Julien, P. Y., (2000), *The two-dimensional upland erosion model CASC2D-SED*, The Hydrology-Geomorphology Interface: Rainfall, Floods, Sedimentation, Land Use (Proceedings of the Jerusalem Conference, May 1999), IAHS Publ. No. 261, pp. 107-125.
- Johnson, D., (1999), *Channel Routing*, (Available at: [http://www.comet.ucar.edu/class/hydromet/07\\_Jan19\\_1999/html/routing/sld001.htm](http://www.comet.ucar.edu/class/hydromet/07_Jan19_1999/html/routing/sld001.htm)).
- Joint Research Centre, (2014), *Forest Fires in Europe, Middle East and North Africa*, Joint Report of JRC and Directorate-General Environment, Report EUR 26791 EN, 107p.
- Julien, P.Y. and Saghafian, B., (1991), *CASC2D User's manual: A two dimensional watershed rainfall-runoff model*, Center for Geosciences—

Hydrologic Modelling Group, Colorado State University (CER90-91PYJ-BS-12). Fort Collins, Colorado, USA.

- Julien, P. Y., Saghafian, B. and Ogden, F.L., (1995), *Raster-based hydrologic modeling of spatially-varied surface runoff*, Water Resources Bulletin, American Water Resources Association, Vol.31, No.3, pp. 523-536, June 1995.
- Kalabokidis, K, Kallos, G., Karavitis, C., Caballero, D., Tettalaar, P., Llorens, J. and Vasilakos, C., (2005), *Automated fire and flood hazard protection system*, Proc. of the 5<sup>th</sup> International Workshop on Remote Sensing and GIS Applications to Forest Fire Management: Fire Effects Assessment, 16-18 June 2005, Zaragoza, Spain, pp. 167-172.
- Kassela, A., (2011), *Hydrological simulation of the greater experimental basin of Eastern Attica: streams of Rafina and Lykorema, using the HEC-HMS model*, Bachelor Thesis, School of Civil Engineers, National Technical University of Athens (in Greek).
- Katsikatsos G., (1992), *Geology of Greece*, Department of Geology, University of Patras (in Greek).
- Keane, R.E., Dillon, G., Jain, T., Hudak, A., Morgan, P., Karau, E., Sikkink, P. and Silverstein, R., (2012), *The problems with fire severity and its application in fire management*, USDA Forest Service, Rocky Mountain Research Station, Research Paper, RMRS-RP-XXX, (Available at: [http://www.firelab.org/ResearchProject\\_Files/ijwf\\_sev\\_text.pdf](http://www.firelab.org/ResearchProject_Files/ijwf_sev_text.pdf)) .
- Keeley, J.E., Brennan, T. and Pfaff, A.H., (2008), *Fire severity and ecosystem responses following crown fires in California shrublands*, Ecological Applications, Vol. 18, No 6, pp. 1530–1546.
- Keeley, J.E., (2009), *Fire intensity, fire severity and burn severity: a brief review and suggested usage*, International Journal of Wildland Fire, Vol. 18, pp. 116-126.
- Key, C.H., (2005), *Remote sensing sensitivity of fire severity and fire recovery*, In De la Riva, J., Pérez-Cabello, F. and Chuvieco, E. (Eds.), Proceedings of the 5th International Workshop on Remote Sensing and GIS Applications to Forest Fire Management: Fire Effects Assessment (pp. 29–39), Zaragoza, Universidad de Zaragoza, GOFC-GOLD, EARSeL.
- Key, C.H. and Benson, N.C., (2006), *Landscape Assessment: Ground measure of severity, the Composite Burn Index; and Remote sensing of severity, the Normalized Burn Ratio*, In Lutes, D.C., Keane, R.E., Caratti, J.F., Key, C.H., Benson, N.C., Sutherland, S. and Gangi, L.J., (2006), FIREMON: Fire Effects Monitoring and Inventory System. USDA Forest Service, Rocky Mountain Research Station, Ogden, UT. Gen. Tech. Rep. RMRS-GTR-164-CD: LA 1-51.
- Kinver, M., (2011), Partnership to tackle Mediterranean forest threats, BBC News, Science and Environment, 6 April 2011, (Available at: <http://www.bbc.com/news/science-environment-12938448>).

- Kirkby, M.J. and Weyman, D.R., (1974), *Measurements of contributing area in very small drainage basins*, Seminar Paper Series B., No 3, Department of Geography, University of Bristol, Bristol, United Kingdom.
- Kochilakis, G., Poursanidis, D., Chrysoulakis, N., Varella, V., Kotroni, V., Eftychidis, G., Lagouvardos, K., Papathanasiou, C., Karavokyros, G., Aivazoglou, M., Makropoulos, C. and Mimikou, M., (2016a), *A web based DSS for the management of floods and wildfires (FLIRE) in urban and periurban areas*, Environmental Monitoring and Software, Vol. 86, pp. 111-115.
- Kochilakis, G., Poursanidis, D., Chrysoulakis, N., Varella, V., Kotroni, V., Eftychidis, G., Lagouvardos, K., Papathanasiou, C., Karavokyros, G., Aivazoglou, M., Makropoulos, C. and Mimikou, M., (2016b), *FLIRE DSS: A web tool for the management of floods and wildfires in urban and periurban areas*, Open Geosciences (accepted).
- Kolditz, O., Bauer, S., Bilke, L., Böttcher, N., Delfs, J. O., Fischer, T., Görke, U. J., Kalbacher, T., Kosakowski, G., McDermott, C. I., Park, C. H., Radu, F., Rink, K., Shao, H., Shao, H. B., Sun, F., Sun, Y. Y., Singh, A. K., Taron, J., Walther, M., Wang, W., Watanabe, N., Wu, Y., Xie, M., Xu, W. and Zehner, B., (2012), *OpenGeoSys: an open-source initiative for numerical simulation of thermo-hydro-mechanical/chemical (THM/C) processes in porous media*, Environmental Earth Sciences, Vol. 67, No 2, pp. 589-599.
- Köppen W., (1901), *Versuch einer Klassifikation der Klimate, vorzugsweise nach ihren Beziehungen zur Pflanzenwelt*, Geographische Zeitschrift, Vol. 6, pp. 593–611 and 657–679 (in German).
- Kotroni, V., Lagouvardos, K., Chrysoulakis, N., Makropoulos, C., Mimikou, M., Papathanasiou, C. and Poursanidis, D., (2015), *Weather monitoring and forecasting over Eastern Attica (Greece) in the frame of FLIRE Project*, European Geosciences Union General Assembly 2015, Vienna, Austria, 12<sup>th</sup> -17<sup>th</sup> April 2015.
- Kottek M., Grieser J., Beck C., Rudolf B. And Rubel F., (2006), *World Map of the Köppen-Geiger climate classification updated*, Meteorologische Zeitschrift, Vol. 15, No. 3, pp. 259-263.
- Kouwen, N., (2010), *WATFLOOD™/WATROUTE: Hydrological model routing and flow forecasting system*, WATFLOOD User's Manual, Revised Edition, Last Revision: Apr. 10/10, p.247.
- Krause, P., Boyle, D.P. and Bäse, F., (2005), *Comparison of different efficiency criteria for hydrological model assessment*, Advances in Geosciences, Vol. 5, pp. 89-97.
- Kruger, F.J., (1983), *Plant community diversity and dynamics in relation to fire*, Mediterranean-Type Ecosystems, Ecological Studies, Vol. 43, pp. 446-472.
- Kutiel, P. Lavee, H. Segev, M and Benyamini, Y., (1995), *The effect of fire-induced surface heterogeneity on rainfall-runoff-erosion relationships in an eastern Mediterranean ecosystem, Israel*, CATENA, Vol. 25, pp.77-87.
- Lastoria, B., (2008), *Hydrological Processes on the land surface: a survey of modelling approaches*, Technical Report for INTERREG IIIB FORALPS

Project, Agency for Environmental Protection and Technical Services, Rome, Italy, 56 p.

- Latron, J., Gallart, F. and Llorens, P., (2004), *Comment on "L. Ciarapica and E. Todini, TOPKAPI: a model for the representation of the rainfall-runoff process at different scales. Hydrological Processes 16 (2002) 207-229"*, Hydrological Processes, Vol. 18, pp. 179-182.
- Lavabre, J., Sempere Torres, D. and Cernesson, F., (1993), *Changes in the hydrological response of a small Mediterranean basin a year after a wildfire*, Journal of Hydrology, Vol. 142, pp. 273-299.
- Le Houérou, H.N, (1987), *Vegetation wildfires in the Mediterranean basin: evolution and trends*, Ecologia Mediterranea, Vol. 13, No. 4, pp. 13-24.
- Lester, T. and McNally, A., (2012), *Cambridgeshire Flood Risk Management Partnership, March Surface Water Management Plan, Detailed Assessment and Options Appraisal Report, Final*, Cambridgeshire County Council, Hyder Consulting (UK), Report No. 5301-UA0021636-BMR-03, 40p.
- Lewis, S.A., Wu, J.Q. and Robichaud, P.R., (2006), *Assessing burn severity and comparing soil water repellency, Hayman Fire, Colorado*, Hydrological Processes, Vol. 20, pp. 1-16.
- Lhermitte, S., Verbesselt, J., Verstraeten, W.W., Veraverbeke, S. and Coppin, P., (2011), *Assessing intra-annual vegetation regrowth after fire using the pixel based regeneration index*, ISPRS Journal of Photogrammetry and Remote Sensing, Vol. 66, No 1, pp. 17-27.
- Liu, Z., Martina, M.L.V. and Todini, E., (2005), *Flood forecasting using a fully distributed model: application of the TOPKAPI model to the Upper Xixian Catchment*, Hydrology and Earth System Sciences, Vol. 9, No 4, pp. 347-364.
- Livingston, R. K., Earles, T. A. and Wright, K. R. (2005), *Los Alamos post-fire watershed recovery: a curve-number-based evaluation*, In: Moglen, Glenn E., eds. Proceedings: 2005 watershed management conference-managing watersheds for human and natural impacts: engineering, ecological, and economic challenges, 19-22 July 2005, Williamsburg, VA. Alexandria, American Society of Civil Engineers, pp. 471-481.
- Machairas Design Office Ltd., (1984), *Final Design Study of River Defenses along the Rafina Stream*, Directorate D3, Ministry of Public Works (in Greek).
- Marinos G., (1955), *Geological reconnaissance of the Rafina lignite basin*, Unpublished report, Institute of Geological and Mineral Exploration (IGME), Athens.
- Marinos P., Valadaki-Plessa K. and Plessas S., (1995), *Process and adjustment of geological data for the risk assessment of erosion and sediment yield at the Marathona and Mesogaia catchments of the Prefecture of Attica, Workshop on the Flood protection of Athens*, Athens, T.C.G. Minutes (in Greek).
- Mariolakos I. and Lekkas S., (1974), *The hydrogeological conditions of the Koropi basin, Attica*, Annales Géologiques des Pays Helléniques XXVI: 186–260 (in Greek).

- Marzano, R., Lingua, E. and Garbarino, M., (2012), *Post-fire effects and short-term regeneration dynamics following high-severity crown fires in a Mediterranean forest*, iForest – Biogeosciences and Forestry, Vol. 5, pp. 93-100.
- Mashriqui, H., Halgren, J. and Reed, S., (2014), *1D river hydraulic model for operational flood forecasting in the tidal Potomac: Evaluation for freshwater, tidal, and wind-driven events*, Journal of Hydraulic Engineering, Vol. 140, No 5, CID: 04014005.
- Massari, C., Brocca, L., Barbetta, S., Papathanasiou, C., Mimikou, M. and Moramarco, T., (2014), *Using globally available soil moisture indicators for flood modelling in Mediterranean catchments*, Hydrology and Earth System Sciences, Vol. 18, pp. 839-853, doi:10.5194/hess-18-839-2014.
- Matgen P., Fenicia F., Heitz S., Plaza D., de Keyser R., Pauwels V.R.N., Wagner W. and Savenije H., (2012), *Can ASCAT-derived soil wetness indices reduce predictive uncertainty in well-gauged areas? A comparison with in situ observed soil moisture in an assimilation application.*, Advances in Water Resources, Vol. 44, pp. 49-65.
- Mayor, A.G., Bautista, S., Llovet, J. and Bellot, J., (2007), *Post-fire hydrological and erosional responses of a Mediterranean landscape: Seven years of catchment-scale dynamics*, Catena, Vol. 71, pp. 68-75.
- McEnroe, B.M. and Zhao, H., (1999), *Lag times and peak coefficients for rural watersheds in Kansas*, Final Report, K-TRAN Research Project KU-98-1, University of Kansas, Kansas Department of Transportation, 45 p.
- McKay, M.D., (1992), *Latin Hypercube Sampling as a tool in uncertainty analysis of computer models*, Proc. of the 24<sup>th</sup> Winter Simulation Conference, 13-16 December, Arlington, VA, USA, pp. 557-564.
- McKay, M.D., Beckman, R.J., and Conover, W.J., (1979), *A comparison of three methods for selecting values of input variables in the analysis of output from a computer code*, Technometrics, Vol. 21, No 2, pp. 239-245.
- Mell, W.E., Manzello, S.L., Maranghides, A., Butry, D. and Rehm, R., (2010), *The wildland–urban interface fire problem—current approaches and research needs*, International Journal of Wildland Fire, Vol. 19, pp. 238–251.
- Melone, F., Barbetta, S., Diomede, T., Peruccacci, S., Rossi, M., Tessarolo, A. and Verdecchia, M., (2005), *Review and selection of hydrological models – integration of hydrological models and meteorological inputs*, Technical Report for Action No 1.13 of the RISK AWARE: RISK-Advanced Weather forecast system to Advise on Risk Events and management, INTEREG IIIB CADSES Programme, 34 p.
- Mérimée P., (1840), *Colomba*, Les Classiques de Poche, Ed. Le Livre de Poche, 264p (in French).
- Merz, R., Blöschl, G. and Parajka, J., (2006), *Spatio-temporal variability of event runoff coefficients*, Journal of Hydrology, Vol. 331, No 3-4, pp. 591-604.
- METER Consulting Engineers Ltd., (1998a), *Preliminary Design Study of the area downstream Valanaris Stream*, EYDAP S.A. (in Greek).

- METER Consulting Engineers Ltd., (1998b), *Final Design Study and Design Study of Local Interventions*, EYDAP S.A. (in Greek).
- Meyer, G.A., Pierce, J.L., Wood, S.H. and Jull, J.T., (2001), *Fire, storms and erosional events in the Idaho batholith*, Hydrological Processes, Vol. 15, pp. 3025-3038.
- Miller, J.D., Knapp, E.E., Key, C.H., Skinner, C.N., Isbell, C.J., Creasy, R.M. and Sherlock, J.W., (2009), *Calibration and validation of the Relative differenced Normalized Burn Ratio (RdNBR) to three measures of fire severity in the Sierra Nevada and Klamath Mountains, California, USA*, Remote Sensing of Environment, Vol. 113, No 3, pp. 645-656.
- Mishra, S. K. and Singh, V. P., (2003), Soil Conservation Service Curve Number (SCS-CN) Methodology, Water Science and Technology Library, Vol. 42, Kluwer Academic Publishers, Louisiana State University, Baton Rouge, U.S.A.
- Mishra, S.K., Singh, V.P., Sansalone, J. and Aravamuthan, V., (2003), *A modified SCS-CN method: characterization and testing*, Water Resources Management, Vol. 17, 2003, pp. 37–68.
- Mishra S.K., and Singh V.P., (2002), *SCS-CN-based hydrologic simulation package*. In: Singh V.P. and Frevert, D.K. (Eds.), *Mathematical Models in Small Watershed Hydrology and Applications*, Water Resources Publications, Littleton, Colorado, pp. 391–464.
- Mishra, S.K. and Singh, V.P., (1999), *Another look at SCS-CN method*, Journal of Hydrological Engineering, Vol. 4, 1999, pp. 257–264
- Mitsopoulos, I., Eftychidis, G., Papathanasiou, C., Makropoulos, C. and Mimikou, M., (2015), *Post-fire debris flow potential in a fire prone Mediterranean landscape*, Proc. 2nd International Conference on Fire Behaviour and Risk, 26<sup>th</sup> – 29<sup>th</sup> May 2015, Alghero, Sardinia, Italy.
- Mitsopoulos, I., Eftychidis, G., Papathanasiou, C., Makropoulos, C. and Mimikou, M., (2015), *Assessing post fire flood risk potential in a typical Mediterranean Wildland-Urban Interface of Greece*, Proc. 2<sup>nd</sup> International Conference on Changing Cities: Spatial Design, Landscape and Socio-economic Dimensions, 22<sup>nd</sup> – 26<sup>th</sup> June 2015, Porto Heli, Peloponnese, Greece.
- Mitsopoulos I., (2013), *A methodology for assessing post fire debris flow potential in Mediterranean ecosystems*, Technical report for Action B4: “Forest fire risk assessment and mitigation planning” of the FLIRE Project (LIFE11 ENV GR 975).
- Moody, J.A. and Martin, D.A., (2001a), *Initial hydrologic and geomorph response following a wildfire in the Colorado front range*, Earth Surface Processes and Landforms, Vol. 26, pp. 1049-1070.
- Moody, J.A. and Martin, D.A., (2001b), *Post-fire, rainfall intensity-peak discharge relations for three mountainous watersheds in the western USA*, Hydrological Processes, Vol. 15, No 15, pp. 2981-2993.

- Moore, R., Gijbbers, P., Fortune, D., Gregersen, J. and Blind, M., (2007), *OpenMI Document Series: Part A – Scope for the OpenMI (Version 1.4)*, The OpenMI Association, 2007, 19p.
- Moore, R.J., Cole, S.J., Bell, V.A. and Jones, D.A., (2006), *Issues in flood forecasting: ungauged basins, extreme floods and uncertainty*, *Frontiers in flood forecasting*, 8<sup>th</sup> Kovacs Colloquium, UNESCO, Paris, June/July 2006, IAHS-AISH, No 305, pp. 103-122.
- Nash, J. and Sutcliffe, J., (1970), *River flow forecasting through conceptual models, Part I – a discussion of principles*, *Journal of Hydrology*, Vol. 10, pp. 282-290.
- National Observatory of Athens (NOA), (2012), *The network of automatic meteorological stations of the National Observatory of Athens*, September 2012, Report available through the website [www.meteo.gr/meteosearch](http://www.meteo.gr/meteosearch) (in Greek).
- Néelz, S. and Pender, G., (2009), *Desktop review of 2D hydraulic modelling packages*, Science Report: SC080035, Joint Defra/Environment Agency Flood and Coastal Erosion Risk Management R & D Programme, 63p.
- Neitsch, S.L., Arnold, J.G., Kiniry, J.R. and Williams, J.R., (2011), *Soil and Water Assessment Tool – Theoretical Documentation, Version 2009*, Texas Water Resources Institute Technical Report No. 406, Texas A & M University System, College Station, Texas 77843-2118, 647 p.
- Nepstad, D., Verissimo, A., Alencar, A., Nobre, C., Lima, E., Lefebvre, P., Schlesinger, P., Potter, C., Moutinho, P., Mendoza, E., Cochrane, M. and Brooks, V., (1999), *Large-scale impoverishment of Amazonian forest by logging and fire*, *Nature*, Vol. 398, pp. 505–508.
- NSW-DPI (New South Wales Government-Department of Primary Industries), *Soil Erosion Factsheets*, (Available at: <http://www.dpi.nsw.gov.au/agriculture/resources/soils/erosion/soil-erosion-factsheets>).
- NWCG – National Wildfire Coordinating Group, (2012), *Glossary of Wildland Fire Terminology*, PMS 205, 190p, (Available at: <http://www.nwcg.gov/pms/pubs/pubs.htm>).
- Ogden, F.L. and Julien, P.Y., (2002), *CASC2D: A two-dimensional, physically-based, hortonian hydrologic model*, In: *Mathematical Models of Small Watershed Hydrology and Applications - Chapter 4*, Ed. Singh V. P. and Frevert D., Water Resources Publications, LLC, 957 p.
- Oliveira, S. and Fernandes, P., (2009), *Regeneration of Pinus and Quercus after fire in Mediterranean-type ecosystems: Natural mechanisms and management practices*, *Silva Lusitana*, Vol. 17, No 2, pp. 181-192.
- O’Sullivan, J.J., Ahilan, S. and Bruen, M., (2012), *A modified Muskingum routing approach for floodplain flows: Theory and practice*, *Journal of Hydrology*, Vol. 470-471, pp. 239-254.
- Pagana, V., (2012), *Elaboration of flood inundation maps in Rafina basin*, Master Thesis, Inter-Departmental Postgraduate Course Water Resources Science and Technology, National Technical University of Athens (in Greek).



- Pallàs, R., Vilaplana, J.M., Guinau, M., Falgàs, E., Alemany, X. and Muñoz, A., (2004), *A pragmatic approach to debris flow hazard mapping in areas affected by Hurricane Mitch: example from NW Nicaragua*, Engineering Geology, Vol. 72, pp. 57-72.
- Panagos, P., Ballabio, C., Borrelli, P., Meusburger, K., Klik, A., Rousseva, S., Tadić, M. P., Michaelides, S., Hrabalíková, M., Olsen, P., Aalto, J., Lakatos, M., Rymaszewicz, A., Dumitrescu, A., Beguería, S., Alewell, C., (2015), *Rainfall erosivity in Europe*, Science of the Total Environment, Vol. 511, pp. 801-814, <https://doi.org/10.1016/j.scitotenv.2015.01.008>.
- Papathanasiou, C., (2015), *Estimating flood risk prior to and after a forest fire*, Services and products for preventive planning of forest fire and post-fire flood management – 3<sup>rd</sup> FLIRE Stakeholders' Meeting, 26<sup>th</sup> of March 2015, Institute of Mediterranean Forest Ecosystems and Forest Products Technology (FRIA), Athens, Greece.
- Papathanasiou, C., Makropoulos, C. and Mimikou, M., (2015a), *Hydrological modelling for flood forecasting: calibrating the post-fire initial conditions*, Journal of Hydrology, Vol. 529, Part 3, pp. 1838-1850, doi: 10.1016/j.hydrol.2015.07.038.
- Papathanasiou C., Pagana V., Makropoulos C., Massari C., Barbetta S., Brocca L., Mimikou M. and Moramarco T. (2015b), *Automating flood hazard mapping in a typical periurban area*, Proc. of "Le Giornate dell' Idrologia 2015" Conference, 6<sup>th</sup>-8<sup>th</sup> October 2015, Perugia.
- Papathanasiou, C., Makropoulos, C., Baltas, E. and Mimikou, M., (2013a), *The Hydrological Observatory of Athens: a state-of-the-art network for the assessment of the hydrometeorological regime of Attica*, Proc. 13<sup>th</sup> International Conference on Environmental Science and Technology, 5<sup>th</sup>-7<sup>th</sup> September 2013, Athens, Greece.
- Papathanasiou, C., Makropoulos, C. and Mimikou, M., (2013b), *An innovative approach to Floods and Fire Risk Assessment and Management: the FLIRE Project*, Proc. 8<sup>th</sup> International Conference of EWRA "Water Resources Management in an Interdisciplinary and Changing Context", 26<sup>th</sup>-29<sup>th</sup> June 2013, Porto, Portugal.
- Papathanasiou, C., Serbis, D. and Mamassis, N., (2013c), *Flood mitigation at the downstream areas of a transboundary river*, Water Utility Journal, Vol. 3, pp. 33-42.
- Papathanasiou C., Pagana V., Varela V., Eftychidis G., Makropoulos C. and Mimikou M., (2013d), *Status Survey report for the study area*, Technical report for Action A2: "Identification of the current status of the study area" of the FLIRE Project (LIFE11 ENV GR 975).
- Papathanasiou, C., Massari, C., Pagana V., Barbetta, S., Brocca, L., Moramarco, T., Makropoulos C. and Mimikou M., (2013e), *Hydrological Study of Rafina catchment*, Technical report for Action B1: "Catchment Hydrological Modelling" of the FLIRE Project (LIFE11 ENV GR 975).
- Papathanasiou, C., Alonistioti, D., Kasella, A., Makropoulos, C. and Mimikou, M., (2012), *The impact of forest fires on the vulnerability of peri-urban catchments to flood events (The case of the Eastern Attica region)*, Special

Issue of the Global NEST Journal on Hydrology and Water Resources, September 2012, Vol. 14, No 3, pp. 294-302.

- Papathanasiou C., Safiolea E., Makropoulos C. and Mimikou M., (2009), *The FLADAR Project and its contribution to the implementation of the EU Flood Directive 2007/60*, Proc. 11<sup>th</sup> International Conference on Environmental Science and Technology, 3 – 5 September 2009, Chania, Crete, Greece.
- Parra, A. and Chuvieco, E., (2005), *Assessing burn severity using Hyperion data*, In De la Riva, J., Pérez-Cabello, F. and Chuvieco, E. (Eds.), Proceedings of the 5th International Workshop on Remote Sensing and GIS Applications to Forest Fire Management: Fire Effects Assessment (pp. 239–244), Paris, Universidad de Zaragoza, GOF-C-GOLD, EARSeL.
- Park, S., Oh, S., Jeon, S, Jung, H. and Choi, C., (2011), *Soil erosion risk in Korean watersheds, assessed using the revised universal soil loss equation*, Journal of Hydrology, Vol. 399, pp. 263-273.
- Pausas, J.G. and Verdú, M., (2005), *Plant persistence traits in the fire-prone ecosystems of the Mediterranean basin: a phylogenetic approach*, Oikos, Vol. 109, pp. 196-202.
- Pausas, J.G., Llovet, J., Rodrigo, A. and Vallejo, R., (2008), *Are wildfires a disaster in the Mediterranean basin? – A review*, International Journal of Wildland Fire, Vol. 17, No 6, pp. 713-723.
- Peng, D., Zhijia, L. and Zhiyu, L., (2008), *Numerical algorithm of distributed TOPKAPI model and its application*, Water Science and Engineering, Vol. 1, No 4, pp. 14-21.
- Perry, C.A., (2000), *Significant floods in the United States during the 20<sup>th</sup> century – USGS measures a century of floods*, USGS Fact Sheet 024-00, March 2000, 4p.
- Polychronaki, A., Gitas, I.Z. and Minchella, A., (2013), *Monitoring post-fire vegetation recovery in the Mediterranean using SPOT and ERS imagery*, International Journal of Wildland Fire, Vol. 23, No 5, pp. 631-642.
- Ponce, V.M. and Hawkins, R., (1996), *Runoff Curve Number: Has it reached maturity?*, Journal of Hydrologic Engineering, ASCE, Vol. 1, No 1, pp. 11-19.
- Ponziani, F., Berni, N., Stelluti, M., Zauri, R., Pandolfo, C., Brocca, L., Moramarco, T., Salciarini, D. and Tamagnini, C., (2013), *Landwarn: an operative early warning systems for landslides forecasting based on rainfall thresholds and soil moisture*, In Margottini C., Canuti P. and Sassa K., (Eds.) *Landslide Science and Practice*, Vol. 2, Early Warning, Instrumentation and Monitoring, Springer-Verlag, Berlin Heidelberg, 685p.
- Poursanidis, D., Kochilakis, G., Chrysoulakis, N, Varella, V., Kotroni, V., Lagouvardos, K., Eftychidis, G., Papathanasiou, C., Makropoulos, C., Mimikou, M., (2015a), *FLIRE: an EO-based DSS for combined flood and fire risk assessment in peri-urban areas*, Mapping Urban Areas from Space (MUAS), 4-5 November 2015, ESA/ESRIN, Frascati, Rome, Italy.
- Poursanidis, D., Kochilakis, G., Chrysoulakis, N., Varella, V., Kotroni, V., Eftychidis, G., Lagouvardos, K., Papathanasiou, C., Karavokyros, G., Aivazoglou, M., Makropoulos, C. and Mimikou, M., (2015b), *FLIRE DSS*, A

*web service system for the management of wildfires and floods in urban and periurban areas*, 13<sup>th</sup> International Symposium on Geo-disaster Reduction, 09-11 August 2015, Prague, Czech Republic.

- Poursanidis, D., Kochilakis, G., Chrysoulakis, N., Varella, V., Kotroni, V., Eftychidis, G., Lagouvardos, K., Papathanasiou, C., Karavokyros, G., Aivazoglou, M., Makropoulos, C., and Mimikou, M., (2015c), *Web-service systems for the management of natural disasters – The case study of the FLIRE DSS in urban and rural areas*, Proc. International Conference SafeChania 2015: The Knowledge Triangle in the Civil Protection Service (Education, Research, Innovation), 10-12 June 2015, Chania, Crete, Greece.
- Poursanidis, D., Kochilakis, G., Chrysoulakis, N., Varella, V., Kotroni, V., Eftychidis, G., Lagouvardos, K., Papathanasiou, C., Karavokyros, G., Aivazoglou, M., Makropoulos, C. and Mimikou, M., (2015d), *The FLIRE DSS, A web service SYSTEM for the management of natural disasters in urban and rural areas*, RSCy2015 – Paphos, Cyprus, 16-19 March 2015.
- Queensland Government, (2011), *Understanding Floods: Questions and Answers*, Report on floods for the State of Queensland, Australia, 38p. (Available on line at: [www.chiefscientist.qld.gov.au](http://www.chiefscientist.qld.gov.au).)
- Raimondi, A. and Becciu, G., (2015), *On pre-filling probability of flood control detention facilities*, Urban Water Journal, Vol. 12, No 4, pp. 344-351.
- Refsgaard, J. C., (1997), *Parameterisation, calibration, and validation of distributed hydrological models*, Journal of Hydrology, Vol. 198, pp. 69-97.
- River Basin Management Plan of Attica (GR06) – Phase A, *Deliverable 8: Analysis of human-made pressures and their impacts on surface and ground water systems*, Special Secretariat for Water, Ministry of Environment, Energy and Climate Change, January 2012.
- Robichaud, P.R. and Hungerford, R.D., (2000), *Water repellency by laboratory burning of four northern Rocky Mountain forest soils*, Journal of Hydrology, Vol. 231-232, pp. 207-219.
- Robichaud, P.R., (2000), *Fire effects on infiltration rates after prescribed fire in Northern Pocky Mountain forests, USA*, Journal of Hydrology, Vol. 231-232, pp. 220-229.
- Rodrigo, A., Retana, J. and Picò, F.X., (2004), *Direct regeneration is not the only response of Mediterranean forest to large fires*, Ecology, Vol. 85, pp. 716-729.
- Rojas, R., (2002), *GIS-based upland erosion modeling, geovisualization and grid size effects on erosion simulations with CASC2D-SED*, Ph.D. Dissertation, Dept. Civil Engr., Colorado State University, Fort Collins, Colorado, USA.
- Roose, E., (1996), *Land husbandry – Components and strategy*, FAO Soils Bulletin 70, Food and Agriculture Organization of the United Nations, Soil Resources Management and Conservation Service Land and Water Development Division, 380p.
- Rossman, L.A., (2010), *Storm Water Management Model User's Manual, Version 5.0*, United States Environmental Protection Agency, Water Supply

and Water Resources Division, National Risk Management Research Laboratory, Cincinnati, OH 45268, Revised July 2010, EPA/600/R-05/040.

- Rulli, M.C. and Rosso, R., (2007), *Hydrologic response of upland catchments to wildfires*, Advances in Water Resources, Vol. 30, pp. 2072-2086.
- Rycroft, H.B., (1947), *A note on the immediate effects of veld burning on storm flow in a Jonkershoek stream catchment*, Journal of the South African Forestry Association, Vol. 15, pp. 80-88.
- Saghafian, B., (1992), *Hydrologic Analysis of Watershed Response to Spatially Varied Infiltration*, Ph.D. Dissertation, 215 pp, Colorado State University, Fort Collins, Colorado, USA.
- Salvati, L. and Carlucci, M., (2015), *Towards sustainability in agro-forest systems? Grazing intensity, soil degradation and the socioeconomic profile of rural communities in Italy*, Ecological Economics, Vol. 112, pp. 1-13.
- San-Miguel-Ayanz, J., Schulte, E., Schmuck, G., Camia, A., Strobl, P., Liberta, G., Giovando, C., Boca, R., Sedano, F., Kempeneers, P., McInerney, D., Withmore, C., Santos de Oliveira, S., Rodrigues, M., Durrant, T., Corti, P., Oehler, F., Vilar, L. and Amatulli, G., (2012), *Comprehensive monitoring of wildfires in Europe: the European Forest FIRE Information System (EFFIS)*, In: Approaches to Managing Disaster – Assessing Hazards, Emergencies and Disaster Impacts - Chapter 5, Ed. Prof. John Tiefenbacher, ISBN: 978-953-51-0294-6, InTech, pp. 87-108.
- Santoni, P.A., Morandini, F. and Barboni, T., (2010), *Steady and un steady fireline intensity of spreading fires at Laboratory Scale*, The Open Thermodynamics Journal, Vol. 4, pp. 2012-219.
- Scharffenberg, W.A. and Fleming, M.J., (2010), *Hydrologic Modeling System – HEC-HMS, User's Manual, Version 3.5*, US Army Corps of Engineers, Hydrologic Engineering Center (HEC), CPD-74A, 318p.
- Schimper, A.F.W., (1903), *Plant-geography upon a physiological basis*, Oxford, Clarendon Press.
- Schoupe, M., (2008), *Sensor networks for Disaster Management – Ongoing Community Research*, GEOSS Sensor Web Workshop – GEO Secretariat at WMO, Geneva, 15-16 May 2008, Switzerland.
- Scott, D.F. and Van Wyk, D.B., (1990), *The effects of wildfire on soil wettability and hydrological behaviour of an afforested catchment*, Journal of Hydrology, Vol. 121, pp. 239-256.
- Shi, Z.H., Chen, L.D., Fang, F.F., Qin, D.F. and Cai, C.F., (2009), *Research on the SCS-CN initial abstraction ratio using rainfall-runoff event analysis in the Three Gorges Area*, Chins, Catena, Vol. 77, No 1, pp. 1-7.
- Shoshany, M., (2000), *Satellite remote sensing of natural Mediterranean vegetation: a review within an ecological context*, Progress in Physical Geography, Vol. 24, No 2, pp. 153–178.
- Shukla, M., (2011), *Soil Hydrology, Land Use and Agriculture: Measurement and Modelling*, CAB International, ISBN-13:978 1 84593 797 3.

- Shultz, M.J., (2007), *Comparison of distributed versus lumped hydrologic simulation models using stationary and moving storm events applied to small synthetic rectangular basins and an actual watershed basin*, PhD Thesis, University of Texas as Arlington.
- Smith, M.B., Seo, D.-J., Koren, V.I., Reed, S.M., Zhang, Z., Duan, Q., Moreda, F. and Cong, S., (2004), *The distributed model intercomparison project (DMIP): Motivation and experiment design*, Journal of Hydrology, Vol. 298, No 1-4, pp. 4-26.
- Snyder, F.F., (1938), *Synthetic unit-graphs: Transactions*, American Geophysical Union, Vol. 19, pp. 447-454.
- Soto, B. and Díaz-Fierros, F., (1998), *Runoff and soil erosion from areas of burnt scrub: comparison of experimental results with those predicted by the WEPP model*, CATENA, Vol. 31, No. 4, pp. 257-270.
- Soulis, K., Londra, P., Alonistioti, D., Pollalis, E. and Valiantzas, J.D., (2009), *Investigation of wildfires effect on flood runoff*, Proceedings of the 6<sup>th</sup> Panhellenic Conference of the Hellenic Society of Agricultural Engineers (HelAgEng), Thessaloniki, 8-10 October 2009, pp. 163-170.
- Soulis K., Dercas N., and Valiantzas J.D., (2007), *Presentation of the Experimental Watershed in the Stream Lykorrema of Penteli Mountain*, Proc. of the 5<sup>th</sup> Congress of the Hellenic Society of Agricultural Engineers, 18 – 20 October 2007, Larisa, Greece.
- Springer, E.P. and Hawkins, R.H., (2005), *Curve number and peakflow responses following the Cerro Grande Fire on a small watershed*. In: Moglen, G.E. (Eds.), Proceedings: 2005 Watershed Management Conference- Managing Watersheds for Human and Natural Impacts: Engineering, Ecological, and Economic Challenges, 19<sup>th</sup> – 22<sup>nd</sup> July 2005, Williamsburg, VA. Alexandria, VA: American Society of Civil Engineers, pp. 459-470.
- Stamatis G., Lambrakis N., Alexakis D. and Zagana E., (2006), *Groundwater quality in Mesogea basin in eastern Attica (Greece)*, Hydrological Processes, Vol. 20, pp. 2803-2818.
- Stickney, P.F., (1986), *First decade plant succession following the Sundance forest fire, northern Idaho*, USDA, Forest Service, Intermountain Research Station, INT-197, Ogden, UT, USA, 26 p., (Available at: <http://babel.hathitrust.org/cgi/pt?id=uiug.30112104053597;view=1up;seq=3>).
- Strahler R.E., (1952), *Hypsometric (area- altitude) analysis of erosional topography*, Geological Society of America Bulletin, Vol. 63, No 11, pp. 1117-1142.
- Su, C.H., Ryu, D., Young, R.I., Western, A.W., Wagner, W., (2013), *Inter-comparison of microwave satellite soil moisture retrievals over the Murrumbidgee Basin, southeast Australia*, Remote Sensing of Environment, Vol. 134, pp. 1-11.
- Szymkiewicz, R., (1991), *Finite-Element Method for the solution of the Saint Venant equations in an open channel network*, Journal of Hydrology, Vol. 122, pp. 275-287.

- Thanos C.A. and Marcou S., (1991), *Post-fire regeneration in Pinus brutia forest ecosystems of Samos island (Greece): 6 years after*, Acta Oecologica, Vol. 12, No 5, pp. 633-642.
- Thanos, C.A., Marcou, S., Christodoulakis, D. and Yannitsaros, A., (1989), *Early post-fire regeneration in Pinus brutia ecosystems of Samos island (Greece)*, Acta Oecologica / Oecologia Plantarum, Vol. 10, No 1, pp. 79-94.
- Todini, E., (1988), *Il modello afflussi deflussi del fiume Arno*, Relazione Generale dello studio per conto della REGIONE Toscana, Technical Report, Bologna, Italy (in Italian).
- Todini, E., (1996), *The Arno rainfall-runoff model*, Journal of Hydrology, Vol. 175, pp. 339-382.
- Tolson, B.A. and Shoemaker, C.A., (2008), *Efficient prediction uncertainty approximation in the calibration of environmental simulation models*, Water Resources Research, Vol. 44, W04411, 19p.
- Trabaud, L., Michels, C. and Grosman, J., (1985), *Recovery of burnt Pinus halepensis Mill. Forests. II Pine reconstitution after wildfire*, Forest Ecology and Management, Vol. 13, pp. 167-179.
- Trabaud, L., (1987), *Fire and survival traits of plants*, In Trabaud L., eds., *The role of fire in ecological systems*, SPB Academic Publishing, The Hague, pp. 65–89.
- Trambly, Y., Bouaicha, R., Brocca, L., Dorigo, W., Bouvier, C., Camici, S. and Servat, E., (2012), *Estimation of antecedent wetness conditions for flood modelling in northern Morocco*, Hydrology and Earth System Sciences, Vol. 16, pp. 4375-4386.
- TUHH, (2008), *Kalypso Risk Anwenderhandbuch*, Institut für Wasserbau, Version 2.0.1, 40 p (in German).
- Urich, C., Burger, G., Mair, M. and Rauch W., (2012), *DynaMind – A software tool for integrated modelling of urban environments and their infrastructure*, Proceedings of the 10<sup>th</sup> International Conference on Hydroinformatics, HIC 2012, Hamburg, Germany, 8p.
- US Department of Agriculture, Natural Resources Conservation Service, (2004a), National Engineering Handbook: Part 630 – Hydrology, *Chapter 9: Hydrologic Soil-Cover Complexes*, (Originally published in the National Engineering Handbook: Part 4 – Hydrology by the U.S.D.A. Soil Conservation Service, 1965).
- US Department of Agriculture, Natural Resources Conservation Service, (2004b), National Engineering Handbook: Part 630 – Hydrology, *Chapter 10: Estimation of Direct Runoff from Storm Rainfall*, (Originally published in the National Engineering Handbook: Part 4 – Hydrology by the U.S.D.A. Soil Conservation Service, 1965).
- US Department of Agriculture, Natural Resources Conservation Service, (2009), National Engineering Handbook: Part 630 – Hydrology, *Chapter 7: Hydrologic Soil Groups*, (Originally published in the National Engineering Handbook: Part 4 – Hydrology by the U.S.D.A. Soil Conservation Service, 1965).

- US Department of Agriculture, Natural Resources Conservation Service, (1986), *Urban Hydrology for Small Watersheds, Technical Release 55*, 210-VI-TR-55, Second Edition, June 1986.
- US Department of Agriculture, Soil Conservation Service, (1985), National Engineering Handbook, *Section 4: Hydrology*, Washington, D.C.
- US NWS, (2004), *Flood Severity Category Evaluation*, United States National Weather Service, Location North America, Period 2004.
- Vallance, J.W. and Iverson, R.M., (2015), *Lahars and their Deposits*, The Encyclopedia of Volcanoes (2<sup>nd</sup> Ed.), Academic Press, Chapter 37, pp. 649-664.
- van Griensven, A., Meixner, T., Grunwald, S., Bishop, T., Diluzio, M. and Srinivasan, R., (2006), *A global sensitivity analysis tool for the parameters of multi-variable catchment models*, Journal of Hydrology, Vol. 324, pp. 10-23.
- van Leeuwen, W.J.D., Casady, G.M., Neary, D.G., Bautista, S., Alloza, J.A., Carmel, Y., Wittenberg, L., Malkinson, D. and Orr, B.J., (2010), *Monitoring post-wildfire vegetation response with remotely sensed time series data in Spain, USA and Israel*, International Journal of Wildland Fire, Vol. 19, No 1, pp. 75-93.
- Vanderkimpen, P., Melger, E. and Peeters, P., (2009), *Flood modeling for risk evaluation – a MIKE FLOOD vs. SOBEK 1D2D benchmark study*, In: Flood Risk Management: Research and Practice, Ed. Samuels, P., Huntington, S., Allsop W. and Harrop., J., Taylor & Francis Group, London, pp. 77-84.
- Van Der Knijff J. and De Roo A., (2008), *LISFLOOD – Distributed water balance and flood simulation model*, Revised User Manual, Joint Research Centre Scientific and Technical Reports, EUR 22166 EN/2 – 2008, Institute for Environment and Sustainability.
- Van Der Knijff J.M., Younis J. and De Roo A.P.J., (2010), *LISFLOOD: a GIS-based distributed model for river basin scale water balance and flood simulation*, International Journal of Geographical Information Science, Vol. 24, No. 2, pp. 189-212.
- van Wagendonk, J.W., (1996), *Use of deterministic fire growth model to test fuel treatments*, In: Sierra Nevada Ecosystem Project: Final Report to Congress, Vol. 2, Chapter 43, University of California, Davis, Wildland Resources Center, Rep. 37, 1528p.
- Veraverbeke, S., Lhermitte, S., Verstraeten, W.W. and Goossens, R., (2010), *The temporal dimension of differenced Normalized Burn Ratio (dNBR) fire/burn severity studies: the case of the large 2007 Peloponnese wildfires in Greece*, Remote Sensing of Environment, Vol. 114, No 11, pp. 2548-2563.
- Viedma, O., Meliá, J., Segarra, D. and García-Haro, J., (1997), *Modeling rates of ecosystem recovery after fires by using Landsat TM data*, Remote Sensing of Environment, Vol. 61, pp. 383-398.
- Viessman, Jr.W. and Lewis, G.L., (1995), *Introduction to Hydrology*, 4<sup>th</sup> Ed., Glenview, Ill: Addison Wesley/Longman, 760 p.

- Viessman, Jr.W. and Lewis, G.L., (2003), *Introduction to Hydrology*, 5<sup>th</sup> Ed., Pearson Education, Inc., Upper Saddle River, New Jersey, USA. 612 p.
- Vieux, B.E. and Vieux, J.E., (2002), *Vflo™: A real-time distributed hydrologic model*, Proceedings of the 2<sup>nd</sup> Federal Interagency Hydrologic Modeling Conference, July 28<sup>th</sup> - August 1<sup>st</sup>, 2002, Las Vegas, Nevada.
- Wagener, T. and Kollat, J., (2007), *Numerical and visual evaluation of hydrological and environmental models using the Monte Carlo analysis toolbox*, Environmental Modelling & Software, Vol. 22, pp. 1021-1033.
- Wanders, N., Hendriks, D. M. D. and Van Der Velde, Y., (2011), *Combined groundwater-surface water modeling with a lumped hydrological model, Deltares*, Project with reference number 1203833-000-BGS-0001, Version 1.1, 9 February 2011, final report.
- Wanders, N., Karssenbergh, D., Bierkens, M., Parinussa, R., De Jeu, R., Van Dam, J. and De Jong, S., (2012), *Observation uncertainty of satellite soil moisture products determined with physically-based modelling*, Remote Sensing of Environment, Vol. 127, pp. 341-356.
- Willgoose, G.R., (2011), *Modelling bushfire impact on hydrology: The implications of the fire modelling approach on the climate change impact*, 19<sup>th</sup> International Congress on Modelling and Simulation, Perth, Australia, 12-16 December 2011.
- WMO - World Meteorological Organization, (2014), Weather Climate Water Hazards, Poster on natural hazards, presented at Natural Hazards Theme of the WMO website, (Available at: [http://www.wmo.int/pages/publications/showcase/documents/hazards\\_wmd.pdf](http://www.wmo.int/pages/publications/showcase/documents/hazards_wmd.pdf)).
- World Meteorological Organization – WMO, (1983), *Guide to Hydrological Instruments and Methods of Observation*, Publication 8, 5<sup>th</sup> Ed., Geneva.
- Wolfram, S., (1982), *Cellular automata as simple self-organizing systems*, Caltech preprint CALT-68-938, 12p.
- Wondzell, S.M. and King, J.G., (2003), *Postfire erosional processes in the Pacific Northwest and Rocky Mountain regions*, Forest Ecology and Management, Vol. 178, pp. 75-87.
- WWF, (2003), *Forest fires in the Mediterranean: a burning issue*, (Available at: <http://assets.panda.org/downloads/forestfires2003factfile.doc>).
- Xanthopoulos G. and Caballero D., (2007), *Fires in the Wildland-Urban Intermix (WUI) zone: lessons learnt from recent disasters*, p. 131-156 In "Tomorrow in Danger: Natural and technological disasters in Europe and Greece", Sapountzaki K., Ed. Gutenberg, Athens, p. 396.
- Xu, C., Dai, F., Xu, X. and Lee, Y.H., (2012), *GIS-based support vector machine modeling of earthquake-triggered landslide susceptibility in the Jianjiang River watershed, China*, Geomorphology, Vol. 145, pp. 70–80.
- Zêzere, J.L., Ferreira, A.B. and Rodrigues, M.L., (1999), *Landslides in the North of Lisbon Region (Portugal): Conditioning and triggering factors*, Physics



and Chemistry of the Earth, Part A: Solid Earth and Geodesy, Vol. 24, No 10, pp. 925-934.

- Zhou Y., Zhang Y., Vaze J., Lane P. and Xu S., (2013), *Impact of bushfire and climate variability on streamflow from forested catchments in southeast Australia*, Hydrology and Earth System Sciences Discussions, Vol. 10, pp. 4397-4437. doi:10.5194/hessd-10-4397-2013.
- Zhu, A.X., Wang, R., Qiao, J., Qin, C.Z., Chen, Y., Liu, J., Du, F., Lin, Y. and Zhu T., (2014), *An expert knowledge-based approach to landslide susceptibility mapping using GIS and fuzzy logic*, Geomorphology, Vol. 214, pp. 128-138.